7-2021

Evaluating Bioenergetics and Mitochondrial Dynamics in Patient Fibroblasts with Pathogenic Mitochondrial DNA Mutations Causing Leigh Syndrome

Ajibola Bakare
University of Arkansas, Fayetteville

Evaluating Bioenergetics and Mitochondrial Dynamics in Patient Fibroblasts with Pathogenic Mitochondrial DNA Mutations Causing Leigh Syndrome

A dissertation submitted in partial fulfillment
of the requirements for the degree of
Doctor of Philosophy in Cell and Molecular Biology

by

Ajibola Bakare
Transylvania University
Bachelor of Arts in Biology, 2015

July 2021
University of Arkansas

This dissertation is approved for recommendation to the Graduate Council.

Shilpa Iyer, Ph.D.
Dissertation Director

Raj R. Rao, Ph.D.
Committee Member

Kyle P. Quinn, Ph.D.
Committee Member

Ines Pinto, Ph.D.
Committee Member

Francis Millett, Ph.D.
Committee Member

Abstract

Leigh syndrome (LS) is a rare fatal mitochondrial disorder of infants caused by pathogenic mutations in the nuclear (nDNA) or mitochondrial DNA (mtDNA) leading to mitochondrial dysfunction. The extent to which pathogenic mtDNA variants regulate disease severity in LS is not well understood. The heterogeneous nature of this disorder, based in part by complex mitochondrial genetics, and the nuclear and mitochondrial cross-talk has made it particularly challenging to investigate and develop therapies for treating LS . While the prognosis is poor, several studies are underway to understand the pathophysiology of LS. This dissertation provides a comprehensive structural and functional analysis of five patient fibroblast cells modeling LS, harboring pathogenic mtDNA variants; in order to gain a better understanding of disease severity and alleviate some of the mitochondrial dysfunction reported in LS.

The influence of pathogenic mtDNA on mitochondrial structure and function in LS is unknown. Therefore, in our first study, we conducted a comprehensive analysis and identified five mitochondrial morphologies individuals, networks, branches, length of branches and size of networks in single cells containing some of the most prevalent pathogenic mtDNA known to cause LS. Results indicated LS cells predominantly contained individual mitochondria with short branch lengths, characteristic of a fragmented state compared to a control line with long-branched mitochondrial networks.

To better understand disease severity in patient fibroblast cells modeling LS, (*T8993G, T9185C, T10158C*, *T12706C*) in *MTATP6*, *MTND3*, *MTND5* genes affecting the function of complex V or complex I. In this study, we estimated a high percentage (> 90%) of pathogenic mtDNA (*T8993G, T9185C*) in LS cells affecting complex V and a low percentage (< 39%) of pathogenic mtDNA (*T10158C*, *T12706C*) in LS cells affecting complex I. Levels of defective enzyme activities of the electron transport chain correlated with the percentage of pathogenic

mtDNA. Subsequent bioenergetics assays showed cell lines relied on both mitochondrial bioenergetics and glycolysis for meeting energy requirements. The CBHI ratio emerged as a sensitive biomarker to ascertain disease severity in LS lines specifically harboring pathogenic mtDNA variants. Higher CBHI values indicated milder forms of the disease and lower CBHI values indicated severe form of the disease. Our results suggest that whereas the precise mechanism of LS has not been elucidated, a multi-pronged approach taking into consideration the specific pathogenic mtDNA variant, and composite BHI ratio, can aid in better understanding the factors influencing disease severity in LS.

Finally, we explored the therapeutic effects of introducing citric acid cycle (TCA) intermediate substrate, succinate, as a cell permeable prodrug-NV118, to alleviate some of the mitochondrial dysfunction in LS. Results suggest that a 24-hour treatment with prodrug NV118 elicited an upregulation of glycolylysis and mitochondrial membrane potential (MMP) while inhibiting intracellular reactive oxygen species (ROS) in LS cells. The results from this study suggests an important role for TCA intermediates in the treatment of mitochondrial dysfunction in LS. With advances in available research tools leading to a better understanding of the mitochondria in health and disease, there is hope for novel treatment options in the future.

Acknowledgments

First, I would like to thank Dr. Iyer for providing me with space and resources to perform the studies for this doctoral dissertation in her lab. Furthermore, I am grateful for the continued guidance and mentorship that Dr. Iyer provides me throughout my graduate degree at the University of Arkansas. Whether it be providing feedback during lab meetings or giving suggestions and recommendations on what experiments to perform or feedbacks on how to write scientific papers and make quality publication style figures, I have gained a lot of expertise from her teachings. I also appreciate all the efforts that were put into critically reviewing the papers that were submitted for publications, some of which have been included in this dissertation.

I would be remorseful if I did not acknowledge Dr. Rao as well for contributing to my growth as a scientist. I am grateful to him for being a committee member that I could rely on to help provide constructive feedback on my work. Thank you for asking tough questions that helped me delve deeper into the basics of my research. I also appreciate your help with reviewing several drafts of the papers that have been submitted for publication.

Furthermore, I am deeply grateful to the other members of my committee for taking the time to listen to my ideas and provide valuable feedback when necessary. I am thankful to Dr. Pinto for lending her ears and listening when I needed to get a different perspective on my project. I am also thankful to Dr. Quinn for the support he provided on collaborative projects I was involved in with his lab. I would also like to thank Dr. Millett for being a valuable member of my committee and providing me with invaluable knowledge on mitochondrial biochemistry and energetics through his wonderful class. I am also grateful to Drs Iyer, Pinto, and, Quinn for writing me recommendation letters to help with my professional development and my future aspirations.

I would like to thank all my collaboration partners, colleagues, lab mates, and undergraduate mentees whom I have worked with over the years. Thank you for your contribution to my various project. I am grateful to Dr. Lesnefsky for the collaborative effort and his involvement in reviewing my work. I would also like to thank Dr. Bailey for being a source of support and providing guidance when I needed it and for also writing me multiple recommendation letters to advance my career. My deepest gratitude goes to Joshua Stabach for his technical assistance in the lab and for the extra joy he added to the lab while he was here. Thanks to Josh for always finding a way to help ease the stress of graduate school with his jokes and memes. Graduate school would have been a lot more stressful without the pleasing and colorful working atmosphere that Josh's presence added to the lab.

Finally, I am grateful to the various support group that has helped me stay focused in following through with my graduate studies. I am most grateful to my partner, Katherine Dupree for her constant support. I am also grateful to my family for the strong faith that they placed in me, and my mum for her constant prayers, that have helped me get through difficult times. I would not even be here, if not for the sacrifice that my family made. For this, I am eternally grateful. I give thanks to the Almighty as well, for the continuous gift of life. It is this gift that makes it possible for me to pursue my desires.

Dedication

I dedicate this dissertation to my father; the one who sacrificed everything he had to help me pursue my goal. Losing you in the first couple of months of starting graduate school was the hardest thing that I have had to endure in my adult life. But your words of wisdom, “Tough times never last, only tough people do,” kept me going. Whenever I was struggling in graduate school, these words would come to me and I would know that you were right there with me and telling me to push on. I also dedicate this to my mum and brothers, who have sacrificed sharing memories over the years owing to the distance that separates us. Thank you for never losing faith in me and for the continuous support from all of you. Even though we are oceans apart, know that you all are always here with me in my heart. I love you all!

Table of Contents

List of Figures

List of Tables

List of Abbreviations

AMPK	AMP-activation Protein Kinase
ATP	Adenosine Triphosphate
BHI	Bioenergetic Heath Index
cBHI	Composite Bioenergetic Health Index
CI	Complex I (NADH:ubiquinone oxidoreductase)
CV	Complex V (ATP synthase)
COX	Cytochrome Oxidase
CNS	Central Nervous System
CPEO	Chronic Progressive External Opthalmoplegia
CSF	Cerebral Spinal Fluid
DCFDA	2',7'-dichlorofluorescein diacetate
DMKG	Dimethyl Ketoglutarate
ES Cells	Embryonic Stem Cells
ETC	Electron Transport Chain
$FADH_2$	Flavin Adenine Dinucleotide
FB	Fibroblast cells
FCCP	Trifluoromethoxy Carbonylcyanide Phenylhydrazone
HIF	Hypoxia Inducible Factor
iDH1	Isocitrate Dehydrogenase 1
iN	Induced Neurons
iPSC	Induced Pluripotent Stem Cell
KSS	Kearns-Sayres syndrome
LS	Leigh syndrome
LHON	Leber's hereditary optic neuropathy

LRPPRC	Leucine Rich Pentatricopeptide Repeat Containing
MELAS	Mitochondrial Encephalomyopathy with Lactic Acidosis and Stroke-like episodes
MERRF	Myoclonic epilepsy with ragged red fibers
MILS	Maternally Inherited Leigh syndrome
MiNA	Mitochondrial Network Analysis
MMP	Mitochondrial Membrane Potential
mtDNA	Mitochondrial DNA
MTND1-6	Mitochondrial NADH dehydrogenase 1-6
MTCYB	Mitochondrial encoded cytochrome B
mTORC1	Mammalian Target of Rapamycin Complex 1
MTR	Mitotracker Red
NADH	Nicotinamide Adenine Dinucleotide
NARP	Neuropathy,ataxia, and retinitis pigmentosa
nDNA	Nuclear DNA
NDUF	NADH dehydrogenase (ubiquinone) Fe-S protein
NSE	Necrotising Encephalomyelopathy
OAA	Oxaloacetate
OCR	Oxygen Consumption Rate
OXPHOS	Oxidative Phosphorylation
PDHC	Pyruvate dehydrogenase complex
PER	Proton Efflux Rate
PGC1α	Peroxisome proliferator-activated receptor gamma coactivator 1-alpha
PNT	Pronuclear transplantation
POLG	DNA polymerase subunit gamma

PS	Pearson syndrome
ROS	Reactive Oxygen Species
SLC	Solute Carrier (gene)
SCNT	Somatic Nuclear Transfer
SDH	Succinate Dehydrogenase
Sirt	Sirtuins
SOD	Superoxide dismutase
SURF	Surfeit locus genes
TALEN	Transcription Activator-like Effector Nuclease
TTC19	Tetratricopeptide Repeat Domain 19
TPK	Thiamine Pyrophosphokinase 1
TPP	Thiamine Pyrophosphate
THTR1,2	Thiamine Transporter 1, 2
TCA cycle	Tricarboxylic Acid cycle
UQCRQ	Ubiquinol-Cytochrome C Reductase Complex III Subunit VII)
VHL	Von Hippel-Lindau
ZFN	Zinc Finger Nuclease

List of Published Papers

Chapter 1

1. **Bakare, A.B.**, Lesnefsky, E.J., Iyer, S. Leigh Syndrome: A tale of two genomes. *Frontiers in Physiology*. Submitted April 2021.

Chapter 2

2. **Bakare, A.B.,** Daniel, J., Stabach, J., Rojas, A., Bell, A., Henry, B., Iyer, S. Quantifying mitochondrial dynamics in patient fibroblasts with multiple developmental defects and mitochondrial disorders. *International Journal of Molecular Sciences*. 2021, 22, 6263.

Chapter 3

3. **Bakare, A.B.,** Dean, J., Chen, Q., Saikia, B., Thorat, V., Huang, Y, LaFramboise, T., Lesnefsky, E.J., and Iyer, S. Evaluating the bioenergetics health index ratio in Leigh syndrome fibroblasts to understand disease severity. *Scientific Reports*. Submitted June 2021.

Chapter 4

4. **Bakare, A.B.,** Rao, R.R., Iyer, S. Cell-permeable succinate increases mitochondrial membrane potential and glycolysis in Leigh syndrome patient fibroblasts. *Cells*. Submitted July 2021.

Introduction

1.1. Rationale for study

Leigh syndrome, also known as subacute necrotizing encephalomyelopathy (NSE), is a complex and incurable early-onset neurodegenerative disease (Ruhoy and Saneto, 2014). It affects 1 in 40, 000 live births and disease onset varies, with the majority of cases developing before the age of 2 (Gerards et al., 2016). Like most other mitochondrial diseases, LS is clinically and genetically heterogeneous, resulting in a diverse phenotypic spectrum. Due in part to mutant load, LS can present as NARP (Neuropathy, ataxia, and retinitis pigmentosa) at low mutant loads between 50-60%; while phenotypically present as LS at higher mutant loads >90%. In recent years, efforts have been made to compile clinical information from various multi centers across Europe, Asia, the USA, and Australia (Sofou et al., 2014;Sofou et al., 2018;Ganetzky et al., 2019;Hayhurst et al., 2019;Hong et al., 2020;Ogawa et al., 2020;Stendel et al., 2020). These have allowed for metadata analysis and systemic retrospective studies to find unifying symptoms for LS. These studies have suggested that certain clinical symptoms such as ataxia, hypotonia, developmental delay, and seizures are common among patients with the same mutations (Sofou et al., 2018).

To this end, we performed a comparative analysis of the structural and functional defects in patient fibroblasts carrying some of the most prevalent mitochondrial mutations involved in Leigh syndrome. This allowed for the investigation of the molecular mechanisms underlying the various pathologies associated with LS in variants containing four different pathological mtDNA mutations. The first three-point mutations were (SBG1& SBG2: *T8993G*, SBG3: *T9185C*) in the *MTATP6* gene known to impact complex V or ATP synthase function (Bakare et al., 2021). The other two point mutations were (SBG4-FB: *T10158C*) in the *MTND3* gene, and (SBG5-FB: *T12706C*) in the *MTND5* gene presumed to impact complex I function (Bakare et al., 2021).

We **hypothesized** that patient cells with a high percentage of pathogenic mtDNA mutations would generate abnormal mitochondrial morphologies, disrupt electron transfer, reduce proton translocation, and have defects in membrane potential and bioenergetics.

Our long-term goal is to better understand the complex relationship between the pathogenic genotypes and their morphological, biochemical, and clinical phenotypes in mitochondrial diseases affecting young children. Understanding this relationship will allow for targeted therapies that might be effective in treating LS and other related metabolic disorders. The current thinking is that Mitochondrial disorders share some traits that are mutation-specific and biomarkers can be developed to identify these traits. Identifying these biomarkers can help with developing better diagnostic and therapeutic tools for LS.

The experiments outlined under the three different specific aims below will enable us to test the hypothesis outlined above.

1.1.1. Specific aim 1 – To characterize the mitochondrial structure and function in five patient-derived fibroblast cells modeling LS

To address this aim, the mitochondrial network analysis (MiNA) tool (Valente et al., 2009), will be used to analyze the mitochondrial morphologies of fluorescently labeled human fibroblast cell lines. Analysis will be performed on one healthy control BJ fibroblast and five diseased fibroblast cell lines. The patient-derived fibroblast cells modeling LS, harbor point mutations in the *MTATP6* gene (*T8993G*, *T9185C*) and *MTND3* gene (*T10158C*), and *MTND5* gene (*T12706C*) impacting complex V or ATP synthase function and complex I function. The rationale behind using these cell lines is because these are some of the most prevalent pathogenic mtDNA mutations that have been reported to be involved in LS to date (Taylor et al., 2002;Piekutowska-Abramczuk et al., 2018;Wei et al., 2018;Yu et al., 2018;Stendel et al., 2020). The mitochondrial uncoupler, FCCP will be used to analyze mitochondrial dynamics in the LS

patient fibroblast cells and control BJ-FB cells under basal conditions and when stressed with FCCP. Finally, mitochondrial membrane potential (MMP) will be investigated to understand how changes in mitochondrial morphologies affect mitochondrial membrane potential.

1.1.2. Specific aim 2 – To identify a sensitive biomarker for determining disease severity in five patient-derived fibroblast cells modeling LS

Specific aim 2 will determine how the five patient cells modeling LS and harboring pathogenic mtDNA (*T8993G*, *T9185C*, *T10158C*, and *T12706C*) along with control BJ cell line affect various mitochondrial functions. This would aid in identifying mutant DNA heteroplasmy levels, enzyme activities of individual subunits, mitochondrial respiration, reactive oxygen species assay, and glycolysis to further understand the underlying mechanisms behind the severity and clinical heterogeneity reported in LS patients. Furthermore, comparing the functional analysis with the reported clinical symptoms will allow us to identify a sensitive biomarker that can assess overall mitochondrial dysfunction, which can be used to make predictions of disease severity in LS.

1.1.3. Specific aim 3 – To test the efficacy of cell membrane permeable complex II substrate, succinate as a potential therapeutic drug in four patient-derived fibroblast cells modeling LS

There is currently no known cure for LS. Therefore, in this aim, we will treat four fibroblast cells modeling LS harboring (*T8993G*, *T10158C*, *T12706C*) pathogenic mtDNA and one control BJ-FB cell line with a cell membrane permeable complex II substrate, succinate (NV118) in the short term. Optimization studies will be performed on the control BJ-FB cell line to determine the appropriate NV118 concentration that is non- toxic to the cells. Biochemical assays to test mitochondrial respiration, membrane potential, and glycolysis will be carried out in the diseased

and healthy cell lines. Furthermore, cellular ROS will be assessed in the diseased and control cell lines after treatment with a pre-determined concentration of NV118.

Overall, the outcomes from this study are important steps towards understanding disease origins and support the beneficial use of a TCA cycle intermediate substrate- succinate prodrug (NV118), in the development of a therapeutic application for LS and mitochondrial diseases in the near future.Introduction.

1.2. References

Bakare, A.B., Daniel, J., Stabach, J., Rojas, A., Bell, A., Henry, B., and Iyer, S. (2021). Quantifying Mitochondrial Dynamics in Patient Fibroblasts with Multiple Developmental Defects and Mitochondrial Disorders. *International Journal of Molecular Sciences* 22.

Ganetzky, R.D., Stendel, C., Mccormick, E.M., Zolkipli-Cunningham, Z., Goldstein, A.C., Klopstock, T., and Falk, M.J. (2019). MT-ATP6 mitochondrial disease variants: Phenotypic and biochemical features analysis in 218 published cases and cohort of 14 new cases. *Human Mutation* 40**,** 499-515.

Gerards, M., Sallevelt, S.C., and Smeets, H.J. (2016). Leigh syndrome: Resolving the clinical and genetic heterogeneity paves the way for treatment options. *Mol Genet Metab* 117**,** 300-312.

Hayhurst, H., De Coo, I.F.M., Piekutowska-Abramczuk, D., Alston, C.L., Sharma, S., Thompson, K., Rius, R., He, L., Hopton, S., Ploski, R., Ciara, E., Lake, N.J., Compton, A.G., Delatycki, M.B., Verrips, A., Bonnen, P.E., Jones, S.A., Morris, A.A., Shakespeare, D., Christodoulou, J., Wesol-Kucharska, D., Rokicki, D., Smeets, H.J.M., Pronicka, E., Thorburn, D.R., Gorman, G.S., Mcfarland, R., Taylor, R.W., and Ng, Y.S. (2019). Leigh syndrome caused by mutations in MTFMT is associated with a better prognosis. *Ann Clin Transl Neurol* 6**,** 515-524.

Hong, C.M., Na, J.H., Park, S., and Lee, Y.M. (2020). Clinical Characteristics of Early-Onset and Late-Onset Leigh Syndrome. *Front Neurol* 11**,** 267.

Ogawa, E., Fushimi, T., Ogawa-Tominaga, M., Shimura, M., Tajika, M., Ichimoto, K., Matsunaga, A., Tsuruoka, T., Ishige, M., Fuchigami, T., Yamazaki, T., Kishita, Y., Kohda, M., Imai-Okazaki, A., Okazaki, Y., Morioka, I., Ohtake, A., and Murayama, K. (2020). Mortality of Japanese patients with Leigh syndrome: Effects of age at onset and genetic diagnosis. *J Inherit Metab Dis* 43**,** 819-826.

Piekutowska-Abramczuk, D., Rutyna, R., Czyżyk, E., Jurkiewicz, E., Pronicka, K.I., Rokicki, D., Stachowicz, S., Strzemecka, J., Guz, W., Gawroński, M., Kosierb, A., Ligas, J., Puchala, M., Drelich-Zbroja, A., Bednarska-Makaruk, M., Dąbrowski, W., Ciara, E., Książyk, J.B., and Pronicka, E. (2018). Leigh syndrome in individuals bearing m.9185T>C MTATP6 variant. Is hyperventilation a factor which starts its development? *Metabolic Brain Disease* 33**,** 191-199.

Ruhoy, I.S., and Saneto, R.P. (2014). The genetics of Leigh syndrome and its implications for clinical practice and risk management. *Appl Clin Genet* 7**,** 221-234.

Sofou, K., De Coo, I.F., Isohanni, P., Ostergaard, E., Naess, K., De Meirleir, L., Tzoulis, C., Uusimaa, J., De Angst, I.B., Lonnqvist, T., Pihko, H., Mankinen, K., Bindoff, L.A., Tulinius, M., and Darin, N. (2014). A multicenter study on Leigh syndrome: disease course and predictors of survival. *Orphanet J Rare Dis* 9**,** 52.

Sofou, K., De Coo, I.F.M., Ostergaard, E., Isohanni, P., Naess, K., De Meirleir, L., Tzoulis, C., Uusimaa, J., Lonnqvist, T., Bindoff, L.A., Tulinius, M., and Darin, N. (2018). Phenotype-genotype correlations in Leigh syndrome: new insights from a multicentre study of 96 patients. *J Med Genet* 55**,** 21-27.

Stendel, C., Neuhofer, C., Floride, E., Yuqing, S., Ganetzky, R.D., Park, J., Freisinger, P., Kornblum, C., Kleinle, S., Schols, L., Distelmaier, F., Stettner, G.M., Buchner, B., Falk, M.J., Mayr, J.A., Synofzik, M., Abicht, A., Haack, T.B., Prokisch, H., Wortmann, S.B., Murayama, K., Fang, F., Klopstock, T., and Group, A.T.P.S. (2020). Delineating MT-ATP6-associated disease: From isolated neuropathy to early onset neurodegeneration. *Neurol Genet* 6**,** e393.

Taylor, R.W., Morris, A.A., Hutchinson, M., and Turnbull, D.M. (2002). Leigh disease associated with a novel mitochondrial DNA ND5 mutation. *European Journal of Human Genetics* 10**,** 141-144.

Valente, L., Piga, D., Lamantea, E., Carrara, F., Uziel, G., Cudia, P., Zani, A., Farina, L., Morandi, L., Mora, M., Spinazzola, A., Zeviani, M., and Tiranti, V. (2009). Identification of novel mutations in five patients with mitochondrial encephalomyopathy. *Biochim Biophys Acta* 1787**,** 491-501.

Wei, Y., Cui, L., and Peng, B. (2018). Mitochondrial DNA mutations in late-onset Leigh syndrome. *J Neurol* 265**,** 2388-2395.

Yu, X.L., Yan, C.Z., Ji, K.Q., Lin, P.F., Xu, X.B., Dai, T.J., Li, W., and Zhao, Y.Y. (2018). Clinical, Neuroimaging, and Pathological Analyses of 13 Chinese Leigh Syndrome Patients with Mitochondrial DNA Mutations. *Chin Med J (Engl)* 131**,** 2705-2712.

Chapter 1

2. Leigh Syndrome: A tale of two genomes

Bakare, A.B., Lesnefsky, E.J., Iyer, S.

2.1. Abstract

Leigh syndrome is a rare, complex, and incurable early-onset (typically infant or early childhood) mitochondrial disorder with both phenotypic and genetic heterogeneity. The heterogeneous nature of this disorder, based in part on the complexity of mitochondrial genetics, and the significant interactions between the nuclear and mitochondrial genomes has made it particularly challenging to research and develop therapies. This review article discusses some of the advances that have been made in the field to date. While the prognosis is poor with no current substantial treatment options, multiple studies are underway to understand the etiology, pathogenesis, and pathophysiology of Leigh syndrome. With advances in available research tools leading to a better understanding of the mitochondria in health and disease, there is hope for novel treatment options in the future.

2.2. Introduction

Leigh syndrome (LS), was first described in 1951 by Denis Archibald Leigh as Subacute Necrotising Encephalomyelopathy (NSE) and is a complex and incurable early-onset neurodegenerative disease (Leigh, 1951). According to the definition used by the Online Mendelian Inheritance in Man Database (OMIM 256000), LS has been defined by these cardinal characteristics: “a neurodegenerative disease with variable symptoms due to mitochondrial dysfunction (caused by hereditary genetic defect) accompanied by bilateral Central Nervous System (CNS) lesions that can be associated with further abnormalities in diagnostic imaging.” Decades of research after the initial description by Denis Leigh have led to the association of LS

with defect(s) in one or several of the electron transport chain (ETC) complexes of the mitochondria. Clinical symptoms include neurodevelopmental deterioration, which is often accompanied by brainstem dysfunction such as abnormalities in tone, power, reflexes, ataxia, dysphagia, and seizures (Nesbitt et al., 2012). While the clinical presentations might differ between individuals, LS symptoms largely represent the areas in the brain (brainstem, cerebellum, basal ganglia, oculomotor and cranial nerves) involved in its pathology (Ruhoy and Saneto, 2014).

Like most other mitochondrial diseases, LS is clinically and genetically heterogeneous, resulting in a diverse phenotypic spectrum. Due in part to mutant load, LS can present as NARP (Neuropathy, ataxia, and retinitis pigmentosa) at low mutant loads between 50-60%; while phenotypically present as LS at higher mutant loads >90%. The heterogeneous nature of LS can also be attributed in part to the complex nature of the mitochondrial ETC, which is composed of subunits that are encoded by both nuclear (nDNA) and mitochondrial DNA (mtDNA) (Nesbitt et al., 2012;Zinovkin et al., 2016;Bailey and Doherty, 2017;Manickam et al., 2017) with mutations in either genomes coding for different ETC subunits resulting in LS. Furthermore, since the mitochondria do not follow the Mendelian inheritance pattern, healthy and diseased mtDNA could co-exist within a cell (Taylor et al., 2001b). This phenomenon, termed heteroplasmy, also contributes to the complexity and diverse phenotypic spectrum characteristic of LS. In some cases, it is believed that a certain heteroplasmic threshold must be attained for the expression of the diseased phenotype.

Here, we review the current knowledge of LS, describing how mutations in various ETC subunits encoded by either nDNA or mtDNA contribute to disease pathogenesis. Emphasis will be placed on the most common mutations that have been reported to result in deficiencies of each of the complexes that comprise the OXPHOS system. This review will also discuss some of the disease models that are currently being used to study LS, the challenges associated with

these models, and the potential for induced pluripotent stem cells (iPSC) technologies contributing to novel models for understanding the pathophysiology of LS. Finally, current and potential treatment options for LS will also be discussed.

2.3. Background of mitochondrial biology and Leigh syndrome

2.3.1. Historical and current perspective of Leigh syndrome

Studies have largely implicated dysfunction in mitochondrial energy metabolism as a frequent cause of LS (Lake et al., 2016). Mitochondria are key organelles that are critical to normal cell and organ function and serve an essential role in maintaining metabolic homeostasis through the production of energy in the form of Adenosine Triphosphate (ATP) (Graeber and Muller, 1998;Shaughnessy et al., 2014;Zinovkin et al., 2016). Mitochondria also serve as the hub for various cellular activities such as lipid metabolism, the citric acid cycle, and oxidative phosphorylation (OXPHOS) (Graeber and Muller, 1998). Mitochondria produce ATP via the OXPHOS pathway; a process that takes place at the inner mitochondrial membrane and involves the channeling of electrons through four ETC complexes. The electron transport results in subsequent translocation of protons from the matrix into the intermembrane space; with the combination of the proton gradient and the inward-negative mitochondrial membrane potential driving the molecular motor, ATP synthase (complex V), to produce ATP. An impairment in the ETC or its assembly complexes (**Supplementary Table 7.3.1.**) results in metabolic disorders like LS. The ETC, as the name suggests is a vast complex comprising of approximately 90 different subunits which make up the four enzyme complexes and complex V of OXPHOS, with the mtDNA encoding 13 subunits and the rest encoded by nuclear DNA (nDNA) (Larsson and Clayton, 1995;Koopman et al., 2013). Together, the nDNA and mtDNA coordinate the synthesis of subunits that come together to form the individual complexes that comprise the ETC,

subsequently allowing the mitochondria to function as the core energy producer for cellular needs.

The human mitochondrial DNA is a 16.6kb pair, double-stranded circular genome containing 37 genes. These genes encode for: 13 subunits (**Figure 2.2.2.**) of the ETC and 24 genes involved in mtDNA translation (2 ribosomal RNAs (rRNAs) and 22 transfer RNAs (tRNAs)) (Larsson and Clayton, 1995;Graeber and Muller, 1998;Wallace, 1999;Taylor et al., 2001b;DiMauro and Schon, 2003;Koopman et al., 2013). The remainder of the mitochondrial ETC and associated assembly factor proteins, replication, transcription, translation, and regulatory proteins are encoded by the nDNA (**see Table 2.3.2.**) (Wallace, 1999;Iyer et al., 2009a). It is widely accepted that all mitochondrial organelles originated from an early endosymbiont event involving an α-protobacterium and a nucleus containing host cell (Gray et al., 1999;DiMauro and Schon, 2003;van Esveld and Huynen, 2018). During evolution, this early endosymbiotic relationship became so intertwined that these organisms became very dependent on one another thus requiring the streamlining of the genome of the protobacterium to create a more efficient organelle (Wallace, 1999;van Esveld and Huynen, 2018). The modern human mitochondria is a product of this evolutionary event; with the loss of some of the early protobacterium genes and insertion of other genes into the host's genome (van Esveld and Huynen, 2018). As a result, the ETC is under the control of two genomes. Therefore, mitochondrial genetics is governed by inheritance patterns, which are slightly different from Mendelian genetics.

During the electron transfer to molecular oxygen, reactive oxygen species (ROS) are generated by leakage of electrons in complex I and III causing oxidative stress to cells (Mitchell, 1961;Murphy, 2009;Nicholls and Ferguson, 2013). ETC defects occurring from mtDNA or nDNA mutations compromise membrane potential and ATP synthesis, and interruption of this pathway renders cells and tissues vulnerable under disease and oxidative stress conditions (Iyer et al.,

2012;Jain et al., 2016). Consequently, an error in either nDNA or mtDNA encoding for proteins that make up any of the subunits could result in disorder(s) of the ETC and the mitochondria. Advances in next-generation and whole-exome sequencing continue to reveal novel nDNA mutations involved in LS; with subsequent inheritance in an autosomal recessive or X-linked inheritance (vs. maternal) pattern. Owing to its ubiquitous role, the mitochondria are present in all human cells (except RBC), and their distribution and copy number vary from cell to cell. ETC defects impairing OXPHOS result in major pathological problems for energy-demanding cells and tissues such as those of the heart, brain, and muscles (Ruhoy and Saneto, 2014;Maglioni et al., 2020). Not surprisingly, many of the symptoms associated with LS and similar metabolic disorders affect the neuromuscular or cardiovascular systems (Leigh, 1951;Ruhoy and Saneto, 2014;Veerapandiyan et al., 2016). While it is widely accepted that both the nDNA and mtDNA contribute to the normal function of the mitochondrial ETC, the mechanism underlying cross-talk and communication between these genomes in the diseased state remains under investigation. While this review focuses largely on mitochondrial dysfunction resulting from pathogenic mutations affecting ETC enzymes, mutations resulting in defective mitochondrial translation machinery (Sweeney et al., 1994;Sue et al., 1999;Antonicka et al., 2003;Tucker et al., 2011;Cox et al., 2012;Ghezzi et al., 2012;Kopajtich et al., 2014;Suzuki and Suzuki, 2014;Tischner et al., 2015), non-ETC enzymes such as pyruvate dehydrogenase (Matthews et al., 1993;Finsterer, 2008;Patel et al., 2012), or cofactors (Gerards et al., 2013;Banka et al., 2014;Smith et al., 2018) can affect OXPHOS and also result in mitochondrial dysfunctions.

2.3.2. Mitochondrial genetics and heteroplasmy

Unlike Mendelian genetics, mtDNA inheritance follows some unique inheritance patterns. Maternal inheritance, heteroplasmy, and mitotic segregation are some of the traits that separate mitochondrial genetics from those of Mendelian genetics (Wallace, 1999;DiMauro and Schon, 2003). During normal human development, only the mtDNA from the mother is inherited by the

offspring (Wallace, 1999). Although there have been rare reports of mtDNA inheritance from the father, this is usually not the case; as mtDNA from the sperm are usually degraded through an unknown mechanism during fertilization (Sutovsky et al., 1999;Schwartz and Vissing, 2002). Therefore, a mother with mutant mtDNA will always pass this to her children and the daughter of this mother will pass this along to her offspring as well. This inheritance pattern termed maternal inheritance is largely involved in cases of maternally inherited mitochondrial disorders such as MILS (Maternally Inherited Leigh Syndrome).

Within a cell, there are hundreds of mitochondria, with each mitochondrion having multiple copies of mtDNA, and a cell comprising of thousands of copies of mtDNA (Wallace, 1999;DiMauro and Schon, 2003;Tachibana et al., 2009). In the first steps of human development, the mitochondria inherited by an individual are derived exclusively from the oocyte during fertilization. In healthy offspring, the inherited mitochondria will contain copies of the same wild-type mtDNA, referred to as homoplasmy. However, owing to its proximity to sites of reactive oxygen species (ROS) production in the mitochondrial matrix, and an error-prone polymerase, mtDNA has a very high mutation rate (Richter et al., 1988;Wallace, 1999;Shaughnessy et al., 2014). Initially, when a mutation occurs, cells will contain a mixture of wild-type and mutant mtDNA, a phenomenon referred to as heteroplasmy. Heteroplasmy can occur at both cellular (and tissue) and organelle levels, just as a cell can harbor mitochondria with wild-type and mutant mtDNA, this process can occur within a mitochondrion as well. Since mtDNA division does not coincide with nDNA division (Larsson and Clayton, 1995); a division of heteroplasmic cells that occurs by a process known as replicative/mitotic segregation, could invariably shift the mtDNA genotype of the daughter cells to those of the mutant or wild-type mtDNA, over many generations (Wallace, 1999). Therefore, heteroplasmy in combination with replicative segregation can shift the phenotype of a healthy cell to a diseased state. For a mutation to be pathogenic, however, the percentage of mutant mtDNA must exceed a threshold

such that oxidative metabolism is affected. If the percentage of mutant mtDNA continues to increase, this will consequently result in a gradual and continuous decrease in energy production until a bioenergetic threshold is reached (Wallace, 1999). Above this threshold, cellular needs cannot be met, invariably, resulting in disease phenotype which is usually characteristic of metabolic disorders such as LS. This phenomenon referred to as the threshold effect is responsible for the clinical signs and heterogeneity in disease penetrance observed in mitochondrial disorders. Tissues that are metabolically active and highly dependent on oxidative phosphorylation -such as the brain, heart, skeletal muscles, retina- tend to have a lower threshold; and are therefore more vulnerable and less tolerant to the pathogenic effects of mtDNA mutations (DiMauro and Schon, 2003).

The variation in copy number and stochastic nature of mitochondrial genetics results in a variable inheritance and expression pattern of heteroplasmic mutations; and largely contributes to the variability and spectrum of disease phenotype associated with LS. The genotype-phenotype relationship in LS patients is difficult to ascertain because different heteroplasmic loads exhibit different phenotypes. For example, *T8993G* (*T8993C*) mutation; a mutation that affects mt-DNA encoded ATP synthase 6 (ATPase 6) gene, when present in low abundance only results in NARP (neurogenic muscle weakness, ataxia, and retinitis pigmentosa), while a high abundance of the same mutation results in MILS (Maternally Inherited Leigh's Syndrome) with rapid lethalities (Iyer et al., 2012). Furthermore, there have been reports of mutations in OXPHOS genes encoded by nDNA presenting with similar phenotypes to those of mtDNA mutations; and cases of different genetic mutations resulting in the same diseased phenotype.

Table 2.3.2. The electron transport chain complexes (ETC) with subunits encoded by mitochondrial (mtDNA) and nuclear DNA (nDNA). Also included are the numbers of assembly subunits encoded by nDNA. Common mutations associated with each complex that causes Leigh's syndrome (LS) are highlighted.

Complexes	Structural Genes (mtDNA/ nDNA)	Assembly Factors	Most common LS Mutations	Affected Subunits	Proposed reason for dysfunction
Complex I (NADH:Ubuiquinone oxidoreductase)	7/37	11	*T10158C* (Ser34Pro), *T10191C* (Ser45Pro), *G10197A* (Ala47Thr)	MTND3	Mutations affect the transition of the active/deactivate state of the enzyme
			G13513A (Asp393Gly), *T12706C* (Phe124Leu)	MTND5	Disruption of proton translocation through this channel
Complex II (Succinate-coenzyme Q reductase)	0/4	2	*G1664A* (Gly555Glu)	SDHA*	This mutation affects an assembly factor, resulting in the production of an unstable enzyme
Complex III (Ubiquinol cytochrome C reductase)	1/10	2	*C208T* (Ser45Phe; UQCRB)	UQCRB (subunit VII)**	Mutation affect gene involved in oxygen sensing and enzyme maintenance
			C14792G (His16Asp)	MTCYB	Potentially affect enzyme's activity
Complex IV (Cytochrome c oxidase)	3/11	18	SURF1**, LRPPRC**, PET100**	COX assembly and biogenesis factors	These are factors involved in the assembly and biogenesis of COX subunits. These mutations would invariably affect the production and stabilization of the complex
Complex V (ATP synthase)	2/17	4	*T8993G* (Leu156Arg), *T8993C* (Leu156Pro)	MTATP6	Mutations are located close to the C-ring (f_o catalytic site). The T>G mutation is more severe than the T>C mutation. Most studies have concluded that these mutations result in less efficient coupling/defects in assembly and stability of the MTATP6 subunit. Some studies have also suggested block in proton translocation
			T9185C (Leu220Pro)	MTATP6	Mutation compromises the function of ATP synthase

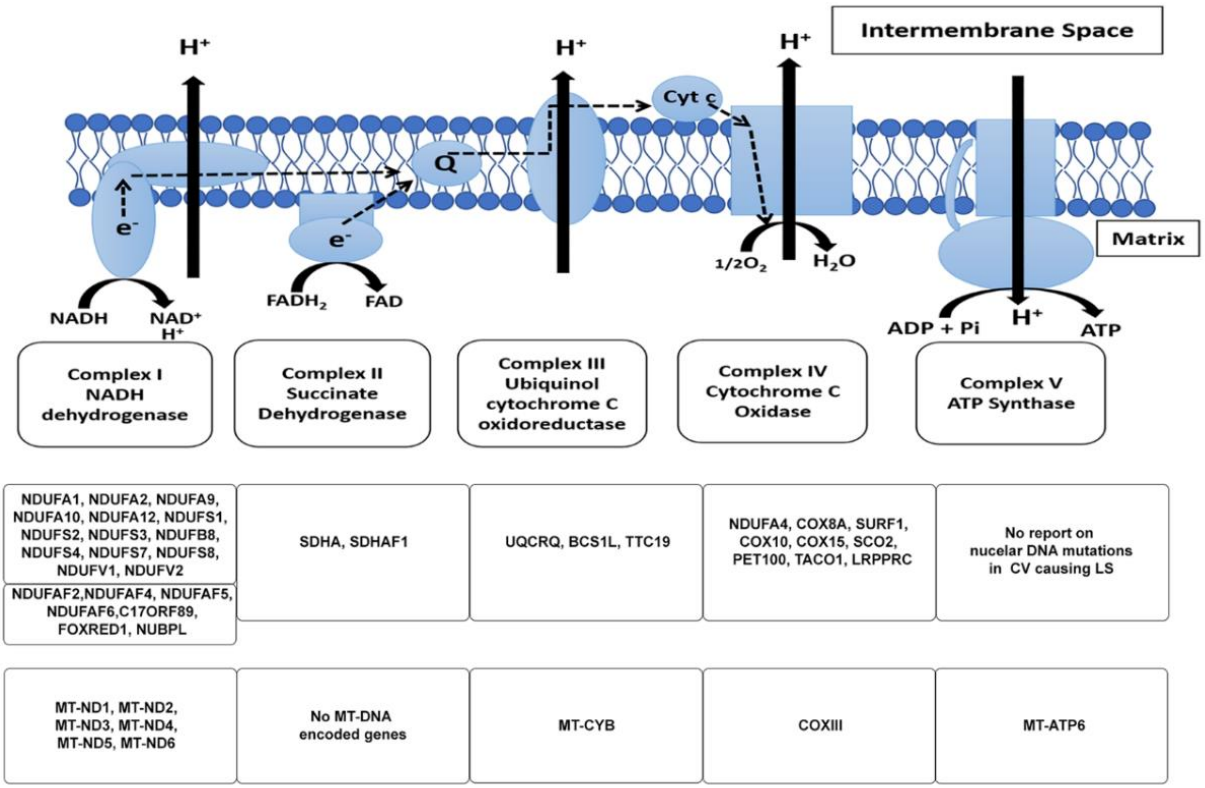

Figure 2.3.2. The mitochondrial electron transport chain. The subunits of the respiratory chain are encoded by nDNA and mtDNA. Mitochondria produce ATP via the OXPHOS pathway; a process that takes place at the inner mitochondrial membrane and involves the channeling of electrons through four-electron transport chain (ETC) complexes (Complex I-IV). The electron transport results in subsequent translocation of protons from the matrix into the intermembrane space, this proton gradient in combination with the inward-negative mitochondrial membrane potential drives the molecular motor, ATP synthase (complex V), to produce ATP. An impairment in the ETC or its assembly complexes results in metabolic malfunction in cells and tissues. The ETC is a vast complex comprising ~90 different subunits which make up the five enzyme complexes of OXPHOS. Of these subunits, mtDNA encodes 13 subunits while the nuclear DNA (nDNA) encodes ~77 subunits. Together, the nDNA and mtDNA coordinate the synthesis of subunits that come together to form the individual complexes that compose the ETC, subsequently allowing the mitochondria to function as the core energy producer for cellular needs. Specific genes encoded by nDNA and mtDNA in the context of LS are listed.

2.3.3. What is Leigh syndrome?

Mitochondrial (mt) disorders represent a large group of severe genetic disorders mainly impacting organ systems with high energy requirements (McFarland et al., 2010;Maglioni et al., 2020). These disorders are clinically complex, often fatal, and occur at an estimated ratio of 1 in

5,000 to 10,000 live births (Skladal et al., 2003;Schaefer et al., 2004). Leigh syndrome (LS) is a classic example of mitochondrial disorder resulting from pathogenic mutations that disrupt OXPHOS capacities. Although first described in 1951, it was not until 1968 when Hommes and colleagues described a case of a one-year-old patient that LS first became associated with defects in mitochondrial energy metabolism (Hommes et al., 1968). By 1983, multiple reports resulted in the first description of LS as a mitochondrial disease (Willems et al., 1977;van Erven et al., 1987;Hammans et al., 1991). During the early years after its initial description, its resemblance to Wernicke's encephalopathy (WE) led many to believe that LS resulted from an error in thiamine metabolism (Worsley et al., 1965;Baertling et al., 2014;Leigh et al., 2015). Many years after its first description, it was noted that some patients with LS presented with deficiencies in either the pyruvate decarboxylase (Evans, 1981) or pyruvate dehydrogenase complex (PDHc) (DeVivo et al., 1979). These variations in disease phenotype allude to the heterogeneous nature of LS.

During its initial description, the characterization of pathological hallmarks of LS was diagnosed postmortem by histopathological observations. However, advances in sequencing, biochemical, and imaging technologies have resulted in better antemortem diagnoses. Furthermore, in the last 15 years, these technologies have resulted in the identification of novel pathogenic mutations in LS patients, with more than 75 genes identified as monogenic causes of LS (Lake et al., 2016). Based on genetic analysis, LS can be inherited in any of these three patterns: maternal inheritance, autosomal recessive manner, and in very rare cases through X-linked transmission, as well as via de novo mutation and, evidence suggests, through complex heterozygosity. (Ruhoy and Saneto, 2014;Leigh et al., 2015;Lake et al., 2016).

2.3.4. Clinical presentations and diagnostic approaches for Leigh syndrome

As highlighted above LS is highly heterogenous, owing to many of the factors discussed previously. There is a continuous effort both in the clinical and scientific research fields to reconcile the relationship between the genetic and phenotypic presentations reported in patients with LS (**Figure 2.3.4.**). Various case reports have described some of the clinical symptoms of LS, however, because of how rare this disorder is, the small sample sizes in these reports restrict analytical studies (Uittenbogaard et al., 2018;Wei et al., 2018;Yu et al., 2018;Edwards et al., 2020). This makes its challenging to fully identify the most predominant symptoms in patients with LS. In recent years, however, efforts have been made to compile clinical information from various multi centers across Europe, Asia, the USA, and Australia (Sofou et al., 2014;Sofou et al., 2018;Ganetzky et al., 2019;Hayhurst et al., 2019;Hong et al., 2020;Ogawa et al., 2020;Stendel et al., 2020). These have allowed for metadata analysis and systemic retrospective studies to find unifying symptoms for LS.

Although LS shows clinical heterogeneity, the most prevalent symptoms that have been reported correlate with the involvement of brain regions such as the basal ganglia, brainstem, thalamus, and cerebellum (Yu et al., 2018;Chang et al., 2020). These regions of the brain control body movement, balance, and basic life functions like breathing, swallowing, and blood circulation (Chang et al., 2020). In most patients with LS, pathological lesions in one or more of these areas of the brain have been found in MRI (Magnetic Resonance Imaging) reports, contributing to observed clinical manifestations of LS (Baertling et al., 2014). It is worth noting that, while pathological lesions in basal ganglia and brainstem are considered the hallmarks of LS, there have been reports of cases where basal ganglia (Sonam et al., 2014) or brainstem lesions (Hayhurst et al., 2019) were not detected in patients with LS (Stendel et al., 2020). However, other neuropathological signs such as delayed myelination, cerebral atrophy, and cerebellar lesions were reported in these cases (Sonam et al., 2014;Chourasia et al.,

2017;Stendel et al., 2020). These findings suggest that LS can present primarily with pathological lesions in other regions of the brain and can predate other neuroimaging features that are considered hallmarks of LS. While these findings demonstrate the need to consider expanding the diagnostic criteria for LS on neuroimaging findings, they also highlight one of the limitations of neuroimaging as a diagnostic tool for LS. Neuroimaging findings need to be combined with other diagnostic tools such as biochemical, histopathological, and sequencing information to properly diagnose LS.

To date, the most common clinical features associated with LS are (**see Figure 2.3.4. for more details**): ataxia, hypotonia, developmental delay, seizures, poor feeding/feeding difficulties associated with dysphagia, failure to thrive, persistent vomiting, elevated serum or cerebrospinal fluid lactate levels, and abnormal ocular disturbances (Gerards et al., 2016;Lee et al., 2019b;Chang et al., 2020;Hong et al., 2020;Ogawa et al., 2020;Stendel et al., 2020). Aside from the neuromuscular and ocular abnormalities, abnormalities in other organ systems have also been reported in some cases (**Figure 2.3.4.**). During the course of the disease, some patients present with gastrointestinal and cardiac problems (Gerards et al., 2016;Sofou et al., 2018). In addition, respiratory distress has been reported to be a common clinical feature in patients with early-onset LS- before the age of 2 (Yu et al., 2018). Recent reports have suggested that certain clinical features are more common in early-onset cases than in late-onset cases of LS. In a study performed in Korea to distinguish clinical features of early and late-onset LS, they found that delayed developmental development was significantly higher in the early-onset (before 2years old) compared to the late-onset (after 2years old) groups. While motor weakness and ataxia were predominant in the late-onset group relative to the early-onset LS patients (Yu et al., 2018;Hong et al., 2020). Further, the onset of disease could also dictate what type of seizures patients present with (focal or generalized seizures) (Wei et al., 2018). The presence of pathological signs at birth and history of epileptic seizures have been strongly

associated with poor prognosis (Sofou et al., 2014;Hong et al., 2020). Because LS induces alteration in mitochondrial activities, many biochemical findings focus on lactic acid levels in serum and cerebrospinal fluid (CSF). However, conflicting reports on lactate levels have been reported, there are some reports of high serum and CSF lactate in LS patients (Sofou et al., 2014;Uittenbogaard et al., 2018;Edwards et al., 2020). While serum and CSF lactate levels are normal in some other patients (Gerards et al., 2016). New evidence suggests that elevated lactate levels could also be associated with disease onset. Elevated lactate in CSF was more common and significantly correlated to a more severe disease course and associated with patients with early-onset (before 6-months) (Sofou et al., 2014;Yu et al., 2018). Therefore, instead of using lactate levels as a diagnosis for LS as previously suggested (Rahman et al., 1996), it could serve as a prognosis to determine the severity of the disease in patients.

Histopathological findings with muscle biopsies have been another source of controversy in defining clinical features of LS. While positive muscle biopsy findings such as COX, SDH deficiency (Sonam et al., 2014), ragged red fibers (RRF), and atrophy of muscle fibers (Sofou et al., 2014) have been used as a diagnosis for LS, nonspecific myopathic changes and negative findings have also been reported in patients with LS (Wei et al., 2018). Furthermore, findings such as RRF are associated with another mitochondria disorder, myoclonic epilepsy with ragged red fibers (MERRF). Finally, biochemical findings highlighting deficiencies in respiratory chain complexes, while important in LS diagnosis have also been inconsistent (Ganetzky et al., 2019;Ogawa et al., 2020). As stated earlier, these observations highlight the need to combine findings from various diagnostic tools including genetic findings for proper diagnosis of LS.

Although the clinical presentations of LS are heterogenous, the collaborative efforts resulting in the collation of clinical data from various sources and the resulting extensive meta-data analysis have provided us valuable information on the most common clinical features associated with LS (**Figure 2.3.4.**). Most importantly, we are beginning to understand the

mutations most involved in specific clinical features and the association between these features and patient survival. For example, in one study, patients with NDUF mutations had a prevalence of early cerebral cortex abnormalities, high occurrence of cardiac and ocular manifestations relative to other LS patients. In the same study, patients with the mtDNA mutation *T8993G* had more severe clinical and radiological manifestations and poorer disease outcomes compared to those with the *T8993C* variant (Sofou et al., 2018). Another study showed that SURF1 deficiency has a more favorable survival outcome (Wedatilake et al., 2013;Sofou et al., 2014). These suggest that certain clinical manifestations and phenotypes might be shared among LS patients with similar mutations and that some mutations have milder disease progression. A better understanding of the genotype and phenotype relationship involved in LS could help with better diagnosis and early treatment of the disease, subsequently resulting in prolonging the lives of patients with LS. As highlighted above, there have been discrepancies in some of the neuroimaging, histopathological, and biochemical findings reported for patients. Some of these differences could potentially result from variability associated with the stage of the disease. As mentioned, some clinical presentations are more prevalent in early-onset compared to late-onset LS patients vice versa. Therefore, the discrepancies recorded could be associated with the progression of the disease. Future longitudinal studies exploring changes in clinical presentation in various cohorts of LS patients could prove invaluable in solving this problem. Since LS is rare, and most patients with the disorder have to be under close supervision, it is difficult to have a controlled study with very large population size. Furthermore, because there are no standardized ways of diagnosing the disorder, the same tests are not performed for every patient, this further confounds our ability to make connections between the clinical presentations and genetic mutations. However, the current approach by the multi-centers will continue to add to our understanding of the disorder. It will be beneficial to understand the effects that different mitochondrial haplotypes have on clinical presentations as well. For instance, it has been reported that environmental factors and polymorphism in mtDNA

haplogroups J1c and J2c are associated with increased penetrance of LHON (Leber's hereditary optic neuropathy) (Carelli et al., 2006).

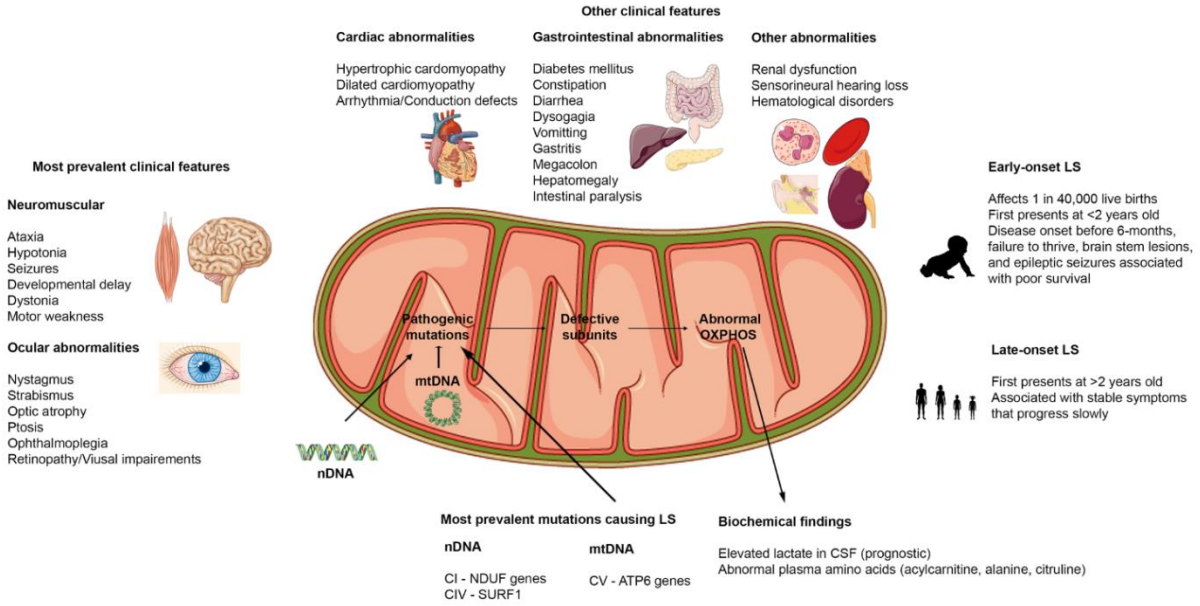

Figure 2.3.4. Clinical features of Leigh syndrome. Figure showing the various clinical features associated with LS. The most prevalent clinical features affect the brain, muscles, and eyes. Other clinical findings include dysfunctions in cardiovascular, gastrointestinal, renal, auditory, and hematological systems. LS can present as early-onset or late-onset with abnormalities in at least three of the organ systems highlighted. LS results from pathogenic mutations in either the nDNA or mtDNA that causes abnormalities in the OXPHOS capacities of the mitochondria. Hence, biochemical findings reflect these defects.

2.4. Factors influencing Leigh syndrome

As previously described, LS results from mutations that cause perturbation to the ETC. Once the ETC becomes overburdened and dysfunction in oxidative processes in the mitochondria persist, various pathogenic processes are initiated (**Figure 2.3.4.**). As a hub for oxygen and electron-rich compounds, perturbation to the flow of electrons and protons could invariably result in reactive oxygen species and superoxide formation. Consequently, leading to the initiation of stress and inflammatory responses, chronic forms of these responses could result in cell death, culminating in the development of the symptoms associated with LS. In this

section, we introduce the ETC and how defects in any of these complexes contribute to LS pathology. We focus largely on the ETC defects resulting from mtDNA mutations that have been reported to be involved in most cases of LS to date. We end this section with a summary of other deficiencies caused by nuclear-encoded genes, not related to ETC enzymes that have also been reported in patients with LS.

2.4.1. Complex I

Complex I also known as NADH:Ubiquinone oxidoreductase (**Figure 2.3.2.**), is the first component and largest complex of the mitochondrial ETC, comprising more than 45 subunits (Sarzi et al., 2007;Nesbitt et al., 2012). The mtDNA encodes only 7 (MTND1-MTND6, MTND4L) of these subunits, while nDNA encodes the remaining structural and assembly factor subunits (Sarzi et al., 2007) **(Table 2.3.2.)**. This enzyme oxidizes NADH (Nicotinamide Adenine Dinucleotide) -produced through glycolysis, the Krebs cycle, and β-oxidation- to reduce ubiquinone (Q); the energy from this redox reaction is coupled to proton translocation across the mitochondrial inner membrane (Sarzi et al., 2007;Nesbitt et al., 2012;Babot and Galkin, 2013;Babot et al., 2014). Owing to its size and location in the OXPHOS pathway, a complex I defect could result in severe respiratory chain dysfunction and has been reported to account for most cases of LS (Kirby et al., 2003). Complex I deficiency can present at any age, with symptoms ranging from isolated myopathy or liver disease to multisystemic disorders (Werner et al., 2009).

To date, approximately 14 nDNA genes encoding for both structural and biogenesis/assembly factor subunits of complex I (**Supplementary Table 7.3.1.**) have been implicated in the etiology of LS (Berger et al., 2008;Koopman et al., 2013). Only three mtDNA genes (*MTND2*, *MTND3*, *MTND5*), however, have been reported to be largely involved in LS, with *MTND3* and *MTND5* mutations being the most prevalent of all three mtDNA mutations

reported thus far. While these mutations are the most common, there have also been isolated reports of patients with *MTND1*, *MTND4*, and *MTND6* mutations resulting in LS or Leigh-like syndrome, albeit, in very rare cases (McFarland et al., 2004). Some of the most recurrent structural subunit mutations which have been reported to contribute to LS include *T10158C* (McFarland et al., 2004), *T10191C* (Taylor et al., 2001a), and *G10197A* (Sarzi et al., 2007) in the *MTND3* gene; *T12706C* (Taylor et al., 2002), *G13513A* (Chol et al., 2003), and *A13514G* (Corona et al., 2001) in the *MTND5* gene; and *G14459A* (Kirby et al., 2000), and *T14487C* (Ugalde et al., 2003) in the *MTND6* gene (**Supplementary Table 7.3.2.**).

Both *T10158C*, and *T10191C* mutations result in amino acid substitutions of a polar serine residue for a hydrophobic proline residue at codons 34 and 45 of the *MTND3* genes respectively. The third mutation, *G10197A* results in a substitution of a hydrophobic alanine residue for a polar threonine residue at codon 47 of the *MTND3* gene (McFarland et al., 2004;Sarzi et al., 2007). Structural analysis of the MTND3 subunit suggests that all of these mutations reside in the transmembrane domain of the *MTND3* gene which projects into the mitochondrial matrix (Sarzi et al., 2007). The location of these mutations suggests that they either act to cause dysregulation in complex I assembly or reduce the enzymatic activity of the enzyme. Studies strongly suggest that, although *T10158C*, and *T10191C* mutations moderately reduced complex I assembly, the decrease is almost negligible when compared to the drastic reduction in enzyme activity of the complex in these mutants (McFarland et al., 2004), thus suggesting that *MTND3* mutations could result in LS through a decrease in the enzymatic activity of complex I.

Studies have reported LS cases resulting from mutations in *G13513A* and *T12706C* of the *MTND5* genes associated with complex I (Kirby et al., 2003). Although it has been reported that disease phenotype only presents in tissues such as muscle and brain at high mutant loads (typically above 90%) for most pathogenic mutations, the *MTND5* gene mutation can result in

diseased phenotype at low mutant loads even below 50% (Kirby et al., 2003). This could potentially be a result of very low heteroplasmy; alternatively, the origin (fibroblast) of the cells used in this analysis could potentially explain this observation. Immunoprecipitation studies allude to MTND5 subunit as being located peripherally in complex I and have been suggested to be the last subunit to be assembled into the complex. Further, the MTND5 synthesis is believed to be a rate-limiting step for the activity of complex I (Liolitsa et al., 2003). Therefore, the MTND5 subunit is a key regulator of complex I assembly and stability, consequently is a key modulator of cellular respiration. Taken together, this could explain why a mutation in MTND5 subunits at lower mutant load could result in severe cases of LS and other complex I related disorders such as MELAS (mitochondrial encephalomyopathy with lactic acidosis and stroke-like episodes) or LHON (Leber's hereditary optic neuropathy).

Given the importance of Complex I in the OxPhos pathway, any mutation that affects its function could gravely perturb the ETC, resulting in decreased ATP synthesis and increased production of ROS and other reactive species. These effects result in a vicious cycle that results in mitochondrial degradation and subsequent cell and tissue death. Studies have suggested that complex I activity has to be reduced by more than 70% before oxygen consumption or ATP production is perturbed (Sarzi et al., 2007), indicating that a high percentage of mutant mtDNA must be present for biochemical or clinical manifestation of disease. However, as mentioned previously, the location of the mutation could determine what percentage of mutant load would result in a diseased phenotype. For example, *MTND3* mutation requires a higher mutant load (greater than 80%) to result in LS phenotype, while *MTND5* mutation could result in LS phenotype at mutant load as low as 50%. Aside from mutation threshold, factors such as additional genetic factors, cell cycle (mitotic cells vs non-mitotic cells), can influence the expression of complex I deficiency (Sarzi et al., 2007). It is worth noting that recent findings from interventional studies have shown improvement in bioenergetics functions without rescuing ETC

defects. Intervention strategies such as those targeting NAD+ metabolism, or mTOR inhibition have alleviated mitochondrial disease in some models of LS and related mitochondrial disorders (Johnson et al., 2013;Lee et al., 2019a;Cheema et al., 2021). These findings again allude to the complexity associated with studying mitochondrial disorders.

2.4.2. Complex II

Complex II, also known as succinate-coenzyme Q reductase, is the smallest of the ETC complexes with all four subunits (Succinate dehydrogenase subunits A to D; SDHA-D) being nuclear-encoded (**Table 2.3.2.**) (Ruhoy and Saneto, 2014). Located in the inner membrane of the mitochondria, this complex participates in both the citric acid cycle and ETC. The largest catalytic subunit, SDHA oxidizes succinate and couples this to the reduction of its flavine cofactor, FAD; while the other catalytic subunit, SDHB shuttles electrons to ubiquinone in a concerted manner (Renkema et al., 2015). Mutations in complex II account for a very small portion of OxPhos disorders, as dysfunction in this complex, is very rare (Pagnamenta et al., 2006;Ohlenbusch et al., 2012;Jain-Ghai et al., 2013;Renkema et al., 2015). More than 10 different autosomal-recessive pathogenic mutations in SDHA have been reported to cause LS, Leigh's-like, and other related mitochondrial disorders, while mutations in SDHAF1 (a complex II assembly factor), SDHB, and SDHD have also been reported to cause LS or LS-like symptoms (**Supplementary Table 7.3.1.**). However, there is still no report of SDHC involvement in the etiology of LS (Renkema et al., 2015). Although clinical phenotype and MRI findings have been used to describe LS or LS-like symptoms in patients with complex II defects, some of the patients presented with other symptoms that were not characteristics of LS (Jain-Ghai et al., 2013). For instance, a case of mild LS was reported to be caused by homozygous *G555E* mutation in the SDHA subunit of complex II; whereas, this same mutation has been reported to be responsible for cases of lethal-infantile presentations of mitochondrial complex II defects (Pagnamenta et al., 2006). While it is typical to observe phenotypic heterogeneity in

heteroplasmic mutations of mtDNA, this is atypical of a nuclear mutation. This observation alludes to the heterogeneous nature of this disease that contributes to its complexity, thus making it difficult to completely understand its etiology.

2.4.3. Complex III

Mitochondrial complex III, also known as ubiquinol cytochrome c reductase (**Figure 2.3.2.**), is located within the mitochondrial inner membrane where it catalyzes the transfer of electrons from succinate and NADH dehydrogenases to cytochrome *c* (de Lonlay et al., 2001;Barel et al., 2008). Further, energy from this electron transfer is used in the translocation of a proton across the inner membrane, contributing to the proton gradient required for OXPHOS. Complex III consists of 11 structural subunits (**Table 2.3.2.**) with only one of these subunits, cytochrome *b* (*MTCYB*), encoded by the mtDNA. Isolated mitochondrial complex III deficiencies are rare and present with heterogeneous clinical symptoms characteristic of LS. In a clinical report of a 15-month-old female LS patient of European descent, two homoplasmic mutations involving *C14792G* and *G14459A* was reported that resulted in p.His16Asp change in *MTCYB* and p.Ala72Val substitution in the ND6 subunit, respectively (Ronchi et al., 2011). Interestingly, the mother of this patient (normal) was homoplasmic for the *C14792G* mutation (*MTCYB*) but heteroplasmic for the *G14459A* mutation. This suggests that the *ND6* mutation and not the *MTCYB* mutation is involved in the LS pathology in this patient. While mutations in nuclear-encoded proteins of complex III have been reported to be involved in LS pathology (**Supplementary Table 7.3.1.**), most pathological cases of *MTCYB* mutations (**Supplementary Table 7.3.2.)** result in skeletal muscle weakness, exercise intolerance, and in some cases sporadic myopathy-rhabdomyolysis associated with ragged-red fibers (Barel et al., 2008).

While various pathogenic mutations in the gene encoding cytochrome *b* (*MTCYB*) have been reported, mutations in nDNA have only been reported in three genes to date: the *BCS1L*,

TTC19, and the *UQCRB* gene (ubiquinol-cytochrome *c* reductase binding protein) (Barel et al., 2008). Both *BCS1L* and *TTC19* genes encode assembly factor proteins of complex III, with the *BCS1L* gene encoding for a complex III assembly factor (de Lonlay et al., 2001), while *TTC19* encoding for tetratricopeptide 19, a protein embedded in the inner mitochondrial membrane (Atwal, 2014). The *UQCRB* gene encodes subunit VI (chromosome 8q22) of complex III, while another study described a large consanguineous inbred Israeli Bedouib kindred with a mutation in the *UQCRQ* gene, which resulted in a *C208T* mutation in exon2 of the subunit (Barel et al., 2008). This mutation resulted in a substitution of serine for phenylalanine at position 45 (p.Ser45Phe) in the encoded protein, UQCRQ, complex III subunit VII and resulted in LS-like symptoms. In addition to decreased activity of complex III, the activity of complex I was also decreased in these patients, a common observation because of the structural interdependence of complex I and complex III. While *TTC19* mutations are rare, *BCS1L* constitutes most cases of LS associated with nDNA mutations(Atwal, 2014). As has been alluded to previously, both isolated complex III and combined complex I and III deficiencies can contribute to LS pathology. Thus, future work needs to focus on understanding supercomplex assembly and dysregulation in this assembly as it relates to LS.

2.4.4. Complex IV

Also referred to as cytochrome c oxidase (COX), complex IV is the terminal enzyme of the mitochondrial ETC (**Figure 2.3.2.**); and is embedded in the inner mitochondrial membrane where it catalyzes the transfer of electrons from reduced cytochrome c to molecular oxygen (Antonicka et al., 2003;Bohm et al., 2006). In humans, COX is a multimeric protein composed of 13 subunits with 3 encoded by the mtDNA (*MTCOX1-3*) and form the catalytic subunits of the enzyme, while the other 10 are nuclear-encoded and contribute to the assembly and biogenesis of the complex (Antonicka et al., 2003).

While isolated cases of COX deficiencies owing to mtDNA mutations have been reported (**Supplementary Table 7.3.2.**), mutations in nuclear-encoded genes have been reported as the most common cause of Complex IV deficiency (**Supplementary Table 7.3.1.**). Approximately 15% of LS cases worldwide are attributed to isolated COX deficiency, with mutations in the SURF1 gene accounting for at least a third of these cases (Li et al., 2018). Mutations in other nuclear genes such as *Sco1*(Mourier et al., 2014), *Sco2* (Joost et al., 2010), *Cox10* (Antonicka et al., 2003), Cox15 (Mourier et al., 2014), LRPPRC (Rolland et al., 2013;Mourier et al., 2014), *TACO1*(Weraarpachai et al., 2009), *PET100* (Lim et al., 2014), *C12orf65* (Wesolowska et al., 2015), which play important roles in COX assembly and biogenesis, have all been implicated in LS pathology.

The *LRPPRC* mutation is one of the most studied founder mutations, which affects the leucine-rich pentatricopeptide repeat domain protein (LRPPRC), involved in post-transcriptional regulation of mitochondrial gene expression (Olahova et al., 2015). This specific mutation is found to be prevalent and unique to the French-Canadian population in the Saguenay-Lac-Saint-Jean region of Quebec. In one of the largest known cohort patient studies, the result showed that 55 of the 56 patients were homozygous for *A354V* mutation in the *LRPPRC* gene and presented with LS or stroke-like episodes. Compared to *SURF1* mutations, *LRPPRC* mutation resulted in a distinct occurrence of a metabolic crisis, consequently resulting in earlier and higher mortality (Mourier et al., 2014).

SURF1 mutation is the other most studied COX deficiencies resulting in LS and other metabolic disorders. Surf1 is an assembly factor of complex IV and is a member of the Surfeit locus protein localized in the mitochondrial inner membrane with multiple transmembrane domains. Although the loss of *SURF1* function has been shown to result in a considerable decrease in complex IV assembly, it does not result in complete loss of the assembly, suggesting that it is important but not indispensable. A recent study reported a case of *SURF1*

mutation associated with LS in the Chinese population with data suggesting the presence of a mutation spectrum and the likelihood of the spectrum being population specific. The specificity of this mutation in Chinese populations related to the presence of more frameshift and nonsense mutations in this gene compared to point mutations noticed in other populations (Li et al., 2018).

Other rare mutations in assembly proteins of COX have been described. For example, eight Australian families with Lebanese ancestry diagnosed with LS or LS-like encephalopathy associated with COX deficiency had mutations in the *PET100* gene (Lim et al., 2014). This mutation resulted in a similar, yet distinct clinical presentation to those of SURF1 LS from patients with Lebanese ancestry. While the exact function of this gene is still unknown, this points to *PET100* as being another case of the founder's mutation. While the SURF1 and LRPPRC seem to retain a homogenous phenotypic presentation in LS, our knowledge of the functions of these and other assembly/biogenesis proteins is still lacking. Therefore, it is still very unclear the specific role of each of these genes in the etiology of LS.

2.4.5. Complex V

A multi-subunit complex, with a molecular mass of approximately 550kDa, the mitochondrial ATP synthase, or complex V (**Figure 2.3.2.**) is the terminal complex of the OxPhos pathway (Kucharczyk et al., 2009b). The ATP synthase has both a hydrophobic domain (F_o), embedded in the mitochondrial inner membrane, and a hydrophilic ATPase domain (F_1), which resides in the matrix. The mitochondrial complex V uses a proton gradient generated by the other ETC complexes (I, III, and IV) to drive the catalytic conversion of ADP (Adenosine diphosphate), and inorganic phosphate (P_i) into ATP (Adenosine triphosphate). In humans, the complex is composed of 19 structural subunits, 2 of which are encoded by mtDNA, the other 17 encoded

by nDNA. Mutations in either of the nuclear or mitochondrial encoded genes could contribute to the dysfunction of this complex, consequently resulting in decreased ATP synthesis.

Although nDNA or mtDNA mutations could affect the functions of complex V (**Supplementary Table 7.3.1.**), mutations in the *MTATP6* gene seem to be the most prevalent pathological cause of LS related to complex V deficiency (**Supplementary Table 7.3.2.**). The *MTATP6* gene is one of the two mtDNA genes that encode proteins forming part of the F_o domain of complex V, with the most common mutation being a point mutation at nucleotide position 8993. Two-point mutations in this specific nucleotide position, *T8993G* and *T8993C* which result in substitution of a highly conserved Leucine156 (Leu) residue for Arginine (Arg) and Proline (Pro) residues respectively have been associated with complex V deficiency (Uziel et al., 1997;Baracca et al., 2007;Debray et al., 2007). Interestingly, the *T8993C* mutation has a milder diseased phenotype compared to the *T8993G* mutation. The *T8993C* mutation, even at a very high mutant load of 94% results in mild cases of NARP while the *T8993G* result in more severe cases of Maternally Inherited Leigh's Syndrome (MILS) (Santorelli et al., 1993). Furthermore, the *T8993C* mutation has been reported to result in late-onset manifestation and slower disease progression. The relative severity of *T8993G* compared to *T8993C* could potentially be attributed to the amino acid substitutions of each mutation. The *T8993C* mutation results in non-polar amino acid, Leu being substituted with another non-polar amino acid, Pro; while the *T8993G* mutation results in substitution of non-polar amino acid for a charged (basic) amino acid, Arg. The change in polarity and introduction of a charged amino acid could result in greater destabilization in the catalytic site of the ATP synthase where this mutation occurs (Kucharczyk et al., 2009a). Further, increased ROS and Superoxide Dismutase (SOD) production by *T8993C* mutants and significantly higher membrane potential in *T8993G* mutants could serve as compensatory mechanisms employed in these mutations, thus serving to explain the varying phenotypes observed between the two mutations (Baracca et al., 2007). However,

other research groups have reported that while both mutations affect cellular energetics and result in varying diseased phenotypes, ATP-synthesis in cells with either of these mutations is not extremely diminished (Pallotti et al., 2004;Baracca et al., 2007). These observations demonstrate that the bioenergetic defect is unlikely to be the main reason for disease pathogenesis with the need for more studies to elucidate the mechanism of disease pathology associated with these mutations.

Another mutation at nucleotide position 9185 of the *MTATP6* gene has been reported to be involved in LS. The *T9185C* results in a substitution of Leu220 for proline and is believed to interfere with the proton pump. Similar to the *T8993G* mutations, lymphoblast studies did not show abnormality in ATP synthesis. The reason for the onset of LS in individuals carrying this mutation is unknown; however, disease onset and exacerbation in *T9185C* cases correspond to febrile viral-like illness or infection (Saneto and Singh, 2010;Piekutowska-Abramczuk et al., 2018). In one case, hypoxia treatment reversed LS in a patient carrying this disorder while the brother of this patient with 100% mutated mtDNA for *T9185C* mutation did not present with NARP/MILS (Piekutowska-Abramczuk et al., 2018). In this specific case, it was postulated that hypocapnia and respiratory alkalosis as a result of hyperventilation could potentially contribute to LS and hypoxia treatment was a recommended therapeutic option to reverse disease symptoms (Piekutowska-Abramczuk et al., 2018). However, these studies could not fully elucidate the mechanism of LS disease pathology due to the very small sample size. Therefore, more extensive studies need to be performed to better understand the role of this mutation in disease etiology.

2.4.6. Other deficiencies involved in LS

Besides deficiencies in the ETC and ATPsyntase enzymes, pathogenic mutations in gene encoding proteins essential for the maintenance of the integrity of the mitochondria have also

been reported to cause LS (Lebon et al., 2007;Ghezzi et al., 2009;Fassone et al., 2010;Debray et al., 2011;Gerards et al., 2013;Baertling et al., 2017;Smith et al., 2018). Genes encoding proteins needed for assembly of OXPHOS enzymes, expression, and maintenance of mtDNA, cofactor biosynthesis, mitochondrial quality control and dynamics, and pyruvate dehydrogenase, and vitamin transport have all been implicated in LS (El-Hattab et al., 1993;Rahman and Thorburn, 1993;Benit et al., 2001;de Lonlay et al., 2001;Antonicka et al., 2003;Calvo et al., 2010;Tucker et al., 2011;Patel et al., 2012;Atwal, 2014;Smith et al., 2018). Many of the genes involved in these processes are nuclear-encoded, as described previously. Likewise, mutation to any of the mtDNA genes encoding the rRNAs and tRNAs involved in protein synthesis in the mitochondria can have a dire effect on the structural and functional integrity of the mitochondria.

Historically, the mutation in a subunit of the pyruvate dehydrogenase complex (PDHc) was one of the first observations recorded in cases of LS patients (DeVivo et al., 1979). In a review of 371 patients with a spectrum of PDHc deficiency, LS was described in 50 of these patients (Patel et al., 2012). The PDHc is a multi-subunit enzyme that is involved in the conversion of pyruvate into acetyl-CoA, an important substrate of the TCA cycle. As such it connects the glycolytic pathway with the oxidative pathway of the TCA cycle (Patel and Korotchkina, 2006). Therefore, mutations affecting any of its subunits can result in disruption to mitochondrial respiration and result in reliance on the glycolytic pathway for the production of ATP. Pathogenic mutations in the *PDHA1* gene have been reported as the most common PDHc deficiency involved in LS (Quintana et al., 2009;Patel et al., 2012).

Aside from PDHc, errors in thiamine metabolism were also considered one of the causes of LS when it was first described. During the early years after its initial description, its resemblance to Wernicke's encephalopathy (WE) led many to believe that LS resulted from an error in thiamine metabolism (Worsley et al., 1965;Baertling et al., 2014;Leigh et al., 2015). Many years after its first description, it was noted that some patients with LS presented with

deficiencies in either the pyruvate decarboxylase (Evans, 1981) or pyruvate dehydrogenase complex (PDHc) (DeVivo et al., 1979). This is because thiamine (vitamin B1) is a cofactor used by a lot of enzymes involved in cellular metabolism (Brown, 2014). Thiamine is transported into the cell by two transporters, THTR1 and THTR2. In the cytosol, thiamine gets converted into its active form, thiamine pyrophosphate (TPP) (Brown, 2014). TPP serves as an essential cofactor for enzymes such as transketolase, PDHc, alpha-ketoglutarate dehydrogenase, and several other enzymes involved in various metabolic pathways (Brown, 2014;Gerards et al., 2016). Mutations in *TPK1* (thiamine pyrophosphokinase) (Banka et al., 2014), *SLC25A19*, and *SLC19A3* (Gerards et al., 2013;Ortigoza-Escobar et al., 2014;Ortigoza-Escobar et al., 2016) have all been implicated as the most common cause of LS resulting from thiamine deficiency. The TPK1 is involved in conversion of thiamine into its active form in the cytosol, while SLC19A3 encodes the gene for one of the thiamine transporters (THTR2). Suggesting that mutations that affect the transport or metabolism of thiamine can result in dysfunction of mitochondrial energetics.

Other mutations have been reported to be involved in LS as well. Mutations resulting in defects to mitochondrial gene expression can also cause LS. Mutations in genes encoding translation machinery such as tRNAs and mitochondrial housekeeping have been reported. These include mutations in the mtDNA encoded tRNA *MTT1*(Cox et al., 2012), a mutation in catalytic subunits of the DNA polymerase gamma (POLG), and several nuclear-encoded translation factors (Antonicka et al., 2003;Valente et al., 2007;Tucker et al., 2011;Ahola et al., 2014;Schwartzentruber et al., 2014). Mutations in nuclear genes encoding structural and assembly subunits (**Supplementary Table 7.3.1.**) of ETC enzymes have also been described. The most common of these are mutations in the *NDUF* (Budde et al., 2000;Bugiani et al., 2004;Hoefs et al., 2008;Tuppen et al., 2010a;Hoefs et al., 2011;Uehara et al., 2014;Lou et al., 2018;Sofou et al., 2018) and *SURF1* (Tiranti et al., 1999;Sonam et al., 2014;Li et al.,

2018)genes. Mutations in nuclear genes resulting in CI or CIV deficiencies (**Supplementary Table 7.3.1.**) account for a large percentage of the nuclear mutations associated with LS (Koene et al., 2012;Gerards et al., 2016). Advances in whole-genome and exome technology continue to result in the identification of isolated and multiple complex deficiencies that contribute to LS.

2.5. Disease models for LS

Owing to the difficulty of manipulating the mammalian mitochondrial genome and the paucity of animal models, several model organisms have been developed over the years to study mitochondrial-related disorders. Some of these models include organisms like yeasts (Srivastava et al., 2018), fruitflies (Scialo et al., 2016), and worms (Lin and Wang, 2017). Much of the structure of the mitochondrial ETC complexes were first determined through crystallization studies using yeast as the model organism (Srivastava et al., 2018). Therefore, it is important to highlight how these models have proven to be invaluable in our quest to understanding mitochondrial disorders such as LS. The following section discusses some of the breakthroughs that have been recorded using the current models. Furthermore, the limitations of each of these models are briefly discussed to accentuate the importance of developing an appropriate disease model for studies of LS and related mitochondrial disorders.

2.5.1. Yeast

Saccharomyces cerevisiae is the most widely used organism for studying mitochondrial genetic disorders (Tuppen et al., 2010b), largely in part to the structural similarity between yeast mt-tRNAs and the possibility of transforming yeast to construct various mitochondrial mutations (Ahlers et al., 2000;Feuermann et al., 2003;Tuppen et al., 2010b). Furthermore, the ability of *S. cerevisiae* to survive in the complete absence of functional mtDNA makes it an attractive model for studying severe mitochondrial defects (Tuppen et al., 2010b;Ceccatelli Berti et al., 2021;di

Punzio et al., 2021). Yeast models have been employed in investigating various mitochondrial tRNA mutations (De Luca et al., 2006;Montanari et al., 2008) involved in MELAS (mitochondrial myopathy, encephalopathy lactic acidosis and stroke-like episodes) (Feuermann et al., 2003), MERRF (myoclonic epilepsy and ragged red fibers), CPEO (chronic progressive external ophthalmoplegia) (Rohou et al., 2001) and other related myopathies. Yeast has also been used to characterize and model the m.*T8993C* mutations which are a common cause of NARP and MILS (Tuppen et al., 2010b). Early studies on caloric restrictions and longevity in *S. cerevisiae* resulted in the discovery that caloric restriction extends lifespan in yeast (Jiang et al., 2000;Lin et al., 2000;Schleit et al., 2013). It was these findings that paved the way for the use of mTOR inhibitors as potential therapies for mitochondrial disease (Johnson et al., 2013;Sage-Schwaede et al., 2019;Cheema et al., 2021).

Although this model has been instrumental in better understanding various mitochondrial-related disorders, marked evolutionary distance between yeast and humans does not allow for conclusive information about the impact of these defects on tissues and organs. Furthermore, fermentative yeast such as *S. cerevisiae* lack complex I, making it impossible to model one of the most common causes of a mitochondrial disorder. The introduction of an alternative model, the obligate aerobic yeast, *Yarrowia lipolytica*, however, could potentially resolve this problem. *Y. lipolytica* possesses a vital proton-pumping NADH:ubiquinone oxidoreductase, making it possible to study the structure and function of complex I in health and disease. In this model system, three missense mutations in nuclear-coded subunits homologous to bovine TYKY (NDUFS8) and PSST (NDUFS7) of the mitochondrial complex I was developed to understand the function of these subunits (Ahlers et al., 2000); and led to conclusions that NDUFS8 and NDUFS7 might be involved in proton translocation by complex I. While this model solves the problem associated with a lack of complex I in *S. cerevisiae*, it still does not address the variation in homology and evolutionary distance between yeast and humans. Therefore, the

yeast model is still not able to answer all the questions regarding mechanisms of disease pathology in various mitochondrial-related disorders.

2.5.2. Worm

The nematode, *Caenorhabditis elegans* (*C. elegans*) is another model organism that has been used for studying LS. *C. elegans* are simple multicellular organisms with only 959 cells, organized into gastrointestinal, reproductive, muscle, nerve, and cuticle tissues. The genome of *C. elegans* has been fully sequenced and it is known to share greater than 83% homology with the human genome (Lai et al., 2000;Maglioni et al., 2020). The transparency of the worm and its small size makes it easier to directly visualize cellular processes and manipulate their genes to model various human diseases (Kuwabara and O'Neil, 2001;Maglioni et al., 2020). Furthermore, the complete outline of the neurons and synaptic connectivities in *C. elegans* have been determined, making it ideal for studying neurodegenerative disorders like LS (Riddle and Albert, 1997;Maglioni et al., 2020). It has been used as a model to study neuronal alterations during aging and as a model for neurodegenerative diseases like Alzheimer's and Parkinson's disease (Lublin and Link, 2013;Alexander et al., 2014). Disease models of LS with human homologs of *NDUFS4* and *NDUFS1* mutations affecting CI were created with *C. elegans* to screen for drugs that can suppress the disease (Maglioni et al., 2020). Not only does the model in this study recapitulate the human pathologies associated with the mutations, but they also led to the discovery that the mutations were causing alterations in acetylcholine synapsis. In another study, a human homolog of the *NDUFS2* mutant model was created to study the preventative and therapeutic effects of various antioxidants that have been proposed for the clinical treatment of respiratory chain diseases (Polyak et al., 2018). Human homologs with missense and deletion mutations have also been created for genes such as *SDH-C* (CII), *UQCRFS1* (CIII), *COQ7*, and *IDH1* (Lai et al., 2000). These mutant strains have allowed for modeling respiratory chain dysfunction and investigating *in vivo* mitochondrial functions associated with

these defects (Kayser et al., 2004;Lemire et al., 2009;Dingley et al., 2010). These types of studies where mutations are introduced to study disease phenotypes while screening for targeted therapeutics continue to provide valuable information on mechanisms underlying the mutation variants involved in LS and other respiratory chain disorders (Diaz, 2010;Polyak et al., 2018;Maglioni et al., 2020;Fox et al., 2021).

While worm models present several advantages such as short lifecycle/lifespan, the relative ease and low cost of generating transgenic strains, and their transparent nature which allows for cellular localization of fluorescently tagged genes, they present with their limitations (Kamath et al., 2001;Timmons et al., 2001;Rea et al., 2010), One of the major challenges of using worms as disease models is in the ability to obtain evidence that observed pathologies are specific and relevant to the disease being studied (Teschendorf and Link, 2009). The evolutionarily conserved genes between worms and humans make it easy to introduce mutations to replicate the involvement of nDNA in mitochondrial disorders. However, mtDNA mutations have a mild effect in *C. elegans* and do not mimic the features associated with these pathogenic variants in humans (Tsang and Lemire, 2003). Since mtDNA mutations can also result in LS, worms might not be ideal models for studying pathophysiological features associated with mutations in the mitochondrial genome. Nevertheless, worm models recapitulate many key features of protein of interest in human respiratory chain disorders and continue to serve as critical foundations for furthering our understanding of these disorders.

2.5.3. Fruit fly

Given that neurodegeneration is one of the hallmarks of LS, the fruit fly, *Drosophila melanogaster*, has proven to be invaluable in understanding the cellular, and molecular genetic mechanisms underlying neurodegeneration (reviewed in (Deal and Yamamoto, 2018)). Studies with *Drosophila* have allowed the identification of certain evolutionarily conserved genes that

contribute to neurodegeneration in humans. Furthermore, the fruit fly has been used to construct models of various LS mutations. Transcriptional silencing of *CG9943*, the Drosophila homolog of *SURF1* resulted in decreased COX activity, mirroring some of the same ETC defects observed in humans with *SURF1* mutations (Da-Re et al., 2014). In addition to dysregulation of COX activity, it was also observed that activity of the F_o-subunit of the ATPsynthase and the other OXPHOS complexes were affected. This suggests an additional role in the organization of OXPHOS complexes for the *SURF1* gene in addition to its role in the assembly of COX (Da-Re et al., 2014). Knockdown in another *D. melanogaster* gene, *ND-18*, an ortholog of the human *NDUFS4* recapitulates the feeding difficulty observed in humans with a defect in this complex I gene (Foriel et al., 2018). One of the biggest advantages the fruit fly model offers is that knockdown models reduce the impact of heteroplasmy, allowing for recapitulation of key features of LS disorder in humans and enabling detailed *in vivo* studies of LS and other associated mitochondrial disorders (Sanchez-Martinez et al., 2006;Foriel et al., 2018;Loewen and Ganetzky, 2018). Although *D. melanogaster* continues to be used as a model to study the effects of mutations on mitochondrial functions and the consequent effect on neurodegeneration (Chen and Feany, 2005;Jeibmann and Paulus, 2009;Chen et al., 2016), the anatomical divergence between humans and fruit fly limits recapitulation of certain morphological features. While the fundamental molecular pathways might be conserved, these differences possess limitations in the *D. melanogaster* models; thus requiring significant follow-up studies in higher model organisms of any genes observed as involved in LS pathology in *D. melanogaster*.

2.5.4. Mouse

Although yeast, worms, and fruitfly models have been invaluable in advancing our understanding of mitochondrial genetics, a mammalian *in vivo* model system is required to fully comprehend the etiology, pathogenesis, and tissue specificity associated with mitochondrial

diseases. Where the yeast, worms and, fruitfly models lack, the mouse model is ideal largely in part to its evolutionary closeness to humans. Advances in gene targeting have revolutionized life sciences and made it possible to generate mouse models that can recapitulate mitochondrial diseases (Vempati et al., 2008), with mouse models of OXPHOS defects (extensively reviewed by (Torraco et al., 2009) proving to be invaluable tools in furthering our understanding of various mitochondrial diseases. Transmitochondrial mice models developed to study mutation selectivity in female mouse germline introduced with two different mutations; a severe *ND6* and milder *CO1* mutations using a heteroplasmic mice model, showed that while some tissues show random genetic drift in their mtDNA; in other tissues, there seems to be a strong, tissue-specific, age-related directional selection for different mt-DNA genotypes even in the same animals (Jenuth et al., 1997;Fan et al., 2008). Few studies have also developed an LS model for neuroprotection studies by using the complex I inhibitor MPTP (1-methyl-4-phenyl-1,2,3,6-tetrahydropyridine). MPTP intoxicated mice served as a good model of LS based on the finding that MPTP affects mainly complex I and complex IV and triggered basal ganglia degeneration (Lagrue et al., 2009;Da Costa et al., 2016).

Mice missing the *NDUFS4* subunit of complex I are the leading models for LS (Quintana et al., 2010;Quintana et al., 2012;Adjobo-Hermans et al., 2020;Grillo et al., 2021). Studies on Ndufs4 knockout (KO) led to the discovery that hypoxia can prevent and reverse neurological effects of CI-defect and LS (Ferrari et al., 2017;Jain et al., 2019). These studies revealed that hypoxia extended the lifespan in KO mice by up to 4times those in normoxic conditions (Ferrari et al., 2017). When KO mice with late-onset encephalopathy were exposed to normobaric 11% O_2, the neurological disease in these mice improved. Once they were returned to normoxia, the *Ndufs4* KO mice died within days (Ferrari et al., 2017). Suggesting that intermittent hypoxia was ineffective in preventing neuropathology. A similar result was observed in another study, where activation of the hypoxia pathway was not sufficient to rescue disease in the *Ndufs4* KO mouse

model. However chronic hypoxic breathing and other intervention to reduce brain oxygen levels were effective at preventing neurological disease in these mouse models (Jain et al., 2019). These studies attributed a role for unused oxygen in the pathology observed under normoxic and intermittent hypoxic conditions (Ferrari et al., 2017;Jain et al., 2019). The *Ndufs4* KO has been beneficial in understanding the potential for hypoxia as a therapeutic strategy for LS. Another study with *Ndufs4* KO showed that not only did the mutation result in a significant decrease in CI subunit levels, but it also induced a near-complete loss of another accessory subunit, *NDUFA12*. The mutation also resulted in a significant increase in a different assembly subunit *NDUFAF2*, leading to the conclusion that NDUFAF12 could stabilize CI in the absence of NDUFS4 and NDUFA12 (Adjobo-Hermans et al., 2020). In addition to the *Ndufs4* KO, mouse models have been engineered for studying deficiencies in other ETC complexes that contribute to LS. Homozygous *Surf1* mutant mice with cytochrome c oxidase deficiency (Agostino et al., 2003), mice lacking mitochondrial superoxide dismutase (Melov et al., 1998), and mice deficient in the mitochondrial membrane protease Presenilins-associated rhomboid-like protein (PARL) (Spinazzi et al., 2019) have all been created to model LS.

Whilst the mouse model has been invaluable in answering many questions associated with mitochondrial disease etiology and pathogenesis, it seems to pose some challenges just like the other models described previously. One of the biggest setbacks involves overcoming problems of embryonic and neonatal lethality of mutant mice to examine if the mice faithfully reproduce targeted disease as expected (Vempati et al., 2008). Nevertheless, mouse models have been beneficial in overcoming challenges associated with the availability of human samples to conduct comprehensive mechanistic analysis and continue to be used as a model for *in vivo* studies of mitochondrial diseases.

2.5.5. Humans

2.5.5.1. Transmitochondrial cybrids

After recognition in 1963 that the mitochondria contain their genome and the realization that under conditions favoring glycolytic metabolism, yeast will undergo depletion and deletion of mtDNA molecules, efforts were made by scientists to artificially induce this phenomenon using ethidium bromide (Swerdlow, 2007). It was not until 1985 that the first report of a total eukaryotic cell mtDNA depletion was reported in a chicken embryo (Desjardins et al., 1985;Morais et al., 1988). In 1989, King and Attardi reported the successful production of human osteosarcoma rho zero (ρ^o) cell lines; a significant progress that gave rise to the development of human transmitochondrial cytoplasmic hybrid (cybrids) models for the investigation of mitochondrial related diseases (King and Attardi, 1989). This model is especially appealing because it delineates donor mtDNA from the original nuclear background, allowing for the study of mitochondrial mutation-dependent differences in isolation (Danielson et al., 2005).

Transmitochondrial cybrids are generated by a cytoplasmic fusion of ρ^o cells from parent cell lines with enucleated cells from donor cell lines and have allowed for studies on the heteroplasmic threshold, mtDNA-nDNA compatibility (Swerdlow, 2007), mtDNA segregation (Jenuth et al., 1996;Jenuth et al., 1997), and most importantly for studying various disorders of the mitochondria such as LHON (Danielson et al., 2005;Iyer, 2013) and LS(Iyer et al., 2009b;Iyer et al., 2012). Transmitochondrial cybrid models have also resulted in questioning the uneven segregation hypothesis that has been used in explaining the genetic-phenotypic variance associated with various mitochondrial diseases (Rorbach et al., 2008). While this model provides an attractive option, it poses some challenges; one of the most obvious being the technique used in generating the cell lines. The ρ^o cells are generated through long-term exposure to a mutagen, ethidium bromide, while the enucleated donor cells are generated by

exposure to cytochalasin B; a mycotoxin (Danielson et al., 2005), a process that could induce significant cellular stress and affect several gene expressions. Furthermore, the fusion process may result in damage and disorganization of multiple cellular organelles and membranes. Another challenge results from the use of aneuploid inherently genetically unstable cancer cell lines as the parental cell lines used in this model (Danielson et al., 2005) as this could potentially result in dysfunctional or variable gene expression. Finally, given that we do not fully understand the cross-talk that exists between nuclear and mitochondrial DNA, a cybrid cell might not fully recapitulate the disease of interest.

2.5.5.2. Induced Pluripotent Stem cell (iPSCs) models

The discovery of induced pluripotent stem cells (iPSCs) by Yamanaka in 2006 opened a plethora of opportunities for biomedical research. Not only does this technology allow for the reprogramming of differentiated cells to an embryonic-like state, but it also opened the door for a new era of personalized medicine; allowing for the generation of patient-specific cell lines for the study of various diseases (Takahashi et al., 2007). This technology is especially useful in investigating mitochondrial diseases owing to their varying phenotypes. One of the challenges associated with understanding the pathogenesis of mitochondrial diseases is the limited availability of human supplies and variability in diseased phenotypes between and within tissues. With iPSCs, some of these problems can be resolved as fibroblast-derived from diseased patients could be reprogrammed and potentially differentiated into any cell/tissue to better elucidate the pathological mechanism of a specific mitochondrial disorder on various cells/tissues. Many recent studies have demonstrated the potential for generating human iPSC patient-specific models from LS carrying mutations in *MTATP6* and *MTND5* genes (Galera-Monge et al., 2016;Zurita-Diaz et al., 2016;Grace et al., 2019). Another study combined somatic cell nuclear transfer (SCNT) and iPSC technology to perform a metabolic rescue in the iPSCs generated from these patients, demonstrating the significant possibilities that iPSC models hold,

as they could potentially be used to simultaneously study pathogenesis and develop treatments for patients with LS and other mitochondrial diseases (Ma et al., 2015). With unique hiPSC model systems that carry defined mtDNA mutations, the potential for a better understanding of key pathways and metabolic regulation during the early development of LS is now possible. The generation of patient-specific hiPSCs and subsequent generation of specialized differentiated cell types also allows us to better understand the variability associated with LS and the development of targeted therapies. In addition, it now allows us to address the extent to which heteroplasmy is preserved in specific cell types during the differentiation process.

One of the challenges with iPSC models is the ability to maintain mutation load in daughter cells after reprogramming and differentiation (Povea-Cabello et al., 2020). To address this problem, direct reprogramming protocols have been developed to ensure that the age and epigenetic markers of donors are maintained (Horvath, 2013;Mertens et al., 2015;Huh et al., 2016). Another challenge is associated with the conversion efficiency and generation of high purity samples that only contain the cell lineages of interest. Recent studies with induced neurons (iN) have developed reprogramming techniques that address this problem, resulting in a high yield and percentage of pure iNs (Drouin-Ouellet et al., 2017;Shrigley et al., 2018). The biggest challenge of all relates to maintaining these cell lines in long-term culture. The long-term culture of iPSC and reprogramming is difficult and extremely expensive, making it difficult to adopt in labs with limited resources (Povea-Cabello et al., 2020). However, direct reprograming, like those done to derive iNs can help reduce the cost of reprogramming hiPSC. Recently, iNs from two MERRF patient-derived fibroblasts harboring the *A8344G* were successfully developed using direct reprogramming (Villanueva-Paz et al., 2019). These iNs retained the heteroplasmy mutation load from the parent fibroblast and showed features of matured neurons. Neuronal maturation markers and functional studies such as electrophysiological recordings further confirmed that these iNs behaved like neurons. Furthermore, the MERRF iNs showed

pathophysiological features that have been described in other MERRF models, making them suitable models for mimicking neurological disorders (Villanueva-Paz et al., 2020). Together, hiPS and directed reprogramming technology hold promise for advancing our understanding of mitochondrial disorders like LS, while allowing for targeted high-throughput drug screening in human cell lines and advancing precision medicine (Villalon-Garcia et al., 2020). This is by far the most accurate model because the same cell line from a single patient has the potential to be differentiated into any cell type to study the effects of pathogenic mutations on the different cells and tissues in humans. Drug screening using this technology could allow for quicker discoveries because it eliminates the need of testing these drugs in other animal models.

2.6. Therapeutic strategies and future directions

Despite the progress that has been made in understanding the molecular mechanisms underlying mitochondrial diseases, there are currently no specific treatment options for LS and other related mitochondrial disorders. Currently, the available therapeutic approaches are limited and are still an area of interest for various research groups. The currently available options are symptomatic treatments; and focus on improving energy state through optimization of ATP production while lowering lactate levels (Ruhoy and Saneto, 2014). EPI-743, an analog of coenzyme Q10, is an antioxidant that has been suggested to improve clinical outcomes in some cases of genetically confirmed LS in a small controlled study (Martinelli et al., 2012), while supplementation with B vitamins such as thiamine, a cofactor of PDH (pyruvate dehydrogenase) is being considered as a treatment option (Bar-Meir et al., 2001). The ketogenic diet has also been proposed to improve symptoms in an adult case of LS (Malojcic et al., 2004) and some studies have also suggested hypoxia treatment as a therapy for mitochondrial disease (Russell et al., 2016;Shoubridge, 2016). While this might seem counterintuitive, studies in mice suggest that hypoxia could potentially be used as a therapy for mitochondrial dysfunction, with the researchers proposing that hypoxia could be beneficial owing to two different mechanisms: the

first involving a reduction in O_2 tension, resulting in a decrease of reactive oxygen species (ROS), while the second involving activation of HIFs (Hypoxia-Inducible Factors), resulting in decreased production of ATP by OXPHOS and a shift to glycolysis (Jain et al., 2016;Ferrari et al., 2017;Jain et al., 2019). Extensive research needs to be performed to validate the mechanism(s) involved in this process before hypoxia is deemed safe/efficient as a treatment for any mitochondrial disorder. Furthermore, the efficacy and safety of many of the supplements and vitamins are still being investigated. Many of these currently lack valid preclinical and clinical evidence to support their efficacy in treating mitochondrial disorders (Garone and Viscomi, 2018). One of the biggest challenges to developing treatment options for LS is the phenotypic and genotypic variability associated with this mitochondrial disorder. Nevertheless, efforts are being made to develop a novel treatment, with efforts focusing on therapies to increase ATP production by the ETC, increasing mitochondrial biogenesis, targeting dysfunctional mitochondria for degradation, or degrading mitochondrial genomes harboring disease-causing mutations. The collective goal of these treatment options is to improve mitochondrial health in specific cells and tissues that are impacted by the disease.

2.6.1. Mitochondrial replacement therapy

Since mtDNA are maternally inherited and mutations in the mt genome can result in a range of pathologies and there is currently no cure for these diseases, mitochondrial replacement therapies have gained attention as a means of limiting inheritance of pathogenic mtDNA (Kang et al., 2016;Greenfield et al., 2017;Saxena et al., 2018;Craven et al., 2020). Two techniques, one developed in the UK and the other in the US, have been established to prevent the transmission of mutations in mtDNA (Saxena et al., 2018;Craven et al., 2020). In the UK, the method that was developed and currently licensed involves pronuclear transplantation (PNT) from an affected donor into an enucleated healthy embryo right after completing meiosis. Reports from preclinical studies using this technique showed that mtDNA carryover was

reduced to <2% in 79% of PNT blastocysts (Hyslop et al., 2016). In the US, the approach developed is based on maternal spindle transfer (Kang et al., 2016;Zhang et al., 2017). This involves the transfer of the nucleus of the affected mother's oocyte to an enucleated donor's oocyte before fertilization with the father's sperm. The maternal spindle transfer resulted in embryos containing >99% of donor mtDNA. While donor mtDNA was stably maintained in embryonic stem cells (ES cells) derived from most embryos, some of the ES cell lines reversed to the maternal haplotype (Kang et al., 2016). Leading to the suggestion that some haplotypes confer proliferative and growth advantages to cells. Therefore, having leftover mtDNA from the affected mother could still result in the development of the mitochondrial disorder in the offspring later on.

In the US, the first baby born by the spindle transfer technique generated a lot of controversies (Zhang et al., 2017;Garone and Viscomi, 2018). There are still so many ethical issues surrounding the use of mitochondrial replacement therapy (Craven et al., 2020). This is evident in the fact that there are very few countries that have adopted this. Even in countries like the UK where its use has been approved, the approval is only for selected patients (Garone and Viscomi, 2018;Craven et al., 2020). Aside from the ethical dilemma, both techniques that have been developed still have a small fraction of the affected mother's mtDNA present (Hyslop et al., 2016;Kang et al., 2016;Zhang et al., 2017). As reported in one of the studies, there was a gradual loss of donor mtDNA in some of the ES cells derived from transplanted embryos. Long-term follow-up on children born as a result of mitochondrial replacement therapy would help clarify if they develop mitochondrial disorders later in life. Another concern that has been raised relates to mitochondrial-nuclear DNA compatibility. However, studies have suggested that switching nuclear genomes between different mitochondrial haplotypes does not result in any detectable difference in mitochondrial gene expression (reviewed extensively by (Greenfield et al., 2017)). The other limitation is that mitochondrial replacement therapy only addresses

mitochondrial disorders resulting from a mutation in the mitochondrial genome, but not the nuclear genome.

2.6.2. Gene therapy

Gene therapy promises to use development from gene-editing technologies to cure mitochondrial diseases. Since mutations in mtDNA contribute to mitochondrial disorders, editing these mutant DNA shift the proportions of mutant to healthy DNA, thereby, reducing the burden of the disease. Early studies focused on using adeno-associated viral vectors (AAVs) to achieve this (Garone and Viscomi, 2018;Viscomi and Zeviani, 2020). The use of AAVs for human gene therapy is attractive because of the favorable safety profile and the availability of several tissue specific serotypes (Garone and Viscomi, 2018;Viscomi and Zeviani, 2020). This approach does come with its limitations, however. The first being the difficulty associated with limited cloning capability. Secondly, it is difficult to achieve therapeutic expression in several tissues. Nevertheless, AAVs have been used to partially rescue the phenotype in of *Ndufs4* KO mouse model with LS (Di Meo et al., 2017). AAVs have also been used in combination with other gene editing tools to deliver therapeutic genes to affected organs (Bacman et al., 2013;Gammage et al., 2016b;Bacman et al., 2018;Gammage et al., 2018).

Currently, restriction endonucleases (RE), zinc finger nuclease (ZFN), transcription activator-like effector nuclease (TALEN), and CRISPR/Cas9 technology are widely used editing tools for this purpose (Greenfield et al., 2017;Reddy et al., 2020;Yang et al., 2021). The RE, SmaI which is usually used for diagnosis of NARP and LS because of its ability to recognize the DNA sequence in the pathogenic variant of the *T8993G* mutation was modified to eliminate this mutant mtDNA. In this study, elimination of this pathogenic mtDNA was followed by repopulation of wild-type mtDNA and restoration of mitochondrial functions (Tanaka et al., 2002). Studies using ZFN (Minczuk et al., 2008;Gammage et al., 2014;Gammage et al., 2016a;Gammage et

al., 2018) and TALENS (Bacman et al., 2013;Reddy et al., 2015;Yang et al., 2018) have also been used to successfully target pathogenic variants in the mitochondrial genome to eliminate these mutant genes and restore wild-type phenotype. Although a lot of these techniques have been readily adapted to editing the nuclear genome, slight modifications have to be made to target them to mitochondria to modify mtDNA (Hussain et al., 2021). For instance, while CRISPR/Cas9 has been adopted for base editing in the nuclear genome, it has been challenging to do the same with the mitochondrial genome because of the difficulty associated with the delivery of guide RNA into the mitochondria (Greenfield et al., 2017;Hussain et al., 2021;Yang et al., 2021). However, a CRISPR-free technology involving the use of bacterial cytidine deaminase toxin has been recently developed for use in mitochondrial base editing (Mok et al., 2020). This new technology has the potential to pave the way for new studies involving the precise manipulation of mtDNA to treat mitochondrial disorders.

2.6.3. Pharmacological treatments and diet

The pharmacological therapies focus on different aspects of mitochondrial functions, ranging from upregulation of mitochondrial biogenesis or autophagy to preventing oxidative damage (Lightowlers et al., 2015;Gerards et al., 2016;Povea-Cabello et al., 2020). The most common targets for pharmacological agents focus on AMP-activated protein kinase (AMPK), Sirtuins (Sirt1), and mammalian target of rapamycin complex 1 (mTORC1) pathways (Garone and Viscomi, 2018;Viscomi and Zeviani, 2020). The peroxisomal proliferator-activated receptor-gamma 1 (PGC1α) is a transcriptional coactivator for several transcription factors. Post-translational modification by AMPK or deacetylation by Sirt1 results in activation of PGC1α (Viscomi and Zeviani, 2020). Therefore, pharmacological modulations on AMPK and Sirt1 are used to activate PGC1α to enhance mitochondrial biogenesis. AMPK is usually activated by AMP, while Sirt1 is activated by NAD+, so analogs of AMP and NAD+ are used to activate this pathway. Compounds such as bezafibrate, AICAR, resveratrol, and nicotinamide riboside are

examples of AMP and NAD+ analogs that have shown some success in treating mitochondrial disorders (Bastin et al., 2008;Wenz et al., 2008;Cerutti et al., 2014;Iannetti et al., 2018). The other pathway that is targeted involves the mTORC1. mTORC1 is a cytosolic Serine/Threonine kinase belonging to the phosphatidylinositol kinase-related protein kinases family. It plays a central role in processes such as protein translation, immune response, nucleotide and lipid synthesis, glucose metabolism, autophagy, and lysosomal biogenesis (Saxton and Sabatini, 2017). As discussed previously, studies on caloric restriction in yeast led to the idea that inhibition of mTORC1 can be used as therapy for mitochondrial disease. Rapamycin and its analogs are potent inhibitors of mTORC1 and have been shown to improve symptoms in some patients with mitochondrial disease (Sage-Schwaede et al., 2019;Martin-Perez et al., 2020). The effect of rapamycin has been tested in *NDUFS4* KO mice, results from this and other studies show that mTORC1 inhibition alleviated mitochondrial disease in the mouse model of LS (Johnson et al., 2013;Cheema et al., 2021). It has been suggested that rapamycin acts by inducing a metabolic shift from glycolysis to amino acid metabolism, reducing the buildup of glycolytic intermediates (Schleit et al., 2013).

In line with the idea of metabolic shift is the ketogenic diet. This type of diet aims to shift metabolism towards beta-oxidation and ketone body production, to increase transcription of OXPHOS, TCA cycle, and glycolysis genes (Bough et al., 2006). In mouse models following a ketogenic diet, a decrease in mitochondrial ROS, and an increase in mitochondrial uncoupling protein and glutathione levels were reported (Sullivan et al., 2004;Jarrett et al., 2008). Suggesting that ketogenic diets might act to reduce mitochondrial-mediated oxidative stress. There is still a lot of controversy regarding the safety and efficacy of this dietary option (Garone and Viscomi, 2018;Kuszak et al., 2018).

Other compounds in use are antioxidants such as CoQ10 and its derivatives idebenone, and EPI-743. Idebenone is taken up more readily by the cells and has been suggested as a

replacement for CoQ10 (Kwong et al., 2002). Although idebenone has been used mainly as a treatment for Leber's hereditary optic neuropathy (LHON), it is now being tested as a treatment option for LS (Haginoya et al., 2009;Carelli et al., 2011;Barboni et al., 2013). EPI-743 has also shown some promise in reversing LS in patients with different mtDNA mutations, however, its efficiency is still being evaluated (Gerards et al., 2016). Recently, cell permeants ETC substrates have gained attention as therapeutic agents for mitochondrial diseases. Supplementation with the cell-permeable dimethyl ketoglutarate (DMKG) extended life and delayed onset of neurological phenotype in an *Ndufs4*-KO mouse model of LS (Lee et al., 2019a). Cell permeate succinate prodrugs have also shown promise in alleviating disease in cellular models of mitochondrial disorders with complex I deficiency (Ehinger et al., 2016;Janowska et al., 2020;Piel et al., 2020). These substrates work by increasing TCA cycle intermediates and providing alternative substrate sources for the mitochondria. Many of the pharmacological agents mentioned in this section are still in pre-clinical and clinical trials, some of them have shown conflicting results in these trials (Garone and Viscomi, 2018). Therefore, a more extensive study needs to be performed to determine the efficacy and safety of these therapeutic agents.

2.6.4. Hypoxia

During aerobic respiration, oxygen acts as the final electron acceptor in the ETC, in a reaction that results in its reduction to water. In excess, oxygen can also result in the formation of reactive oxygen species (ROS) and other radicals that can damage proteins, nucleic acids, phospholipids, and other molecular species (Viscomi and Zeviani, 2019). Physiologic levels of ROS act as signaling molecules to regulate key mitochondrial functions (Butow and Avadhani, 2004). However, too much ROS can be detrimental to cells as previously highlighted. It is for this reason that cells have devised ways of neutralizing the debilitating effects of ROS and other free radicals with ROS scavengers and antioxidants. Mitochondrial disorders are problematic

because they cause defects in mitochondrial ETC, compromising the efficient utilization of oxygen and electron transport. This could result in electron leakage and further result in the production of ROS and other free radicals (Viscomi and Zeviani, 2019). It is this understanding that has led to the use of antioxidants as therapeutic agents for mitochondrial disorders. However, reducing oxygen below a certain threshold, as in the case of hypoxia can be detrimental to cellular respiration as well. This is why the use of hypoxia as therapy might seem counterintuitive as a treatment for diseases wherein ETC activities are already compromised.

The use of hypoxia as a therapy for mitochondrial disorders became popular when CRISPR/Cas9 screening identified the Von Hippel-Lindau (VHL) factor as the most effective suppressor of antimycin-induced mitochondrial dysfunction (Jain et al., 2016). VHL is a ubiquitin ligase that targets hypoxia-induced transcription factors (HIFs) for degradation (Garone and Viscomi, 2018;Viscomi and Zeviani, 2019). However, hypoxia stabilizes HIF and results in the activation of hypoxia response. In a 30day exposure to chronic hypoxic conditions (11% O_2) *Ndufs4* KO mice showed drastic improvement in lifespan and delay in clinical progression of LS. When mice with the same KO mutation were exposed to hyperoxic conditions (50% O_2), their conditions worsened. Further, when exposed to intermediate levels of hypoxia (17%), there was no beneficial effect seen in the *Ndufs4* KO mice (Jain et al., 2016). Interestingly, transcriptional activation of HIF in *Ndufs4* KO mice did not result in the same beneficial effects observed under hypoxic conditions in the previous study (Jain et al., 2019). In the study, the researchers suggest that interventions to reduce brain oxygen levels are effective at preventing neurological disease in mouse models. One of the biggest challenges with the hypoxia treatment is that most studies have only been performed in the *Ndufs4* KO mouse models (Jain et al., 2016;Ferrari et al., 2017;Grange et al., 2021). Studies on models with other mutations involved in LS will provide more insight into the efficacy of this therapy. Furthermore, the mechanism behind the observed response to hypoxia is still unclear and more studies need to be done to explore this

(Garone and Viscomi, 2018;Viscomi and Zeviani, 2019). Finally, the methods that have been proposed in this study to lower pO_2 are unlikely to be transferred for use in patients that are already severely sick (Jain et al., 2019).

2.7. Conclusion

While advances in mitochondrial genetics and structural analysis coupled with sequencing have furthered our understanding of LS, observations that bioenergetic defects might not be the sole explanation for the pathology observed in LS merits further investigation (Kucharczyk et al., 2009b). Another unanswered question stems from the role of assembly/accessory factors in disease pathology. As discussed earlier, novel pathogenic roles for assembly and biogenesis factors of the ETC are being reported. Although previous studies largely focused on mutations affecting structural subunits of the ETC, we are now starting to observe that more than just the structural unit, the assembly factors, also play key roles in regulating bioenergetics of the cell (D'Aurelio et al., 2010;Pitceathly et al., 2013). Future studies thus need to be performed to understand the roles of the accessory subunits of each of the various complexes of the ETC. In addition, future research also needs to focus on mtDNA segregation in tissues, due to genetic drift in mtDNA segregation, and observations show that this drift is tissue-specific. Therefore, a better understanding of this issue could potentially provide a better understanding of the genotype-phenotype variability associated with LS and other mitochondrial diseases. Finally, the mitochondria are dynamic organelles that constantly undergo rounds of fission and fusion to maintain a healthy pool and sustain energy production. There is thus significant interest in understanding how the dynamic nature of this organelle contributes to health and disease. As outlined above, there is still much to learn about the mitochondria, as new tools and technology continue to develop, and our understanding is further enhanced. hiPSC technology is a novel tool that would allow us to bypass the paucity of human samples and provide the amount of material required to aid with studies on mitochondria. Furthermore, in combination with various

gene-editing tools, hiPSC technology could potentially open doors for new drug discovery and therapeutic approaches that could invariably lead to the discovery of treatments for patients with LS.

2.8. References

Adjobo-Hermans, M.J.W., De Haas, R., Willems, P., Wojtala, A., Van Emst-De Vries, S.E., Wagenaars, J.A., Van Den Brand, M., Rodenburg, R.J., Smeitink, J.a.M., Nijtmans, L.G., Sazanov, L.A., Wieckowski, M.R., and Koopman, W.J.H. (2020). NDUFS4 deletion triggers loss of NDUFA12 in Ndufs4(-/-) mice and Leigh syndrome patients: A stabilizing role for NDUFAF2. *Biochim Biophys Acta Bioenerg* 1861**,** 148213.

Agostino, A., Invernizzi, F., Tiveron, C., Fagiolari, G., Prelle, A., Lamantea, E., Giavazzi, A., Battaglia, G., Tatangelo, L., Tiranti, V., and Zeviani, M. (2003). Constitutive knockout of Surf1 is associated with high embryonic lethality, mitochondrial disease and cytochrome c oxidase deficiency in mice. *Hum Mol Genet* 12**,** 399-413.

Ahlers, P.M., Garofano, A., Kerscher, S.J., and Brandt, U. (2000). Application of the obligate aerobic yeast Yarrowia lipolytica as a eucaryotic model to analyse Leigh syndrome mutations in the complex I core subunits PSST and TYKY. *Biochim Biophys Acta* 1459**,** 258-265.

Ahola, S., Isohanni, P., Euro, L., Brilhante, V., Palotie, A., Pihko, H., Lonnqvist, T., Lehtonen, T., Laine, J., Tyynismaa, H., and Suomalainen, A. (2014). Mitochondrial EFTs defects in juvenile-onset Leigh disease, ataxia, neuropathy, and optic atrophy. *Neurology* 83**,** 743-751.

Alexander, A.G., Marfil, V., and Li, C. (2014). Use of Caenorhabditis elegans as a model to study Alzheimer's disease and other neurodegenerative diseases. *Front Genet* 5**,** 279.

Antonicka, H., Leary, S.C., Guercin, G.H., Agar, J.N., Horvath, R., Kennaway, N.G., Harding, C.O., Jaksch, M., and Shoubridge, E.A. (2003). Mutations in COX10 result in a defect in mitochondrial heme A biosynthesis and account for multiple, early-onset clinical phenotypes associated with isolated COX deficiency. *Hum Mol Genet* 12**,** 2693-2702.

Atwal, P.S. (2014). Mutations in the Complex III Assembly Factor Tetratricopeptide 19 Gene TTC19 Are a Rare Cause of Leigh Syndrome. *JIMD Rep* 14**,** 43-45.

Babot, M., Birch, A., Labarbuta, P., and Galkin, A. (2014). Characterisation of the active/de-active transition of mitochondrial complex I. *Biochim Biophys Acta* 1837**,** 1083-1092.

Babot, M., and Galkin, A. (2013). Molecular mechanism and physiological role of active-deactive transition of mitochondrial complex I. *Biochem Soc Trans* 41**,** 1325-1330.

Bacman, S.R., Kauppila, J.H.K., Pereira, C.V., Nissanka, N., Miranda, M., Pinto, M., Williams, S.L., Larsson, N.G., Stewart, J.B., and Moraes, C.T. (2018). MitoTALEN reduces mutant mtDNA load and restores tRNA(Ala) levels in a mouse model of heteroplasmic mtDNA mutation. *Nat Med* 24**,** 1696-1700.

Bacman, S.R., Williams, S.L., Pinto, M., Peralta, S., and Moraes, C.T. (2013). Specific elimination of mutant mitochondrial genomes in patient-derived cells by mitoTALENs. *Nat Med* 19**,** 1111-1113.

Baertling, F., Rodenburg, R.J., Schaper, J., Smeitink, J.A., Koopman, W.J., Mayatepek, E., Morava, E., and Distelmaier, F. (2014). A guide to diagnosis and treatment of Leigh syndrome. *J Neurol Neurosurg Psychiatry* 85**,** 257-265.

Baertling, F., Sanchez-Caballero, L., Van Den Brand, M.a.M., Wintjes, L.T., Brink, M., Van Den Brandt, F.A., Wilson, C., Rodenburg, R.J.T., and Nijtmans, L.G.J. (2017). NDUFAF4 variants are associated with Leigh syndrome and cause a specific mitochondrial complex I assembly defect. *Eur J Hum Genet* 2**5,** 1273-1277.

Bailey, L.J., and Doherty, A.J. (2017). Mitochondrial DNA replication: a PrimPol perspective. *Biochem Soc Trans* 45**,** 513-529.

Banka, S., De Goede, C., Yue, W.W., Morris, A.A., Von Bremen, B., Chandler, K.E., Feichtinger, R.G., Hart, C., Khan, N., Lunzer, V., Matakovic, L., Marquardt, T., Makowski, C., Prokisch, H., Debus, O., Nosaka, K., Sonwalkar, H., Zimmermann, F.A., Sperl, W., and Mayr, J.A. (2014). Expanding the clinical and molecular spectrum of thiamine pyrophosphokinase deficiency: a treatable neurological disorder caused by TPK1 mutations. *Mol Genet Metab* 113**,** 301-306.

Bar-Meir, M., Elpeleg, O.N., and Saada, A. (2001). Effect of various agents on adenosine triphosphate synthesis in mitochondrial complex I deficiency. *J Pediatr* 139**,** 868-870.

Baracca, A., Sgarbi, G., Mattiazzi, M., Casalena, G., Pagnotta, E., Valentino, M.L., Moggio, M., Lenaz, G., Carelli, V., and Solaini, G. (2007). Biochemical phenotypes associated with the mitochondrial ATP6 gene mutations at nt8993. *Biochim Biophys Acta* 1767**,** 913-919.

Barboni, P., Valentino, M.L., La Morgia, C., Carbonelli, M., Savini, G., De Negri, A., Simonelli, F., Sadun, F., Caporali, L., Maresca, A., Liguori, R., Baruzzi, A., Zeviani, M., and Carelli, V. (2013). Idebenone treatment in patients with OPA1-mutant dominant optic atrophy. *Brain* 136**,** e231.

Barel, O., Shorer, Z., Flusser, H., Ofir, R., Narkis, G., Finer, G., Shalev, H., Nasasra, A., Saada, A., and Birk, O.S. (2008). Mitochondrial complex III deficiency associated with a homozygous mutation in UQCRQ. *Am J Hum Genet* 82**,** 1211-1216.

Bastin, J., Aubey, F., Rotig, A., Munnich, A., and Djouadi, F. (2008). Activation of peroxisome proliferator-activated receptor pathway stimulates the mitochondrial respiratory chain and can correct deficiencies in patients' cells lacking its components. *J Clin Endocrinol Metab* 93**,** 1433-1441.

Benit, P., Chretien, D., Kadhom, N., De Lonlay-Debeney, P., Cormier-Daire, V., Cabral, A., Peudenier, S., Rustin, P., Munnich, A., and Rotig, A. (2001). Large-scale deletion and point mutations of the nuclear NDUFV1 and NDUFS1 genes in mitochondrial complex I deficiency. *Am J Hum Genet* 68**,** 1344-1352.

Berger, I., Hershkovitz, E., Shaag, A., Edvardson, S., Saada, A., and Elpeleg, O. (2008). Mitochondrial complex I deficiency caused by a deleterious NDUFA11 mutation. *Ann Neurol* 63**,** 405-408.

Bohm, M., Pronicka, E., Karczmarewicz, E., Pronicki, M., Piekutowska-Abramczuk, D., Sykut-Cegielska, J., Mierzewska, H., Hansikova, H., Vesela, K., Tesarova, M., Houstkova, H.,

Houstek, J., and Zeman, J. (2006). Retrospective, multicentric study of 180 children with cytochrome C oxidase deficiency. *Pediatr Res* 59**,** 21-26.

Bough, K.J., Wetherington, J., Hassel, B., Pare, J.F., Gawryluk, J.W., Greene, J.G., Shaw, R., Smith, Y., Geiger, J.D., and Dingledine, R.J. (2006). Mitochondrial biogenesis in the anticonvulsant mechanism of the ketogenic diet. *Ann Neurol* 60**,** 223-235.

Brown, G. (2014). Defects of thiamine transport and metabolism. *J Inherit Metab Dis* 37**,** 577-585.

Budde, S.M., Van Den Heuvel, L.P., Janssen, A.J., Smeets, R.J., Buskens, C.A., Demeirleir, L., Van Coster, R., Baethmann, M., Voit, T., Trijbels, J.M., and Smeitink, J.A. (2000). Combined enzymatic complex I and III deficiency associated with mutations in the nuclear encoded NDUFS4 gene. *Biochem Biophys Res Commun* 275**,** 63-68.

Bugiani, M., Invernizzi, F., Alberio, S., Briem, E., Lamantea, E., Carrara, F., Moroni, I., Farina, L., Spada, M., Donati, M.A., Uziel, G., and Zeviani, M. (2004). Clinical and molecular findings in children with complex I deficiency. *Biochim Biophys Acta* 1659**,** 136-147.

Butow, R.A., and Avadhani, N.G. (2004). Mitochondrial signaling: the retrograde response. *Mol Cell* 14**,** 1-15.

Calvo, S.E., Tucker, E.J., Compton, A.G., Kirby, D.M., Crawford, G., Burtt, N.P., Rivas, M., Guiducci, C., Bruno, D.L., Goldberger, O.A., Redman, M.C., Wiltshire, E., Wilson, C.J., Altshuler, D., Gabriel, S.B., Daly, M.J., Thorburn, D.R., and Mootha, V.K. (2010). High-throughput, pooled sequencing identifies mutations in NUBPL and FOXRED1 in human complex I deficiency. *Nat Genet* 42**,** 851-858.

Carelli, V., Achilli, A., Valentino, M.L., Rengo, C., Semino, O., Pala, M., Olivieri, A., Mattiazzi, M., Pallotti, F., Carrara, F., Zeviani, M., Leuzzi, V., Carducci, C., Valle, G., Simionati, B., Mendieta, L., Salomao, S., Belfort, R., Jr., Sadun, A.A., and Torroni, A. (2006). Haplogroup effects and recombination of mitochondrial DNA: novel clues from the analysis of Leber hereditary optic neuropathy pedigrees. *Am J Hum Genet* 78**,** 564-574.

Carelli, V., La Morgia, C., Valentino, M.L., Rizzo, G., Carbonelli, M., De Negri, A.M., Sadun, F., Carta, A., Guerriero, S., Simonelli, F., Sadun, A.A., Aggarwal, D., Liguori, R., Avoni, P., Baruzzi, A., Zeviani, M., Montagna, P., and Barboni, P. (2011). Idebenone treatment in Leber's hereditary optic neuropathy. *Brain* 134**,** e188.

Ceccatelli Berti, C., Di Punzio, G., Dallabona, C., Baruffini, E., Goffrini, P., Lodi, T., and Donnini, C. (2021). The Power of Yeast in Modelling Human Nuclear Mutations Associated with Mitochondrial Diseases. *Genes (Basel)* 12.

Cerutti, R., Pirinen, E., Lamperti, C., Marchet, S., Sauve, A.A., Li, W., Leoni, V., Schon, E.A., Dantzer, F., Auwerx, J., Viscomi, C., and Zeviani, M. (2014). NAD(+)-dependent activation of Sirt1 corrects the phenotype in a mouse model of mitochondrial disease. *Cell Metab* 19**,** 1042-1049.

Chang, X., Wu, Y., Zhou, J., Meng, H., Zhang, W., and Guo, J. (2020). A meta-analysis and systematic review of Leigh syndrome: clinical manifestations, respiratory chain enzyme complex deficiency, and gene mutations. *Medicine (Baltimore)* 99**,** e18634.

Cheema, N.J., Cameron, J.M., and Hood, D.A. (2021). Effect of rapamycin on mitochondria and lysosomes in fibroblasts from patients with mtDNA mutations. *Am J Physiol Cell Physiol*.

Chen, K., Lin, G., Haelterman, N.A., Ho, T.S., Li, T., Li, Z., Duraine, L., Graham, B.H., Jaiswal, M., Yamamoto, S., Rasband, M.N., and Bellen, H.J. (2016). Loss of Frataxin induces iron toxicity, sphingolipid synthesis, and Pdk1/Mef2 activation, leading to neurodegeneration. *Elife* 5.

Chen, L., and Feany, M.B. (2005). Alpha-synuclein phosphorylation controls neurotoxicity and inclusion formation in a Drosophila model of Parkinson disease. *Nat Neurosci* 8**,** 657-663.

Chol, M., Lebon, S., Benit, P., Chretien, D., De Lonlay, P., Goldenberg, A., Odent, S., Hertz-Pannier, L., Vincent-Delorme, C., Cormier-Daire, V., Rustin, P., Rotig, A., and Munnich, A. (2003). The mitochondrial DNA G13513A MELAS mutation in the NADH dehydrogenase 5 gene is a frequent cause of Leigh-like syndrome with isolated complex I deficiency. *J Med Genet* 40**,** 188-191.

Chourasia, N., Adejumo, R.B., Patel, R.P., and Koenig, M.K. (2017). Involvement of Cerebellum in Leigh Syndrome: Case Report and Review of the Literature. *Pediatr Neurol* 74**,** 97-99.

Corona, P., Antozzi, C., Carrara, F., D'incerti, L., Lamantea, E., Tiranti, V., and Zeviani, M. (2001). A novel mtDNA mutation in the ND5 subunit of complex I in two MELAS patients. *Ann Neurol* 49**,** 106-110.

Cox, R., Platt, J., Chen, L.C., Tang, S., Wong, L.J., and Enns, G.M. (2012). Leigh syndrome caused by a novel m.4296G>A mutation in mitochondrial tRNA isoleucine. *Mitochondrion* 12**,** 258-261.

Craven, L., Murphy, J.L., and Turnbull, D.M. (2020). Mitochondrial donation - hope for families with mitochondrial DNA disease. *Emerg Top Life Sci* 4**,** 151-154.

D'aurelio, M., Vives-Bauza, C., Davidson, M.M., and Manfredi, G. (2010). Mitochondrial DNA background modifies the bioenergetics of NARP/MILS ATP6 mutant cells. *Hum Mol Genet* 19**,** 374-386.

Da-Re, C., Von Stockum, S., Biscontin, A., Millino, C., Cisotto, P., Zordan, M.A., Zeviani, M., Bernardi, P., De Pitta, C., and Costa, R. (2014). Leigh syndrome in Drosophila melanogaster: morphological and biochemical characterization of Surf1 post-transcriptional silencing. *J Biol Chem* 289**,** 29235-29246.

Da Costa, B., Dumon, E., Le Moigno, L., Bodard, S., Castelnau, P., Letellier, T., and Rocher, C. (2016). Respiratory chain inhibition: one more feature to propose MPTP intoxication as a Leigh syndrome model. *J Bioenerg Biomembr* 48**,** 483-491.

Danielson, S.R., Carelli, V., Tan, G., Martinuzzi, A., Schapira, A.H., Savontaus, M.L., and Cortopassi, G.A. (2005). Isolation of transcriptomal changes attributable to LHON mutations and the cybridization process. *Brain* 128**,** 1026-1037.

De Lonlay, P., Valnot, I., Barrientos, A., Gorbatyuk, M., Tzagoloff, A., Taanman, J.W., Benayoun, E., Chretien, D., Kadhom, N., Lombes, A., De Baulny, H.O., Niaudet, P., Munnich, A., Rustin, P., and Rotig, A. (2001). A mutant mitochondrial respiratory chain assembly protein causes complex III deficiency in patients with tubulopathy, encephalopathy and liver failure. *Nat Genet* 29**,** 57-60.

De Luca, C., Besagni, C., Frontali, L., Bolotin-Fukuhara, M., and Francisci, S. (2006). Mutations in yeast mt tRNAs: specific and general suppression by nuclear encoded tRNA interactors. *Gene* 377**,** 169-176.

Deal, S.L., and Yamamoto, S. (2018). Unraveling Novel Mechanisms of Neurodegeneration Through a Large-Scale Forward Genetic Screen in Drosophila. *Front Genet* 9**,** 700.

Debray, F.G., Lambert, M., Lortie, A., Vanasse, M., and Mitchell, G.A. (2007). Long-term outcome of Leigh syndrome caused by the NARP-T8993C mtDNA mutation. *Am J Med Genet A* 143A**,** 2046-2051.

Debray, F.G., Morin, C., Janvier, A., Villeneuve, J., Maranda, B., Laframboise, R., Lacroix, J., Decarie, J.C., Robitaille, Y., Lambert, M., Robinson, B.H., and Mitchell, G.A. (2011). LRPPRC mutations cause a phenotypically distinct form of Leigh syndrome with cytochrome c oxidase deficiency. *J Med Genet* 48**,** 183-189.

Desjardins, P., Frost, E., and Morais, R. (1985). Ethidium bromide-induced loss of mitochondrial DNA from primary chicken embryo fibroblasts. *Mol Cell Biol* 5**,** 1163-1169.

Devivo, D.C., Haymond, M.W., Obert, K.A., Nelson, J.S., and Pagliara, A.S. (1979). Defective activation of the pyruvate dehydrogenase complex in subacute necrotizing encephalomyelopathy (Leigh disease). *Ann Neurol* 6**,** 483-494.

Di Meo, I., Marchet, S., Lamperti, C., Zeviani, M., and Viscomi, C. (2017). AAV9-based gene therapy partially ameliorates the clinical phenotype of a mouse model of Leigh syndrome. *Gene Ther* 24**,** 661-667.

Di Punzio, G., Di Noia, M.A., Delahodde, A., Sellem, C., Donnini, C., Palmieri, L., Lodi, T., and Dallabona, C. (2021). A Yeast-Based Screening Unravels Potential Therapeutic Molecules for Mitochondrial Diseases Associated with Dominant ANT1 Mutations. *Int J Mol Sci* 22.

Diaz, F. (2010). Cytochrome c oxidase deficiency: patients and animal models. *Biochim Biophys Acta* 1802**,** 100-110.

Dimauro, S., and Schon, E.A. (2003). Mitochondrial respiratory-chain diseases. *N Engl J Med* 348**,** 2656-2668.

Dingley, S., Polyak, E., Lightfoot, R., Ostrovsky, J., Rao, M., Greco, T., Ischiropoulos, H., and Falk, M.J. (2010). Mitochondrial respiratory chain dysfunction variably increases oxidant stress in Caenorhabditis elegans. *Mitochondrion* 10**,** 125-136.

Drouin-Ouellet, J., Lau, S., Brattas, P.L., Rylander Ottosson, D., Pircs, K., Grassi, D.A., Collins, L.M., Vuono, R., Andersson Sjoland, A., Westergren-Thorsson, G., Graff, C., Minthon, L., Toresson, H., Barker, R.A., Jakobsson, J., and Parmar, M. (2017). REST suppression mediates neural conversion of adult human fibroblasts via microRNA-dependent and -independent pathways. *EMBO Mol Med* 9**,** 1117-1131.

Edwards, L.S., Halmagyi, G.M., Mallawaarachchi, A., Thompson, E.O., and Kiernan, M.C. (2020). Fatal cerebellar oedema in adult Leigh syndrome. *Pract Neurol* 20**,** 336-337.

Ehinger, J.K., Piel, S., Ford, R., Karlsson, M., Sjovall, F., Frostner, E.A., Morota, S., Taylor, R.W., Turnbull, D.M., Cornell, C., Moss, S.J., Metzsch, C., Hansson, M.J., Fliri, H., and Elmer, E. (2016). Cell-permeable succinate prodrugs bypass mitochondrial complex I deficiency. *Nat Commun* 7**,** 12317.

El-Hattab, A.W., Craigen, W.J., Wong, L.J.C., and Scaglia, F. (1993). "Mitochondrial DNA Maintenance Defects Overview," in *GeneReviews((R)),* eds. M.P. Adam, H.H. Ardinger, R.A. Pagon, S.E. Wallace, L.J.H. Bean, G. Mirzaa & A. Amemiya. (Seattle (WA)).

Evans, O.B. (1981). Pyruvate decarboxylase deficiency in subacute necrotizing encephalomyelopathy. *Arch Neurol* 38**,** 515-519.

Fan, W., Waymire, K.G., Narula, N., Li, P., Rocher, C., Coskun, P.E., Vannan, M.A., Narula, J., Macgregor, G.R., and Wallace, D.C. (2008). A mouse model of mitochondrial disease reveals germline selection against severe mtDNA mutations. *Science* 319**,** 958-962.

Fassone, E., Duncan, A.J., Taanman, J.W., Pagnamenta, A.T., Sadowski, M.I., Holand, T., Qasim, W., Rutland, P., Calvo, S.E., Mootha, V.K., Bitner-Glindzicz, M., and Rahman, S. (2010). FOXRED1, encoding an FAD-dependent oxidoreductase complex-I-specific molecular chaperone, is mutated in infantile-onset mitochondrial encephalopathy. *Hum Mol Genet* 19**,** 4837-4847.

Ferrari, M., Jain, I.H., Goldberger, O., Rezoagli, E., Thoonen, R., Cheng, K.H., Sosnovik, D.E., Scherrer-Crosbie, M., Mootha, V.K., and Zapol, W.M. (2017). Hypoxia treatment reverses neurodegenerative disease in a mouse model of Leigh syndrome. *Proc Natl Acad Sci U S A* 114**,** E4241-E4250.

Feuermann, M., Francisci, S., Rinaldi, T., De Luca, C., Rohou, H., Frontali, L., and Bolotin-Fukuhara, M. (2003). The yeast counterparts of human 'MELAS' mutations cause mitochondrial dysfunction that can be rescued by overexpression of the mitochondrial translation factor EF-Tu. *EMBO Reports* 4**,** 53-58.

Finsterer, J. (2008). Leigh and Leigh-like syndrome in children and adults. *Pediatr Neurol* 39**,** 223-235.

Foriel, S., Beyrath, J., Eidhof, I., Rodenburg, R.J., Schenck, A., and Smeitink, J.a.M. (2018). Feeding difficulties, a key feature of the Drosophila NDUFS4 mitochondrial disease model. *Dis Model Mech* 11.

Fox, B.C., Slade, L., Torregrossa, R., Pacitti, D., Szabo, C., Etheridge, T., and Whiteman, M. (2021). The mitochondria-targeted hydrogen sulfide donor AP39 improves health and mitochondrial function in a C. elegans primary mitochondrial disease model. *J Inherit Metab Dis* 44**,** 367-375.

Galera-Monge, T., Zurita-Diaz, F., Gonzalez-Paramos, C., Moreno-Izquierdo, A., Fraga, M.F., Fernandez, A.F., Garesse, R., and Gallardo, M.E. (2016). Generation of a human iPSC line from a patient with Leigh syndrome caused by a mutation in the MT-ATP6 gene. *Stem Cell Res* 16**,** 766-769.

Gammage, P.A., Gaude, E., Van Haute, L., Rebelo-Guiomar, P., Jackson, C.B., Rorbach, J., Pekalski, M.L., Robinson, A.J., Charpentier, M., Concordet, J.P., Frezza, C., and Minczuk, M. (2016a). Near-complete elimination of mutant mtDNA by iterative or dynamic dose-controlled treatment with mtZFNs. *Nucleic Acids Res* 44**,** 7804-7816.

Gammage, P.A., Rorbach, J., Vincent, A.I., Rebar, E.J., and Minczuk, M. (2014). Mitochondrially targeted ZFNs for selective degradation of pathogenic mitochondrial genomes bearing large-scale deletions or point mutations. *EMBO Mol Med* 6**,** 458-466.

Gammage, P.A., Van Haute, L., and Minczuk, M. (2016b). Engineered mtZFNs for Manipulation of Human Mitochondrial DNA Heteroplasmy. *Methods Mol Biol* 1351**,** 145-162.

Gammage, P.A., Viscomi, C., Simard, M.L., Costa, A.S.H., Gaude, E., Powell, C.A., Van Haute, L., Mccann, B.J., Rebelo-Guiomar, P., Cerutti, R., Zhang, L., Rebar, E.J., Zeviani, M.,

Frezza, C., Stewart, J.B., and Minczuk, M. (2018). Genome editing in mitochondria corrects a pathogenic mtDNA mutation in vivo. *Nat Med* 24**,** 1691-1695.

Ganetzky, R.D., Stendel, C., Mccormick, E.M., Zolkipli-Cunningham, Z., Goldstein, A.C., Klopstock, T., and Falk, M.J. (2019). MT-ATP6 mitochondrial disease variants: Phenotypic and biochemical features analysis in 218 published cases and cohort of 14 new cases. *Human Mutation* 40**,** 499-515.

Garone, C., and Viscomi, C. (2018). Towards a therapy for mitochondrial disease: an update. *Biochem Soc Trans* 46**,** 1247-1261.

Gerards, M., Kamps, R., Van Oevelen, J., Boesten, I., Jongen, E., De Koning, B., Scholte, H.R., De Angst, I., Schoonderwoerd, K., Sefiani, A., Ratbi, I., Coppieters, W., Karim, L., De Coo, R., Van Den Bosch, B., and Smeets, H. (2013). Exome sequencing reveals a novel Moroccan founder mutation in SLC19A3 as a new cause of early-childhood fatal Leigh syndrome. *Brain* 136**,** 882-890.

Gerards, M., Sallevelt, S.C., and Smeets, H.J. (2016). Leigh syndrome: Resolving the clinical and genetic heterogeneity paves the way for treatment options. *Mol Genet Metab* 117**,** 300-312.

Ghezzi, D., Baruffini, E., Haack, T.B., Invernizzi, F., Melchionda, L., Dallabona, C., Strom, T.M., Parini, R., Burlina, A.B., Meitinger, T., Prokisch, H., Ferrero, I., and Zeviani, M. (2012). Mutations of the mitochondrial-tRNA modifier MTO1 cause hypertrophic cardiomyopathy and lactic acidosis. *Am J Hum Genet* 90**,** 1079-1087.

Ghezzi, D., Goffrini, P., Uziel, G., Horvath, R., Klopstock, T., Lochmuller, H., D'adamo, P., Gasparini, P., Strom, T.M., Prokisch, H., Invernizzi, F., Ferrero, I., and Zeviani, M. (2009). SDHAF1, encoding a LYR complex-II specific assembly factor, is mutated in SDH-defective infantile leukoencephalopathy. *Nat Genet* 41**,** 654-656.

Grace, H.E., Galdun, P., 3rd, Lesnefsky, E.J., West, F.D., and Iyer, S. (2019). mRNA Reprogramming of T8993G Leigh's Syndrome Fibroblast Cells to Create Induced Pluripotent Stem Cell Models for Mitochondrial Disorders. *Stem Cells Dev* 28**,** 846-859.

Graeber, M.B., and Muller, U. (1998). Recent developments in the molecular genetics of mitochondrial disorders. *J Neurol Sci* 153**,** 251-263.

Grange, R.M.H., Sharma, R., Shah, H., Reinstadler, B., Goldberger, O., Cooper, M.K., Nakagawa, A., Miyazaki, Y., Hindle, A.G., Batten, A.J., Wojtkiewicz, G.R., Schleifer, G., Bagchi, A., Marutani, E., Malhotra, R., Bloch, D.B., Ichinose, F., Mootha, V.K., and Zapol, W.M. (2021). Hypoxia ameliorates brain hyperoxia and NAD(+) deficiency in a murine model of Leigh syndrome. *Mol Genet Metab* 133**,** 83-93.

Gray, M.W., Burger, G., and Lang, B.F. (1999). Mitochondrial evolution. *Science* 283**,** 1476-1481.

Greenfield, A., Braude, P., Flinter, F., Lovell-Badge, R., Ogilvie, C., and Perry, A.C.F. (2017). Assisted reproductive technologies to prevent human mitochondrial disease transmission. *Nat Biotechnol* 35**,** 1059-1068.

Grillo, A.S., Bitto, A., and Kaeberlein, M. (2021). The NDUFS4 Knockout Mouse: A Dual Threat Model of Childhood Mitochondrial Disease and Normative Aging. *Methods Mol Biol* 2277**,** 143-155.

Haginoya, K., Miyabayashi, S., Kikuchi, M., Kojima, A., Yamamoto, K., Omura, K., Uematsu, M., Hino-Fukuyo, N., Tanaka, S., and Tsuchiya, S. (2009). Efficacy of idebenone for respiratory failure in a patient with Leigh syndrome: a long-term follow-up study. *J Neurol Sci* 278**,** 112-114.

Hammans, S.R., Sweeney, M.G., Brockington, M., Morgan-Hughes, J.A., and Harding, A.E. (1991). Mitochondrial encephalopathies: molecular genetic diagnosis from blood samples. *Lancet* 337**,** 1311-1313.

Hayhurst, H., De Coo, I.F.M., Piekutowska-Abramczuk, D., Alston, C.L., Sharma, S., Thompson, K., Rius, R., He, L., Hopton, S., Ploski, R., Ciara, E., Lake, N.J., Compton, A.G., Delatycki, M.B., Verrips, A., Bonnen, P.E., Jones, S.A., Morris, A.A., Shakespeare, D., Christodoulou, J., Wesol-Kucharska, D., Rokicki, D., Smeets, H.J.M., Pronicka, E., Thorburn, D.R., Gorman, G.S., Mcfarland, R., Taylor, R.W., and Ng, Y.S. (2019). Leigh syndrome caused by mutations in MTFMT is associated with a better prognosis. *Ann Clin Transl Neurol* 6**,** 515-524.

Hoefs, S.J., Dieteren, C.E., Distelmaier, F., Janssen, R.J., Epplen, A., Swarts, H.G., Forkink, M., Rodenburg, R.J., Nijtmans, L.G., Willems, P.H., Smeitink, J.A., and Van Den Heuvel, L.P. (2008). NDUFA2 complex I mutation leads to Leigh disease. *Am J Hum Genet* 82**,** 1306-1315.

Hoefs, S.J., Van Spronsen, F.J., Lenssen, E.W., Nijtmans, L.G., Rodenburg, R.J., Smeitink, J.A., and Van Den Heuvel, L.P. (2011). NDUFA10 mutations cause complex I deficiency in a patient with Leigh disease. *Eur J Hum Genet* 19**,** 270-274.

Hommes, F.A., Polman, H.A., and Reerink, J.D. (1968). Leigh's encephalomyelopathy: an inborn error of gluconeogenesis. *Arch Dis Child* 43**,** 423-426.

Hong, C.M., Na, J.H., Park, S., and Lee, Y.M. (2020). Clinical Characteristics of Early-Onset and Late-Onset Leigh Syndrome. *Front Neurol* 11**,** 267.

Horvath, S. (2013). DNA methylation age of human tissues and cell types. *Genome Biol* 14**,** R115.

Huh, C.J., Zhang, B., Victor, M.B., Dahiya, S., Batista, L.F., Horvath, S., and Yoo, A.S. (2016). Maintenance of age in human neurons generated by microRNA-based neuronal conversion of fibroblasts. *Elife* 5.

Hussain, S.A., Yalvac, M.E., Khoo, B., Eckardt, S., and Mclaughlin, K.J. (2021). Adapting CRISPR/Cas9 System for Targeting Mitochondrial Genome. *Front Genet* 12**,** 627050.

Hyslop, L.A., Blakeley, P., Craven, L., Richardson, J., Fogarty, N.M., Fragouli, E., Lamb, M., Wamaitha, S.E., Prathalingam, N., Zhang, Q., O'keefe, H., Takeda, Y., Arizzi, L., Alfarawati, S., Tuppen, H.A., Irving, L., Kalleas, D., Choudhary, M., Wells, D., Murdoch, A.P., Turnbull, D.M., Niakan, K.K., and Herbert, M. (2016). Towards clinical application of pronuclear transfer to prevent mitochondrial DNA disease. *Nature* 534**,** 383-386.

Iannetti, E.F., Smeitink, J.a.M., Willems, P., Beyrath, J., and Koopman, W.J.H. (2018). Rescue from galactose-induced death of Leigh Syndrome patient cells by pyruvate and NAD(.). *Cell Death Dis* 9**,** 1135.

Iyer, S. (2013). Novel therapeutic approaches for Leber's hereditary optic neuropathy. *Discov Med* 15**,** 141-149.

Iyer, S., Alsayegh, K., Abraham, S., and Rao, R.R. (2009a). Stem cell-based models and therapies for neurodegenerative diseases. *Crit Rev Biomed Eng* 37**,** 321-353.

Iyer, S., Bergquist, K., Young, K., Gnaiger, E., Rao, R.R., and Bennett, J.P., Jr. (2012). Mitochondrial gene therapy improves respiration, biogenesis, and transcription in G11778A Leber's hereditary optic neuropathy and T8993G Leigh's syndrome cells. *Hum Gene Ther* 23**,** 647-657.

Iyer, S., Thomas, R.R., Portell, F.R., Dunham, L.D., Quigley, C.K., and Bennett, J.P., Jr. (2009b). Recombinant mitochondrial transcription factor A with N-terminal mitochondrial transduction domain increases respiration and mitochondrial gene expression. *Mitochondrion* 9**,** 196-203.

Jain-Ghai, S., Cameron, J.M., Al Maawali, A., Blaser, S., Mackay, N., Robinson, B., and Raiman, J. (2013). Complex II deficiency--a case report and review of the literature. *Am J Med Genet A* 161A**,** 285-294.

Jain, I.H., Zazzeron, L., Goldberger, O., Marutani, E., Wojtkiewicz, G.R., Ast, T., Wang, H., Schleifer, G., Stepanova, A., Brepoels, K., Schoonjans, L., Carmeliet, P., Galkin, A., Ichinose, F., Zapol, W.M., and Mootha, V.K. (2019). Leigh Syndrome Mouse Model Can Be Rescued by Interventions that Normalize Brain Hyperoxia, but Not HIF Activation. *Cell Metab* 30**,** 824-832 e823.

Jain, I.H., Zazzeron, L., Goli, R., Alexa, K., Schatzman-Bone, S., Dhillon, H., Goldberger, O., Peng, J., Shalem, O., Sanjana, N.E., Zhang, F., Goessling, W., Zapol, W.M., and Mootha, V.K. (2016). Hypoxia as a therapy for mitochondrial disease. *Science* 352**,** 54-61.

Janowska, J.I., Piel, S., Saliba, N., Kim, C.D., Jang, D.H., Karlsson, M., Kilbaugh, T.J., and Ehinger, J.K. (2020). Mitochondrial respiratory chain complex I dysfunction induced by N-methyl carbamate ex vivo can be alleviated with a cell-permeable succinate prodrug. *Toxicol In Vitro* 65**,** 104794.

Jarrett, S.G., Milder, J.B., Liang, L.P., and Patel, M. (2008). The ketogenic diet increases mitochondrial glutathione levels. *J Neurochem* 106**,** 1044-1051.

Jeibmann, A., and Paulus, W. (2009). Drosophila melanogaster as a model organism of brain diseases. *Int J Mol Sci* 10**,** 407-440.

Jenuth, J.P., Peterson, A.C., Fu, K., and Shoubridge, E.A. (1996). Random genetic drift in the female germline explains the rapid segregation of mammalian mitochondrial DNA. *Nat Genet* 14**,** 146-151.

Jenuth, J.P., Peterson, A.C., and Shoubridge, E.A. (1997). Tissue-specific selection for different mtDNA genotypes in heteroplasmic mice. *Nat Genet* 16**,** 93-95.

Jiang, J.C., Jaruga, E., Repnevskaya, M.V., and Jazwinski, S.M. (2000). An intervention resembling caloric restriction prolongs life span and retards aging in yeast. *FASEB J* 14**,** 2135-2137.

Johnson, S.C., Yanos, M.E., Kayser, E.B., Quintana, A., Sangesland, M., Castanza, A., Uhde, L., Hui, J., Wall, V.Z., Gagnidze, A., Oh, K., Wasko, B.M., Ramos, F.J., Palmiter, R.D., Rabinovitch, P.S., Morgan, P.G., Sedensky, M.M., and Kaeberlein, M. (2013). mTOR inhibition alleviates mitochondrial disease in a mouse model of Leigh syndrome. *Science* 342**,** 1524-1528.

Joost, K., Rodenburg, R., Piirsoo, A., Van Den Heuvel, B., Zordania, R., and Ounap, K. (2010). A novel mutation in the SCO2 gene in a neonate with early-onset cardioencephalomyopathy. *Pediatr Neurol* 42**,** 227-230.

Kamath, R.S., Martinez-Campos, M., Zipperlen, P., Fraser, A.G., and Ahringer, J. (2001). Effectiveness of specific RNA-mediated interference through ingested double-stranded RNA in Caenorhabditis elegans. *Genome Biol* 2**,** RESEARCH0002.

Kang, E., Wu, J., Gutierrez, N.M., Koski, A., Tippner-Hedges, R., Agaronyan, K., Platero-Luengo, A., Martinez-Redondo, P., Ma, H., Lee, Y., Hayama, T., Van Dyken, C., Wang, X., Luo, S., Ahmed, R., Li, Y., Ji, D., Kayali, R., Cinnioglu, C., Olson, S., Jensen, J., Battaglia, D., Lee, D., Wu, D., Huang, T., Wolf, D.P., Temiakov, D., Belmonte, J.C., Amato, P., and Mitalipov, S. (2016). Mitochondrial replacement in human oocytes carrying pathogenic mitochondrial DNA mutations. *Nature* 540**,** 270-275.

Kayser, E.B., Sedensky, M.M., and Morgan, P.G. (2004). The effects of complex I function and oxidative damage on lifespan and anesthetic sensitivity in Caenorhabditis elegans. *Mech Ageing Dev* 125**,** 455-464.

King, M.P., and Attardi, G. (1989). Human cells lacking mtDNA: repopulation with exogenous mitochondria by complementation. *Science* 246**,** 500-503.

Kirby, D.M., Boneh, A., Chow, C.W., Ohtake, A., Ryan, M.T., Thyagarajan, D., and Thorburn, D.R. (2003). Low mutant load of mitochondrial DNA G13513A mutation can cause Leigh's disease. *Ann Neurol* 54**,** 473-478.

Kirby, D.M., Kahler, S.G., Freckmann, M.L., Reddihough, D., and Thorburn, D.R. (2000). Leigh disease caused by the mitochondrial DNA G14459A mutation in unrelated families. *Ann Neurol* 48**,** 102-104.

Koene, S., Rodenburg, R.J., Van Der Knaap, M.S., Willemsen, M.A., Sperl, W., Laugel, V., Ostergaard, E., Tarnopolsky, M., Martin, M.A., Nesbitt, V., Fletcher, J., Edvardson, S., Procaccio, V., Slama, A., Van Den Heuvel, L.P., and Smeitink, J.A. (2012). Natural disease course and genotype-phenotype correlations in Complex I deficiency caused by nuclear gene defects: what we learned from 130 cases. *J Inherit Metab Dis* 35**,** 737-747.

Koopman, W.J., Distelmaier, F., Smeitink, J.A., and Willems, P.H. (2013). OXPHOS mutations and neurodegeneration. *EMBO J* 32**,** 9-29.

Kopajtich, R., Nicholls, T.J., Rorbach, J., Metodiev, M.D., Freisinger, P., Mandel, H., Vanlander, A., Ghezzi, D., Carrozzo, R., Taylor, R.W., Marquard, K., Murayama, K., Wieland, T., Schwarzmayr, T., Mayr, J.A., Pearce, S.F., Powell, C.A., Saada, A., Ohtake, A., Invernizzi, F., Lamantea, E., Sommerville, E.W., Pyle, A., Chinnery, P.F., Crushell, E., Okazaki, Y., Kohda, M., Kishita, Y., Tokuzawa, Y., Assouline, Z., Rio, M., Feillet, F., Mousson De Camaret, B., Chretien, D., Munnich, A., Menten, B., Sante, T., Smet, J., Regal, L., Lorber, A., Khoury, A., Zeviani, M., Strom, T.M., Meitinger, T., Bertini, E.S., Van Coster, R., Klopstock, T., Rotig, A., Haack, T.B., Minczuk, M., and Prokisch, H. (2014). Mutations in GTPBP3 cause a mitochondrial translation defect associated with hypertrophic cardiomyopathy, lactic acidosis, and encephalopathy. *Am J Hum Genet* 95**,** 708-720.

Kucharczyk, R., Rak, M., and Di Rago, J.P. (2009a). Biochemical consequences in yeast of the human mitochondrial DNA 8993T>C mutation in the ATPase6 gene found in NARP/MILS patients. *Biochim Biophys Acta* 1793**,** 817-824.

Kucharczyk, R., Zick, M., Bietenhader, M., Rak, M., Couplan, E., Blondel, M., Caubet, S.D., and Di Rago, J.P. (2009b). Mitochondrial ATP synthase disorders: molecular mechanisms and the quest for curative therapeutic approaches. *Biochim Biophys Acta* 1793**,** 186-199.

Kuszak, A.J., Espey, M.G., Falk, M.J., Holmbeck, M.A., Manfredi, G., Shadel, G.S., Vernon, H.J., and Zolkipli-Cunningham, Z. (2018). Nutritional Interventions for Mitochondrial OXPHOS Deficiencies: Mechanisms and Model Systems. *Annu Rev Pathol* 13**,** 163-191.

Kuwabara, P.E., and O'neil, N. (2001). The use of functional genomics in C. elegans for studying human development and disease. *Journal of Inherited Metabolic Disease* 24**,** 127-138.

Kwong, L.K., Kamzalov, S., Rebrin, I., Bayne, A.C., Jana, C.K., Morris, P., Forster, M.J., and Sohal, R.S. (2002). Effects of coenzyme Q(10) administration on its tissue concentrations, mitochondrial oxidant generation, and oxidative stress in the rat. *Free Radic Biol Med* 33**,** 627-638.

Lagrue, E., Abert, B., Nadal, L., Tabone, L., Bodard, S., Medja, F., Lombes, A., Chalon, S., and Castelnau, P. (2009). MPTP intoxication in mice: a useful model of Leigh syndrome to study mitochondrial diseases in childhood. *Metab Brain Dis* 24**,** 321-335.

Lai, C.H., Chou, C.Y., Ch'ang, L.Y., Liu, C.S., and Lin, W. (2000). Identification of novel human genes evolutionarily conserved in Caenorhabditis elegans by comparative proteomics. *Genome Res* 10**,** 703-713.

Lake, N.J., Compton, A.G., Rahman, S., and Thorburn, D.R. (2016). Leigh syndrome: One disorder, more than 75 monogenic causes. *Ann Neurol* 79**,** 190-203.

Larsson, N.G., and Clayton, D.A. (1995). Molecular genetic aspects of human mitochondrial disorders. *Annu Rev Genet* 29**,** 151-178.

Lebon, S., Rodriguez, D., Bridoux, D., Zerrad, A., Rotig, A., Munnich, A., Legrand, A., and Slama, A. (2007). A novel mutation in the human complex I NDUFS7 subunit associated with Leigh syndrome. *Mol Genet Metab* 90**,** 379-382.

Lee, C.F., Caudal, A., Abell, L., Nagana Gowda, G.A., and Tian, R. (2019a). Targeting NAD(+) Metabolism as Interventions for Mitochondrial Disease. *Sci Rep* 9**,** 3073.

Lee, S., Na, J.H., and Lee, Y.M. (2019b). Epilepsy in Leigh Syndrome With Mitochondrial DNA Mutations. *Front Neurol* 10**,** 496.

Leigh, D. (1951). Subacute necrotizing encephalomyelopathy in an infant. *J Neurol Neurosurg Psychiatry* 14**,** 216-221.

Leigh, P.N., Al-Sarraj, S., and Dimauro, S. (2015). Impact commentaries. Subacute necrotising encephalomyelopathy (Leigh's disease; Leigh syndrome). *J Neurol Neurosurg Psychiatry* 86**,** 363-365.

Lemire, B.D., Behrendt, M., Decorby, A., and Gaskova, D. (2009). C. elegans longevity pathways converge to decrease mitochondrial membrane potential. *Mech Ageing Dev* 130**,** 461-465.

Li, Y., Wen, S., Li, D., Xie, J., Wei, X., Li, X., Liu, Y., Fang, H., Yang, Y., and Lyu, J. (2018). SURF1 mutations in Chinese patients with Leigh syndrome: Novel mutations, mutation spectrum, and the functional consequences. *Gene* 674**,** 15-24.

Lightowlers, R.N., Taylor, R.W., and Turnbull, D.M. (2015). Mutations causing mitochondrial disease: What is new and what challenges remain? *Science* 349**,** 1494-1499.

Lim, S.C., Smith, K.R., Stroud, D.A., Compton, A.G., Tucker, E.J., Dasvarma, A., Gandolfo, L.C., Marum, J.E., Mckenzie, M., Peters, H.L., Mowat, D., Procopis, P.G., Wilcken, B., Christodoulou, J., Brown, G.K., Ryan, M.T., Bahlo, M., and Thorburn, D.R. (2014). A founder mutation in PET100 causes isolated complex IV deficiency in Lebanese individuals with Leigh syndrome. *Am J Hum Genet* 94**,** 209-222.

Lin, C.J., and Wang, M.C. (2017). Microbial metabolites regulate host lipid metabolism through NR5A-Hedgehog signalling. *Nat Cell Biol* 19**,** 550-557.

Lin, S.J., Defossez, P.A., and Guarente, L. (2000). Requirement of NAD and SIR2 for life-span extension by calorie restriction in Saccharomyces cerevisiae. *Science* 289**,** 2126-2128.

Liolitsa, D., Rahman, S., Benton, S., Carr, L.J., and Hanna, M.G. (2003). Is the mitochondrial complex I ND5 gene a hot-spot for MELAS causing mutations? *Ann Neurol* 53**,** 128-132.

Loewen, C.A., and Ganetzky, B. (2018). Mito-Nuclear Interactions Affecting Lifespan and Neurodegeneration in a Drosophila Model of Leigh Syndrome. *Genetics* 208**,** 1535-1552.

Lou, X., Shi, H., Wen, S., Li, Y., Wei, X., Xie, J., Ma, L., Yang, Y., Fang, H., and Lyu, J. (2018). A Novel NDUFS3 mutation in a Chinese patient with severe Leigh syndrome. *J Hum Genet* 63**,** 1269-1272.

Lublin, A.L., and Link, C.D. (2013). Alzheimer's disease drug discovery: in vivo screening using Caenorhabditis elegans as a model for beta-amyloid peptide-induced toxicity. *Drug Discov Today Technol* 10**,** e115-119.

Ma, H., Folmes, C.D., Wu, J., Morey, R., Mora-Castilla, S., Ocampo, A., Ma, L., Poulton, J., Wang, X., Ahmed, R., Kang, E., Lee, Y., Hayama, T., Li, Y., Van Dyken, C., Gutierrez, N.M., Tippner-Hedges, R., Koski, A., Mitalipov, N., Amato, P., Wolf, D.P., Huang, T., Terzic, A., Laurent, L.C., Izpisua Belmonte, J.C., and Mitalipov, S. (2015). Metabolic rescue in pluripotent cells from patients with mtDNA disease. *Nature* 524**,** 234-238.

Maglioni, S., Schiavi, A., Melcher, M., Brinkmann, V., Luo, Z., Raimundo, N., Laromaine, A., Meyer, J.N., Distelmaier, F., and Ventura, N. (2020). Lutein restores synaptic functionality in a C. elegans model for mitochondrial complex I deficiency. *bioRxiv***,** 2020.2002.2020.957225.

Malojcic, B., Brinar, V., Poser, C., and Djakovic, V. (2004). An adult case of Leigh disease. *Clin Neurol Neurosurg* 106**,** 237-240.

Manickam, A.H., Michael, M.J., and Ramasamy, S. (2017). Mitochondrial genetics and therapeutic overview of Leber's hereditary optic neuropathy. *Indian J Ophthalmol* 65**,** 1087-1092.

Martin-Perez, M., Grillo, A.S., Ito, T.K., Valente, A.S., Han, J., Entwisle, S.W., Huang, H.Z., Kim, D., Yajima, M., Kaeberlein, M., and Villen, J. (2020). PKC downregulation upon rapamycin treatment attenuates mitochondrial disease. *Nat Metab* 2**,** 1472-1481.

Martinelli, D., Catteruccia, M., Piemonte, F., Pastore, A., Tozzi, G., Dionisi-Vici, C., Pontrelli, G., Corsetti, T., Livadiotti, S., Kheifets, V., Hinman, A., Shrader, W.D., Thoolen, M., Klein, M.B., Bertini, E., and Miller, G. (2012). EPI-743 reverses the progression of the pediatric mitochondrial disease--genetically defined Leigh Syndrome. *Mol Genet Metab* 107**,** 383-388.

Matthews, P.M., Marchington, D.R., Squier, M., Land, J., Brown, R.M., and Brown, G.K. (1993). Molecular genetic characterization of an X-linked form of Leigh's syndrome. *Ann Neurol* 33**,** 652-655.

Mcfarland, R., Kirby, D.M., Fowler, K.J., Ohtake, A., Ryan, M.T., Amor, D.J., Fletcher, J.M., Dixon, J.W., Collins, F.A., Turnbull, D.M., Taylor, R.W., and Thorburn, D.R. (2004). De novo mutations in the mitochondrial ND3 gene as a cause of infantile mitochondrial encephalopathy and complex I deficiency. *Ann Neurol* 55**,** 58-64.

Mcfarland, R., Taylor, R.W., and Turnbull, D.M. (2010). A neurological perspective on mitochondrial disease. *The Lancet. Neurology* 9**,** 829-840.

Melov, S., Schneider, J.A., Day, B.J., Hinerfeld, D., Coskun, P., Mirra, S.S., Crapo, J.D., and Wallace, D.C. (1998). A novel neurological phenotype in mice lacking mitochondrial manganese superoxide dismutase. *Nat Genet* 18**,** 159-163.

Mertens, J., Paquola, A.C.M., Ku, M., Hatch, E., Bohnke, L., Ladjevardi, S., Mcgrath, S., Campbell, B., Lee, H., Herdy, J.R., Goncalves, J.T., Toda, T., Kim, Y., Winkler, J., Yao, J., Hetzer, M.W., and Gage, F.H. (2015). Directly Reprogrammed Human Neurons Retain Aging-Associated Transcriptomic Signatures and Reveal Age-Related Nucleocytoplasmic Defects. *Cell Stem Cell* 17**,** 705-718.

Minczuk, M., Papworth, M.A., Miller, J.C., Murphy, M.P., and Klug, A. (2008). Development of a single-chain, quasi-dimeric zinc-finger nuclease for the selective degradation of mutated human mitochondrial DNA. *Nucleic Acids Res* 36**,** 3926-3938.

Mitchell, P. (1961). Coupling of phosphorylation to electron and hydrogen transfer by a chemi-osmotic type of mechanism. *Nature* 191**,** 144-148.

Mok, B.Y., De Moraes, M.H., Zeng, J., Bosch, D.E., Kotrys, A.V., Raguram, A., Hsu, F., Radey, M.C., Peterson, S.B., Mootha, V.K., Mougous, J.D., and Liu, D.R. (2020). A bacterial cytidine deaminase toxin enables CRISPR-free mitochondrial base editing. *Nature* 583**,** 631-637.

Montanari, A., Besagni, C., De Luca, C., Morea, V., Oliva, R., Tramontano, A., Bolotin-Fukuhara, M., Frontali, L., and Francisci, S. (2008). Yeast as a model of human mitochondrial tRNA base substitutions: investigation of the molecular basis of respiratory defects. *RNA* 14**,** 275-283.

Morais, R., Desjardins, P., Turmel, C., and Zinkewich-Peotti, K. (1988). Development and characterization of continuous avian cell lines depleted of mitochondrial DNA. *In Vitro Cell Dev Biol* 24**,** 649-658.

Mourier, A., Ruzzenente, B., Brandt, T., Kuhlbrandt, W., and Larsson, N.G. (2014). Loss of LRPPRC causes ATP synthase deficiency. *Hum Mol Genet* 23**,** 2580-2592.

Murphy, M.P. (2009). How mitochondria produce reactive oxygen species. *Biochem J* 417**,** 1-13.

Nesbitt, V., Morrison, P.J., Crushell, E., Donnelly, D.E., Alston, C.L., He, L., Mcfarland, R., and Taylor, R.W. (2012). The clinical spectrum of the m.10191T>C mutation in complex I-deficient Leigh syndrome. *Dev Med Child Neurol* 54**,** 500-506.

Nicholls, D.G., and Ferguson, S.J. (2013). *Bioenergetics 4.* Elsevier.

Ogawa, E., Fushimi, T., Ogawa-Tominaga, M., Shimura, M., Tajika, M., Ichimoto, K., Matsunaga, A., Tsuruoka, T., Ishige, M., Fuchigami, T., Yamazaki, T., Kishita, Y.,

Kohda, M., Imai-Okazaki, A., Okazaki, Y., Morioka, I., Ohtake, A., and Murayama, K. (2020). Mortality of Japanese patients with Leigh syndrome: Effects of age at onset and genetic diagnosis. *J Inherit Metab Dis* 43**,** 819-826.

Ohlenbusch, A., Edvardson, S., Skorpen, J., Bjornstad, A., Saada, A., Elpeleg, O., Gartner, J., and Brockmann, K. (2012). Leukoencephalopathy with accumulated succinate is indicative of SDHAF1 related complex II deficiency. *Orphanet J Rare Dis* 7**,** 69.

Olahova, M., Hardy, S.A., Hall, J., Yarham, J.W., Haack, T.B., Wilson, W.C., Alston, C.L., He, L., Aznauryan, E., Brown, R.M., Brown, G.K., Morris, A.A., Mundy, H., Broomfield, A., Barbosa, I.A., Simpson, M.A., Deshpande, C., Moeslinger, D., Koch, J., Stettner, G.M., Bonnen, P.E., Prokisch, H., Lightowlers, R.N., Mcfarland, R., Chrzanowska-Lightowlers, Z.M., and Taylor, R.W. (2015). LRPPRC mutations cause early-onset multisystem mitochondrial disease outside of the French-Canadian population. *Brain* 138**,** 3503-3519.

Ortigoza-Escobar, J.D., Molero-Luis, M., Arias, A., Oyarzabal, A., Darin, N., Serrano, M., Garcia-Cazorla, A., Tondo, M., Hernandez, M., Garcia-Villoria, J., Casado, M., Gort, L., Mayr, J.A., Rodriguez-Pombo, P., Ribes, A., Artuch, R., and Perez-Duenas, B. (2016). Free-thiamine is a potential biomarker of thiamine transporter-2 deficiency: a treatable cause of Leigh syndrome. *Brain* 139**,** 31-38.

Ortigoza-Escobar, J.D., Serrano, M., Molero, M., Oyarzabal, A., Rebollo, M., Muchart, J., Artuch, R., Rodriguez-Pombo, P., and Perez-Duenas, B. (2014). Thiamine transporter-2 deficiency: outcome and treatment monitoring. *Orphanet J Rare Dis* 9**,** 92.

Pagnamenta, A.T., Hargreaves, I.P., Duncan, A.J., Taanman, J.W., Heales, S.J., Land, J.M., Bitner-Glindzicz, M., Leonard, J.V., and Rahman, S. (2006). Phenotypic variability of mitochondrial disease caused by a nuclear mutation in complex II. *Mol Genet Metab* 89**,** 214-221.

Pallotti, F., Baracca, A., Hernandez-Rosa, E., Walker, W.F., Solaini, G., Lenaz, G., Melzi D'eril, G.V., Dimauro, S., Schon, E.A., and Davidson, M.M. (2004). Biochemical analysis of respiratory function in cybrid cell lines harbouring mitochondrial DNA mutations. *Biochem J* 384**,** 287-293.

Patel, K.P., O'brien, T.W., Subramony, S.H., Shuster, J., and Stacpoole, P.W. (2012). The spectrum of pyruvate dehydrogenase complex deficiency: clinical, biochemical and genetic features in 371 patients. *Mol Genet Metab* 106**,** 385-394.

Patel, M.S., and Korotchkina, L.G. (2006). Regulation of the pyruvate dehydrogenase complex. *Biochem Soc Trans* 34**,** 217-222.

Piekutowska-Abramczuk, D., Rutyna, R., Czyzyk, E., Jurkiewicz, E., Iwanicka-Pronicka, K., Rokicki, D., Stachowicz, S., Strzemecka, J., Guz, W., Gawronski, M., Kosierb, A., Ligas, J., Puchala, M., Drelich-Zbroja, A., Bednarska-Makaruk, M., Dabrowski, W., Ciara, E., Ksiazyk, J.B., and Pronicka, E. (2018). Leigh syndrome in individuals bearing m.9185T>C MTATP6 variant. Is hyperventilation a factor which starts its development? *Metab Brain Dis* 33**,** 191-199.

Piel, S., Chamkha, I., Dehlin, A.K., Ehinger, J.K., Sjovall, F., Elmer, E., and Hansson, M.J. (2020). Cell-permeable succinate prodrugs rescue mitochondrial respiration in cellular models of acute acetaminophen overdose. *PLoS One* 15**,** e0231173.

Pitceathly, R.D., Rahman, S., Wedatilake, Y., Polke, J.M., Cirak, S., Foley, A.R., Sailer, A., Hurles, M.E., Stalker, J., Hargreaves, I., Woodward, C.E., Sweeney, M.G., Muntoni, F., Houlden, H., Taanman, J.W., Hanna, M.G., and Consortium, U.K. (2013). NDUFA4 mutations underlie dysfunction of a cytochrome c oxidase subunit linked to human neurological disease. *Cell Rep* 3**,** 1795-1805.

Polyak, E., Ostrovsky, J., Peng, M., Dingley, S.D., Tsukikawa, M., Kwon, Y.J., Mccormack, S.E., Bennett, M., Xiao, R., Seiler, C., Zhang, Z., and Falk, M.J. (2018). N-acetylcysteine and vitamin E rescue animal longevity and cellular oxidative stress in pre-clinical models of mitochondrial complex I disease. *Mol Genet Metab* 123**,** 449-462.

Povea-Cabello, S., Villanueva-Paz, M., Suarez-Rivero, J.M., Alvarez-Cordoba, M., Villalon-Garcia, I., Talaveron-Rey, M., Suarez-Carrillo, A., Munuera-Cabeza, M., and Sanchez-Alcazar, J.A. (2020). Advances in mt-tRNA Mutation-Caused Mitochondrial Disease Modeling: Patients' Brain in a Dish. *Front Genet* 11**,** 610764.

Quintana, A., Kruse, S.E., Kapur, R.P., Sanz, E., and Palmiter, R.D. (2010). Complex I deficiency due to loss of Ndufs4 in the brain results in progressive encephalopathy resembling Leigh syndrome. *Proc Natl Acad Sci U S A* 107**,** 10996-11001.

Quintana, A., Zanella, S., Koch, H., Kruse, S.E., Lee, D., Ramirez, J.M., and Palmiter, R.D. (2012). Fatal breathing dysfunction in a mouse model of Leigh syndrome. *J Clin Invest* 122**,** 2359-2368.

Quintana, E., Mayr, J.A., Garcia Silva, M.T., Font, A., Tortoledo, M.A., Moliner, S., Ozaez, L., Lluch, M., Cabello, A., Ricoy, J.R., Koch, J., Ribes, A., Sperl, W., and Briones, P. (2009). PDH E1beta deficiency with novel mutations in two patients with Leigh syndrome. *J Inherit Metab Dis* 32 Suppl 1**,** S339-343.

Rahman, S., Blok, R.B., Dahl, H.H., Danks, D.M., Kirby, D.M., Chow, C.W., Christodoulou, J., and Thorburn, D.R. (1996). Leigh syndrome: clinical features and biochemical and DNA abnormalities. *Ann Neurol* 39**,** 343-351.

Rahman, S., and Thorburn, D. (1993). "Nuclear Gene-Encoded Leigh Syndrome Spectrum Overview," in *GeneReviews((R)),* eds. M.P. Adam, H.H. Ardinger, R.A. Pagon, S.E. Wallace, L.J.H. Bean, G. Mirzaa & A. Amemiya. (Seattle (WA)).

Rea, S.L., Graham, B.H., Nakamaru-Ogiso, E., Kar, A., and Falk, M.J. (2010). Bacteria, yeast, worms, and flies: exploiting simple model organisms to investigate human mitochondrial diseases. *Developmental Disabilities Research Reviews* 16**,** 200-218.

Reddy, P., Ocampo, A., Suzuki, K., Luo, J., Bacman, S.R., Williams, S.L., Sugawara, A., Okamura, D., Tsunekawa, Y., Wu, J., Lam, D., Xiong, X., Montserrat, N., Esteban, C.R., Liu, G.H., Sancho-Martinez, I., Manau, D., Civico, S., Cardellach, F., Del Mar O'callaghan, M., Campistol, J., Zhao, H., Campistol, J.M., Moraes, C.T., and Izpisua Belmonte, J.C. (2015). Selective elimination of mitochondrial mutations in the germline by genome editing. *Cell* 161**,** 459-469.

Reddy, P., Vilella, F., Izpisua Belmonte, J.C., and Simón, C. (2020). Use of Customizable Nucleases for Gene Editing and Other Novel Applications. *Genes* 11**,** 976.

Renkema, G.H., Wortmann, S.B., Smeets, R.J., Venselaar, H., Antoine, M., Visser, G., Ben-Omran, T., Van Den Heuvel, L.P., Timmers, H.J., Smeitink, J.A., and Rodenburg, R.J. (2015). SDHA mutations causing a multisystem mitochondrial disease: novel mutations and genetic overlap with hereditary tumors. *Eur J Hum Genet* 23**,** 202-209.

Richter, C., Park, J.W., and Ames, B.N. (1988). Normal oxidative damage to mitochondrial and nuclear DNA is extensive. *Proc Natl Acad Sci U S A* 85**,** 6465-6467.

Riddle, D.L., and Albert, P.S. (1997). "Genetic and Environmental Regulation of Dauer Larva Development," in *C. elegans II,* eds. Nd, D.L. Riddle, T. Blumenthal, B.J. Meyer & J.R. Priess. (Cold Spring Harbor (NY)).

Rohou, H., Francisci, S., Rinaldi, T., Frontali, L., and Bolotin-Fukuhara, M. (2001). Reintroduction of a characterized Mit tRNA glycine mutation into yeast mitochondria provides a new tool for the study of human neurodegenerative diseases. *Yeast* 18**,** 219-227.

Rolland, S.G., Motori, E., Memar, N., Hench, J., Frank, S., Winklhofer, K.F., and Conradt, B. (2013). Impaired complex IV activity in response to loss of LRPPRC function can be compensated by mitochondrial hyperfusion. *Proc Natl Acad Sci U S A* 110**,** E2967-2976.

Ronchi, D., Cosi, A., Tonduti, D., Orcesi, S., Bordoni, A., Fortunato, F., Rizzuti, M., Sciacco, M., Collotta, M., Cagdas, S., Capovilla, G., Moggio, M., Berardinelli, A., Veggiotti, P., and Comi, G.P. (2011). Clinical and molecular features of an infant patient affected by Leigh Disease associated to m.14459G>A mitochondrial DNA mutation: a case report. *BMC Neurol* 11**,** 85.

Rorbach, J., Yusoff, A.A., Tuppen, H., Abg-Kamaludin, D.P., Chrzanowska-Lightowlers, Z.M., Taylor, R.W., Turnbull, D.M., Mcfarland, R., and Lightowlers, R.N. (2008). Overexpression of human mitochondrial valyl tRNA synthetase can partially restore levels of cognate mt-tRNAVal carrying the pathogenic C25U mutation. *Nucleic Acids Res* 36**,** 3065-3074.

Ruhoy, I.S., and Saneto, R.P. (2014). The genetics of Leigh syndrome and its implications for clinical practice and risk management. *Appl Clin Genet* 7**,** 221-234.

Russell, O.M., Lightowlers, R.N., and Turnbull, D.M. (2016). Applying the Airbrakes: Treating Mitochondrial Disease with Hypoxia. *Mol Cell* 62**,** 5-6.

Sage-Schwaede, A., Engelstad, K., Salazar, R., Curcio, A., Khandji, A., Garvin, J.H., Jr., and De Vivo, D.C. (2019). Exploring mTOR inhibition as treatment for mitochondrial disease. *Ann Clin Transl Neurol* 6**,** 1877-1881.

Sanchez-Martinez, A., Luo, N., Clemente, P., Adan, C., Hernandez-Sierra, R., Ochoa, P., Fernandez-Moreno, M.A., Kaguni, L.S., and Garesse, R. (2006). Modeling human mitochondrial diseases in flies. *Biochim Biophys Acta* 1757**,** 1190-1198.

Saneto, R.P., and Singh, K.K. (2010). Illness-induced exacerbation of Leigh syndrome in a patient with the MTATP6 mutation, m. 9185 T>C. *Mitochondrion* 10**,** 567-572.

Santorelli, F.M., Shanske, S., Macaya, A., Devivo, D.C., and Dimauro, S. (1993). The mutation at nt 8993 of mitochondrial DNA is a common cause of Leigh's syndrome. *Ann Neurol* 34**,** 827-834.

Sarzi, E., Brown, M.D., Lebon, S., Chretien, D., Munnich, A., Rotig, A., and Procaccio, V. (2007). A novel recurrent mitochondrial DNA mutation in ND3 gene is associated with isolated complex I deficiency causing Leigh syndrome and dystonia. *Am J Med Genet A* 143A**,** 33-41.

Saxena, N., Taneja, N., Shome, P., and Mani, S. (2018). Mitochondrial Donation: A Boon or Curse for the Treatment of Incurable Mitochondrial Diseases. *J Hum Reprod Sci* 11**,** 3-9.

Saxton, R.A., and Sabatini, D.M. (2017). mTOR Signaling in Growth, Metabolism, and Disease. *Cell* 168**,** 960-976.

Schaefer, A.M., Taylor, R.W., Turnbull, D.M., and Chinnery, P.F. (2004). The epidemiology of mitochondrial disorders--past, present and future. *Biochim Biophys Acta* 1659**,** 115-120.

Schleit, J., Johnson, S.C., Bennett, C.F., Simko, M., Trongtham, N., Castanza, A., Hsieh, E.J., Moller, R.M., Wasko, B.M., Delaney, J.R., Sutphin, G.L., Carr, D., Murakami, C.J., Tocchi, A., Xian, B., Chen, W., Yu, T., Goswami, S., Higgins, S., Holmberg, M., Jeong, K.S., Kim, J.R., Klum, S., Liao, E., Lin, M.S., Lo, W., Miller, H., Olsen, B., Peng, Z.J., Pollard, T., Pradeep, P., Pruett, D., Rai, D., Ros, V., Singh, M., Spector, B.L., Vander Wende, H., An, E.H., Fletcher, M., Jelic, M., Rabinovitch, P.S., Maccoss, M.J., Han, J.D., Kennedy, B.K., and Kaeberlein, M. (2013). Molecular mechanisms underlying genotype-dependent responses to dietary restriction. *Aging Cell* 12**,** 1050-1061.

Schwartz, M., and Vissing, J. (2002). Paternal inheritance of mitochondrial DNA. *N Engl J Med* 347**,** 576-580.

Schwartzentruber, J., Buhas, D., Majewski, J., Sasarman, F., Papillon-Cavanagh, S., Thiffault, I., Sheldon, K.M., Massicotte, C., Patry, L., Simon, M., Zare, A.S., Mckernan, K.J., Consortium, F.C., Michaud, J., Boles, R.G., Deal, C.L., Desilets, V., Shoubridge, E.A., and Samuels, M.E. (2014). Mutation in the nuclear-encoded mitochondrial isoleucyl-tRNA synthetase IARS2 in patients with cataracts, growth hormone deficiency with short stature, partial sensorineural deafness, and peripheral neuropathy or with Leigh syndrome. *Hum Mutat* 35**,** 1285-1289.

Scialo, F., Sriram, A., Fernandez-Ayala, D., Gubina, N., Lohmus, M., Nelson, G., Logan, A., Cooper, H.M., Navas, P., Enriquez, J.A., Murphy, M.P., and Sanz, A. (2016). Mitochondrial ROS Produced via Reverse Electron Transport Extend Animal Lifespan. *Cell Metab* 23**,** 725-734.

Shaughnessy, D.T., Mcallister, K., Worth, L., Haugen, A.C., Meyer, J.N., Domann, F.E., Van Houten, B., Mostoslavsky, R., Bultman, S.J., Baccarelli, A.A., Begley, T.J., Sobol, R.W., Hirschey, M.D., Ideker, T., Santos, J.H., Copeland, W.C., Tice, R.R., Balshaw, D.M., and Tyson, F.L. (2014). Mitochondria, energetics, epigenetics, and cellular responses to stress. *Environ Health Perspect* 122**,** 1271-1278.

Shoubridge, E.A. (2016). MITOCHONDRIA. Mitochondrial disease therapy from thin air? *Science* 352**,** 31-32.

Shrigley, S., Pircs, K., Barker, R.A., Parmar, M., and Drouin-Ouellet, J. (2018). Simple Generation of a High Yield Culture of Induced Neurons from Human Adult Skin Fibroblasts. *J Vis Exp*.

Skladal, D., Halliday, J., and Thorburn, D.R. (2003). Minimum birth prevalence of mitochondrial respiratory chain disorders in children. *Brain* 126**,** 1905-1912.

Smith, A.C., Ito, Y., Ahmed, A., Schwartzentruber, J.A., Beaulieu, C.L., Aberg, E., Majewski, J., Bulman, D.E., Horsting-Wethly, K., Koning, D.V., Care4rare Canada, C., Rodenburg, R.J., Boycott, K.M., and Penney, L.S. (2018). A family segregating lethal neonatal coenzyme Q10 deficiency caused by mutations in COQ9. *J Inherit Metab Dis* 41**,** 719-729.

Sofou, K., De Coo, I.F., Isohanni, P., Ostergaard, E., Naess, K., De Meirleir, L., Tzoulis, C., Uusimaa, J., De Angst, I.B., Lonnqvist, T., Pihko, H., Mankinen, K., Bindoff, L.A.,

Tulinius, M., and Darin, N. (2014). A multicenter study on Leigh syndrome: disease course and predictors of survival. *Orphanet J Rare Dis* 9**,** 52.

Sofou, K., De Coo, I.F.M., Ostergaard, E., Isohanni, P., Naess, K., De Meirleir, L., Tzoulis, C., Uusimaa, J., Lonnqvist, T., Bindoff, L.A., Tulinius, M., and Darin, N. (2018). Phenotype-genotype correlations in Leigh syndrome: new insights from a multicentre study of 96 patients. *J Med Genet* 55**,** 21-27.

Sonam, K., Khan, N.A., Bindu, P.S., Taly, A.B., Gayathri, N., Bharath, M.M., Govindaraju, C., Arvinda, H.R., Nagappa, M., Sinha, S., and Thangaraj, K. (2014). Clinical and magnetic resonance imaging findings in patients with Leigh syndrome and SURF1 mutations. *Brain Dev* 36**,** 807-812.

Spinazzi, M., Radaelli, E., Horre, K., Arranz, A.M., Gounko, N.V., Agostinis, P., Maia, T.M., Impens, F., Morais, V.A., Lopez-Lluch, G., Serneels, L., Navas, P., and De Strooper, B. (2019). PARL deficiency in mouse causes Complex III defects, coenzyme Q depletion, and Leigh-like syndrome. *Proc Natl Acad Sci U S A* 116**,** 277-286.

Srivastava, A.P., Luo, M., Zhou, W., Symersky, J., Bai, D., Chambers, M.G., Faraldo-Gomez, J.D., Liao, M., and Mueller, D.M. (2018). High-resolution cryo-EM analysis of the yeast ATP synthase in a lipid membrane. *Science* 360**,** eaas9699-eaas9699.

Stendel, C., Neuhofer, C., Floride, E., Yuqing, S., Ganetzky, R.D., Park, J., Freisinger, P., Kornblum, C., Kleinle, S., Schols, L., Distelmaier, F., Stettner, G.M., Buchner, B., Falk, M.J., Mayr, J.A., Synofzik, M., Abicht, A., Haack, T.B., Prokisch, H., Wortmann, S.B., Murayama, K., Fang, F., Klopstock, T., and Group, A.T.P.S. (2020). Delineating MT-ATP6-associated disease: From isolated neuropathy to early onset neurodegeneration. *Neurol Genet* 6**,** e393.

Sue, C.M., Bruno, C., Andreu, A.L., Cargan, A., Mendell, J.R., Tsao, C.Y., Luquette, M., Paolicchi, J., Shanske, S., Dimauro, S., and De Vivo, D.C. (1999). Infantile encephalopathy associated with the MELAS A3243G mutation. *J Pediatr* 134**,** 696-700.

Sullivan, P.G., Rippy, N.A., Dorenbos, K., Concepcion, R.C., Agarwal, A.K., and Rho, J.M. (2004). The ketogenic diet increases mitochondrial uncoupling protein levels and activity. *Ann Neurol* 55**,** 576-580.

Sutovsky, P., Moreno, R.D., Ramalho-Santos, J., Dominko, T., Simerly, C., and Schatten, G. (1999). Ubiquitin tag for sperm mitochondria. *Nature* 402**,** 371-372.

Suzuki, T., and Suzuki, T. (2014). A complete landscape of post-transcriptional modifications in mammalian mitochondrial tRNAs. *Nucleic Acids Res* 42**,** 7346-7357.

Sweeney, M.G., Hammans, S.R., Duchen, L.W., Cooper, J.M., Schapira, A.H., Kennedy, C.R., Jacobs, J.M., Youl, B.D., Morgan-Hughes, J.A., and Harding, A.E. (1994). Mitochondrial DNA mutation underlying Leigh's syndrome: clinical, pathological, biochemical, and genetic studies of a patient presenting with progressive myoclonic epilepsy. *J Neurol Sci* 121**,** 57-65.

Swerdlow, R.H. (2007). Mitochondria in cybrids containing mtDNA from persons with mitochondriopathies. *J Neurosci Res* 85**,** 3416-3428.

Tachibana, M., Sparman, M., Sritanaudomchai, H., Ma, H., Clepper, L., Woodward, J., Li, Y., Ramsey, C., Kolotushkina, O., and Mitalipov, S. (2009). Mitochondrial gene replacement in primate offspring and embryonic stem cells. *Nature* 461**,** 367-372.

Takahashi, K., Tanabe, K., Ohnuki, M., Narita, M., Ichisaka, T., Tomoda, K., and Yamanaka, S. (2007). Induction of pluripotent stem cells from adult human fibroblasts by defined factors. *Cell* 131**,** 861-872.

Tanaka, M., Borgeld, H.J., Zhang, J., Muramatsu, S., Gong, J.S., Yoneda, M., Maruyama, W., Naoi, M., Ibi, T., Sahashi, K., Shamoto, M., Fuku, N., Kurata, M., Yamada, Y., Nishizawa, K., Akao, Y., Ohishi, N., Miyabayashi, S., Umemoto, H., Muramatsu, T., Furukawa, K., Kikuchi, A., Nakano, I., Ozawa, K., and Yagi, K. (2002). Gene therapy for mitochondrial disease by delivering restriction endonuclease SmaI into mitochondria. *J Biomed Sci* 9**,** 534-541.

Taylor, R.W., Morris, A.A., Hutchinson, M., and Turnbull, D.M. (2002). Leigh disease associated with a novel mitochondrial DNA ND5 mutation. *Eur J Hum Genet* 10**,** 141-144.

Taylor, R.W., Singh-Kler, R., Hayes, C.M., Smith, P.E., and Turnbull, D.M. (2001a). Progressive mitochondrial disease resulting from a novel missense mutation in the mitochondrial DNA ND3 gene. *Ann Neurol* 50**,** 104-107.

Taylor, R.W., Taylor, G.A., Durham, S.E., and Turnbull, D.M. (2001b). The determination of complete human mitochondrial DNA sequences in single cells: implications for the study of somatic mitochondrial DNA point mutations. *Nucleic Acids Res* 29**,** E74-74.

Teschendorf, D., and Link, C.D. (2009). What have worm models told us about the mechanisms of neuronal dysfunction in human neurodegenerative diseases? *Molecular Neurodegeneration* 4**,** 38.

Timmons, L., Court, D.L., and Fire, A. (2001). Ingestion of bacterially expressed dsRNAs can produce specific and potent genetic interference in Caenorhabditis elegans. *Gene* 263**,** 103-112.

Tiranti, V., Jaksch, M., Hofmann, S., Galimberti, C., Hoertnagel, K., Lulli, L., Freisinger, P., Bindoff, L., Gerbitz, K.D., Comi, G.P., Uziel, G., Zeviani, M., and Meitinger, T. (1999). Loss-of-function mutations of SURF-1 are specifically associated with Leigh syndrome with cytochrome c oxidase deficiency. *Ann Neurol* 46**,** 161-166.

Tischner, C., Hofer, A., Wulff, V., Stepek, J., Dumitru, I., Becker, L., Haack, T., Kremer, L., Datta, A.N., Sperl, W., Floss, T., Wurst, W., Chrzanowska-Lightowlers, Z., De Angelis, M.H., Klopstock, T., Prokisch, H., and Wenz, T. (2015). MTO1 mediates tissue specificity of OXPHOS defects via tRNA modification and translation optimization, which can be bypassed by dietary intervention. *Hum Mol Genet* 24**,** 2247-2266.

Torraco, A., Diaz, F., Vempati, U.D., and Moraes, C.T. (2009). Mouse models of oxidative phosphorylation defects: powerful tools to study the pathobiology of mitochondrial diseases. *Biochim Biophys Acta* 1793**,** 171-180.

Tsang, W.Y., and Lemire, B.D. (2003). The role of mitochondria in the life of the nematode, Caenorhabditis elegans. *Biochim Biophys Acta* 1638**,** 91-105.

Tucker, E.J., Hershman, S.G., Kohrer, C., Belcher-Timme, C.A., Patel, J., Goldberger, O.A., Christodoulou, J., Silberstein, J.M., Mckenzie, M., Ryan, M.T., Compton, A.G., Jaffe, J.D., Carr, S.A., Calvo, S.E., Rajbhandary, U.L., Thorburn, D.R., and Mootha, V.K. (2011). Mutations in MTFMT underlie a human disorder of formylation causing impaired mitochondrial translation. *Cell Metab* 14**,** 428-434.

Tuppen, H.A., Hogan, V.E., He, L., Blakely, E.L., Worgan, L., Al-Dosary, M., Saretzki, G., Alston, C.L., Morris, A.A., Clarke, M., Jones, S., Devlin, A.M., Mansour, S., Chrzanowska-Lightowlers, Z.M., Thorburn, D.R., Mcfarland, R., and Taylor, R.W. (2010a). The p.M292T NDUFS2 mutation causes complex I-deficient Leigh syndrome in multiple families. *Brain* 133**,** 2952-2963.

Tuppen, H.a.L., Blakely, E.L., Turnbull, D.M., and Taylor, R.W. (2010b). Mitochondrial DNA mutations and human disease. *Biochimica et Biophysica Acta (BBA) - Bioenergetics* 1797**,** 113-128.

Uehara, N., Mori, M., Tokuzawa, Y., Mizuno, Y., Tamaru, S., Kohda, M., Moriyama, Y., Nakachi, Y., Matoba, N., Sakai, T., Yamazaki, T., Harashima, H., Murayama, K., Hattori, K., Hayashi, J., Yamagata, T., Fujita, Y., Ito, M., Tanaka, M., Nibu, K., Ohtake, A., and Okazaki, Y. (2014). New MT-ND6 and NDUFA1 mutations in mitochondrial respiratory chain disorders. *Ann Clin Transl Neurol* 1**,** 361-369.

Ugalde, C., Triepels, R.H., Coenen, M.J., Van Den Heuvel, L.P., Smeets, R., Uusimaa, J., Briones, P., Campistol, J., Majamaa, K., Smeitink, J.A., and Nijtmans, L.G. (2003). Impaired complex I assembly in a Leigh syndrome patient with a novel missense mutation in the ND6 gene. *Ann Neurol* 54**,** 665-669.

Uittenbogaard, M., Brantner, C.A., Fang, Z., Wong, L.C., Gropman, A., and Chiaramello, A. (2018). Novel insights into the functional metabolic impact of an apparent de novo m.8993T>G variant in the MT-ATP6 gene associated with maternally inherited form of Leigh Syndrome. *Mol Genet Metab* 124**,** 71-81.

Uziel, G., Moroni, I., Lamantea, E., Fratta, G.M., Ciceri, E., Carrara, F., and Zeviani, M. (1997). Mitochondrial disease associated with the T8993G mutation of the mitochondrial ATPase 6 gene: a clinical, biochemical, and molecular study in six families. *J Neurol Neurosurg Psychiatry* 63**,** 16-22.

Valente, L., Tiranti, V., Marsano, R.M., Malfatti, E., Fernandez-Vizarra, E., Donnini, C., Mereghetti, P., De Gioia, L., Burlina, A., Castellan, C., Comi, G.P., Savasta, S., Ferrero, I., and Zeviani, M. (2007). Infantile encephalopathy and defective mitochondrial DNA translation in patients with mutations of mitochondrial elongation factors EFG1 and EFTu. *Am J Hum Genet* 80**,** 44-58.

Van Erven, P.M., Gabreels, F.J., Ruitenbeek, W., Renier, W.O., Lamers, K.J., and Sloof, J.L. (1987). Familial Leigh's syndrome: association with a defect in oxidative metabolism probably restricted to brain. *J Neurol* 234**,** 215-219.

Van Esveld, S.L., and Huynen, M.A. (2018). Does mitochondrial DNA evolution in metazoa drive the origin of new mitochondrial proteins? *IUBMB Life* 70**,** 1240-1250.

Veerapandiyan, A., Chaudhari, A., Traba, C.M., and Ming, X. (2016). Novel mutation in mitochondrial DNA in 2 siblings with Leigh syndrome. *Neurol Genet* 2**,** e99.

Vempati, U.D., Torraco, A., and Moraes, C.T. (2008). Mouse models of oxidative phosphorylation dysfunction and disease. *Methods* 46**,** 241-247.

Villalon-Garcia, I., Alvarez-Cordoba, M., Suarez-Rivero, J.M., Povea-Cabello, S., Talaveron-Rey, M., Suarez-Carrillo, A., Munuera-Cabeza, M., and Sanchez-Alcazar, J.A. (2020). Precision Medicine in Rare Diseases. *Diseases* 8.

Villanueva-Paz, M., Povea-Cabello, S., Villalon-Garcia, I., Alvarez-Cordoba, M., Suarez-Rivero, J.M., Talaveron-Rey, M., Jackson, S., Falcon-Moya, R., Rodriguez-Moreno, A., and Sanchez-Alcazar, J.A. (2020). Parkin-mediated mitophagy and autophagy flux disruption in cellular models of MERRF syndrome. *Biochim Biophys Acta Mol Basis Dis* 1866**,** 165726.

Villanueva-Paz, M., Povea-Cabello, S., Villalon-Garcia, I., Suarez-Rivero, J.M., Alvarez-Cordoba, M., De La Mata, M., Talaveron-Rey, M., Jackson, S., and Sanchez-Alcazar, J.A. (2019). Pathophysiological characterization of MERRF patient-specific induced neurons generated by direct reprogramming. *Biochim Biophys Acta Mol Cell Res* 1866**,** 861-881.

Viscomi, C., and Zeviani, M. (2019). Breathe: Your Mitochondria Will Do the Rest... If They Are Healthy! *Cell Metab* 30**,** 628-629.

Viscomi, C., and Zeviani, M. (2020). Strategies for fighting mitochondrial diseases. *J Intern Med* 287**,** 665-684.

Wallace, D.C. (1999). Mitochondrial diseases in man and mouse. *Science* 283**,** 1482-1488.

Wedatilake, Y., Brown, R.M., Mcfarland, R., Yaplito-Lee, J., Morris, A.A., Champion, M., Jardine, P.E., Clarke, A., Thorburn, D.R., Taylor, R.W., Land, J.M., Forrest, K., Dobbie, A., Simmons, L., Aasheim, E.T., Ketteridge, D., Hanrahan, D., Chakrapani, A., Brown, G.K., and Rahman, S. (2013). SURF1 deficiency: a multi-centre natural history study. *Orphanet J Rare Dis* 8**,** 96.

Wei, Y., Cui, L., and Peng, B. (2018). Mitochondrial DNA mutations in late-onset Leigh syndrome. *J Neurol* 265**,** 2388-2395.

Wenz, T., Diaz, F., Spiegelman, B.M., and Moraes, C.T. (2008). Activation of the PPAR/PGC-1alpha pathway prevents a bioenergetic deficit and effectively improves a mitochondrial myopathy phenotype. *Cell Metab* 8**,** 249-256.

Weraarpachai, W., Antonicka, H., Sasarman, F., Seeger, J., Schrank, B., Kolesar, J.E., Lochmuller, H., Chevrette, M., Kaufman, B.A., Horvath, R., and Shoubridge, E.A. (2009). Mutation in TACO1, encoding a translational activator of COX I, results in cytochrome c oxidase deficiency and late-onset Leigh syndrome. *Nat Genet* 41**,** 833-837.

Werner, K.G., Morel, C.F., Kirton, A., Benseler, S.M., Shoffner, J.M., Addis, J.B., Robinson, B.H., Burrowes, D.M., Blaser, S.I., Epstein, L.G., and Feigenbaum, A.S. (2009). Rolandic mitochondrial encephalomyelopathy and MT-ND3 mutations. *Pediatr Neurol* 41**,** 27-33.

Wesolowska, M., Gorman, G.S., Alston, C.L., Pajak, A., Pyle, A., He, L., Griffin, H., Chinnery, P.F., Miller, J.A., Schaefer, A.M., Taylor, R.W., Lightowlers, R.N., and Chrzanowska-Lightowlers, Z.M. (2015). Adult Onset Leigh Syndrome in the Intensive Care Setting: A Novel Presentation of a C12orf65 Related Mitochondrial Disease. *J Neuromuscul Dis* 2**,** 409-419.

Willems, J.L., Monnens, L.A., Trijbels, J.M., Veerkamp, J.H., Meyer, A.E., Van Dam, K., and Van Haelst, U. (1977). Leigh's encephalomyelopathy in a patient with cytochrome c oxidase deficiency in muscle tissue. *Pediatrics* 60**,** 850-857.

Worsley, H.E., Brookfield, R.W., Elwood, J.S., Noble, R.L., and Taylor, W.H. (1965). Lactic acidosis with necrotizing encephalopathy in two sibs. *Arch Dis Child* 40**,** 492-501.

Yang, X., Jiang, J., Li, Z., Liang, J., and Xiang, Y. (2021). Strategies for mitochondrial gene editing. *Comput Struct Biotechnol J* 19**,** 3319-3329.

Yang, Y., Wu, H., Kang, X., Liang, Y., Lan, T., Li, T., Tan, T., Peng, J., Zhang, Q., An, G., Liu, Y., Yu, Q., Ma, Z., Lian, Y., Soh, B.S., Chen, Q., Liu, P., Chen, Y., Sun, X., Li, R., Zhen, X., Liu, P., Yu, Y., Li, X., and Fan, Y. (2018). Targeted elimination of mutant mitochondrial DNA in MELAS-iPSCs by mitoTALENs. *Protein Cell* 9**,** 283-297.

Yu, X.L., Yan, C.Z., Ji, K.Q., Lin, P.F., Xu, X.B., Dai, T.J., Li, W., and Zhao, Y.Y. (2018). Clinical, Neuroimaging, and Pathological Analyses of 13 Chinese Leigh Syndrome Patients with Mitochondrial DNA Mutations. *Chin Med J (Engl)* 131**,** 2705-2712.

Zhang, J., Liu, H., Luo, S., Lu, Z., Chavez-Badiola, A., Liu, Z., Yang, M., Merhi, Z., Silber, S.J., Munne, S., Konstantinidis, M., Wells, D., Tang, J.J., and Huang, T. (2017). Live birth derived from oocyte spindle transfer to prevent mitochondrial disease. *Reprod Biomed Online* 34**,** 361-368.

Zinovkin, R.A., Skulachev, M.V., and Skulachev, V.P. (2016). Mitochondrial Genome and Longevity. *Biochemistry (Mosc)* 81**,** 1401-1405.

Zurita-Diaz, F., Galera-Monge, T., Moreno-Izquierdo, A., Fraga, M.F., Ayuso, C., Fernandez, A.F., Garesse, R., and Gallardo, M.E. (2016). Generation of a human iPSC line from a patient with a mitochondrial encephalopathy due to mutations in the GFM1 gene. *Stem Cell Res* 16**,** 124-127.

Chapter 2

3. Quantifying mitochondrial dynamics in patient fibroblasts with multiple developmental defects and mitochondrial disorders

Bakare, A.B., Daniel, J., Stabach, J., Rojas, A., Bell, A., Henry, B., Iyer, S.

3.1. Abstract:

Mitochondria are dynamic organelles that undergo rounds of fission and fusion and exhibit a wide range of morphologies that contribute to the regulation of different signaling pathways and various cellular functions. It is important to understand the differences between mitochondrial structure in health and disease so that therapies can be developed to maintain the homeostatic balance of mitochondrial dynamics. Mitochondrial disorders are multi-systemic and characterized by complex and variable clinical pathologies. The dynamics of mitochondria in mitochondrial disorders are thus worthy of investigation. Therefore, in this study, we performed a comprehensive analysis of mitochondrial dynamics in five patient-derived fibroblasts containing different pathogenic mitochondrial DNA mutations associated with Leigh syndrome. Our results suggest that the most predominant morphological signature for mitochondria in the diseased state is fragmentation; with four out of the five cell lines exhibiting characteristics consistent with fragmented mitochondria. To our knowledge, this is the first comprehensive study that quantifies mitochondrial dynamics in cell lines with a wide array of developmental and mitochondrial disorders. A more thorough analysis of the correlations between mitochondrial dynamics, mitochondrial genome perturbations, and bioenergetic dysfunction will aid in identifying unique morphological signatures of various mitochondrial disorders in the future.

3.2. Introduction

Mitochondria are highly dynamic organelles responsible for a host of cellular functions, which include regulation of oxidative metabolism, control of apoptosis, and generation of signaling metabolites, with the production of adenosine triphosphate (ATP) being the most prominent of functions (Sprenger and Langer, 2019). In live cells, work has shown that ATP production is regulated by remodeling of the mitochondria (McCarron et al., 2013). In healthy cells, mitochondrial structure differs from cell-to-cell, with the difference in morphology dictated by the function of the specific cell (McCarron et al., 2013). Mitochondria undergo rounds of fission and fusion to replenish the content of the organelle and to maintain structural integrity to continue to perform their function (Picard et al., 2013;Ni et al., 2015). Alterations in mitochondrial morphology can cause bioenergetic defects, and underlie a heterogeneous group of human diseases including myopathies (Wallace, 1999), neurodegeneration (Liu and Hajnoczky, 2009;Gao et al., 2017), cancer (Chan, 2006), diabetes mellitus (Ogawa et al., 2003;Duchen, 2004), and a host of other disorders (Picard et al., 2013). Owing to the involvement of mitochondrial dynamics in regulating cellular functions, studies have focused on understanding the relationship between the morphology and function of the mitochondria in health and disease.

Much is still unknown about the role of mitochondrial dynamics in human diseases. However, it has been suggested that in a diseased state, mitochondrial fission and fusion may be modulated as a compensatory mechanism to maintain the pool of healthy mitochondria within cells (Yoneda et al., 1994;Nakada et al., 2001;Rolland et al., 2013;Ni et al., 2015). Mitochondrial fusion allows for replenishment of depleted cellular resources such as lipids, and proteins between organelles, while fission generates new organelles and is involved in mitochondrial quality control (Youle and van der Bliek, 2012). While there have been reports implicating mitochondrial dynamics in neurodegenerative disorders and cardiovascular diseases (Trimmer et al., 2000;Hoppel et al.,

2009), not much is known about the involvement of mitochondrial dynamics in mitochondrial disorders that result from perturbations in the mitochondrial genome.

In this study, we used the mitochondrial network morphology analysis (MiNA) tool (Valente et al., 2017), an Image J macros to analyze the mitochondrial structure of fluorescently labeled human fibroblast cell lines. Live-cells stained with Mitotracker Red CM-H_2Xros (MTR), a dye that localizes in actively respiring mitochondria, were analyzed to quantify mitochondrial morphology in health and disease. We analyzed one control healthy fibroblast and five diseased fibroblast cell lines carrying various mitochondrial DNA (mtDNA) mutations. The diseased cell lines carry some of the most prevalent mutations involved in Leigh syndrome (LS). We analyzed mitochondrial morphologies in these cell lines under coupled and uncoupled respiration conditions, wherein trifluoromethoxy carbonylcyanide phenylhydrazone (FCCP) –a mitochondrial uncoupler was used to induce maximal respiration. FCCP treatment promotes mitochondrial depolarization, subsequently resulting in the fragmentation of mitochondrial networks (Liesa and Shirihai, 2013). Our results suggest that mitochondria from diseased fibroblast cells exhibit various remodeling of their mitochondria to regulate bioenergetic efficiency and energy expenditure, with the most prevalent morphological adaptation being fragmentation in the diseased cell lines. Furthermore, we noticed that the diseased cell lines tend to have fewer actively respiring mitochondria, suggesting reduced mitochondrial mass in the diseased state. Treatment with FCCP resulted in fragmentation in both healthy and diseased cell lines. By observing mitochondrial morphology in the presence and absence of FCCP, our work provides a better understanding of how healthy and diseased cells adapt to changes in ATP demand and supply. To our knowledge, this is the first comprehensive study that quantifies mitochondrial dynamics of cell lines with a wide array of developmental and mitochondrial disorders. These results could give us a broader view on how mitochondrial genome perturbations in the form of various point mutations could contribute to altered mitochondrial dynamics and lead to bioenergetic dysfunction in mitochondrial disorders.

3.3. Results

3.3.1. Clinical information and cell line characteristics

The patient fibroblast cell lines were obtained from five different patients with varying developmental and mitochondrial disorders. Three of the patient cell lines carry point mutations in the MTATP6 subunits (SBG1, SGB2: *T8993G*, SBG3: *T9185C*) of complex V (ATP synthase). Two of the patient cell lines have mtDNA mutations affecting the MTND3 (SBG4-FB: *T10158C*) and MTND5 (SBG5-FB: *T12706C*) subunits of complex I of the electron transport chain. These mutations affecting complex I and V have been implicated in Leigh syndrome (LS) (Taylor et al., 2002;McFarland et al., 2004;Baracca et al., 2007;Iyer et al., 2009;Piekutowska-Abramczuk et al., 2018). LS is a classic mitochondrial disorder that affects mental and motor activity, where disease severity and developmental defects are tied to specific mutations and mutant load (Leigh, 1951;Loeffen et al., 2000;Iyer et al., 2009). The healthy control fibroblast cell line BJ was obtained from the American Type Culture Collection (Manassas, VA, USA). All patient fibroblast cell lines were obtained under approved IRB protocols at the source. We cultured all fibroblast cell lines at passage 8, to minimize variability in our analysis. In general, we observed differences in cellular proliferation rates with the healthy control BJ fibroblasts exhibiting a ~45 hours doubling time, while the diseased lines exhibited a significantly longer (range of 50-100 hours) doubling time (**supplementary figure 7.1.**). The significantly longer doubling time could be attributed to the presence of the mtDNA mutations that also correlate with reduced bioenergetics.

3.3.2. Descriptors of mitochondrial morphology

Understanding mitochondrial morphology is important in determining the health status of the cell with descriptors such as tubular, fragmented, and hyperfused (Tilokani et al., 2018) often used to characterize mitochondrial morphology. These descriptors are important in identifying

different mitochondrial morphologies in healthy and diseased cells and are also invaluable in making predictions on mitochondrial dynamics as it relates to cellular health. In our study, we have used the Mitochondrial Network Analysis (MiNA) toolset, a relatively simple pair of macros making use of existing ImageJ plug-ins, allowing for semi-automated analysis of mitochondrial morphologies in cultured mammalian cells (Valente et al., 2017). MiNA combines rods, punctate, and large/round-shaped morphology in a group as Individuals, while branched morphologies are categorized as networks (**Figure 3.3.2.**). Previous studies have indicated fragmented mitochondria to be the predominant morphology observed in mitochondrial dysfunctions (Kiryu-Seo et al., 2016;Zemirli et al., 2018), while fused mitochondria are associated with cell survival mechanisms (Rambold et al., 2011;Wai and Langer, 2016). It is therefore imperative that we identify these different morphologies to further delineate their contributions to cellular health and disease, in the context of mitochondrial disorders.

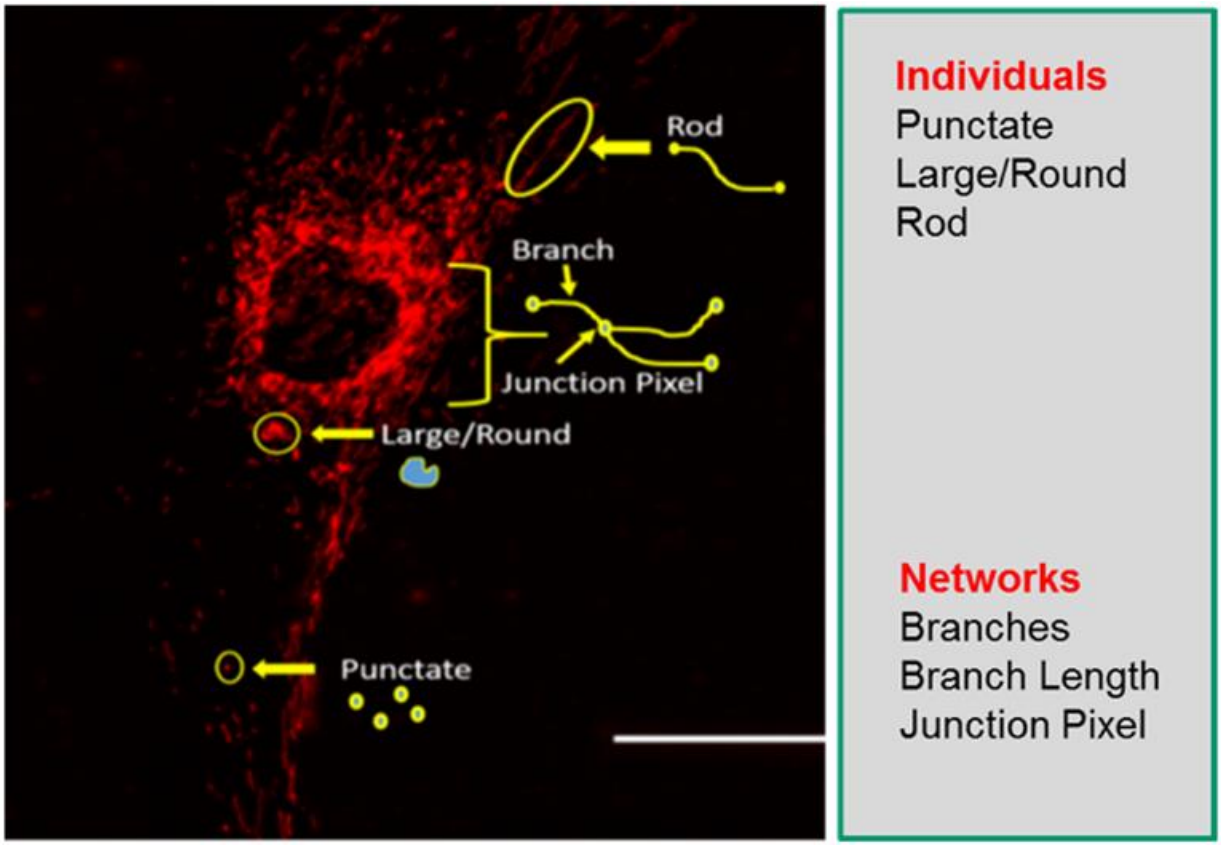

Figure 3.3.2. Mitochondrial morphology descriptors. The mitochondria morphology is classified as Individuals or Networks. Individuals consist of structures without a junction pixel while networks contain branches with one or more junction pixels.

3.3.3. Healthy fibroblast cell lines undergo mitochondrial fission when substrate is abundant

Mitochondrial morphology in fibroblast cell lines was determined with the aid of live-cell fluorescent microscopy. To streamline our procedures, we first analyzed with healthy BJ fibroblasts which are expected to exhibit various morphologies balanced between network and fragmented mitochondria (**Figure 3.3.3.a**). In addition, we also treated the fibroblasts with FCCP to promote mitochondrial fragmentation. When the mitochondria undergo fission, fragmentation of networks occurs. Conversely, mitochondrial fusion results in the formation of larger networks of mitochondria. The predictions for changes to be observed in mitochondrial morphology during fission and fusion events are detailed in **Table 3.3.3.** We predicted that healthy cells should be

able to rapidly remodel their mitochondria to maintain energy homeostasis. This is evident by an increase in the number of individuals, and networked mitochondria (**Table 3.3.3.**), and a subsequent decrease in the mean branch lengths and network size. Our results support this prediction, as we recorded a 45% and 32% increase in the number of individuals and number of networks (**Figure 3.3.3.b**). Total respiring mitochondria, which is the sum of individual and networked mitochondria also increased by 46% in the FCCP treatment group. Although not statistically significant, mean branch length, and mean network size with FCCP treatment were 7% and 5% lower respectively. Using the MiNA macros, we were able to faithfully observe the dynamic nature of mitochondria in BJ healthy fibroblast cell lines.

Table 3.3.3. Mitochondrial morphology predictions with MiNA descriptors. Mitochondrial fission and fusion cause changes to mitochondrial morphology. The most predominant process dictates mitochondrial morphology and can provide an insight into mitochondrial health.

Mitochondrial morphology/ MiNA descriptors	Number of individuals	Number of networks	Mean Branch Length	Mean Network Size
Fission	Increase	Increase[1]	Decrease	Decrease
Fusion	Decrease	Decrease[2] / Increase[3]	Increase	Increase

[1]Smaller networks; [2]Larger networks form; [3]Individuals form networks

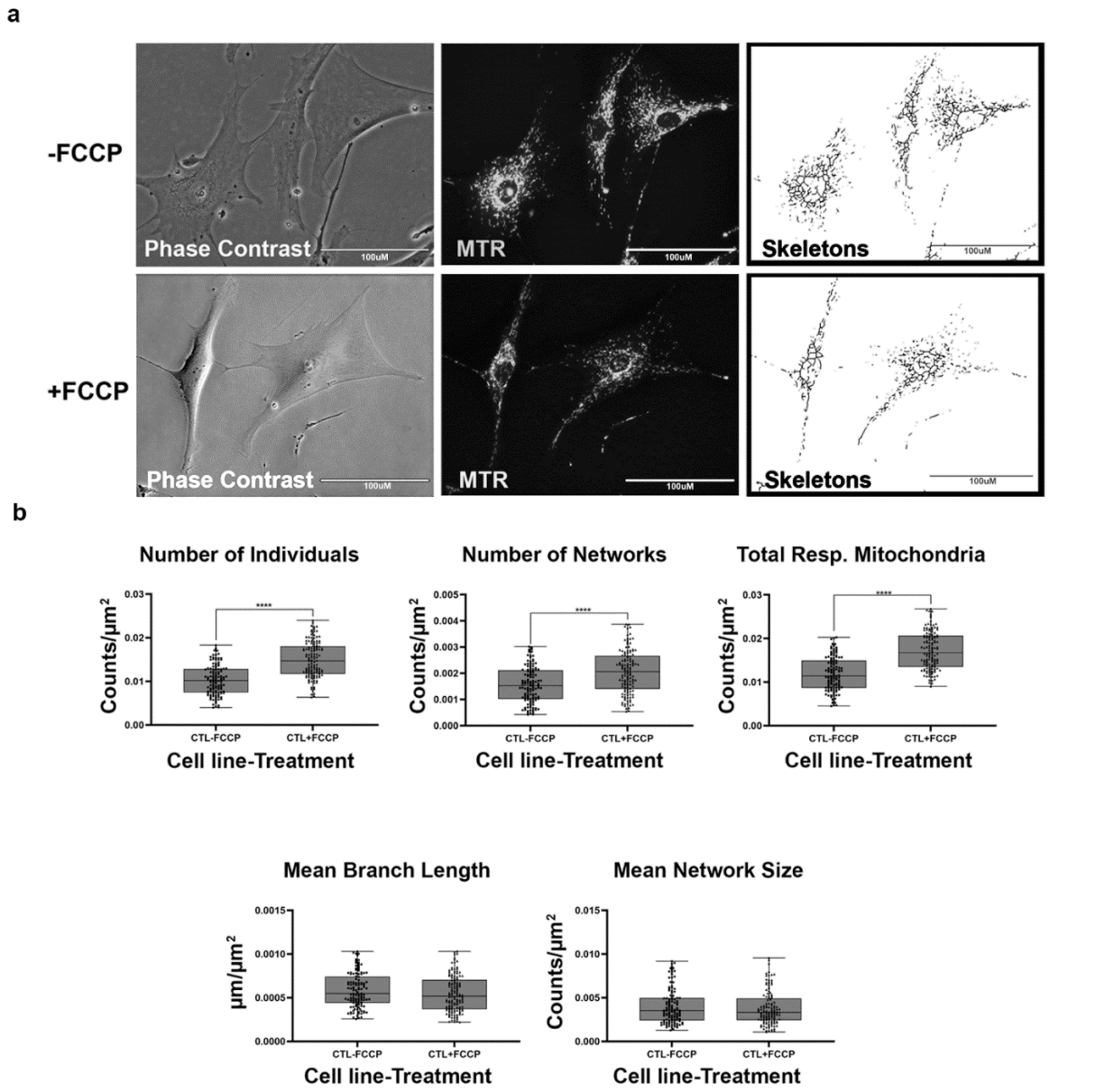

Figure 3.3.3. Mitochondrial morphology of healthy BJ FB in the absence and presence of FCCP. a) Representative images of fibroblast cell lines stained with Mitotracker Red CM-H2Xros (MTR), a dye that localizes to actively respiring mitochondria. The top images are phase contrast, RFP, and skeletonized images of healthy control cell lines without FCCP treatment. The bottom images are phase contrast, RFP, and skeletonized images of healthy control cell lines with FCCP treatment. b) MiNA descriptors showing differences in mitochondrial morphology in untreated and FCCP treated groups. FCCP treatment resulted in mitochondrial fission and resulted in a significant increase in the number of individuals, networks, and total respiring mitochondria. The mean branch length and mean network size are lower after FCCP treatment, albeit not statistically significant. All data are representative of 10-14 images taken from five independent dishes per treatment group. The bars represent minimum and maximal values, and each black dot represents different data points. ****p<0.0001. Scale bar = 100 µm.

3.3.4. Fibroblasts with *T8993G*, *T9185C* mutations in *MTATP6* gene impacting complex V have smaller, fragmented mitochondria

Having confirmed that the MiNA toolset would detect changes in mitochondrial dynamics in healthy control BJ fibroblasts, we proceeded to analyze differences between healthy control and diseased cell lines carrying mutations in subunits of the Complex V-ATP synthase. We analyzed three patient fibroblast cell lines (SBG1, SBG2: *T8993G*; SBG3: *T9185C*) carrying mutations that are most prevalent in patients with LS (Castagna et al., 2007;Debray et al., 2007). We analyzed mitochondrial morphology in the diseased fibroblasts under basal conditions and after FCCP treatment. Although not statistically significant, SBG1 (*T8993G*) cell lines had slightly more fragmented mitochondria than the healthy control (**Figure 3.3.4.1.a**). This is evident by the 4% and 1% increase in both the number of individuals and networks and the subsequent decrease in mean branch length and mean network size (**Figure 3.3.4.1.b**). However, the SBG2-FB (*T8993G*) cell line with the same mutation had a different mitochondrial profile (**Figure 3.3.4.2.a-b**). Both SBG2-FB (*T8993G*) and SBG3-FB (*T9185C*) (**Figure 3.3.4.3.a-b**) had total respiring mitochondria counts that were lower than those of the control BJ-FB suggesting fewer actively respiring mitochondria. Although there was a trend towards less individual and networked mitochondria in SBG2-FB (*T8993G*) and SBG3-FB (*T9185C*) relative to the control fibroblasts, all diseased lines had lower mean branch length and mean network size, supporting the presence of more fragmented morphology in the diseased fibroblasts. Treatment with FCCP resulted in fragmentation in both SBG1-FB (*T8993G*) and SBG3-FB (*T9185C*); with both of these cell lines following the same trend as seen in the healthy control BJ-FB. However, SBG2-FB (*T8993G*) was not as responsive to FCCP treatment; and there was no marked increase in either number of individual or networked mitochondria ((**Figure 3.3.4.2.b**). Furthermore, the mean branch length and mean network size exhibited similar values between the untreated and FCCP treatment groups. Together these results indicate that

the presence of the same mutations could result in different compensatory responses by the mitochondria and variable bioenergetic demand within the fibroblasts could result in different mitochondrial dynamics.

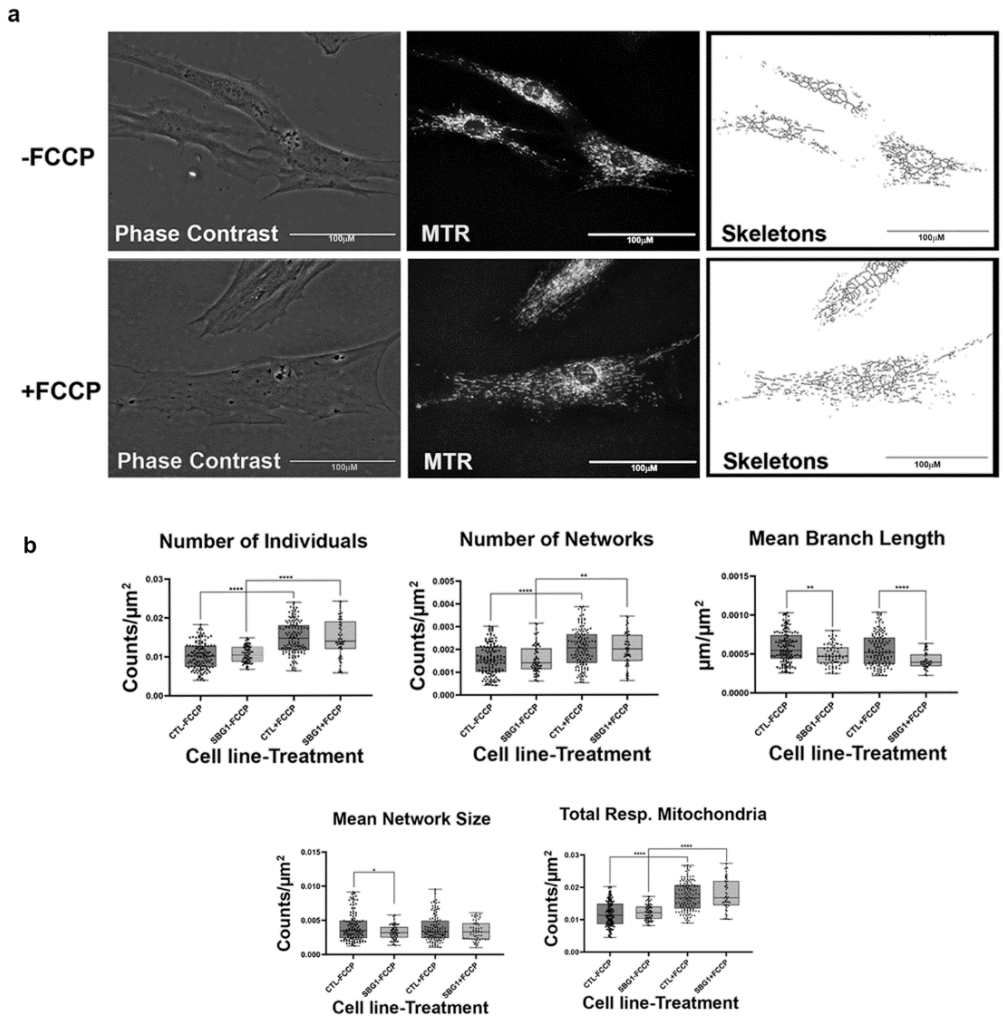

Figure 3.3.4.1. Mitochondrial morphology of SBG1-FB (*T8993G*) in the absence and presence of FCCP. a) Representative images of SBG1-FB (*T8993G*) cell lines stained with MTR. The top images are phase contrast, RFP, and skeletonized images of SBG1-FB (*T8993G*) without FCCP treatment. The bottom images are phase contrast, RFP, and skeletonized images of SBG1-FB with FCCP treatment. b) Although SBG1-FB (*T8993G*) cell lines have a comparable number of individual and networked mitochondria to control, the mitochondria in these lines are smaller. This is evident in the significant decrease in mean branch length and mean network size relative to control under basal conditions, without FCCP treatment. Treatment with FCCP resulted in mitochondrial fission, with SBG1-FB (*T8993G*) showing similar response to FCCP like the healthy control. All data are representative of 10-14 images taken from three independent dishes per treatment group. The bars represent minimum and maximal values, and each black dot represents different data points. ****p<0.0001, **p<0.01, *p<0.05. Scale bar = 100 µm.

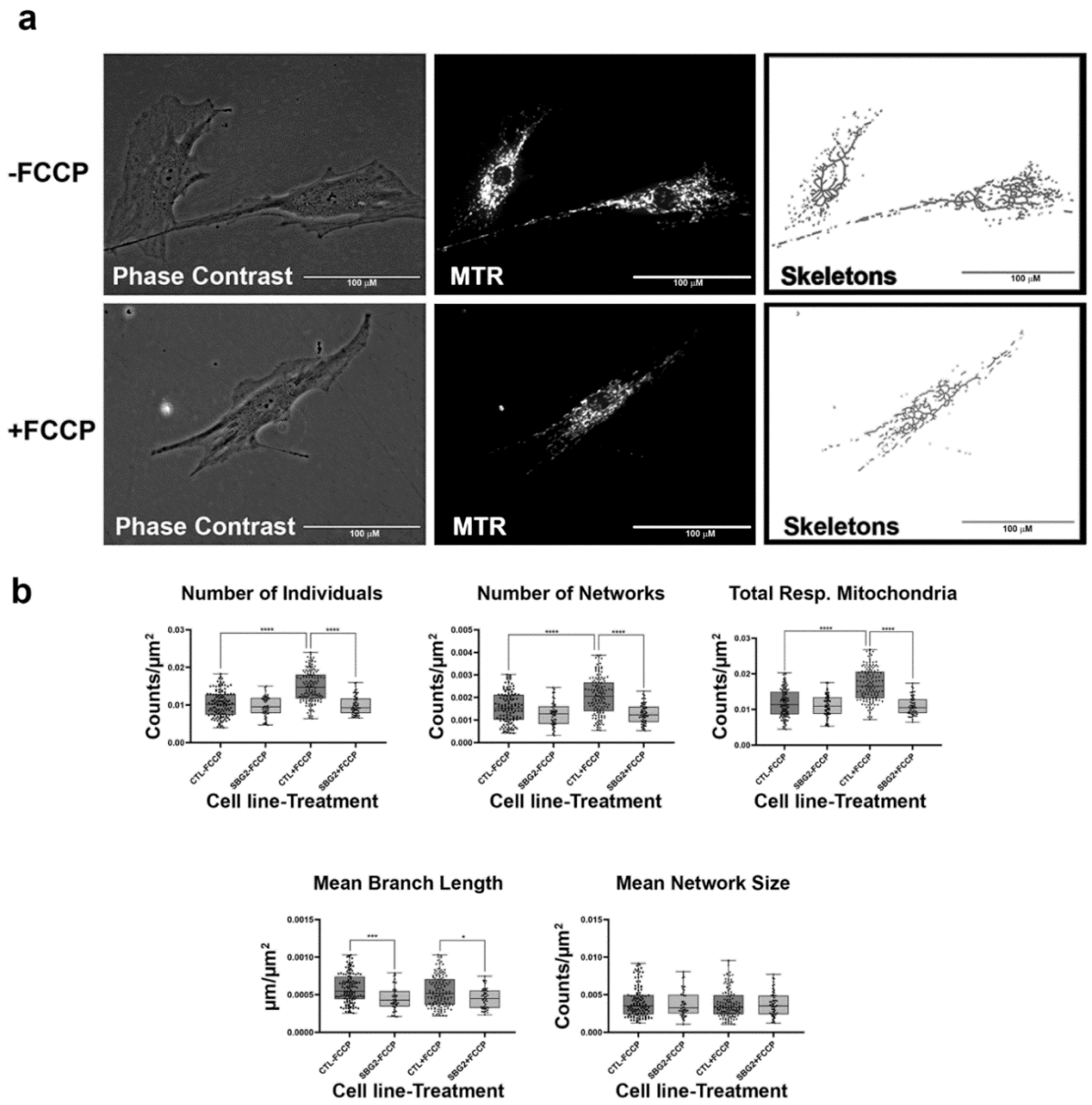

Figure 3.3.4.2. Mitochondrial morphology of SBG2-FB (*T8993G*) in the absence and presence of FCCP. a) Representative images of SBG2-FB (*T8993G*) fibroblast cell lines stained with MTR. The top images are phase contrast, RFP, and skeletonized images of SBG2-FB (*T8993G*) without FCCP treatment. The bottom images are phase contrast, RFP, and skeletonized images of SBG2-FB (*T8993G*) with FCCP treatment. b) SBG2-FB (*T8993G*) have a slightly lower number of individual and networked mitochondria compared to control BJ-FB. The significantly lower mean branch length relative to control fibroblasts under basal conditions further suggests fragmentation. SBG2-FB (*T8993G*) are not responsive to FCCP treatment. All data are representative of 10-14 images taken from three independent dishes per treatment group. The bars represent minimum and maximal values, and each black dot represents different data points. ****p<0.0001, ***p<0.001, *p<0.05. Scale bar = 100 µm.

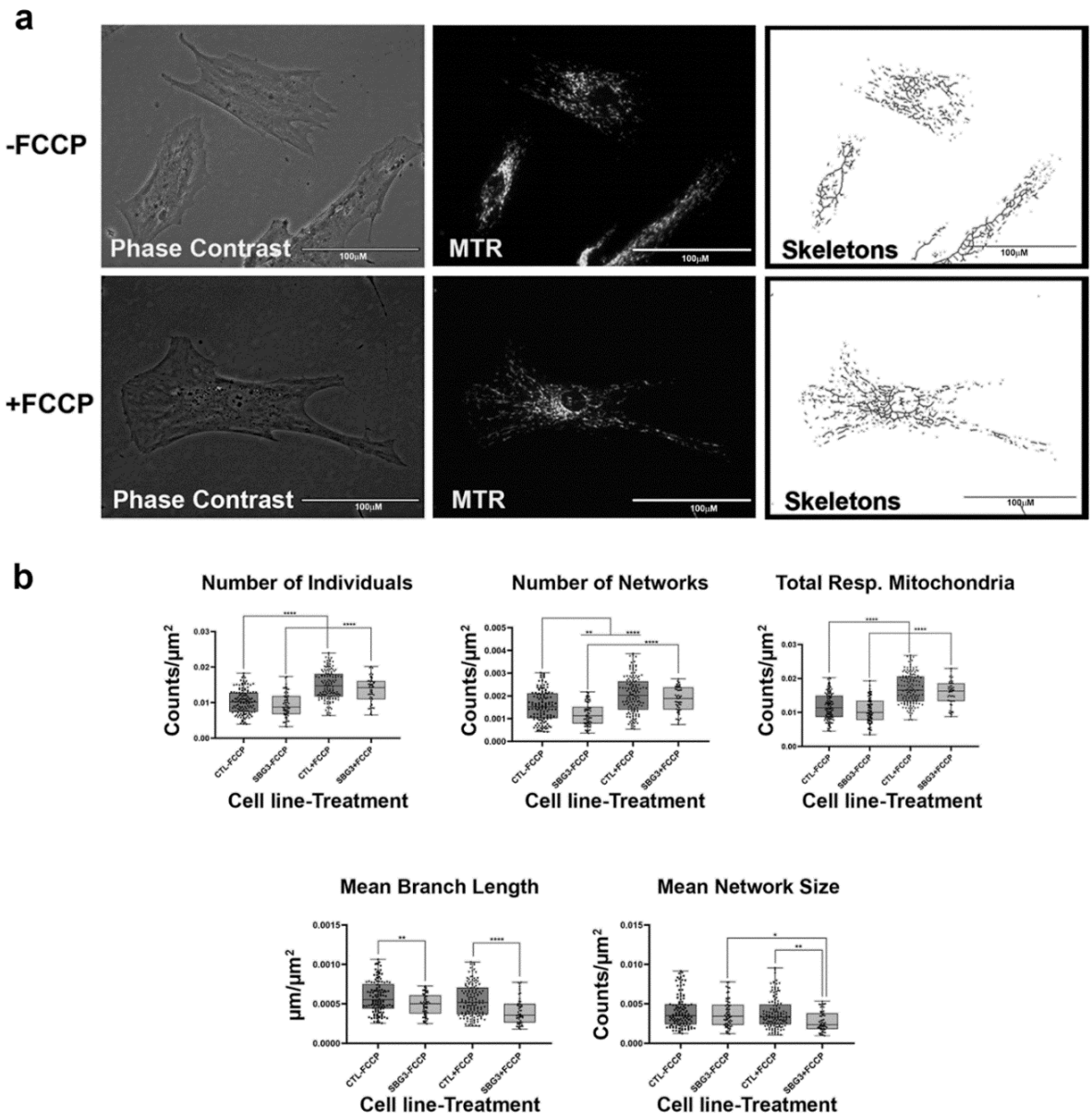

Figure 3.3.4.3. Mitochondrial morphology of SBG3-FB (*T9185C)* in the absence and presence of FCCP. a) Representative images of SBG3-FB (*T9185C*) stained with MTR. The top images are phase contrast, RFP, and skeletonized images of SBG3-FB (*T9185C*) without FCCP treatment. The bottom images are phase contrast, RFP, and skeletonized images of SBG3-FB (*T9185C*) with FCCP treatment. b) While the number of individuals in SBG3-FB (*T9185C*) is comparable to the healthy control BJ-FB, the number of networks is significantly lower. This shows that SBG3-FB (*T9185C*) have fewer networks, with significantly lower mean branch length further suggesting that the networks have smaller branches. Together, this demonstrates a more fragmented morphology in SBG3-FB (*T9185C*) with FCCP treatment resulting in more fragmentation as expected. All data are representative of 10-14 images taken from three independent dishes per treatment group. The bars represent minimum and maximal values, and each black dot represents different data points. ****p<0.0001, **p<0.01, *p<0.05. Scale bar = 100 µm.

3.3.5. Fibroblasts with *T12706C* mutation in the *MTND5* gene exhibit hyperfused mitochondria

We next wanted to determine how mutations in other complexes that impact mitochondrial function affect mitochondrial morphology. We assessed this using two patient fibroblast cell lines with mutations affecting subunits of complex I of the electron transport chain. The SBG4-FB (*T10158C*) cell line has the *T10158C* point mutation while the SBG5-FB (*T12706C*) has the *T12706C* point mutation affecting MTND3 and MTND5 subunits respectively. On average both SBG4-FB (*T10158C*) and SBG5-FB (*T12706C*) trended towards having fewer actively respiring mitochondria than the healthy control BJ-FB, as evidenced by the relatively lower total respiring mitochondria (**Figure 3.3.5.1. & 3.3.5.2**). This difference is more pronounced in the SBG5-FB (*T12706C*), which has a 37% decrease compared to the 9% decrease recorded for SBG4-FB (*T10158C*). As expected, FCCP treatment resulted in fragmented mitochondria in the SBG4-FB (*T10158C*) (**Figure 3.3.5.1.b**). The SBG5-FB (*T12706C*) exhibit a hyperfused morphology (**Figure 3.3.5.2.b**), under basal conditions with significantly elevated ($p<0.0001$) mean branch length and mean network size compared to healthy control BJ fibroblasts. FCCP treatment reversed this phenotype, with mean branch length and mean network size within the SBG5-FB (*T12706C*) group decreased by 21% and 14% respectively after FCCP treatment. This is consistent with mitochondria fragmentation by FCCP, breaking down the larger networks of mitochondria in this cell line. Unlike what we observed with the SBG1-FB (*T8993G*), SBG2-FB (*T8993G*), SBG3-FB (*T9185C*) (with mutations impacting Complex V), SBG4-FB (*T10158C*) & SBG5-FB (*T12706C*) (with mutations impacting Complex I) appear to exhibit different morphologies. These differences could be attributed to the location of the subunits affected by each mutation. The mutation in SBG5-FB (*T12706C*) may affect the function of the mitochondria more than that of SBG4-FB (*T10158C*), requiring remodeling of the mitochondria to maintain optimal function of the respiratory chain.

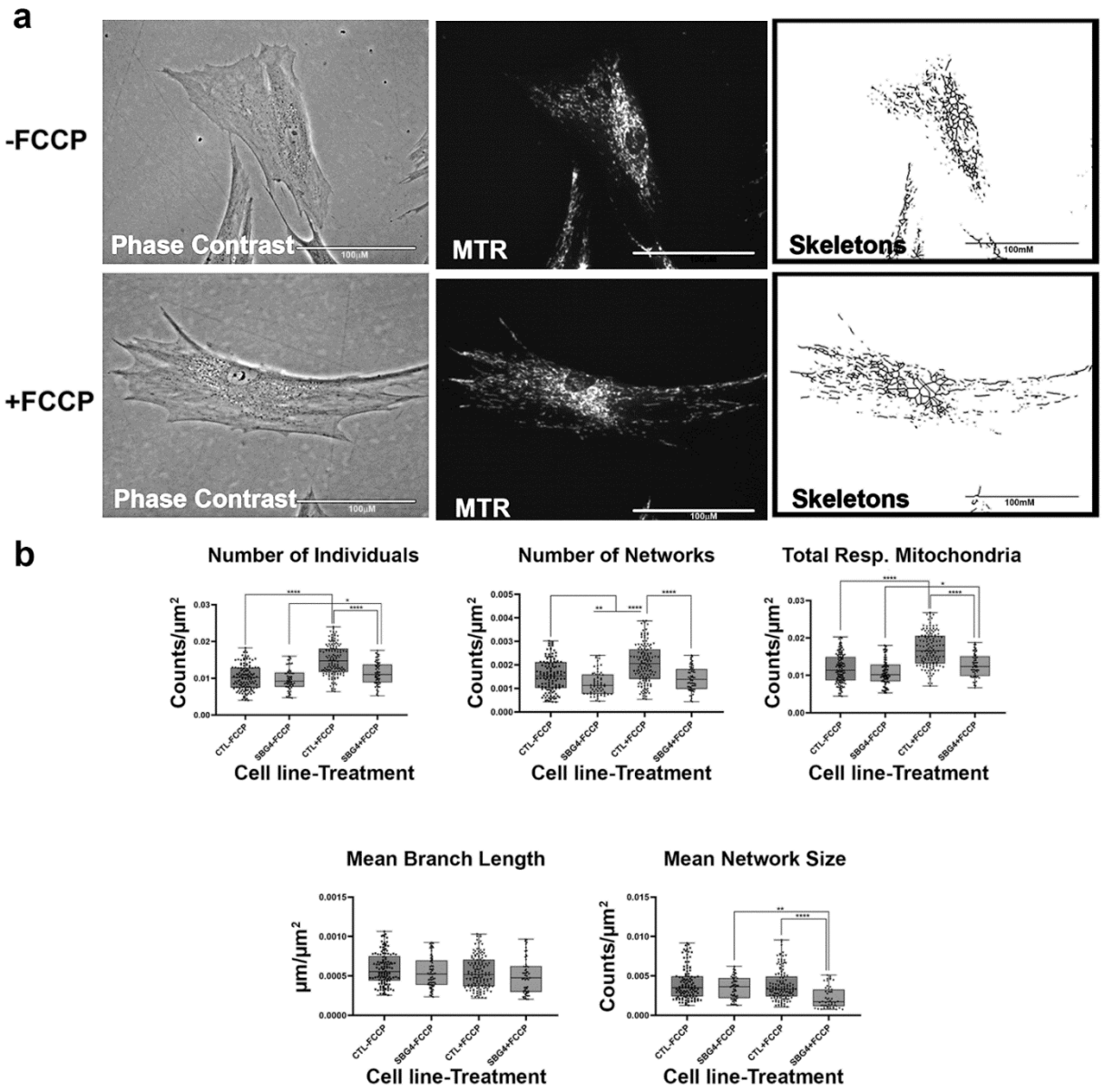

Figure 3.3.5.1. Mitochondrial morphology of SBG4-FB (*T10158C*) in the absence and presence of FCCP. a) Representative images of SBG4-FB (*T10158C*) cell lines stained with MTR. The top images are phase contrast, RFP, and skeletonized images of SBG4-FB (*T10158C*) without FCCP treatment. The bottom images are phase contrast, RFP, and skeletonized images of SBG4-FB (*T10158C*) with FCCP treatment. b) Aside from having fewer networks, SBG4-FB (*T10158C*) are not significantly different from the control BJ-FB. However, they are also responsive to FCCP treatment like the healthy control BJ fibroblasts. All data are representative of 10-14 images taken from three independent dishes per treatment group. The bars represent minimum and maximal values, and each black dot represents different data points. ****p<0.0001, **p<0.01, *p<0.05. Scale bar = 100 µm.

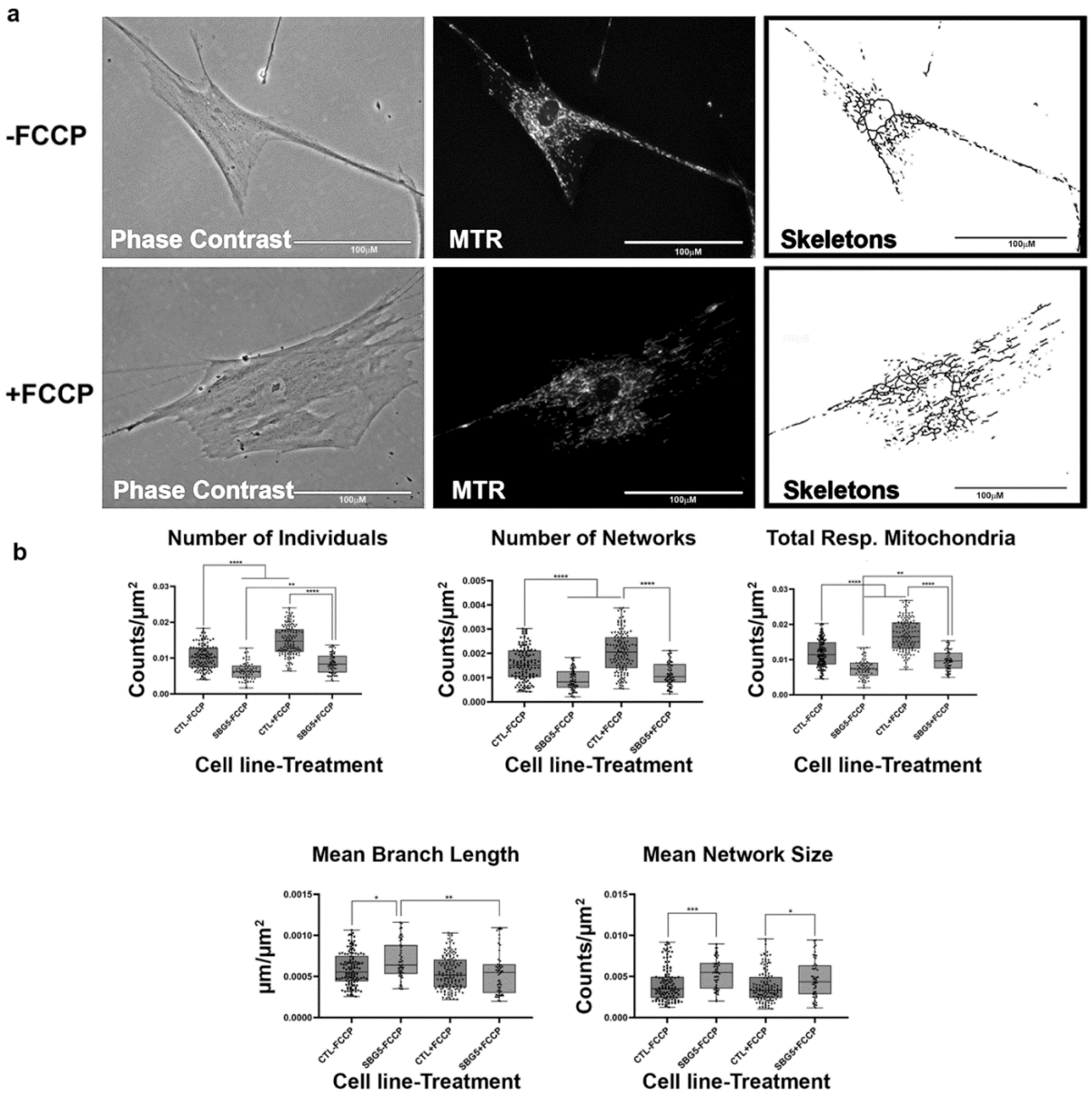

Figure 3.3.5.2. Mitochondrial morphology of SBG5-FB (*T12706C*) in the absence and presence of FCCP. a) Representative images of SBG5-FB (*T12706C*) cell lines stained with MTR. The top images are phase contrast, RFP, and skeletonized images of SBG5-FB (*T12706C*) without FCCP treatment. The bottom images are phase contrast, RFP, and skeletonized images of SBG5-FB (*T12706C*) with FCCP treatment. b) The amount of actively respiring mitochondria in SBG5-FB (*T12706C*) is lower than those of the healthy control BJ-FB. The significantly lower number of individuals, network, and total respiring mitochondria in the SBG5-FB (*T12706C*) support this observation. The SBG5-FB (*T12706C*) also have hyperfused mitochondria, as they have longer branches and more branches within their networks. All data are representative of 10-14 images taken from three independent dishes per treatment group. The bars represent minimum and maximal values, and each black dot represents different data points. ****p<0.0001, ***p<0.001, **p<0.01, *p<0.05. Scale bar = 100 µm.

3.3.6. Mitochondrial membrane potential was decreased in all LS fibroblasts

To investigate how the changes in mitochondrial dynamics affect mitochondrial function, we recorded mitochondrial membrane potential (MMP) in the diseased and healthy control fibroblast cell lines. We hypothesized that MMP would be perturbed in the diseased cell lines by different mechanisms. MMP generated by proton pumps at complexes I, III, and IV is an essential component in the process of energy storage (Mitchell, 1966;Zorova et al., 2018). Flow cytometry methods have been used to measure MMP with tetramethylrhodamine, ethyl ester (TMRE) in live cells with no quenching effect (Scaduto and Grotyohann, 1999). TMRE is a positively charged dye that is attracted to the negative potential across the inner mitochondrial membrane and thus accumulates in functionally active mitochondria in live cells (Cottet-Rousselle et al., 2011). As active mitochondria maintain a net negative charge in the matrix, TMRE is sequestered in the matrix of these mitochondria. Depolarized or inactive mitochondria are not able to sequester TMRE as the MMP is compromised in these mitochondria. In our study, MMP was measured as mean fluorescent intensity (MFI) in all cell lines. Results indicate a significant ($p<0.0001$) decrease in MMP by 83% in SBG1-FB (*T8993G*), 74.13% in SBG2-FB (*T8993G*), 99.23% in SBG3-FB (*T9185C*), 80.47% in SBG4-FB (*T10158C*), 84.92% in SBG5-FB (*T12706C*) compared to healthy control BJ-FB cells (**Figure 3.3.6.a&c**). Although the uncoupler, cyanide p-trifluoromethoxyphenylhydrazone (FCCP) decreased the MMP significantly for most of the diseased cell lines relative to control BJ-FB ($p<0.05$), SBG2-FB (*T8993G*) was not significantly different from the healthy control BJ-FB (**Figure 3.3.6.b,d**).

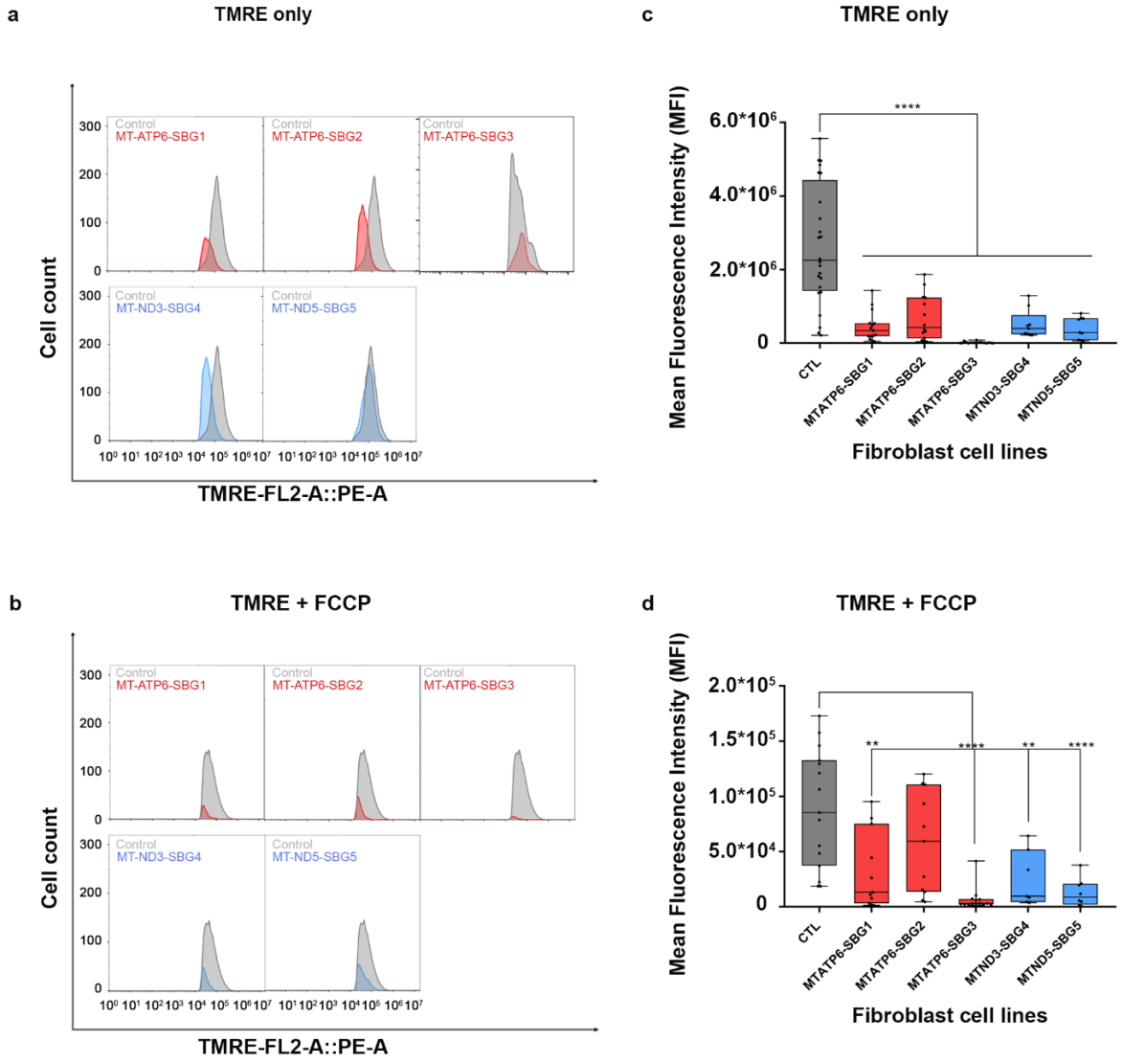

Figure 3.3.6 Mitochondrial membrane potential (MMP) analysis of BJ-FB and LS fibroblast cell lines. Using flow cytometry, along with membrane-potential sensitive dye (TMRE), MMP was evaluated. Representative flow cytometry histogram of five fibroblasts (SBG1-5 and Control BJ) (a) stained with TMRE only (b) stained with TMRE after treatment with FCCP. Mean fluorescence intensity (MFI) was calculated based on three independent runs and are shown for (Control BJ-FB in grey; SBG1-FB (*MTATP6-T8993G*), SBG2-FB (*MTATP6-T8993G*), SBG3-FB (*MTATP6-T9185C*) in red; SBG4-FB (*MTND3-T10158C*), and SBG5-FB (*MTND5-T12706C*) in blue) all samples (c) stained with TMRE only (d) stained with TMRE after treatment with FCCP. ** p<0.01, ****p<0.00001.

3.4. Discussion

Mitochondria are a dynamic organelle that performs a plethora of cellular processes including ATP production, regulation of ions, apoptosis, and cellular signaling; processes that depend on tight regulation of mitochondrial shapes and ultrastructure (Gomes et al., 2011;Sprenger and Langer, 2019). Recent studies are providing evidence that highlights the importance of mitochondrial dynamics in various diseases (Chan, 2006;Hoppel et al., 2009;Gao et al., 2017;Harwig et al., 2018). Additionally, studies have demonstrated the mitochondria's ability to display various net morphologies, depending on the cell type and/or metabolic state (Willems et al., 2015). Under physiological conditions, a balance between fission and fusion helps facilitate normal mitochondrial function (**Figure 3.4.**). However, in a diseased/stressed state, our findings indicate that the mitochondrial dynamics can be predisposed to an overt fission or fusion rate, depending upon the mitochondrial mutation. Under these conditions, the mitochondria response that upregulates fission or fusion mechanisms results in a fragmented or hyperfused morphology respectively (**Figure 3.4.**). In a fragmented state, mitochondria are more spherical, rounded individuals, while hyperfused mitochondria morph into large networks (**Figure 3.4.**). The degree to which mitochondria in a cell undergo such alterations could vary depending on various factors. Therefore, understanding the role of mitochondrial dynamics in various mitochondrial disorders could be instrumental in filling the knowledge gap that exists in the context of the relationship between mtDNA mutations/deletions and mitochondrial morphology.

Previous studies have focused on mitochondrial dynamics in various diseases (Koopman et al., 2005;Hoppel et al., 2009;Willems et al., 2015;Valente et al., 2017;Tokuyama et al., 2020) and have provided key insights on its importance in the context of understanding changes that occur during pathological states. However, this is the first study that provides a comprehensive view of mitochondrial morphology and dynamics across different mitochondrial disorders based on an analysis of five fibroblasts derived from patients diagnosed with LS. To ensure that the MiNA tool

that quantifies mitochondrial morphology based on networked and unbranched mitochondria (Valente et al., 2017) was effective in our analysis, we treated healthy control cell lines with FCCP. FCCP is an uncoupler that stimulates maximal respiratory capacity and stresses the mitochondria, consequently causing mitochondrial network fragmentation (Legros et al., 2002;Liesa and Shirihai, 2013). Treatment of the control fibroblast cell lines with FCCP resulted in a significant increase in the number of individuals, and networks (**Figure 3.3.3.b**). This increase coupled with a 7% and 5% decrease in mean branch length and mean network size respectively confirms mitochondrial fragmentation induced by FCCP. Total respiring mitochondria, the sum of the number of individuals and networks also increased significantly; a result that is consistent with previous studies that have suggested that fragmentation is advantageous for uncoupled respiration (Goyal et al., 2007;Liesa and Shirihai, 2013).

After confirming that MiNA is sensitive and can be used to characterize mitochondrial morphology, we used it to quantify the morphology of the diseased fibroblast cell lines containing specific mutations. Across all five cell lines with different mitochondrial disorders, three have the same mitochondrial morphology profile when compared to the healthy BJ control fibroblast (**Table 3.4.**). In these cell lines (SBG2-FB (*T8993G*), SBG3-FB (*T9185C*), and SBG4-FB (*T10158C*)), there is a trend towards smaller fragmented mitochondria, with a relatively lower number of individuals, networks, mean branch length, mean network size, and total respiring mitochondria. The shorter branch length and fewer network branches suggest that the networks of mitochondria in these cell lines are smaller than observed in the healthy control BJ fibroblasts. Even in the other fibroblast cell line (SBG1-FB (*T8993G*)) that have slightly different profiles, we still observe a significant decrease in the mean branch length. These results suggest that the fibroblasts that contain specific mtDNA mutations exhibit mitochondrial fragmentation, with only SBG5-FB (*T12706C*) fibroblast cell lines deviating from this morphology profile. In the SBG5-FB (*T12706C*) cell lines, the mean branch length and mean network size are significantly greater than the healthy control with the potential for *MTND5* mutation in this cell line favoring mitochondrial fusion.

Therefore, we surmise that the SBG5-FB (*T12706C*) cell lines exhibit an extreme form of fusion, with SBG5-FB (*T12706C*) cell lines exhibiting hyperfused morphology.

When the cell lines were treated with FCCP, we noted that some of the diseased cell lines exhibited the same response to FCCP as the healthy control cell lines, while others did not. This is in line with our observations of basal and maximal respiration values based on oxygen consumption rate (OCR) measurements using a Seahorse Flux Analyzer. The basal respiration values were significantly reduced for 4 out of the 5 fibroblasts, while only SBG1-FB (*T8993G*) exhibited a slight increase when compared with healthy control BJ-FB. Upon addition of FCCP, the maximal respiration values were significantly increased for 3 of the fibroblasts (SBG1-FB (*T8993G*), SBG3-FB (*T9185C*), and SBG4-FB (*T10158C*)), reduced for SBG2-FB (*T8993G*), and SBG5-FB (*T12706C*) exhibited no change when compared with healthy control BJ-FB. These results indicate the presence of differential respiration rates based on specific mtDNA mutations and deletions in the different disease fibroblasts. (Bakare and Iyer, Personal communication). A common view of mitochondrial disorders harboring mtDNA mutations is that there is a direct correlation between disease severity and outcomes to the degree of heteroplasmy. Based on comprehensive next-generation sequencing analysis, we have observed varying heteroplasmy levels (between 25-95%) in the different fibroblasts, consistent with a recent study that noted that the phenotypic spectrum of mitochondrial disorders did not directly correlate with the degree of mutation heteroplasmy (Stendel et al., 2020).

Our findings support previous results where fragmented mitochondria are the predominant morphology in the diseased state (Liu and Hajnoczky, 2011;Wu et al., 2011;Srinivasan et al., 2017;Tokuyama et al., 2020). In addition, the mitochondrial functional analysis based on mitochondrial membrane potential (MMP) measurements demonstrates the differences that exist between diseased and healthy states. This is in line with numerous studies that have demonstrated that changes in MMP and mitochondrial morphological alterations often occur in parallel (Mortiboys et al., 2008;Iannetti et al., 2015;Esteras et al., 2020). Our study for the first

time has characterized mitochondrial morphology across five different patient cell lines with varying mitochondrial disorders. Our results describe a strong relationship between mtDNA genome perturbations and alterations in mitochondrial morphology in these patient fibroblast cell lines. While analysis using MiNA was able to provide us with the necessary information required for this comprehensive comparative study, there are still some limitations to this tool. For example, MiNA groups round, punctate, and rods together as individuals. It would be beneficial to distinguish between fragmentations that result in the formation of more round, punctate mitochondria as opposed to rods, as this would help with better delineation of the mitochondrial dynamics in diseased cell lines. In addition, comparative analysis has been conducted with one healthy control fibroblast (BJ-FB) cell line. Its use in these studies was based on its neonatal origin and used in the context of comparing with disease fibroblasts related to 'pediatric' mitochondrial disorders. Future studies will be conducted with multiple control fibroblasts that will allow us to address gender and age as well as allow comparison of mitochondrial dynamics across the lifespan. Nevertheless, this quantitative analysis allowed us to identify differences in mitochondrial dynamics in fibroblasts that exhibit candidate mtDNA mutations. In the long-term, we hope that a thorough evaluation of mitochondrial dynamics along with correlations with bioenergetic and genetic analyses will aid in identifying the 'signature' of complex mitochondrial disorders and contribute to the development of effective therapies.

Table 3.4. Mitochondrial morphology summary for fibroblast cell lines. Comparison of mitochondrial morphology of diseased and healthy fibroblast cell lines under basal conditions. This result suggests that diseased cell lines tend to have fewer respiring mitochondria with small branches and fragmented networks. In some cases, however, as seen in SBG5-FB (*T12706C*), hyperfusion serves as a compensatory mechanism. * is used to signify data that is statistically significant.

Cell Line	Mutation/Deletion	Number of individuals	Number of networks	Mean Branch Length	Mean Network Size	Total Respiring Mitochondria
SBG1	*MTATP6* (8993T>G)	↑	↑	↓*	↓	↑
SBG2	*MTATP6* (8993T>G)	↓	↓	↓*	↓	↓
SBG3	*MTATP6* (9185T>C)	↓	↓*	↓	↓	↓
SBG4	*MTND3*	↓	↓*	↓	↓	↓
SBG5	*MTND5*	↓*	↓*	↑*	↑*	↓*

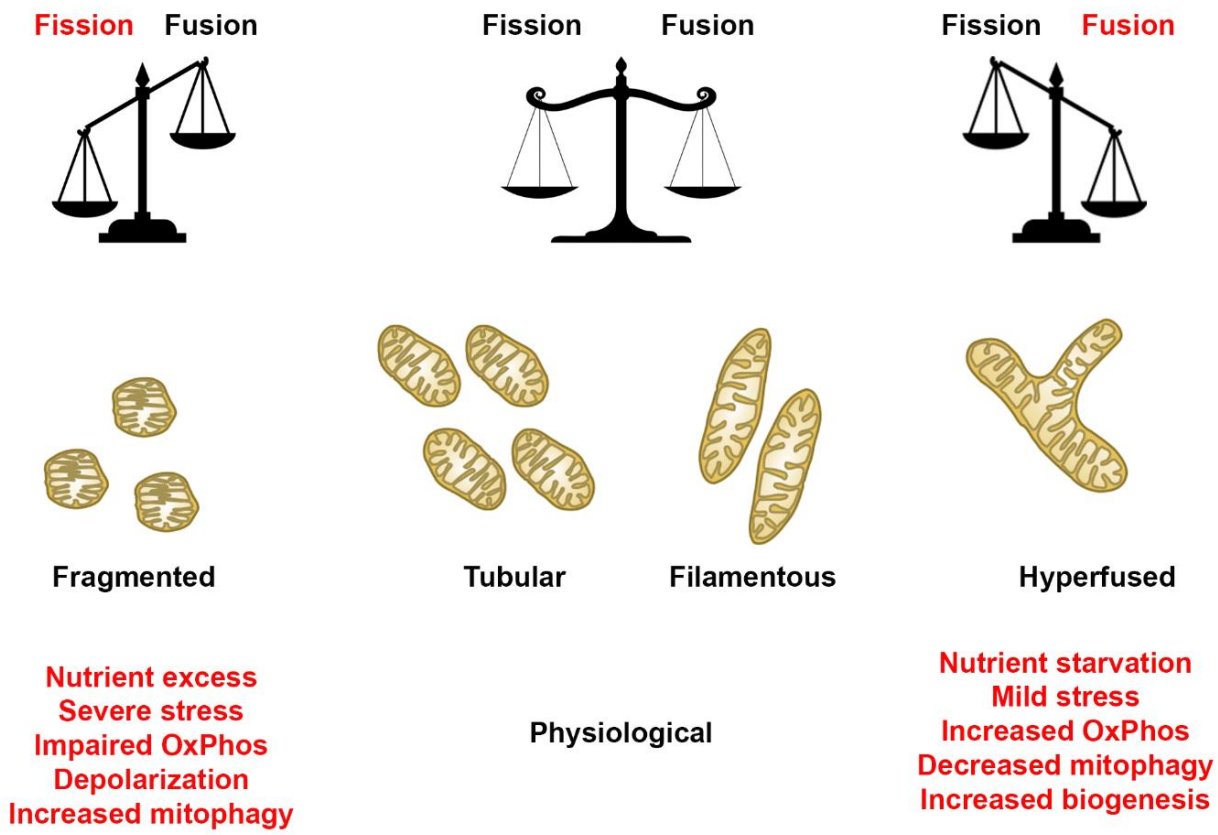

Figure 3.4. Mitochondrial morphology summary for fibroblast cell lines. Comparison of mitochondrial morphology of diseased and healthy fibroblast cell lines under basal conditions. This result suggests that diseased cell lines tend to have fewer respiring mitochondria with small branches and fragmented networks. In some cases, however, as seen in SBG5-FB (*T12706C*), hyperfusion serves as a compensatory mechanism.

3.5. Materials and methods

3.5.1. Fibroblast cell culture

Cultures of healthy control BJ-FB (ATCC® CRL-2522™) were obtained from ATCC (ATCC, Manassas, VA) and the patient-derived diseased fibroblasts (SBG1-FB (*T8993G*), SBG2-FB (*T8993G*), SBG3-FB (*T9185C*), SBG4-FB (*T10158C*), SBG5-FB (*T12706C*)) were obtained from the Medical University of Salzburg, Austria. These cells were maintained in a fibroblast expansion medium that consisted of minimal essential medium (MEM) (Thermo Fisher

Scientific, Waltham, MA), 10% fetal bovine serum (FBS) (GE Healthcare - HyClone™, Chicago, IL), and 2mM L-glutamine. Fibroblasts were enzymatically passaged in 0.05% Trypsin-EDTA (Thermo Fisher Scientific). All cell cultures were maintained without the use of antibiotics, handled in Biosafety Type II sterile hoods regularly cleaned with UV irradiation and 70% ethanol, and grown in 37°C incubators at 5% CO_2 and 95% humidity. The culture medium was replenished every two days until cells became 80% confluent. Prior to use in experimentation, cells were dissociated using 0.05% trypsin-EDTA (Thermo Fisher Scientific) and 20,000cells were seeded into 35mm dishes for fluorescence labeling and image analysis.

3.5.2. Fluorescence labeling of mitochondria

To label the mitochondria, fibroblast cells were incubated with MEM NEAA basal medium (Thermo Fisher Scientific) containing 150nM Mitotracker Red CM-H2Xros (Invitrogen) for 30mins. In the FCCP treatment group, fibroblast cells were incubated with 0.7µM FCCP for 30 minutes before the addition of the Mitotracker Red CM-H2Xros. At the end of the incubation period, the cells were washed 3x times with pre-warmed Dulbecco's phosphate-buffered saline (dPBS). The nucleus was stained by further incubating cells with basal medium containing Nucblue Hoechst (Invitrogen) for 15mins. Following this incubation, cells were washed several times with pre-warmed dPBS to remove excess dye. At the end of the wash, MEM NEAA basal medium was added to each dish prior to image acquisition.

3.5.3. Live-cell fluorescence microscopy

Fluorescence images of live cells were acquired using an EVOS FL inverted light/epifluorescence microscope with 40X/0.65 objective and a Sony ICX445 monochrome CCD digital camera. Red fluorescence from Mitotracker Red CM-H2Xros was measured using a 530nm excitation and a 593nm emission filter set. Blue fluorescence from Nuncblue Hoechst was measured using a 360nm excitation and a 447nm emission filter set. All live cells were imaged on

35mm dishes containing phenol-red-free basal medium. Image acquisition was performed one dish at a time with a maximum time of 30minutes between dishes. All dishes were stored in a humidified 37^{o}C, 5% CO_2 incubator until image acquisition. All images of live cells were taken on the same day as the labeling of mitochondria. All live-cell images were exported as TIFF files for further analysis. Ten to fourteen images were acquired per dish and three dishes were stained per trial. Three independent trials were performed for each of the fibroblast cell lines used in the study.

3.5.4. MINA network analysis

The images generated for the human fibroblast cell lines were pre-processed on Image-J following steps previously outlined (Valente et al., 2017). After pre-processing, the images were skeletonized. Post-skeletonization, images were segmented using Adobe Photoshop CC 2018. These segmented images were opened in Image-J and the MiNA macros were used to quantify mitochondrial morphological parameters of each segmented image. Since fibroblast cell lines have different cellular morphologies, we normalized the parameters generated through MiNA by the cell surface area which was also measured using Image-J.

3.5.5. Mitochondrial membrane potential measurements

In this study, all fibroblasts were maintained in culture following established protocols until the desired passage (p8) is reached. Prior to use in flow cytometry analysis, cells were cultured until 70-80% confluence was reached. On the day of the experiment, cells were enzymatically detached using 0.05% Trypsin-EDTA (Thermo Fisher Scientific) and centrifuged at 400xg for 5 mins. Cells were then resuspended in basal medium, after which the desired amount of tetramethylrhodamine, ethyl ester (TMRE- Abcam, Cambridge, MA, USA) was added (for a final concentration of 50nM). For FCCP and Oligomycin treatment groups, 20 µM and 5 µM of FCCP and Oligomycin were added respectively for 10 mins prior to treatment with TMRE. Cells were

incubated with TMRE in a 37^{o}C 5% CO2 incubator for 25 mins. At the end of the incubation period, cells were centrifuged at 400xg for 5 mins. To wash off the excess dye, cells were resuspended in 1x dPBS solution and centrifuged for another 5 mins. At the end of the wash, the cells were resuspended in phenol-red free basal medium and transferred to Accuri C6 plus flow cytometer (BD Biosciences; Franklin Lakes, NJ, USA) for data acquisition. 10,000 events were recorded for each cell line. After data acquisition, the data were exported as FCS files and analyzed using FlowJo_v10.6.2 software. To gate for the TMRE-positive population, cells that were not stained with TMRE were used to gate for the TMRE negative cell populations. Mean fluorescent intensity (MFI) values, a measure of the geometric mean of TMRE positive cells was obtained for statistical analysis.

3.5.6. Statistical analysis

To ensure scientific rigor and reproducibility, an ANOVA design accounting for 3 biological and 10-14 images from healthy control (BJ-fibroblast) and diseased (SBG1-FB (*T8993G*), SBG2-FB (*T8993G*), SBG3-FB (*T9185C*), SBG4-FB (*T10158C*), SBG5-FB (*T12706C*)) was used to identify any differences with respect to control BJ fibroblasts. Post-hoc Tukey HSD test was used to identify differences among specific groups. Data are presented as the mean ± standard deviation (SD) and were analyzed using the GraphPad Prism 8 program (GraphPad Software, San Diego, CA, USA). A $p<0.05$ was considered significant.

3.6. Conclusions

In summary, we report the effects of specific mtDNA perturbations (mutations) on mitochondrial dynamics in the context of specific mitochondrial disorders like LS. Our results demonstrate that specific point mutations affecting the OXPHOS complexes and translation machinery could upregulate fission dynamics; creating a dysfunction that favors hyper-fragmentation of the mitochondria. Although certain mutations and cellular demand cause

hyperfused mitochondria, our observations indicate that this is not the predominant morphological adaptation in fibroblast cells with mitochondrial disorders. This study improves our understanding of mitochondrial dynamics in patient fibroblasts with multiple developmental defects and mitochondrial disorders and could lead to a better correlation of mitochondrial dynamics, genetics, and bioenergetics, the specific role of mitochondria in patient diagnosis and prognosis, and focused therapies to treat various mitochondrial disorders.

3.7. References

Baracca, A., Sgarbi, G., Mattiazzi, M., Casalena, G., Pagnotta, E., Valentino, M.L., Moggio, M., Lenaz, G., Carelli, V., and Solaini, G. (2007). Biochemical phenotypes associated with the mitochondrial ATP6 gene mutations at nt8993. *Biochim Biophys Acta* 1767**,** 913-919.

Castagna, A.E., Addis, J., Mcinnes, R.R., Clarke, J.T.R., Ashby, P., Blaser, S., and Robinson, B.H. (2007). Late onset Leigh syndrome and ataxia due to a T to C mutation at bp 9,185 of mitochondrial DNA. *American Journal of Medical Genetics Part A* 143A**,** 808-816.

Chan, D.C. (2006). Mitochondria: dynamic organelles in disease, aging, and development. *Cell* 125**,** 1241-1252.

Cottet-Rousselle, C., Ronot, X., Leverve, X., and Mayol, J.F. (2011). Cytometric assessment of mitochondria using fluorescent probes. *Cytometry A* 79**,** 405-425.

Debray, F.G., Lambert, M., Lortie, A., Vanasse, M., and Mitchell, G.A. (2007). Long-term outcome of Leigh syndrome caused by the NARP-T8993C mtDNA mutation. *Am J Med Genet A* 143A**,** 2046-2051.

Duchen, M.R. (2004). Roles of mitochondria in health and disease. *Diabetes* 53 Suppl 1**,** S96-102.

Esteras, N., Adjobo-Hermans, M.J.W., Abramov, A.Y., and Koopman, W.J.H. (2020). Visualization of mitochondrial membrane potential in mammalian cells. *Methods Cell Biol* 155**,** 221-245.

Gao, J., Wang, L., Liu, J., Xie, F., Su, B., and Wang, X. (2017). Abnormalities of Mitochondrial Dynamics in Neurodegenerative Diseases. *Antioxidants (Basel)* 6.

Gomes, L.C., Di Benedetto, G., and Scorrano, L. (2011). During autophagy mitochondria elongate, are spared from degradation and sustain cell viability. *Nat Cell Biol* 13**,** 589-598.

Goyal, G., Fell, B., Sarin, A., Youle, R.J., and Sriram, V. (2007). Role of mitochondrial remodeling in programmed cell death in Drosophila melanogaster. *Dev Cell* 12**,** 807-816.

Harwig, M.C., Viana, M.P., Egner, J.M., Harwig, J.J., Widlansky, M.E., Rafelski, S.M., and Hill, R.B. (2018). Methods for imaging mammalian mitochondrial morphology: A prospective on MitoGraph. *Anal Biochem* 552**,** 81-99.

Hoppel, C.L., Tandler, B., Fujioka, H., and Riva, A. (2009). Dynamic organization of mitochondria in human heart and in myocardial disease. *Int J Biochem Cell Biol* 41**,** 1949-1956.

Iannetti, E.F., Willems, P.H., Pellegrini, M., Beyrath, J., Smeitink, J.A., Blanchet, L., and Koopman, W.J. (2015). Toward high-content screening of mitochondrial morphology and membrane potential in living cells. *Int J Biochem Cell Biol* 63**,** 66-70.

Iyer, S., Alsayegh, K., Abraham, S., and Rao, R.R. (2009). Stem cell-based models and therapies for neurodegenerative diseases. *Crit Rev Biomed Eng* 37**,** 321-353.

Kiryu-Seo, S., Tamada, H., Kato, Y., Yasuda, K., Ishihara, N., Nomura, M., Mihara, K., and Kiyama, H. (2016). Mitochondrial fission is an acute and adaptive response in injured motor neurons. *Sci Rep* 6**,** 28331.

Koopman, W.J., Visch, H.J., Verkaart, S., Van Den Heuvel, L.W., Smeitink, J.A., and Willems, P.H. (2005). Mitochondrial network complexity and pathological decrease in complex I activity are tightly correlated in isolated human complex I deficiency. *Am J Physiol Cell Physiol* 289**,** C881-890.

Legros, F., Lombes, A., Frachon, P., and Rojo, M. (2002). Mitochondrial fusion in human cells is efficient, requires the inner membrane potential, and is mediated by mitofusins. *Mol Biol Cell* 13**,** 4343-4354.

Leigh, D. (1951). Subacute necrotizing encephalomyelopathy in an infant. *J Neurol Neurosurg Psychiatry* 14**,** 216-221.

Liesa, M., and Shirihai, O.S. (2013). Mitochondrial dynamics in the regulation of nutrient utilization and energy expenditure. *Cell Metab* 17**,** 491-506.

Liu, X., and Hajnoczky, G. (2009). Ca2+-dependent regulation of mitochondrial dynamics by the Miro-Milton complex. *Int J Biochem Cell Biol* 41**,** 1972-1976.

Liu, X., and Hajnoczky, G. (2011). Altered fusion dynamics underlie unique morphological changes in mitochondria during hypoxia-reoxygenation stress. *Cell Death Differ* 18**,** 1561-1572.

Loeffen, J.L., Smeitink, J.A., Trijbels, J.M., Janssen, A.J., Triepels, R.H., Sengers, R.C., and Van Den Heuvel, L.P. (2000). Isolated complex I deficiency in children: clinical, biochemical and genetic aspects. *Hum Mutat* 15**,** 123-134.

Mccarron, J.G., Wilson, C., Sandison, M.E., Olson, M.L., Girkin, J.M., Saunter, C., and Chalmers, S. (2013). From structure to function: mitochondrial morphology, motion and shaping in vascular smooth muscle. *J Vasc Res* 50**,** 357-371.

Mcfarland, R., Kirby, D.M., Fowler, K.J., Ohtake, A., Ryan, M.T., Amor, D.J., Fletcher, J.M., Dixon, J.W., Collins, F.A., Turnbull, D.M., Taylor, R.W., and Thorburn, D.R. (2004). De novo mutations in the mitochondrial ND3 gene as a cause of infantile mitochondrial encephalopathy and complex I deficiency. *Annals of Neurology* 55**,** 58-64.

Mitchell, P. (1966). Chemiosmotic coupling in oxidative and photosynthetic phosphorylation. *Biol Rev Camb Philos Soc* 41**,** 445-502.

Mortiboys, H., Thomas, K.J., Koopman, W.J., Klaffke, S., Abou-Sleiman, P., Olpin, S., Wood, N.W., Willems, P.H., Smeitink, J.A., Cookson, M.R., and Bandmann, O. (2008).

Mitochondrial function and morphology are impaired in parkin-mutant fibroblasts. *Ann Neurol* 64**,** 555-565.

Nakada, K., Inoue, K., Ono, T., Isobe, K., Ogura, A., Goto, Y.I., Nonaka, I., and Hayashi, J.I. (2001). Inter-mitochondrial complementation: Mitochondria-specific system preventing mice from expression of disease phenotypes by mutant mtDNA. *Nat Med* 7**,** 934-940.

Ni, H.M., Williams, J.A., and Ding, W.X. (2015). Mitochondrial dynamics and mitochondrial quality control. *Redox Biol* 4**,** 6-13.

Ogawa, K., Noguchi, H., Tsuji, M., and Sasaki, F. (2003). Starvation induces the formation of giant mitochondria in gastric parietal cells of guinea pigs. *J Electron Microsc (Tokyo)* 52**,** 217-225.

Picard, M., Shirihai, O.S., Gentil, B.J., and Burelle, Y. (2013). Mitochondrial morphology transitions and functions: implications for retrograde signaling? *Am J Physiol Regul Integr Comp Physiol* 304**,** R393-406.

Piekutowska-Abramczuk, D., Rutyna, R., Czyzyk, E., Jurkiewicz, E., Iwanicka-Pronicka, K., Rokicki, D., Stachowicz, S., Strzemecka, J., Guz, W., Gawronski, M., Kosierb, A., Ligas, J., Puchala, M., Drelich-Zbroja, A., Bednarska-Makaruk, M., Dabrowski, W., Ciara, E., Ksiazyk, J.B., and Pronicka, E. (2018). Leigh syndrome in individuals bearing m.9185T>C MTATP6 variant. Is hyperventilation a factor which starts its development? *Metab Brain Dis* 33**,** 191-199.

Rambold, A.S., Kostelecky, B., Elia, N., and Lippincott-Schwartz, J. (2011). Tubular network formation protects mitochondria from autophagosomal degradation during nutrient starvation. *Proc Natl Acad Sci U S A* 108**,** 10190-10195.

Rolland, S.G., Motori, E., Memar, N., Hench, J., Frank, S., Winklhofer, K.F., and Conradt, B. (2013). Impaired complex IV activity in response to loss of LRPPRC function can be compensated by mitochondrial hyperfusion. *Proc Natl Acad Sci U S A* 110**,** E2967-2976.

Scaduto, R.C., Jr., and Grotyohann, L.W. (1999). Measurement of mitochondrial membrane potential using fluorescent rhodamine derivatives. *Biophys J* 76**,** 469-477.

Sprenger, H.G., and Langer, T. (2019). The Good and the Bad of Mitochondrial Breakups. *Trends Cell Biol* 29**,** 888-900.

Srinivasan, S., Guha, M., Kashina, A., and Avadhani, N.G. (2017). Mitochondrial dysfunction and mitochondrial dynamics-The cancer connection. *Biochim Biophys Acta Bioenerg* 1858**,** 602-614.

Stendel, C., Neuhofer, C., Floride, E., Yuqing, S., Ganetzky, R.D., Park, J., Freisinger, P., Kornblum, C., Kleinle, S., Schols, L., Distelmaier, F., Stettner, G.M., Buchner, B., Falk, M.J., Mayr, J.A., Synofzik, M., Abicht, A., Haack, T.B., Prokisch, H., Wortmann, S.B., Murayama, K., Fang, F., Klopstock, T., and Group, A.T.P.S. (2020). Delineating MT-ATP6-associated disease: From isolated neuropathy to early onset neurodegeneration. *Neurol Genet* 6**,** e393.

Taylor, R.W., Morris, A.A., Hutchinson, M., and Turnbull, D.M. (2002). Leigh disease associated with a novel mitochondrial DNA ND5 mutation. *Eur J Hum Genet* 10**,** 141-144.

Tilokani, L., Nagashima, S., Paupe, V., and Prudent, J. (2018). Mitochondrial dynamics: overview of molecular mechanisms. *Essays Biochem* 62**,** 341-360.

Tokuyama, T., Hirai, A., Shiiba, I., Ito, N., Matsuno, K., Takeda, K., Saito, K., Mii, K., Matsushita, N., Fukuda, T., Inatome, R., and Yanagi, S. (2020). Mitochondrial Dynamics Regulation in Skin Fibroblasts from Mitochondrial Disease Patients. *Biomolecules* 10.

Trimmer, P.A., Swerdlow, R.H., Parks, J.K., Keeney, P., Bennett, J.P., Jr., Miller, S.W., Davis, R.E., and Parker, W.D., Jr. (2000). Abnormal mitochondrial morphology in sporadic Parkinson's and Alzheimer's disease cybrid cell lines. *Exp Neurol* 162**,** 37-50.

Valente, A.J., Maddalena, L.A., Robb, E.L., Moradi, F., and Stuart, J.A. (2017). A simple ImageJ macro tool for analyzing mitochondrial network morphology in mammalian cell culture. *Acta Histochem* 119**,** 315-326.

Wai, T., and Langer, T. (2016). Mitochondrial Dynamics and Metabolic Regulation. *Trends Endocrinol Metab* 27**,** 105-117.

Wallace, D.C. (1999). Mitochondrial diseases in man and mouse. *Science* 283**,** 1482-1488.

Willems, P.H., Rossignol, R., Dieteren, C.E., Murphy, M.P., and Koopman, W.J. (2015). Redox Homeostasis and Mitochondrial Dynamics. *Cell Metab* 22**,** 207-218.

Wu, S., Zhou, F., Zhang, Z., and Xing, D. (2011). Mitochondrial oxidative stress causes mitochondrial fragmentation via differential modulation of mitochondrial fission-fusion proteins. *FEBS J* 278**,** 941-954.

Yoneda, M., Miyatake, T., and Attardi, G. (1994). Complementation of mutant and wild-type human mitochondrial DNAs coexisting since the mutation event and lack of complementation of DNAs introduced separately into a cell within distinct organelles. *Mol Cell Biol* 14**,** 2699-2712.

Youle, R.J., and Van Der Bliek, A.M. (2012). Mitochondrial fission, fusion, and stress. *Science* 337**,** 1062-1065.

Zemirli, N., Morel, E., and Molino, D. (2018). Mitochondrial Dynamics in Basal and Stressful Conditions. *Int J Mol Sci* 19.

Zorova, L.D., Popkov, V.A., Plotnikov, E.Y., Silachev, D.N., Pevzner, I.B., Jankauskas, S.S., Babenko, V.A., Zorov, S.D., Balakireva, A.V., Juhaszova, M., Sollott, S.J., and Zorov, D.B. (2018). Mitochondrial membrane potential. *Anal Biochem* 552**,** 50-59.

Chapter 3

4. Evaluating the bioenergetics health index ratio in Leigh syndrome fibroblasts to understand disease severity

Bakare, A.B., Dean, J., Chen, Q., Saikia, B., Thorat, V., Huang, Y, LaFramboise, T., Lesnefsky, E.J., and Iyer, S.

4.1. Abstract

Several pediatric mitochondrial disorders including Leigh syndrome (LS) impact mitochondrial (mt) genetics, development, and metabolism; leading to complex pathologies and energy failure. The extent to which pathogenic mtDNA variants regulate disease severity in LS is currently not well understood. To better understand this relationship, we computed a glycolytic bioenergetics health index (BHI) for measuring mitochondrial dysfunction in LS patient fibroblast cells harboring varying percentages of pathogenic mutant mtDNA (*T8993G, T9185C*) exhibiting deficiency in complex V or complex I (*T10158C*, *T12706C*). A high percentage (> 90%) of pathogenic mtDNA in cells affecting complex V and a low percentage (< 39%) of pathogenic mtDNA in cells affecting complex I were quantified. Levels of defective enzyme activities of the electron transport chain correlated with the percentage of pathogenic mtDNA. Subsequent bioenergetics assays showed cell lines relied on both OXPHOS and glycolysis for meeting energy requirements. Results suggest that whereas the precise mechanism of LS has not been elucidated, a multi-pronged approach taking into consideration the specific pathogenic mtDNA variant, glycolytic BHI, and the composite BHI (average ratio of oxphos to glycolysis) can aid in better understanding the factors influencing disease severity in LS.

4.2. Introduction

Mitochondrial (mt) disorders represent a large group of severe genetic disorders mainly impacting organ systems with high energy requirements (McFarland et al., 2010). These disorders are clinically complex, often fatal, and occur at an estimated ratio of 1 in 5000 live births (Skladal et al., 2003;Schaefer et al., 2004). Although much progress has been made since the discovery of pathogenic mtDNA, we still do not understand whether pathogenic mtDNA directly or indirectly influences clinical severity. Previous studies indicate that the unorthodox genetics of a pathogenic mtDNA variant can influence clinical pathologies (Wallace and Chalkia, 2013) because each mitochondrion contains hundreds of mtDNA existing as mixtures of wild type and pathogenic mtDNA molecules within a single cell termed as heteroplasmy. Heteroplasmy at both the cellular and tissue level is capable of shifting the fraction of mutant mtDNA that is present within the daughter cells by replicative segregation (Coller et al., 2002;Nekhaeva et al., 2002a;Nekhaeva et al., 2002b).

In addition, each cell contains a varying number of mitochondria based on the energy requirement of the specific tissue. Key processes including adenosine triphosphate (ATP) synthesis (Mitchell, 1961), tricarboxylic acid cycle (TCA) and fatty acid beta-oxidation (Nicholls and Ferguson, 2013) provide cellular ATP by transporting electrons generated from the oxidation of TCA cycle intermediates through the four-electron transport chain (ETC) subunits coupled to the vectorial transport of protons to generate the proton motive force used by complex V to synthesize ATP (Mitchell, 1961). During the electron transfer to molecular oxygen, reactive oxygen species (ROS) are generated by leakage of electrons in complex I and III causing oxidative stress to cells (Mitchell, 1961;Murphy, 2009;Nicholls and Ferguson, 2013). ETC defects occurring from mtDNA mutations compromise mitochondrial membrane potential and ATP synthesis via oxidative phosphorylation, and interruption of this pathway renders cells

and tissues vulnerable under disease and oxidative stress conditions (Iyer et al., 2012;Jain et al., 2016).

In this study, Leigh Syndrome (LS) a classic mitochondrial disorder, was selected to better understand the relationship between disease severity and its associated pathogenic mtDNA variants, heteroplasmy, and biochemical phenotypes reported in LS (Leigh, 1951;Holt et al., 1990;Shoffner et al., 1992;Tatuch et al., 1992;Loeffen et al., 2000;Baertling et al., 2014;Rahman et al., 2017;Schubert Baldo and Vilarinho, 2020). To date, the mechanisms causing LS are not well understood. Studies have reported LS symptoms as symmetrical necrotic lesions in the brain stem, basal ganglia, and thalamus (Lake et al., 2016). Other studies have reported lactic acidosis, psychomotor retardation, failure to thrive, vomiting, seizures, respiratory failure, and ultimately death; thus restricting treatment options. Many LS patients have also shown elevated lactate in blood and cerebral spinal fluid (CSF) (Uziel et al., 1997;Moslemi et al., 2005;Debray et al., 2007). Currently, ~100 genes have been identified as monogenic causes of LS (Lake et al., 2016;Rahman and Rahman, 2018;Rahman, 2020).

Earlier studies demonstrated that a high percentage of pathogenic mtDNA causing complex V deficiency contributes to maternally inherited LS (MILS) (Tatuch et al., 1992). Results pointed out that *T8993G* mutation in high abundance (> 90%) in the *MTATP6* gene resulted in MILS and caused neurologic findings including seizures, respiratory dysfunction, and rapid fatality (Schubert Baldo and Vilarinho, 2020). Recent studies in LS patients exhibiting varying levels of heteroplasmy in pathogenic mtDNA variants in the *MTATP6* gene reported hyperventilation at the onset of the disease (Piekutowska-Abramczuk et al., 2018). Seminal studies in samples containing pathogenic mtDNA variants causing complex I deficiency showed that clinical symptoms were present even at low levels of heteroplasmy, with heterogeneous clinical outcomes ranging from neonatal lactic acidosis (Kirby et al., 2004), optic neuropathy to LS (Fassone and Rahman, 2012) in children.

To better comprehend the clinical presentation associated with the pathogenic mtDNA variants, heteroplasmy levels, and their biochemical defects in LS, we selected five pediatric patient fibroblast cell lines with varying clinical presentations; from mild myopathies to severe LS. These cell lines carried point mutations in their mtDNA at *T8993G, T9185C* in *MTATP6* gene causing complex V deficiency and *T10158C* in *MTND3* gene and *T12706C* in *MTND5* gene causing complex I deficiency. A commercially available fibroblast cell line (BJ-FB) was used as a healthy control line. In this study, we attempt to systematically connect pathogenic mtDNA variants and associated bioenergetic defects and propose a composite bioenergetic health index ratio as a sensitive marker for assessing patient health in young children suffering from Leigh syndrome.

4.3. Results

4.3.1. Skin fibroblasts from patients

The clinical information of the patients from whom fibroblasts were obtained is detailed in **Table 4.3.1.** All of the mitochondrial disease subjects selected for this study are pediatric patients exhibiting a range of clinical symptoms from mild myopathy to LS to severe neonatal lactic acidosis. All patients carried inherited pathogenic point mutations in mtDNA. One subject (SBG5-FB (*T12706C*)) was diagnosed with severe neonatal lactic acidosis at the time of disease onset and had the most impaired respiration of all fibroblast lines used in this study. We cultured six fibroblast cell lines (five LS: SBG1-FB (*MTATP6-T8993G*), SBG2-FB (*MTATP6-T8993G*), SBG3-FB (*MTATP6-T9185C*), SBG4-FB (*MTND3-T10158C*), SBG5-FB (*MTND5-T12706C*) one CTL: BJ-FB) at passage eight, to minimize variability in results. Cells from three biological replicates from each patient line and respective control line were passaged in culture and samples were frozen and examined at a later time point for genetic analysis.

Table 4.3.1. Clinical information of five patient fibroblast cell lines with pathogenic mtDNA mutations and CTL control cell line

Sample Name	Mutation	Gene	Clinical Information	Age at Diagnosis	Sex
BJ-FB	None	-		-	M
SBG1-FB	*T8993G*	*MTATP6*	Morbus Leigh	3 years	F
SBG2-FB	*T8993G*	*MTATP6*	Developmental delay, abnormal gait	4 years	M
SBG3-FB	*T9185C*	*MTATP6*	Myopathy	23 years	F
SBG4-FB	*T10158C*	*MTND3*	Epilepsy, dystonic tetraparesis	9 years	M
SBG5-FB	*T12706C*	*MTND5*	Severe neonatal lactic acidosis	8 months	F

4.3.2. High heteroplasmy was detected in disease lines affecting ATP synthase and low heteroplasmy was detected in disease lines affecting NADH dehydrogenase

Genomic DNA from different patient and healthy control samples were extracted and mtDNA purified and sequenced (see methods section for details). The percentage of mutant DNA was estimated using high-throughput next-generation sequencing for whole exome, based on approaches developed in our previous study (Grace et al., 2019) and detailed in the methods section. The sequencing results yielded a range of total reads to be analyzed between 64 to 302 in the different cell samples. This large sample size allows confidence regarding the percentages measured. The results indicate high heteroplasmy levels between 96% for SBG1-FB (*T8993G*), 91% for SBG2-FB (*T8993G*), and 98% for SBG3-FB (*T9185C*) cell lines containing mutations in *MTATP6* gene impacting complex V. These results are consistent with other published results on *T8993G* and *T9185C* mutations present in high abundance (>90%) that result in MILS (Childs et al., 2007;Schubert Baldo and Vilarinho, 2020). Estimation of heteroplasmy for pathogenic mutations in mitochondrial encoded *MTND3* and *MTND5* genes of complex I indicated low levels between 30% for SBG4-FB (*T10158C*) and 39% for SBG5-FB (*T12706C).* The low heteroplasmy level for pathogenic mutation in the *MTND5* gene is consistent with other results in the literature (Kirby et al., 2003). Since all samples were cultured at passage eight, we observed a lower than expected level of heteroplasmy for *T10158C* mutation in this study (**Table 4.3.2.**).

Table 4.3.2. Quantification of heteroplasmy by next-generation sequencing. The extracted mtDNA was sequenced using whole-exome sequencing methods. The sequencing results were compiled and analyzed as detailed in the methods section. This allows us to compute heteroplasmic variants based on the sequencing reads. Results demonstrate the presence of pathogenic mtDNA burden in all LS fibroblast samples.

Sample Name	Mutation	Total Reads Analyzed	Normal	Variant	Percentage of Mutation
SBG1-FB	*T8993G*	136	6 (T)	130 (G)	96%
SBG2-FB	*T8993G*	68	6 (T)	62 (G)	91%
SBG3-FB	*T9185C*	302	6 (T)	296 (C)	98%
SBG4-FB	*T10158C*	64	45 (T)	19 (C)	30%
SBG5-FB	*T12706C*	146	89 (T)	59 (C)	39%

4.3.3. Levels of defective enzyme activities of the ETC correlated with the percentage of pathogenic mtDNA

ETC assays measure electron transport through individual components of the respiratory chain (Chance and Williams, 1955). Since the mutations mainly impacted the activity of Complex I and V, we conducted two main assays, one rotenone sensitive and the other rotenone insensitive to provide measurements of the proximal portion of complex I and a measure of the function of the entire complex (Hoppel et al., 1987). Additional assays included complex III (Hatefi, 1978), and complex V activity (described in the methods section) in these cell lines. The activity of complex I was estimated in solubilized mitochondria by measuring rotenone sensitive mitochondrial NADH dehydrogenase cytochrome c-reductase (NCR) which is dependent on complexes I-III and determines the electron transport from donor NADH through complex I, ubiquinone (Q), and complex III where cytochrome *c* is the electron acceptor. Complex I activity is the rate-limiting step in this assay. The second assay (NFR) is NADH ferricyanide reductase which measures the activity of ferricyanide, as an artificial electron acceptor, proximal to the rotenone –sensitive site of complex I. Therefore, NFR activity was measured to estimate the function of the NADH dehydrogenase portion of complex I.

The results (summarized in **Table 4.3.3.**) for cell lines with pathogenic mtDNA variants affecting ATP synthase indicate a statistically significant ($p<0.05$) increase in NFR activities for SBG1-FB (*T8993G*) by 53%, and SBG3-FB (*T9185C*) by 58% when compared with the control BJ-FB cell line. NFR activity showed a 36% higher trend for SBG2-FB *(T8993G)* cell line compared with the control BJ-FB cell line. These results suggested a greater capacity for NADH oxidation to NAD^+ in these lines. Results for NCR showed increasing trends of 28% for SBG1-FB (*T8993G*) and 31% for SBG3-FB(*T9185C*) lines compared to the control BJ-FB cell line. The increases in NFR and NCR activities suggested a potential compensating effect due to downstream defects in ATP synthase activity. Interestingly the NCR activity showed a 13% decrease, although not significantly different in the SBG2-FB (*T8993G*) line carrying (*T8993G*) mutation. The activities of antimycin A-sensitive decylubiquinone-cytochrome-c reductase (complex III) remained indistinguishable in SBG2-FB (*T8993G*) and SBG3-FB (*T9185C*) lines compared to the control cell line indicating that complex III activity was not impacted. However, in SBG1-FB line carrying *(T8993G)* mutation, results showed a significant reduction by ~200% in complex III activity compared to the control BJ-FB cell line. The activity of oligomycin-sensitive complex V activity showed decreasing trends in all cell lines affecting ATP synthase function. Given the low heteroplasmy percentage for pathogenic mtDNA mutations affecting NADH dehydrogenase, results (summarized in **Table 4.3.3.**) for cell lines, SBG4-FB (*T10158C*) & SBG5-FB (*T12706C*) showed decreasing trends for NFR activities; while NCR, complex III, and oligomycin-sensitive complex V activities remained similar to the control cell line. All the data were normalized to citrate synthase activity which was used as an indicator of mitochondrial mass in each line.

Table 4.3.3. Electron transport chain activity of CTL BJ-FB and five LS fibroblast cell lines. The electron transport chain activities for NFR (proximal part of CI), NCR (distal part of CI), CIII, CV of mitochondria isolated from control and diseased cells have been normalized to citrate synthase activity measured in the same samples. Activities are expressed in nmol/mg protein/min/CS. Results are mean +/- S.D, n=3-5 for all individual disease lines, and n= 9 for the BJ-FB control cell line. NCR, NADH:cytochrome c oxidoreductase; NFR, NADH:ferricyanide oxidoreductase; CS, citrate synthase; CIII, cytochrome bc1; CV, ATP synthase. *p <0.05 ***p <0.001 ****p <0.0001 vs. control.

Cell lines	CS	NFR	NCR	CIII	CV
Control	42.22±13.1	16.08±5.5	0.051±0.04	0.67±0.17	0.080±0.12
MT-ATP6					
SBG1	31.00±5.4	34.02±3.8***	0.071±0.04	0.29±0.16*	0.063±0.039
SBG2	38.00±7.4	25.48±8.0	0.045±0.06	0.60±0.20	0.030±0.018
SBG3	26.75±5.6	38.60±5.6****	0.103±0.08	0.66±0.24	0.086±0.060
MT-ND3					
SBG4	44.50±9.2	15.83±0.92	0.053±0.0097	0.75±0.23	0.038±0.013
MT-ND5					
SBG5	41.40±8.26	13.48±1.91	0.063±0.014	0.50±0.16	0.042±0.0033

4.3.4. Mitochondrial reactive oxygen species production was decreased in all diseased cell lines and dependent on mitochondrial membrane potential

Tightly coupled mitochondria ensure electron flow and proton translocation are coupled appropriately with ATP production. When electron transport and ATP production in the mitochondria are not tightly coupled, electrons could potentially leak from ETC complexes, resulting in the production of reactive oxygen species (ROS) (Murphy, 2009;Cheng et al., 2017), which can be further detrimental to mitochondrial function. Results of NFR and NCR data from ETC studies led us to hypothesize that the SBG 1-3FB lines supported a leaky mitochondrial membrane because of a defective ATP synthase (Boyer et al., 1973), while SBG4-5FB lines exhibited overall complex I defect because of defective NADH dehydrogenase function. Using flow cytometry analysis, ROS production was measured using MitoSOX, a fluorescent dye that selectively targets mitochondria in live cells, where it can be readily oxidized by superoxide (Robinson et al., 2008). A significant decrease ($p<0.05$) in ROS production was observed in the

diseased cell lines (SBG1-5FB) relative to the control BJ-FB cell line (**Figure 4.3.4.a**). As experimental controls, two potent mitochondrial inhibitors, rotenone, and antimycin A were used to induce ROS production. Rotenone inhibits the activity of complex I, while antimycin A inhibits the activity of complex III. Inhibition at these sites perturbed electron flow and increased the production of oxygen radicals. As expected, increased ROS production was observed in the sites of complex I and III subunits in the diseased lines. However, the levels were significantly lower ($p<0.0001$) than the BJ-FB control cell line (**Figure 4.3.4.b-c**). It has been reported elsewhere that MitoSOX fluorescence is dependent on MMP fluorescence (Polster et al., 2014;Roelofs et al., 2015). In parallel studies conducted in our laboratory and reported elsewhere, lower MMP was observed for all of our diseased cell lines (manuscript in review). The low mitochondrial ROS could be attributed to the depolarization of the mitochondria caused by the different mutations. The mitochondria are potentially “uncoupled” with a permeable inner mitochondrial membrane and thus electrons do not accumulate on redox centers of complex I and complex III.

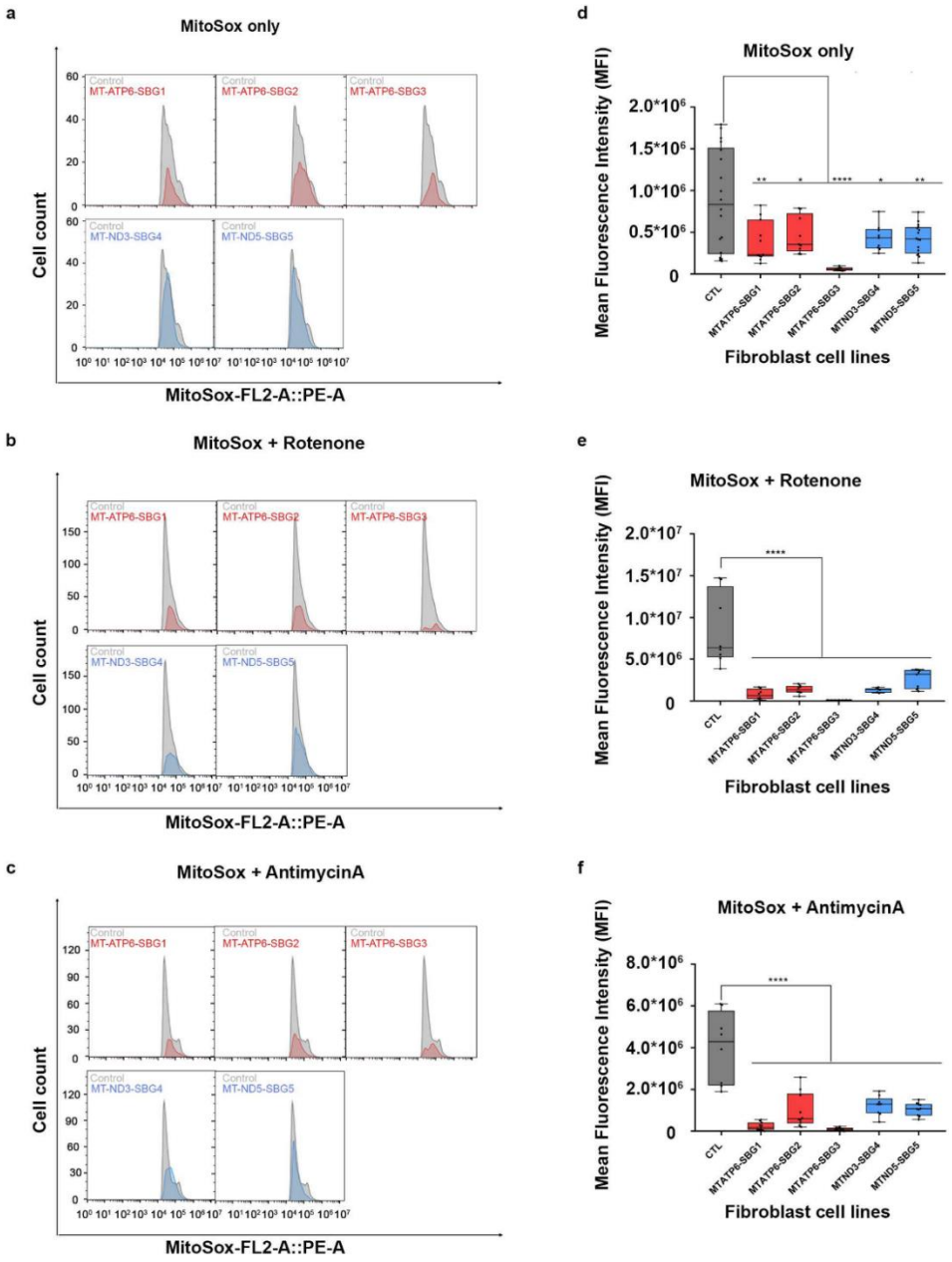

Figure 4.3.4. Mitochondrial reactive oxygen species (ROS) analysis of BJ-FB and five LS fibroblast cell lines. Using flow cytometry, along with MitoSOX™ Red reagent, ROS was evaluated. Representative flow cytometry histogram of all fibroblasts (Control BJ-FB in grey; SBG1-FB (*MTATP6-T8993G*), SBG2-FB (*MTATP6- T8993G*), SBG3-FB (*MTATP6-T9185C*) in red; SBG4-FB (*MTND3-T10158C*) and SBG5-FB (*MTND5-T12706C*) in blue of samples (a) stained with MitoSOX™ Red only (b) stained with MitoSOX™ Red after treatment with Rotenone and (c) stained with MitoSOX™ Red after treatment with Antimycin A. Mean fluorescence intensity (MFI) was calculated based on three independent runs and are shown for all the samples in (d) stained with MitoSOX™ Red only (e) stained with MitoSOX™ Red after treatment with Rotenone and (f) stained with MitoSOX™ Red after treatment with Antimycin. *p<0.05** p<0.01*** p<0.001 ****p<0.00001.

4.3.5. Mitochondrial respiration was disrupted in diseased cell lines with variable spare respiratory reserve capacity

It was hypothesized that an increase in mutation burden disrupts electron transfer (measured as oxygen consumption) leading to altered ETC activity and abnormal mitochondrial bioenergetics. As shown in **Figure 4.3.5.a-c,** oxygen consumption rate (OCR) using a Seahorse XFe96 flux analyzer was measured. Analysis was conducted in all cell lines (n=3-5) at passage eight, in conjunction with quantitative measurements of heteroplasmy levels and ETC activity. The oxidative phosphorylation properties included basal respiration, leak, maximal respiration, and non-mitochondrial respiration, after sequential injections of ATP synthase inhibitor oligomycin, the uncoupler carbonyl cyanide-4-(trifluoromethoxy) phenylhydrazone FCCP, complex I inhibitor Rotenone, and complex III inhibitor Antimycin A into the wells.

Results show (**Figure 4.3.5.d**) a significant increase (30%; $p<0.0001$) in basal respiration in SBG1-FB (*T8993G*) cell line because disruption of ATP synthase function causes the protons to leak rapidly (**Figure 4.3.5.g**) by (33 %; $p<0.0001$) to maintain the circuit; thus signaling the cells to accelerate the demand for ATP-linked basal respiration. However, proton leak was not increased in SBG2-FB (*T8993G*), SBG3-FB (*T9185C*) cell lines, which correlated with significantly (*p<0.0001*) decreased basal respiration (**Figure 4.3.5.d,g**) when compared to the control line. A similar analysis was performed on the other two cell lines SBG4-FB (*T10158C*) & SBG5-FB (*T12706C*) impacting NADH dehydrogenase function. Results indicated a decrease by 23% and 21% in basal respiration (**Figure 4.3.5.d**) for SBG4-FB (*T10158C*) & SBG5-FB (*T12706C*) respectively relative to control. Proton leak was also reduced (**Figure 4.3.5.g**) in the SBG4-FB (*T10158C*) line compared to the control BJ-FB cell line.

The maximum respiration rate caused by the addition of FCCP (**Figure 4.3.5.e**) showed a significant increase by 98% (*p<0.0001*) in SBG1-FB(*T8993G*) and 57% (*p<0.0001*) increase in SBG3-FB (*T9185C*) cell line compared to the control BJ-FB line, mimicking the physiological

energy demand due to a defective ATP synthase. Therefore, rapid oxidation of substrates could occur to meet this metabolic challenge, thus stimulating the respiratory chain to operate at maximum capacity (Zorov et al., 2014;Smith et al., 2018). However, in SBG2-FB (*T8993G*) line, the observed decrease by 23% (p=0.0084) in maximal respiration (**Figure 4.3.5.e**) indicates the cell was unable to meet the metabolic challenge due to inefficient ATP synthase. Similarly, maximum respiration rate was measured on SBG4-FB (*T10158C*) & SBG5-FB (*T12706C*) cell lines impacting NADH dehydrogenase function. Since the *T12706C* mutation disrupts the proton translocation in the transmembrane arm of the complex I subunit (Ni et al., 2019), we expected that the maximum rate of respiration would be severely impacted. Results indicate a mild increase in maximum respiration by 12.5% ($p<0.05$) in SBG4-FB (*T10158C*) cell line; and a severe decrease in maximum respiration by 47.5% ($p<0.0001$) in SBG5-FB (*T12706C*) compared to the control BJ-FB cell line (**Figure 4.3.5.e**).

An important bioenergetics variable of a cell that can experience variable energy demands is the spare respiratory capacity (SRC); which is the ability of the electron transport and substrate supply to respond to an increase in ATP demand (Marchetti et al., 2020). SRC is measured by the difference between maximal respiration and basal respiration (**Figure 4.3.5.a**). Results show a significant increase in spare respiratory capacity values by 150% ($p<0.0001$) in SBG1-FB (*T8993G*) and 190% ($p<0.0001$) increase in SBG3-FB (*T9185C*) cell line, and an 11% ($p<0.0001$) decrease in SBG2-FB (*T8993G*) compared with the control BJ-FB cell line. Next, SRC values were measured in SBG4-FB *(T10158C)* & SBG5-FB (*T12706C*) cell lines impacting NADH dehydrogenase function. We observed a slight increase in SRC values in SBG4-FB (*T10158C*) cell line and a significant decrease by 50% ($p<0.0001$) in SRC values in SBG5-FB (*T12706C*) cell line compared with the control BJ-FB line (**Figure 4.3.5.h**). This suggests that the SBG5-FB (*T12706C*) has a more severe defect in complex I activity versus SBG4-FB

(*T10158C*). These results are in line with other studies that have shown cells with very low SRC values have poor adaptability to stress conditions (Marchetti et al., 2020).

Finally, the mitochondrial respiration was inhibited by simultaneously treating cells with rotenone and antimycin A. Non-mitochondrial respiration was measured as the difference between basal respiration and the final values obtained after the treatment, which is typically attributed to the non-ETC oxidases present in the cell (Hill et al., 2012). Results showed that non-mitochondrial respiration was significantly elevated ($p<0.0001$) in all SBG1-FB (*T8993G*), SBG2-FB (*T8993G*), SBG3-FB (*T9185C*) ($p<0.05$), SBG4-FB *(T10158C)* cell lines compared to the control BJ-FB line (**Figure 4.3.5.f**). The non-mitochondrial respiration was however similar in the SBG5-FB (*T12706C*) line when compared with the BJ-FB control cell line.

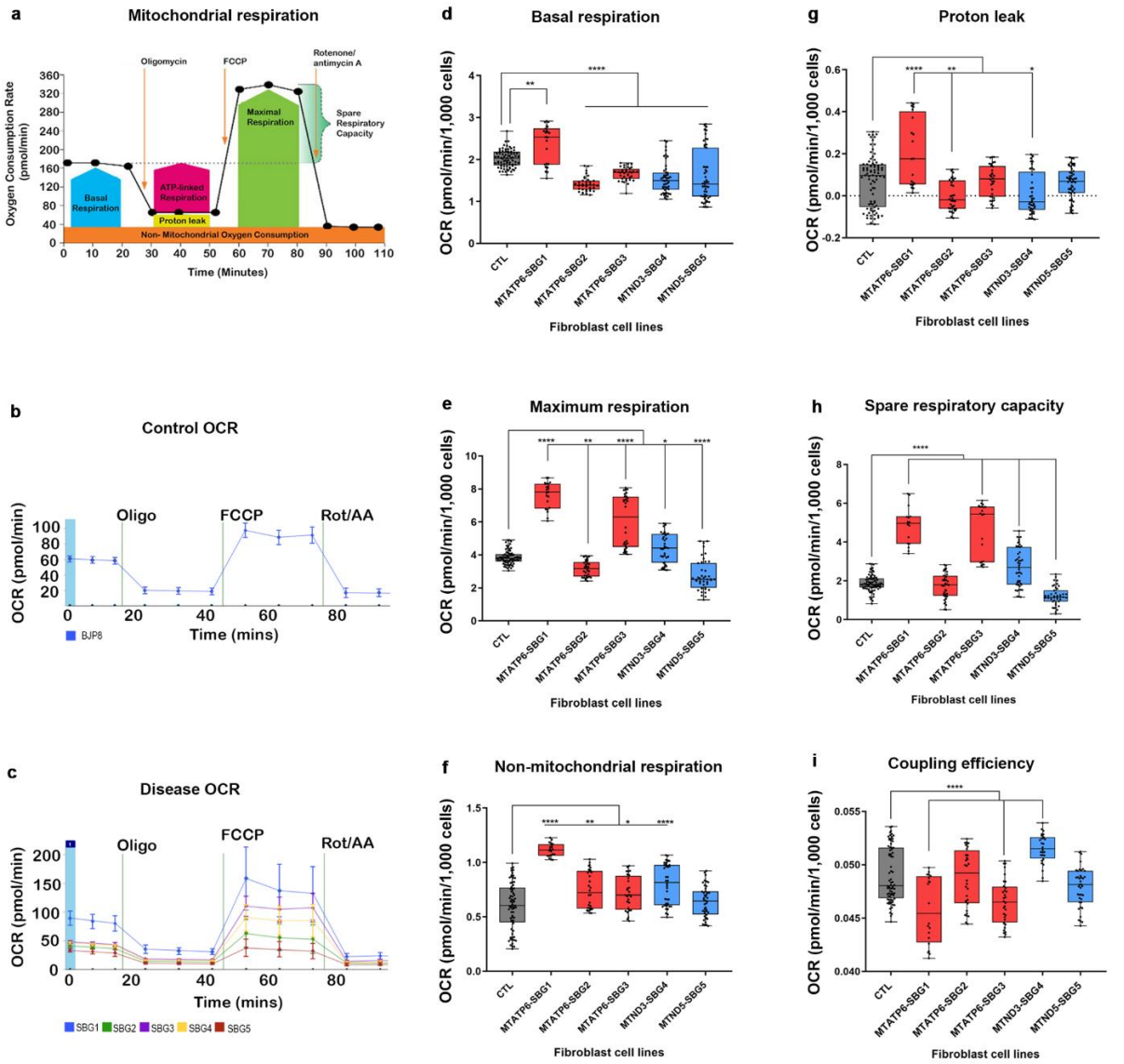

Figure 4.3.5. Mitochondria respiratory profile of CTL BJ-FB and five LS fibroblast cell lines. (a) Scheme of expected oxygen consumption rate (OCR) under basal conditions, (b) OCR profile of BJ-FB, (c) OCR profile of diseased (SBG1-FB (*MTATP6-T8993G*), SBG2-FB (*MTATP6- T8993G*), SBG3-FB (*MTATP6-T9185C*), SBG4-FB (*MTND3-T10158C*) and SBG5-FB (*MTND5-T12706C*) cell lines showing (d) basal respiration, (e) maximal respiration (f) non-mitochondrial respiration after Rot/AA injection proton leak, (g) proton leak (h) spare respiratory capacity, (i) coupling efficiency. All parameters are in pmol/min/1000 cells. Data are mean +/- SD. Experiments were repeated at least three times on different days under the same conditions. *p<0.05 **p<0.01 ***p<0.001 ****p<0.00001. Comparative analyses for all diseased (SBG1-5) FBs were conducted with the healthy control BJ-FB line.

4.3.6. Glycolytic rate is significantly increased in LS fibroblasts harboring *T8993G*, *T9185C*, and *T12706C* mutations affecting CI and CV function

The mitochondrial bioenergetics assay confirmed that all the patient lines except SBG1-FB (*T8993G*) showed significant decreases (~35%) in mitochondrial ATP production (**Figure 4.3.7.a**) in line with other reports (Kirby et al., 2003;Crimi et al., 2004;Schubert Baldo and Vilarinho, 2020). Since clinical data from LS patients showed elevated lactate levels (Crimi et al., 2004), a glycolytic rate assay was performed in these lines and compared with the control BJ-FB line. This allowed for the measurement of basal proton efflux rate (PER)- a measure of pH change from glycolysis only and not by carbon dioxide and water in the mitochondria via the citric acid cycle and oxidative phosphorylation (see schematics **Figure 4.3.6.a**). At the end of the assay, basal glycolysis, glycolytic capacity, and non-glycolytic respiration values were obtained. Basal glycolysis, a measure of basal extracellular proton efflux (PER), is significantly elevated (*p<0.0001*) by 36% in SBG1-FB(*T8993G*) and 26% in SBG3-FB(*T9185C*) and 70% in SBG5-FB (*T12706C*) line compared to control BJ-FB line (**Figure 4.3.6.b**). Increasing trends were observed in basal glycolysis rates in SBG2-FB (*T8993G*) and SBG4-FB *(T10158C)* lines when compared with the control cells.

The addition of mitochondrial inhibitors, rotenone and antimycin A, forced cells to compensate solely through the glycolytic pathway. Glycolytic capacity, a measure of this compensatory change in cellular metabolism increased by 34%, 25%, and 66.67% (*p<0.0001*) in SBG1-FB (*T8993G*), SBG3-FB (*T9185C*), and SBG5-FB (*T12706C*) lines respectively when compared to control BJ-FB cell line (**Figure 4.3.6.c**), further supporting the glycolytic dependence of these cell lines. As observed with the basal glycolysis, glycolytic capacity in the SBG2-FB (*T8993G*) and SBG4-FB *(T10158C)* cell lines were not significantly different from the control BJ-FB cell line. Finally, post-2-DG acidification was recorded after treating the cells with 2-deoxyglucose, to inhibit glycolysis. Post-2-DG acidification, a measure of proton efflux not

associated with either mitochondrial respiration or glycolysis rose by 13% in SBG1-FB(*T8993G*), 30% in SBG2-FB (*T8993G*), and 91% in SBG3-FB (*T9185C*) (*p<0.05*) cell lines with a defective ATP synthase function (**Figure 4.3.6.d**). The post-2-DG acidification was indistinguishable compared to the healthy control line in SBG4-FB *(T10158C)* and SBG5-FB (T12706C) mutant fibroblast cell lines.

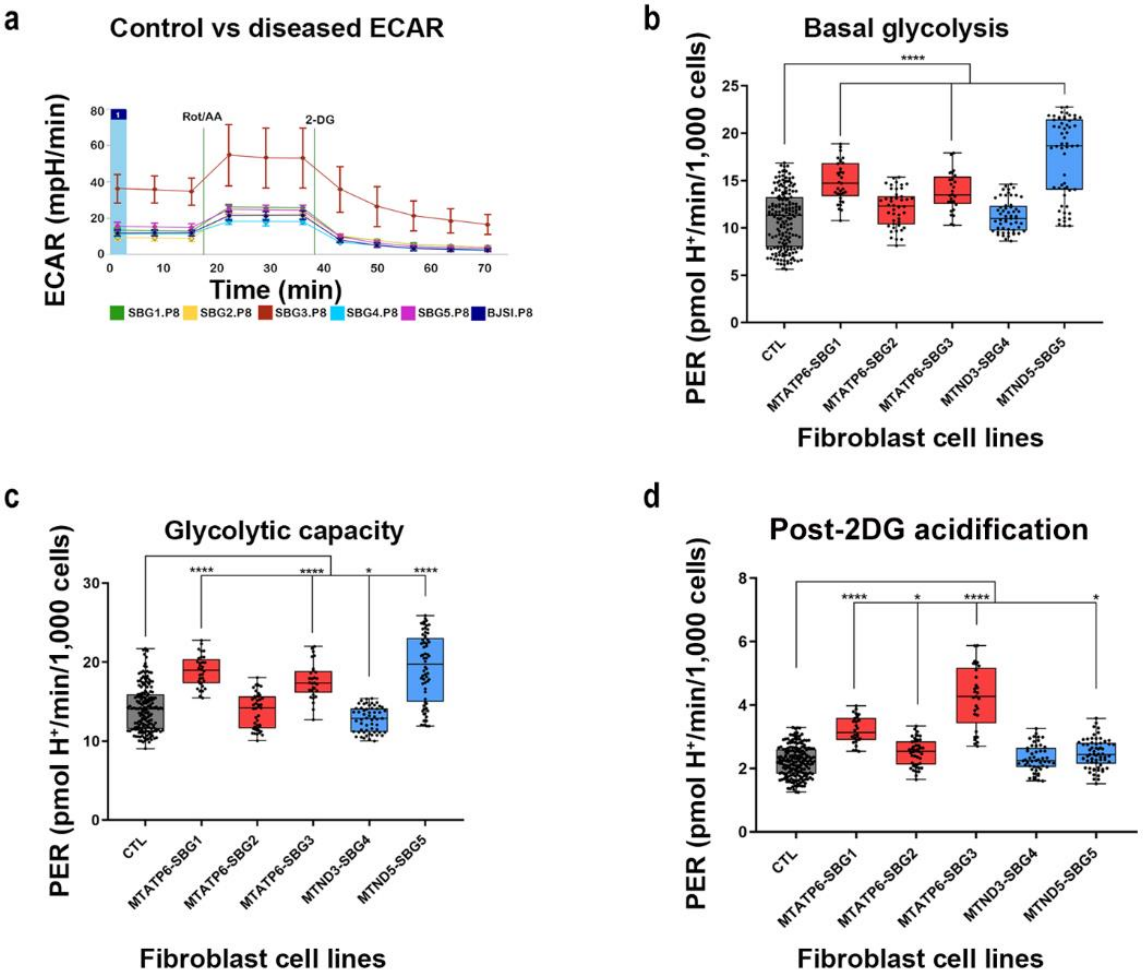

Figure 4.3.6. Glycolytic profile of CTL BJ-FB and five LS fibroblast cell lines. (a) a real-time profile shows the glycolytic acidification; PER of BJ-FB and diseased (SBG1-FB (*MTATP6-T8993G*), SBG2-FB (*MTATP6- T8993G*), SBG3-FB (*MTATP6-T9185C*), SBG4-FB (*MTND3-T10158C*), and SBG5-FB (*MTND5-T12706C*) cell lines showing (b) basal glycolysis (c) glycolytic capacity after ETC blocking using Rot/AA (d) post-2DG (non-glycolytic acidification). Data are shown in pmol H+/min/1000 cells as mean +/- SD. Experiments were repeated at least three times on different days under the same conditions. *p<0.05** p<0.01*** p<0.001 ****p<0.00001. Comparative analyses for all diseased (SBG1-5) FBs were conducted with the healthy control BJ-FB line. PER: proton efflux rate.

4.3.7. Mitochondrial ATP synthesis rate is decreased while glycolytic ATP synthesis rate is elevated in diseased cell lines

The defect in the function of ATP synthase or NADH dehydrogenase resulted in a decrease in mitochondrial ATP synthesis rate (**Figure 4.3.7.a**) and a subsequent increase in glycolytic ATP synthesis rate (**Figure 4.3.7.b**). As expected, we observed significant decreases ($p<0.05$) in mitochondrial ATP synthesis rate ($p<0.05$) by 33% in SBG2-FB (*T8993G*), 16% in SBG3-FB (*T9185C*), 30% in SBG4-FB *(T10158C)* and 37% in SBG5-FB (T12706C) lines compared to control BJ-FB cell lines. Although SBG1-FB (*T8993G*) had a 19.4% increase in mitochondrial ATP synthesis rate, it was due to compensatory oxygen flux (Gnaiger and MitoEAGLE, 2020) due to increased proton leak (**Figure 4.3.5.g**). The glycolytic ATP production rate was increased by 40% in SBG1-FB(*T8993G*), 43% in SBG3-FB (*T9185C*), and 60% in SBG5-FB (T12706C) when compared to control BJ-FB cells, supporting the prediction that dysfunctional mitochondrial-derived ATP, results in activation of adaptive pathways of ATP production. The glycolysis ATP rate was similar in SBG2-FB (*T8993G*) and SBG4-FB *(T10158C)* cell lines compared with the control cells (**Figure 4.3.7.b**) with less severe defects.

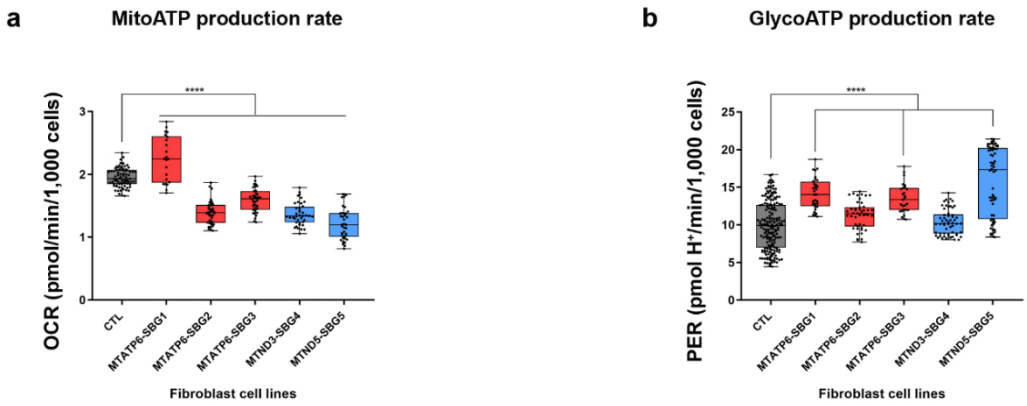

Figure 4.3.7. Production of ATP in BJ-FB and five LS fibroblast cell lines. The LS lines are (SBG1-FB (*MTATP6-T8993G*), SBG2-FB (*MTATP6- T8993G*), SBG3-FB (*MTATP6-T9185C*), SBG4-FB (*MTND3-T10158C*), and SBG5-FB (*MTND5-T12706C*) impacting the function of ATP synthase or NADH dehydrogenase. (a) Mitochondrial ATP rate and (b) Glyco-ATP rate. Data are shown in pmol H+/min/1000 cells as mean +/- SD. Experiments were repeated at least three times on different days under the same conditions. *p<0.05** p<0.01*** p<0.001 ****p<0.00001. Comparative analyses for all diseased (SBG1-5) FBs were conducted with the healthy control BJ-FB line. OCR: oxygen consumption rate. PER: proton efflux rate.

4.3.8. Glycolytic bioenergetic health index (BHI) ratio is a sensitive marker for predicting disease severity in all cell lines

To understand the relationship between disease severity and cellular markers of mitochondrial dysfunction, a single value concept termed “bioenergetics health Index or BHI” was recently proposed as a biomarker for measuring overall mitochondrial dysfunction (Chacko et al., 2014;Chacko et al., 2016). The BHI values were based on mitochondrial bioenergetics parameters and captured positive aspects of bioenergetics function (SRC and ATP-linked respiration) and contrasted these with potentially deleterious aspects (non-mitochondrial oxygen consumption and proton leak) shown in the formula in (**Figure 4.3.8.a**) (Chacko et al., 2016). In this study, the BHI based on mitochondrial parameters has been designated as ‘mitoBHI’. Individual ‘mitoBHI’ values as per the formula in **Figure 4.3.8.a** was highest for SBG3-FB (*T9185C*) at 1.92, followed by SBG1-FB (*T8993G*) at 1.83 and 1.61 for both SBG2-FB (*T8993G*) and SBG4-FB *(T10158C)* and SBG5-FB (*T12706C*) had a reduced value of 1.46, while the

control BJ-FB cell line was estimated to be at 1.61 (**Figure 4.3.8.b**). The 'mitoBHI' values in this study were found to be highly variable.

Since the results obtained with the disease cells also demonstrated a reliance on glycolysis, we introduced a similar concept that we have designated as 'glycoBHI'. Similar to the 'mitoBHI', the 'glycoBHI' captures positive aspects of glycolysis (Basal PER, compensatory glycolysis) and contrasts these with potentially deleterious non-glycolytic parameters (mitoPER and post-2DG-acidification) (**Figure 4.3.8.a**). The first term in the numerator for the glycoBHI is the Basal PER, which refers to the proton efflux rate in live cells by glycolysis only. The second term in the numerator, compensatory glycolysis, is the rate of glycolysis in cells after the addition of mitochondrial inhibitors, which inhibits mitochondrial bioenergetics and drives compensatory changes in the cell to use glycolysis to meet the cells' energy demands. For the denominator, the mitoPER refers to the contribution of the mitochondria to oxygen consumption and proton production, which is non-glycolytic. The final term in the denominator is the post-2-DG-acidification, which includes other sources of extracellular acidification that are not attributed to glycolysis or mitochondrial TCA activity as well as any residual glycolysis not fully inhibited by 2-DG. The terms *a, b, c,* and *d* in both 'mitoBHI' and 'glycoBHI' are exponents (linear in log-space), which modify the relative weighting of the respiratory parameters (Chacko et al., 2016). Individual glycolytic 'glycoBHI' values (**Figure 4.3.8.c**) were calculated using the four parameters as per the formula in **Figure 4.3.8.a**. All 'glycoBHI' values for diseased FBs were statistically significant and higher when compared with the control BJ-FB line (**Figure 4.3.8.c**). The high 'glycoBHI' values corresponded to 3.09, 2.97, and 2.95 for SBG3-FB (*T9185C*), SBG5-FB (*T12706C*), and SBG1-FB (*T8993G*) respectively, which aligns with high basal glycolysis values (**Figure 4.3.6.b**). In support of the basal glycolysis and glycolytic capacity data (**Figure 4.3.6.b, Figure 4.3.6.c**), the 'glycoBHI' values were 2.65 and 2.52 for SBG2-FB (*T8993G*) and SBG4-FB (*T10158C*) respectively. Consistent with our findings, the 'glycoBHI' values exhibited

a 25%, 12%, 31%, 7%, and 26% increase for SBG1-FB, SBG2-FB (*T8993G*), SBG3-FB (*T9185C*), SBG4-FB (*T10158C*), and SBG5-FB (*T12706C*) respectively when compared with the control BJ-FB cell line (**Figure 4.3.8.c**).

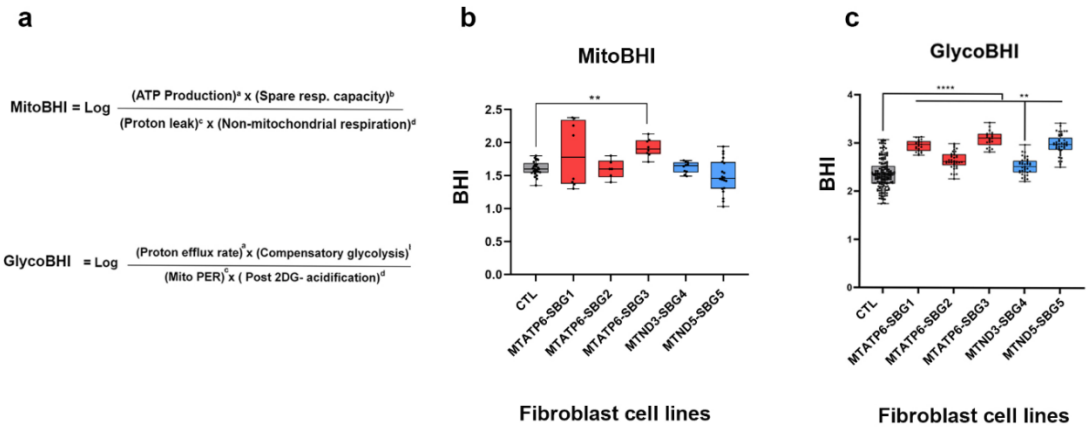

Figure 4.3.8. Composite Bioenergetic Health Index (BHI) ratio for BJ-FB and five LS fibroblast cell lines. The LS lines are (SBG1-FB (*MTATP6-T8993G*), SBG2-FB (*MTATP6-T8993G*), SBG3-FB (*MTATP6-T9185C*), SBG4-FB (*MTND3-T10158C*) and SBG5-FB (*MTND5-T12706C)* impacting the function of ATP synthase or NADH dehydrogenase. (a) The formula used to calculate the MitoBHI and GlycoBHI (b) Mito-BHI values were quantitated based on four bioenergetic parameters: mitoATP production, spare reserve capacity, proton leak and non-mitochondrial respiration. (c) Glyco-BHI values were quantitated based on four glycolytic parameters: Basal glycolysis (Basal PER), compensatory glycolysis, mitochondrial acidification (MitoPER), and post 2-DG acidification. *p<0.05** p<0.01*** p<0.001 ****p<0.00001.

4.4. Discussion

To better understand and connect the mitochondrial dysfunction contributing to clinical severity in LS, we selected five patient fibroblast lines from four young children and one young adult with mtDNA variants with clinical presentations ranging from mild myopathies to severe LS. The three cell lines contained pathogenic mtDNA with point mutations in the *MTATP6* gene [SBG1-FB (*T8993G*)and SBG2-FB (*T8993G*), SBG3-FB: (*T9185C*)] affecting the function of ATP synthase. The other two cell lines contained pathogenic mtDNA with point mutations in the *MTND3* gene [SBG4-FB (*T10158C*)] and *MTND5* gene [SBG5-FB (*T12706C*)] affecting the function of complex I. A commercially available fibroblast cell line (BJ-FB) was used as the

control line to minimize variability and all experiments were designed and analyzed at the same early passage (P8) in this study.

In this study, for the first time, we have introduced ‘glycoBHI’ as a more significant and sensitive indicator of the cells (**Figure 4.3.8.c**) that have mitochondrial dysfunction. In our study, we noted that the mitoBHI was highly variable, perhaps due to the mtDNA variants, heteroplasmy, or the functional aspects of the specific bioenergetics parameters. Since the disease fibroblasts had adapted and were dependent on both OXPHOS and glycolysis, we also computed one composite BHI ratio (‘mitoBHI’/ ‘glycoBHI’), based on the averages of the individual replicates associated with the mitoBHI and the glycoBHI for each line. This allowed us to evaluate the overall ability of the cell to meet energy demand due to its diseased state. In this study, we estimated the values to be 0.68 for the control BJ-FB, 0.64 for SBG4-FB (*T10158C*), 0.62 for SBG3-FB (*T9185C*), 0.62 for SBG1-FB, 0.61 for SBG2-FB (*T8993G*) and 0.49 for SBG5-FB (*T12706C*). With the value for BJ-FB set at 100 (normal), the composite BHI ratio values were 94 for SBG4-FB (*T10158C*) (mild), 91 for SBG3-FB (*T9185C*) (intermediate), 91 for SBG1-FB (*T8993G*) (intermediate), 89 for SBG2-FB (*T8993G*) (intermediate) and 72 for SBG5-FB (*T12706C*) (severe) respectively (**Figure 4.4.**).

Given the clinical variability and bioenergetic differences among patients with mitochondrial disorders, and LS in particular (as illustrated in **Figure 4.4.**); an important first step was to comprehensively analyze the range of bioenergetic parameters regulating the BHI ratio across the five lines and compare it with the BJ-FB control. By using the XFe96 extracellular flux analyzer, we were able to measure OCR as an indicator of mitochondrial respiration and PER for glycolysis. Mitochondrial and glycolysis specific inhibitors were used to measure different parameters such as basal respiration, ATP turnover, maximal respiration, spare respiratory reserve capacity, proton leak, non-mitochondrial respiration, proton efflux rate, compensatory glycolysis, and ATP production rates in real-time.

In this study, we have analyzed two major pathways involved in cellular respiration and ATP production. The first, mitochondrial respiration (OXPHOS), the pathway of ATP generation in the presence of oxygen. The second, basal glycolysis (PER), is the cell's pathway to synthesize ATP, which is non-mitochondrial. Overall, results demonstrate that SBG2-FB (*T8993G*), SBG3-FB (*T9185C*), SBG4-FB (*T10158C*), and SBG5-FB (*T12706C*) have decreased mitochondrial respiration and ATP production, while SBG1-FB (*T8993G*) cell line was driven by compensatory oxygen flux, most likely due to proton leak across the inner mitochondrial membrane. Although all diseased FBs adapted to the mitochondrial defects with variable increases in the glycolytic pathway; SBG1-FB, SBG3-FB (*T9185C*), and SBG5-FB (*T12706C*) showed significantly higher basal glycolysis (**Figure 4.3.6.b**), glycolytic capacity (**Figure 4.3.6.c**); and 'glycoBHI' (**Figure 4.3.8.c**) when compared to the control BJ-FB. SBG2-FB (*T8993G*) and SBG4-FB (*T10158C*) showed only a mild increase in basal glycolysis (**Figure 4.3.6.b**) and 'glycoBHI' (**Figure 4.3.8.c**) values when compared with the control BJ-FB. A question then may arise as to why do SBG1-FB, SBG3-FB (*T9185C*) and SBG5-FB (*T12706C*) cells activate the glycolytic pathway? What was the mechanism driving it?

We hypothesized that SRC values were an important contributing factor, in the cell's decision to compensate for the lowered mitochondrial ATP rate and activate the glycolytic pathway. In support of our hypothesis, previous studies have reported that a decrease in SRC negatively affects cardiac muscles, making them more vulnerable to bioenergetic exhaustion (Gong et al., 2003). Studies on mouse myocytes and iPSC-derived myocytes further support the importance of SRC in cell survival (Pfleger et al., 2015). Other studies have also shown SRC depends on the oxidation of glucose-derived pyruvate (Pfleger et al., 2015;Marchetti et al., 2020), which is then oxidized into Acetyl-CoA and enters the TCA cycle to produce reduced electron carries, NADH and FAD which enters the ETC complex to ultimately produce ATP, via the ATP synthase. In line with these findings, results in this study indicated that the LS diseased

cell lines demonstrated a decrease in mitochondrial ATP synthesis rate (**Figure 4.3.7.a**), prompting a need to activate the glycolysis pathway, perhaps for continued maintenance of high SRC levels (150% & 190%), seen in SBG1-FB (*T8993G*) and SBG3-FB (*T9185C*) cells (**Figure 4.3.5.h**). However, SBG5-FB (*T12706C*) cells displayed significantly low (50%) SRC levels (**Figure 4.3.5.h**), yet very high (70%) glycolysis rate (**Figure 4.3.6.b**). In this scenario, the cells likely have a severe defect in complex I (Ni et al., 2019) and switch to the glycolysis pathway to satisfy the energy requirement of the cells. Therefore, the low SRC levels perhaps diverted the fate of pyruvate to produce lactate during glycolysis, which supports the clinical outcomes associated with LS (Ni et al., 2019). The other cell line with significantly low (11%) SRC levels below the threshold (**Figure 4.3.5.h**) was SBG2-FB (*T8993G*). Here the cells triggered a mild increase in basal glycolysis (**Figure 4.3.6.b**) to generate pyruvate for minimally maintaining SRC levels. SRC is measured as oxygen consumption in the presence of uncoupler-FCCP and is an indicator of ETC's capacity to move protons from the mitochondrial matrix into the intermembrane space (Nicholls et al., 2010) in the uncoupled state (Gnaiger and MitoEAGLE, 2020). Therefore, increasing defects in ATP synthase compromised the ETC capacity, leading to a collapse in membrane potential and reduced ROS levels (**Figure 4.3.4.**) with a concomitant increase in complex I activity indicated by NFR (**Table 4.3.3.**).

Lastly, modest increase (**Figure 4.3.5.h**) in SRC levels in SBG4-FB (*T10158C*) cells compared with the control BJ-FB line. SBG4-FB (*T10158C*) cells did not increase basal glycolysis (**Figure 4.3.6.b**) for ATP synthesis because of the milder complex I defect or low heteroplasmy levels of 30% (**Table 4.3.2.**)**.** Here, we showed for the first time in LS, the importance of SRC as a balancing factor in promoting cell adaptability due to functional mitochondrial defects. More importantly, for the first time, we also demonstrate the relevance of glycolysis and the 'glycoBHI' as a very significant and sensitive index of mitochondrial defects in the LS diseased lines.

Taking all the cellular dysfunction in LS patient cells into consideration, we have attempted to group the clinical severity presented in **Table 4.3.1.** and **Figure 4.4.** into severe, intermediate, and mild categories. In this study, we note that the most severely affected line is SBG5-FB (*T12706C*), based on the comprehensive assessment of bioenergetic parameters (**Figure 4.2.5-4.2.8.**). The cell respiration assays confirmed that SBG5-FB (*T12706C*), exhibited the lowest composite BHI ratio value of 72 (**Figure 4.4.**), due to decreased SRC and high glycolysis. Furthermore, the maximal respiration (**Figure 4.3.5.e**) and SRC (**Figure 4.3.5.h**) was significantly reduced (~50 %) when compared to the healthy control BJ-FB, leading to a low 'mitoBHI' of 1.46 (**Figure 4.3.8.b**). In order to compensate for the loss in mitochondrial ATP production by OXPHOS, the SBG5-FB (*T12706C*) cells adapt and increase glycolysis derived ATP (**Figure 4.3.7.b**), leading to a high 'glycoBHI' value of 2.97 (**Figure 4.3.8.c**). Since the SRC values were the lowest, the resulting pyruvate was converted into lactate to regenerate NAD+, since NADH oxidation by the ETC is decreased. It is thus not surprising that our findings are in agreement with the clinical diagnosis of 'severe neonatal lactic acidosis' and resulting in a fatality at 9.5 months within a month of clinical diagnosis (Ni et al., 2019).

Based on our comprehensive assessment of the different bioenergetic parameters, we grouped three cell lines SBG1-FB (*T8993G*), SBG2-FB (*T8993G*), and SBG3-FB (*T9185C)*, as 'intermediate' with respect to the severity of the disease. Detailed below are the subtle dissimilarities between the three lines to distinguish the bioenergetic differences that contribute to the composite BHI ratios. The first intermediate-to-severe diseased line was SBG2-FB (*T8993G*) with a clinical diagnosis of 'developmental delay and abnormal gait' (**Figure 4.4.**). Although SBG2-FB (*T8993G*), carries the same mutation as SBG1-FB (*T8993G*), the patient exhibited different levels of disease severity reflected in the glycoBHI of 2.64 and a composite BHI ratio value of 89 (**Figure 4.4.**). We also observed a decrease of 33% in mitochondrial ATP synthesis rate (**Figure 4.3.7.a**), the SRC (11.1%) (**Figure 4.3.5.h**), and maximal respiration

(23%) (**Figure 4.3.5.e**) when compared with the control BJ-FB line. When the SRC is consumed and decreases below the threshold, the mitochondria can no longer respond to energetic demand; thus likely contributing to developmental defects in high-energy tissues such as the brain, heart, and muscle.

The second intermediate diseased line is SBG1-FB (*T8993G*), with a clinical diagnosis as LS (**Figure 4.4.**) (Stendel et al., 2020), a 'glycoBHI' of 2.95, and a composite BHI ratio of 91 (**Figure 4.4.**). Furthermore, the maximal respiration rate increased significantly by 98% (**Figure 4.3.5.e**) and SRC by 150% (**Figure 4.3.5.h**) when compared to the control BJ-FB line. However, results also showed an increase in proton leak by 33% when compared with the control BJ-FB (**Figure 4.3.5.g**), indicating a 'pathologically dyscoupled respiration state' (Gnaiger and MitoEAGLE, 2020). Thus the mitochondria appear to compensate by significantly increasing the basal glycolysis (PER) by 36% (**Figure 4.3.6.b**) to preserve the ATP production rate (**Figure 4.3.7.a**). However, the increase in glycolytic capacity by 34% (**Figure 4.3.6.c**) and the trend to increased glycolytic ATP production rate (**Figure 4.3.7.b**) supports that glycolytic compensation is likely incomplete. It is also possible that the pyruvate is diverted to produce lactate to preserve glycolytic rates, leading to elevated blood lactate levels as seen in LS patients (Lake et al., 2016).

The third intermediate-to-mild disease variant is SBG3-FB (*T9185C*), in which the patient was diagnosed at age 23 years with 'mild myopathy' (**Figure 4.4.**). The cell respiration assays confirmed that SBG3-FB (*T9185C*), exhibited the highest increase in SRC (190%) (**Figure 4.3.5.h**) and increased maximal respiration (57%) (**Figure 4.3.5.e**), compared to the control BJ-FB; while the glycolytic ATP was mildly elevated (**Figure 4.3.7.b**), accompanied by a glycoBHI of 3.09 and composite BHI ratio of 91 (**Figure 4.4.**), representing a milder form of LS. The significant increase in post-2DG-acidification (**Figure 4.3.6.d**) indicates the possibility of other pathways not attributed to glycolysis or TCA cycle activity being activated to maintain high SRC levels and is worthy of future investigation.

Finally, the mild disease variant is SBG4-FB (*T10158C*) with a clinical diagnosis of 'epilepsy, dystonic tetraparesis', a glycoBHI of 2.52, and a composite BHI ratio of 94 (**Figure 4.4.**). Furthermore, we observed a slight increase in maximal respiration (13%) (**Figure 4.3.5.e**) and SRC (**Figure 4.3.5.h**), which indicated that the cells were barely able to meet energy demands, by either increasing ATP production within the mitochondria (**Figure 4.3.7.a**) or by adapting to the glycolytic pathway. The glycolytic capacity (**Figure 4.3.6.c**) and basal glycolysis (PER) (**Figure 4.3.6.b**) were only mildly higher when compared with the control line; possibly contributing to a very mild clinical phenotype in the LS patient.

Based on the overall analysis of the five diseased patient-specific fibroblasts, the 'glycoBHI' emerged as a sensitive indicator of mitochondrial defects as the cells had switched 'on' the glycolytic pathway. As shown in (**Figure 4.3.8.c**) glycoBHI was significantly increased in all the cell lines compared to control BJ-FB and was indeed sensitive to the mitochondrial dysfunction.

We also computed the 'composite BHI ratio' (oxphos/glycolysis because the cell lines were utilizing both oxphos (although highly defective) and glycolysis pathways to maintain the energy requirements in the individual cell line. As noted in **Figure 4.4.**, the composite BHI ratio (100 was deemed healthy), while the decreased composite BHI ratio (72 was unhealthy), and indicative of a very diseased state. Two important parameters associated with the composite BHI ratio were basal glycolysis (PER) which was a measure of mitochondrial defect and SRC, which was an indicator of the cell's capacity to adapt to the defect.

Another important consideration is pathogenic mtDNA variants and heteroplasmy levels associated with the specific mtDNA variant. The current study indicates that in addition to the bioenergetic parameters, there must be consideration of the specific pathogenic mtDNA variant, rather than solely relying on the percentage heteroplasmy. In line with previous studies (Tatuch et al., 1992;Ganetzky et al., 2019;Stendel et al., 2020), we also measured a high heteroplasmy for pathogenic mtDNA *MTATP6* variants SBG1-FB: 96%; SBG2-FB (*T8993G*): 91%; SBG3-FB

(*T9185C*): 98%, that is associated with LS, and impacting ATP synthase function. As other studies have reported (Ganetzky et al., 2019;Stendel et al., 2020), the clinical phenotype for SBG1-FB-*MTATP6-T8993G* was classic 'LS', while for SBG2-FB *MTATP6-T8993G* was 'developmental delay, abnormal gait'; and for SBG3-FB-*MTATP6-T9185C* a mild myopathy and late disease onset. Despite the high heteroplasmy and identical mutation, the composite BHI ratio was able to distinguish the different *MTATP6* variants with regard to the disease severity.

Previous studies (Kirby et al., 2004;McFarland et al., 2004), have shown that the pathogenic *MTND3-T10158C* and *MTND5-T12706C* mtDNA variants have also been observed in patients exhibiting LS phenotype. In the current study, heteroplasmy was measured to be 30% in the SBG4-FB-*MTND3-T10158C*. The subtle increase in SRC (**Figure 4.3.5.h**), lowered basal respiration (**Figure 4.3.5.d**) and basal glycolysis (**Figure 4.3.6.b**) is in line with a milder metabolic defect manifested as epilepsy and muscle weakness for the patient from whom SBG4-FB (*T10158C*) was derived. Heteroplasmy was measured at 39% in SBG5-FB-*MTND5-T12706C*, associated with the most severe clinical phenotype. Previous studies have reported varying heteroplasmy levels (from 30-70%) for this mtDNA variant with severe clinical phenotypes associated with LS, which indicates that even a low mutation burden could contribute to disease severity (Taylor et al., 2002;Lebon et al., 2003;Zhadanov et al., 2007;Ni et al., 2019). The present study demonstrates that SBG5-FB (*T12706C*) exhibited low SRC (**Figure 4.3.5.h**); low mitochondrial ATP production (**Figure 4.3.7.a**), very high glycolytic ATP production (**Figure 4.3.7.b**); and high basal glycolysis (**Figure 4.3.6.b**), which is in line with the observed clinical phenotype of neonatal lactic acidosis. In the current study, we have shown that low heteroplasmy in SBG4- FB-*MTND3-T10158C* contributed to a milder clinical phenotype, while SBG5-FB-*MTND5-T12706C* contributed to a very severe phenotype in the context of LS. However, the composite BHI ratio emerged as a comprehensive biomarker based on the value of 94 for SBG4-FB- *MTND3-T10158C* and 72 for SBG5-FB-*MTND5-T12706C* and correlated with the severity of the clinical phenotype (**Figure 4.4.**). Overall, these results suggest that as

long as the precise mechanism of LS has not been elucidated, a multi-pronged approach that takes into consideration the specific pathogenic mtDNA variant, along with a composite BHI ratio, can aid in better diagnosis and understanding the factors influencing disease severity and rapid fatality in LS.

Another possibility suggested by our work beyond mitochondrial disorders is incorporating the composite BHI ratio as a measure of overall mitochondrial health and fitness in different cell types utilizing both glycolytic and oxidative phosphorylation pathways to maintain energy production. Specifically, in adult metabolic disorders such as diabetes, cancer, or obesity, our findings here suggest that drugs that target mitochondrial SRC (Roy Chowdhury et al., 2012;Corazao-Rozas et al., 2016;Yamamoto et al., 2016;Zhang et al., 2016) could hold promise as therapeutic potential and might warrant further study for their ability to alter ATP levels and restore the BHI ratio to physiological levels.

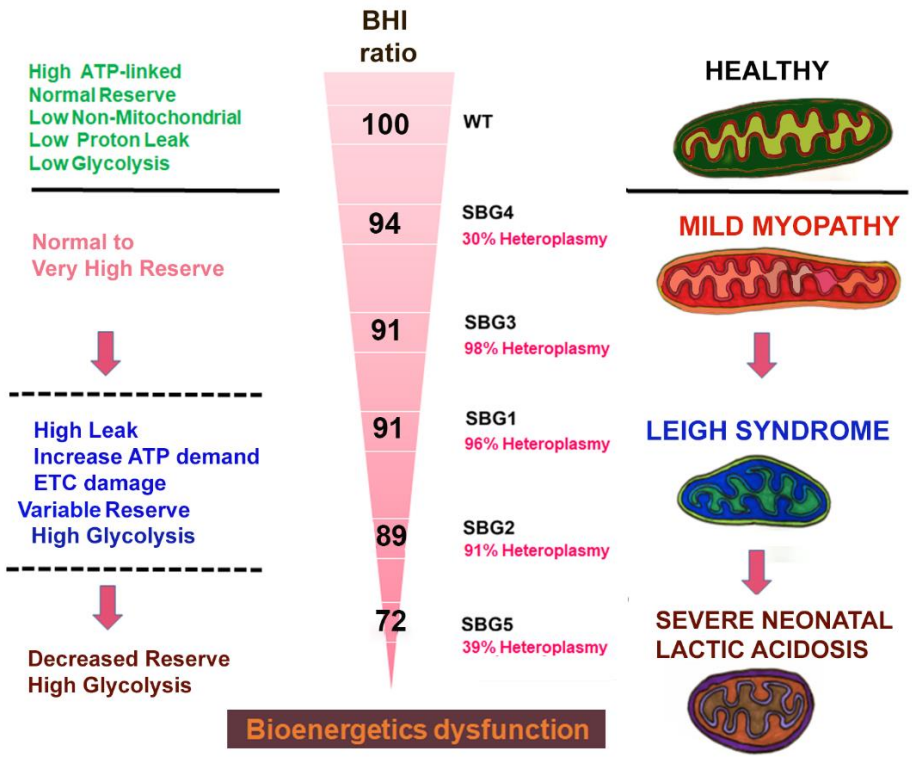

Figure 4.4. A model for predicting disease severity in LS. Our results indicate that during stress triggered by specific pathogenic mtDNA variants or other factors, cells (SBG4-FB (*MTND3-T10158C*) with high spare reserve capacity (SRC), low heteroplasmy and high composite BHI ratio exhibit delayed onset and mild clinical symptoms. However, as SRC and composite BHI ratio decreases, cells (SBG5-FB (*MTND5-T12706C)* are unable to handle stress and exhibit early-onset and severe clinical symptoms despite low heteroplasmy levels. Whereas cells carrying pathogenic disease mtDNA variants in *ATP6* gene (SBG1-FB (*MTATP6-T8993G*), SBG2-FB (*MTATP6- T8993G*), SBG3-FB (*MTATP6-T9185C*) exhibit very high heteroplasmy levels, lower composite BHI ratio when compared with control BJ-FB and can be grouped as 'intermediate' in disease severity.

4.5. Methods

4.5.1. Ethics statement

This study protocol conformed to the guidelines of the Declaration of Helsinki. The current study was conducted with patient fibroblasts provided by the Medical University of Salzburg (SBG), Austria. Fibroblasts were obtained for diagnostic purposes from patients with defined disorders. Informed consent was obtained to use these samples for research in an anonymized

way. In accordance with federal regulations regarding the protection of human research subjects (32 CFR 219.101(b)(4)), the University of Arkansas Office of Research Compliance determined that the project was exempt from Institutional Review Board (IRB) oversight and human research subjects protection regulations.

4.5.2. Clinical information

The clinical information associated with the five patient fibroblasts is summarized in **Table 4.3.1**. The first (SBG1-FB (*T8993G*)) patient was a girl with a clinical presentation of Morbus Leigh while the second (SBG2-FB (*T8993G*)) patient was a boy with a clinical presentation of developmental defects. Pathogenic mtDNA mutation *T8993G* was present in the *ATP6* gene in both the patient cell lines. The third (SBG3-FB (*T9185C*)) patient was a girl with a mild clinical myopathy with pathogenic mtDNA mutation *T9185C* present in the *ATP6* gene. The fourth (SBG4-FB (*T10158C*)) patient was a boy with clinical presentation of epilepsy with pathogenic mtDNA mutation *T10158C* present in mitochondrial *ND3* gene, the core subunit of complex I. The fifth (SBG5-FB (*T12706C*)) patient was a girl with clinical presentation of severe neonatal lactic acidosis with pathogenic mtDNA mutation *T12706C* present in mitochondrial *ND5* gene, in the core subunit of complex I. Unaffected healthy control (BJ-FB- ATCC® CRL-2522™) fibroblast cell line was obtained from the American Type Culture Collection (ATCC, Manassas, VA, USA).

4.5.3. Cell culture

Cultures of healthy control and five patient-derived diseased fibroblast cell lines were maintained in a fibroblast expansion medium that consisted of minimal essential medium (MEM) (Thermo Fisher Scientific, Waltham, MA, USA) supplemented with 10% fetal bovine serum (FBS) (GE healthcare- HyClone™; Chicago, IL) and 2mM L-glutamine (Thermo Fisher Scientific, Waltham, MA, USA). All cell lines were cultured and maintained at 37^{o}C in a humidified

atmosphere of 5% CO_2. The culture medium was replenished every two days and passaged when cells reached 80% confluence. Fibroblasts were enzymatically passaged in 0.05% Trypsin-EDTA (Thermo Fisher Scientific, Waltham, MA, USA). All experiments were performed with cells at passage 8 for consistency and to minimize experimental variability.

4.5.4. Next-generation sequencing for heteroplasmy analysis

Frozen cell pellets from different samples containing ~ 2 x 10^6 cells were thawed and processed. The QIAamp DNA mini kit (Qiagen, Valencia, CA, USA) manufacturer protocol was followed to extract total DNA, which resulted in elution of 100 µL of distilled water (dH2O) and total DNA from all cells. The 100 µL solution containing the genomic DNA was further treated with 1 µL of RNaseA for 1 hour at 37°C to avoid RNA contamination. The gDNA was quantified using DeNovix UV/Vis Spectrophotometer (DeNovix Inc. Wilmington, DE, USA). A blank of 1.0µL of dH2O was used to establish a zero, and 1.0µL of each sample was used to determine the concentration.

The DNA concentration was verified using a Qubit fluorometer (Thermo Scientific). Instead of the standard DNA fragmentation, an enzymatic fragmentation was performed using the KAPA Frag Enzyme from the KAPA HyperPlus Library Preparation Kit (KAPA Biosystems, Wilmington, MA). This alternative was performed to increase yield during the fragmentation step. Fragmented DNA was purified using Ampure beads (Beckman Coulter, Brea, CA). DNA libraries were prepared using the Accel-NGS 2S Plus DNA Library Kit (Swift Biosciences, Ann Arbor, MI). Ten PCR cycles were carried out during the Library Amplification step. The final libraries were analyzed with a 2100 Bioanalyzer to assess library size distribution (Agilent Technologies, Santa Clara, CA). DNA libraries were quantified with the KAPA Library Quantification Kit to ensure accuracy (KAPA Biosystems). Based on the qPCR results, the DNA

libraries were compiled in equimolar amounts and sequenced with the HiSeq 2500 using TruSeq v3 reagents according to the 2 x 100 bp protocol (Illumina, San Diego, CA).

Heteroplasmy fractions were extracted from the FASTQ files as previously described (Grandhi et al., 2017). Briefly, we first filtered out reads that were likely to be nuclear mitochondrial sequences (NuMTs). NuMTs are DNA sequences that are harbored in the nuclear genome, but closely match sequences in the mitochondrial genome (Hazkani-Covo et al., 2010). Specifically, reads that aligned, using Burrows-Wheeler Alignment Tool (Li and Durbin, 2009), with up to one mismatch to the nuclear reference sequence GRCh38 (having removed the mitochondrial revised Cambridge reference sequence (rCRS) (Andrews et al., 1999) were excluded from downstream analysis. The resulting reads were realigned to rCRS, and read counts of the mutant and wild-type alleles were extracted using SAMtools mpileup (Li et al., 2009). From these counts, the mutant heteroplasmy level was computed as: (mutant allele counts)/(total counts).

4.5.5. Mitochondrial oxygen consumption detection, glycolysis function test, and bioenergetics health index (BHI)

In this study, we evaluated the metabolic state in the patient-derived fibroblasts to further understand the influence of mtDNA mutations on cellular bioenergetics. Changes in oxygen consumption were measured in real-time using an XFe96 extracellular flux analyzer. Seahorse XFe96 Cell Mito Stress Test Kit and glycolytic rate assay kit (Seahorse Biosciences, USA) were used as per the manufacturer's instructions. Prior to use in XFe96, fibroblasts were detached using mild trypsin and seed into the plates with a previously optimized number of 20,000 cells per well. All fibroblasts were seeded in 10-12 replicate wells per plate, with the experiment repeated at least 4-5 times.

The cells were supplemented with 180 µl Mito-stress complete Seahorse medium, after which the cells were incubated in a non-CO_2 incubator at 37ºC for one hour. Respiration was measured using the classic mitochondrial inhibitors, specific for complex I and III subunits, such as Rotenone and Antimycin A (0.5 µM final concentrations each). Maximum respiration was measured by the addition of an uncoupler carbonyl cyanide-4-(trifluoromethoxy) phenylhydrazone- FCCP (0.7 µM final concentration); and Oligomycin (1 µM final concentration) was added to measure proton leak. The readouts were normalized to cell number and analyzed using Seahorse XF96 Wave software.

Given the presence of point mutations impacting ATP6, ND5, and ND3, we also analyzed glycolytic function in all fibroblasts. A classical glycolytic rate assay was performed using the XFe96 based on the following procedure: 1) cells were cultured in buffered (5 mM HEPES buffer) Seahorse medium supplemented with glucose and pyruvate; 2) the proton efflux rate (PER) was measured after the addition of saturating amounts of glucose; 3) rotenone and antimycin A were added to inhibit mitochondrial-derived ADP phosphorylation, and 4) 2-DG was added to inhibit glycolysis. The different assay parameters: basal glycolysis, compensatory glycolysis, total proton efflux, and post 2-DG acidification were normalized to cell number and analyzed using Seahorse XFe96 Wave software.

The mitochondrial-derived bioenergetic health index (mitoBHI), a composite index of mitochondrial quality was determined using the formula in **Figure 4.3.8.d**, where a, b, c, and d exponents modify the relative weight of each respiratory parameter and by default are equivalent to 1 in this experiment. The glycolytic BHI (glycoBHI), an index of glycolytic respiration was determined using the formula in **Figure 4.3.8.d.** The composite BHI index was calculated by taking a ratio of the means of mitoBHI and glycoBHI.

4.5.6. Measurement of electron transport chain activity

The activity of electron transport chain complexes I, III, and V were measured in frozen-thawed, detergent-solubilized fibroblast cell lines. The overall approach of Hoppel and colleagues was used (Stephan KrahenbuhlS and Charles, 1991;Lesnefsky et al., 1997). The assay was optimized for the use of smaller volume incubations (300 µl) with preliminary experiments first using isolated mouse heart mitochondria followed by the use of H9c2 cardiomyoblast cells. In these initial experiments, the solubilization method and volumes used preserved complex activity compared to the use of larger assay volumes and greater amounts of mitochondrial and cellular protein. The amount of cell protein used was based on initial work that established linear ranges of total enzyme activity vs. protein content. The fibroblast cell lines SBG 1-5 and control non-diseased fibroblasts were maintained as above. They were pelleted by centrifugation [400 xg] and flash-frozen with liquid nitrogen. They were shipped by overnight express from SI to EJL and immediately placed at -80^{o}C. On the day of the experiment, cells (approximately 2-5 million cells) were thawed on ice, suspended, and centrifuged at 10,000 rcf. The supernatant was removed, and pellets were suspended in 4^{0}C mannitol (220 mM)-sucrose (70 mM)- MOPS (5 mM) buffer with Na_2EDTA (2 mM), pH 7.4. Sodium cholate hydrate (5 g/100 mL Milli-Q water) was added, the mixture briefly vortexed, two additional volumes of MSM-EDTA added to decrease the final cholate concentration to 1%. Protein content was measured using the Lowry assay. Citrate synthase activity was measured using 10 µg of cell protein by the oxaloacetate mediated reduction of DTNB at 412 nm. *Complex I* activity was assessed using NADH:ferricyanide oxidoreductase (NFR) and NADH:cytochrome c oxidoreductase (NCR; rotenone sensitive). NFR was measured using the artificial electron acceptor potassium ferricyanide using 50 µg of cell protein at 340 nm following the decrease in NADH content. NCR was measured by following the rotenone-sensitive reduction of cytochrome *c* using the increase in absorbance at 550 nm using 100 µg of cell

protein. NCR measures the activities of complex I and III with complex I the rate-limiting step. *Complex III* activity (decylubiquinol: cytochrome *c* oxidoreductase, antimycin A sensitive) was measured using 50 µg of cell protein at 550 nm by following the increase in the content of reduced cytochrome *c*. *Complex V* activity (oligomycin sensitive) was measured using 45 µg of cell protein using a commercially available kit (Cayman Chemical, Ann Arbor, MI, USA) according to the manufacturer's instructions.

4.5.7. Mitochondrial reactive oxygen species measurement

In this study, all fibroblasts were maintained in culture following established protocols until the desired passage (p8) is reached. Prior to use in flow cytometry analysis, cells were cultured until 70-80% confluence was reached. On the day of the experiment, cells were enzymatically detached using 0.05% Trypsin-EDTA (Thermo Fisher Scientific) and centrifuged at 400xg for 5 mins. The cells were then resuspended in basal medium, after which the desired amount of MitoSOX Red (Thermo Fisher Scientific) was added (for a final concentration of 3 µM). For Rotenone and Antimycin A treatment groups, 5 µM of each was added for 10 mins before MitoSOX treatment. Cells were incubated with MitoSOX in a 37^{o}C 5% CO2 incubator for 25 mins. At the end of the incubation period, cells were centrifuged at 400xg for 5 mins. To wash off the excess dye, cells were resuspended in 1x dPBS solution and centrifuged for another 5 mins. At the end of the wash, the cells were resuspended in phenol-red free basal medium and transferred to Accuri C6 plus flow cytometer (BD Biosciences; Franklin Lakes, New Jersey) for data acquisition. 10,000 events were recorded for each cell line. After data acquisition, the data were exported as FCS files and analyzed using FlowJo_v10.6.2 software. To gate for the MitoSOX-positive population, we had cells that were not treated with the dye and used these to gate for our negative and positive cell populations. Mean fluorescent intensity (MFI) values, a measure of the geometric mean of MitoSOX positive cells was obtained for statistical analysis.

4.5.8. Statistical analysis

In order to ensure scientific rigor and reproducibility, for the bioenergetics analysis, an ANOVA design accounting for 4-5 biological and 10-12 technical replicated from control (BJ-FB) and diseased (SBG1-FB (*T8993G*), SBG2-FB (*T8993G*), SBG3-FB (*T9185C*), SBG4-FB (*T10158C*), SBG5-FB (*T12706C*)) that are nested within groups was used to identify any differences with respect to control BJ-FBs. Post-hoc Tukey HSD tests were used to identify differences among specific groups. Data are presented as the mean ± standard deviation (SD) and were analyzed using the GraphPad Prism 8 software (GraphPad Software, San Diego, CA, USA). A $p<0.05$ was considered significant.

4.6. References

Andrews, R.M., Kubacka, I., Chinnery, P.F., Lightowlers, R.N., Turnbull, D.M., and Howell, N. (1999). Reanalysis and revision of the Cambridge reference sequence for human mitochondrial DNA. *Nat Genet* 23**,** 147.

Baertling, F., Rodenburg, R.J., Schaper, J., Smeitink, J.A., Koopman, W.J., Mayatepek, E., Morava, E., and Distelmaier, F. (2014). A guide to diagnosis and treatment of Leigh syndrome. *J Neurol Neurosurg Psychiatry* 85**,** 257-265.

Boyer, P.D., Cross, R.L., and Momsen, W. (1973). A new concept for energy coupling in oxidative phosphorylation based on a molecular explanation of the oxygen exchange reactions. *Proc Natl Acad Sci U S A* 70**,** 2837-2839.

Chacko, B.K., Kramer, P.A., Ravi, S., Benavides, G.A., Mitchell, T., Dranka, B.P., Ferrick, D., Singal, A.K., Ballinger, S.W., Bailey, S.M., Hardy, R.W., Zhang, J., Zhi, D., and Darley-Usmar, V.M. (2014). The Bioenergetic Health Index: a new concept in mitochondrial translational research. *Clinical Science (London)* 127**,** 367-373.

Chacko, B.K., Zhi, D., Darley-Usmar, V.M., and Mitchell, T. (2016). The Bioenergetic Health Index is a sensitive measure of oxidative stress in human monocytes. *Redox Biology* 8**,** 43-50.

Chance, B., and Williams, G.R. (1955). Respiratory enzymes in oxidative phosphorylation. IV. The respiratory chain. *J Biol Chem* 217**,** 429-438.

Cheng, J., Nanayakkara, G., Shao, Y., Cueto, R., Wang, L., Yang, W.Y., Tian, Y., Wang, H., and Yang, X. (2017). Mitochondrial Proton Leak Plays a Critical Role in Pathogenesis of Cardiovascular Diseases. *Adv Exp Med Biol* 982**,** 359-370.

Childs, A.M., Hutchin, T., Pysden, K., Highet, L., Bamford, J., Livingston, J., and Crow, Y.J. (2007). Variable phenotype including Leigh syndrome with a 9185T>C mutation in the MTATP6 gene. *Neuropediatrics* 38**,** 313-316.

Coller, H.A., Bodyak, N.D., and Khrapko, K. (2002). Frequent intracellular clonal expansions of somatic mtDNA mutations: significance and mechanisms. *Ann N Y Acad Sci* 959**,** 434-447.

Corazao-Rozas, P., Guerreschi, P., Andre, F., Gabert, P.E., Lancel, S., Dekiouk, S., Fontaine, D., Tardivel, M., Savina, A., Quesnel, B., Mortier, L., Marchetti, P., and Kluza, J. (2016). Mitochondrial oxidative phosphorylation controls cancer cell's life and death decisions upon exposure to MAPK inhibitors. *Oncotarget* 7**,** 39473-39485.

Crimi, M., Papadimitriou, A., Galbiati, S., Palamidou, P., Fortunato, F., Bordoni, A., Papandreou, U., Papadimitriou, D., Hadjigeorgiou, G.M., Drogari, E., Bresolin, N., and Comi, G.P. (2004). A new mitochondrial DNA mutation in ND3 gene causing severe Leigh syndrome with early lethality. *Pediatr Res* 55**,** 842-846.

Debray, F.G., Lambert, M., Lortie, A., Vanasse, M., and Mitchell, G.A. (2007). Long-term outcome of Leigh syndrome caused by the NARP-T8993C mtDNA mutation. *Am J Med Genet A* 143A**,** 2046-2051.

Fassone, E., and Rahman, S. (2012). Complex I deficiency: clinical features, biochemistry and molecular genetics. *J Med Genet* 49**,** 578-590.

Ganetzky, R.D., Stendel, C., Mccormick, E.M., Zolkipli-Cunningham, Z., Goldstein, A.C., Klopstock, T., and Falk, M.J. (2019). MT-ATP6 mitochondrial disease variants: Phenotypic and biochemical features analysis in 218 published cases and cohort of 14 new cases *Human Mutation* 40**,** 499-515.

Gnaiger, E., and Mitoeagle, T.G. (2020). Mitochondrial physiology. *Bioenergetics Communications* 2020.1.

Gong, G., Liu, J., Liang, P., Guo, T., Hu, Q., Ochiai, K., Hou, M., Ye, Y., Wu, X., Mansoor, A., From, A.H.L., Ugurbil, K., Bache, R.J., and Zhang, J. (2003). Oxidative capacity in failing hearts. *American Journal of Physiology-Heart and Circulatory Physiology* 285**,** H541-H548.

Grace, H.E., Galdun, P., 3rd, Lesnefsky, E.J., West, F.D., and Iyer, S. (2019). mRNA Reprogramming of T8993G Leigh's Syndrome Fibroblast Cells to Create Induced Pluripotent Stem Cell Models for Mitochondrial Disorders. *Stem Cells Dev* 28**,** 846-859.

Grandhi, S., Bosworth, C., Maddox, W., Sensiba, C., Akhavanfard, S., Ni, Y., and Laframboise, T. (2017). Heteroplasmic shifts in tumor mitochondrial genomes reveal tissue-specific signals of relaxed and positive selection. *Hum Mol Genet* 26**,** 2912-2922.

Hatefi, Y. (1978). Preparation and properties of dihydroubiquinone: cytochrome c oxidoreductase (complex III). *Methods Enzymol* 53**,** 35-40.

Hazkani-Covo, E., Zeller, R.M., and Martin, W. (2010). Molecular poltergeists: mitochondrial DNA copies (numts) in sequenced nuclear genomes. *PLoS Genet* 6**,** e1000834.

Hill, B.G., Benavides, G.A., Lancaster, J.R., Jr., Ballinger, S., Dell'italia, L., Jianhua, Z., and Darley-Usmar, V.M. (2012). Integration of cellular bioenergetics with mitochondrial quality control and autophagy. *Biol Chem* 393**,** 1485-1512.

Holt, I.J., Harding, A.E., Petty, R.K., and Morgan-Hughes, J.A. (1990). A new mitochondrial disease associated with mitochondrial DNA heteroplasmy. *Am J Hum Genet* 46**,** 428-433.

Hoppel, C.L., Kerr, D.S., Dahms, B., and Roessmann, U. (1987). Deficiency of the reduced nicotinamide adenine dinucleotide dehydrogenase component of complex I of mitochondrial electron transport. Fatal infantile lactic acidosis and hypermetabolism with skeletal-cardiac myopathy and encephalopathy. *J Clin Invest* 80**,** 71-77.

Iyer, S., Bergquist, K., Young, K., Gnaiger, E., Rao, R.R., and Bennett, J.P., Jr. (2012). Mitochondrial gene therapy improves respiration, biogenesis, and transcription in G11778A Leber's hereditary optic neuropathy and T8993G Leigh's syndrome cells. *Hum Gene Ther* 23**,** 647-657.

Jain, I.H., Zazzeron, L., Goli, R., Alexa, K., Schatzman-Bone, S., Dhillon, H., Goldberger, O., Peng, J., Shalem, O., Sanjana, N.E., Zhang, F., Goessling, W., Zapol, W.M., and Mootha, V.K. (2016). Hypoxia as a therapy for mitochondrial disease. *Science* 352**,** 54-61.

Kirby, D.M., Boneh, A., Chow, C.W., Ohtake, A., Ryan, M.T., Thyagarajan, D., and Thorburn, D.R. (2003). Low mutant load of mitochondrial DNA G13513A mutation can cause Leigh's disease. *Ann Neurol* 54**,** 473-478.

Kirby, D.M., Salemi, R., Sugiana, C., Ohtake, A., Parry, L., Bell, K.M., Kirk, E.P., Boneh, A., Taylor, R.W., Dahl, H.H., Ryan, M.T., and Thorburn, D.R. (2004). NDUFS6 mutations are a novel cause of lethal neonatal mitochondrial complex I deficiency. *J Clin Invest* 114**,** 837-845.

Lake, N.J., Compton, A.G., Rahman, S., and Thorburn, D.R. (2016). Leigh syndrome: One disorder, more than 75 monogenic causes. *Annals of Neurology* 79**,** 190-203.

Lebon, S., Chol, M., Benit, P., Mugnier, C., Chretien, D., Giurgea, I., Kern, I., Girardin, E., Hertz-Pannier, L., De Lonlay, P., Rotig, A., Rustin, P., and Munnich, A. (2003). Recurrent de novo mitochondrial DNA mutations in respiratory chain deficiency. *J Med Genet* 40**,** 896-899.

Leigh, D. (1951). Subacute Necrotizing Encephalomyelopathy In An Infant. *J. Neurol. Neurosurg. Psychiat* 14**,** 216-221.

Lesnefsky, E.J., Tandler, B., Ye, J., Slabe, T.J., Turkaly, J., and Hoppel, C.L. (1997). Myocardial ischemia decreases oxidative phosphorylation through cytochrome oxidase in subsarcolemmal mitochondria. *The American journal of physiology* 273**,** H1544-1554.

Li, H., and Durbin, R. (2009). Fast and accurate short read alignment with Burrows-Wheeler transform. *Bioinformatics* 25**,** 1754-1760.

Li, H., Handsaker, B., Wysoker, A., Fennell, T., Ruan, J., Homer, N., Marth, G., Abecasis, G., Durbin, R., and Genome Project Data Processing, S. (2009). The Sequence Alignment/Map format and SAMtools. *Bioinformatics* 25**,** 2078-2079.

Loeffen, J.L., Smeitink, J.A., Trijbels, J.M., Janssen, A.J., Triepels, R.H., Sengers, R.C., and Van Den Heuvel, L.P. (2000). Isolated complex I deficiency in children: clinical, biochemical and genetic aspects. *Hum Mutat* 15**,** 123-134.

Marchetti, P., Fovez, Q., Germain, N., Khamari, R., and Kluza, J. (2020). Mitochondrial spare respiratory capacity: Mechanisms, regulation, and significance in non-transformed and cancer cells. *FASEB J* 34**,** 13106-13124.

Mcfarland, R., Kirby, D.M., Fowler, K.J., Ohtake, A., Ryan, M.T., Amor, D.J., Fletcher, J.M., Dixon, J.W., Collins, F.A., Turnbull, D.M., Taylor, R.W., and Thorburn, D.R. (2004). De novo mutations in the mitochondrial ND3 gene as a cause of infantile mitochondrial encephalopathy and complex I deficiency. *Annals of Neurology* 55**,** 58-64.

Mcfarland, R., Taylor, R.W., and Turnbull, D.M. (2010). A neurological perspective on mitochondrial disease. *The Lancet. Neurology* 9**,** 829-840.

Mitchell, P. (1961). Coupling of phosphorylation to electron and hydrogen transfer by a chemi-osmotic type of mechanism. *Nature* 191**,** 144-148.

Moslemi, A.R., Darin, N., Tulinius, M., Oldfors, A., and Holme, E. (2005). Two new mutations in the MTATP6 gene associated with Leigh syndrome. *Neuropediatrics* 36**,** 314-318.

Murphy, M.P. (2009). How mitochondria produce reactive oxygen species. *Biochem J* 417**,** 1-13.

Nekhaeva, E., Bodyak, N.D., Kraytsberg, Y., Mcgrath, S.B., Van Orsouw, N.J., Pluzhnikov, A., Wei, J.Y., Vijg, J., and Khrapko, K. (2002a). Clonally expanded mtDNA point mutations are abundant in individual cells of human tissues. *Proc Natl Acad Sci U S A* 99**,** 5521-5526.

Nekhaeva, E., Kraytsberg, Y., and Khrapko, K. (2002b). mtLOH (mitochondrial loss of heteroplasmy), aging, and 'surrogate self'. *Mech Ageing Dev* 123**,** 891-898.

Ni, Y., Hagras, M.A., Konstantopoulou, V., Mayr, J.A., Stuchebrukhov, A.A., and Meierhofer, D. (2019). Mutations in NDUFS1 Cause Metabolic Reprogramming and Disruption of the Electron Transfer. *Cells* 8.

Nicholls, D.G., Darley-Usmar, V.M., Wu, M., Jensen, P.B., Rogers, G.W., and Ferrick, D.A. (2010). Bioenergetic profile experiment using C2C12 myoblast cells. *J Vis Exp*.

Nicholls, D.G., and Ferguson, S.J. (2013). *Bioenergetics 4.* Elsevier.

Pfleger, J., He, M., and Abdellatif, M. (2015). Mitochondrial complex II is a source of the reserve respiratory capacity that is regulated by metabolic sensors and promotes cell survival. *Cell Death and Disease* 6**,** e1835-e1835.

Piekutowska-Abramczuk, D., Rutyna, R., Czyzyk, E., Jurkiewicz, E., Iwanicka-Pronicka, K., Rokicki, D., Stachowicz, S., Strzemecka, J., Guz, W., Gawronski, M., Kosierb, A., Ligas, J., Puchala, M., Drelich-Zbroja, A., Bednarska-Makaruk, M., Dabrowski, W., Ciara, E., Ksiazyk, J.B., and Pronicka, E. (2018). Leigh syndrome in individuals bearing m.9185T>C MTATP6 variant. Is hyperventilation a factor which starts its development? *Metab Brain Dis* 33**,** 191-199.

Polster, B.M., Nicholls, D.G., Ge, S.X., and Roelofs, B.A. (2014). Use of potentiometric fluorophores in the measurement of mitochondrial reactive oxygen species. *Methods Enzymol* 547**,** 225-250.

Rahman, J., Noronha, A., Thiele, I., and Rahman, S. (2017). Leigh map: A novel computational diagnostic resource for mitochondrial disease. *Ann Neurol* 81**,** 9-16.

Rahman, J., and Rahman, S. (2018). Mitochondrial medicine in the omics era. *Lancet* 391**,** 2560-2574.

Rahman, S. (2020). Mitochondrial disease in children. *J Intern Med* 287**,** 609-633.

Robinson, K.M., Janes, M.S., and Beckman, J.S. (2008). The selective detection of mitochondrial superoxide by live cell imaging. *Nat Protoc* 3**,** 941-947.

Roelofs, B.A., Ge, S.X., Studlack, P.E., and Polster, B.M. (2015). Low micromolar concentrations of the superoxide probe MitoSOX uncouple neural mitochondria and inhibit complex IV. *Free Radic Biol Med* 86**,** 250-258.

Roy Chowdhury, S.K., Smith, D.R., Saleh, A., Schapansky, J., Marquez, A., Gomes, S., Akude, E., Morrow, D., Calcutt, N.A., and Fernyhough, P. (2012). Impaired adenosine monophosphate-activated protein kinase signalling in dorsal root ganglia neurons is linked to mitochondrial dysfunction and peripheral neuropathy in diabetes. *Brain* 135**,** 1751-1766.

Schaefer, A.M., Taylor, R.W., Turnbull, D.M., and Chinnery, P.F. (2004). The epidemiology of mitochondrial disorders--past, present and future. *Biochim Biophys Acta* 1659**,** 115-120.

Schubert Baldo, M., and Vilarinho, L. (2020). Molecular basis of Leigh syndrome: a current look. *Orphanet J Rare Dis* 15**,** 31.

Shoffner, J.M., Fernhoff, P.M., Krawiecki, N.S., Caplan, D.B., Holt, P.J., Koontz, D.A., Takei, Y., Newman, N.J., Ortiz, R.G., Polak, M., and Et Al. (1992). Subacute necrotizing encephalopathy: oxidative phosphorylation defects and the ATPase 6 point mutation. *Neurology* 42**,** 2168-2174.

Skladal, D., Halliday, J., and Thorburn, D.R. (2003). Minimum birth prevalence of mitochondrial respiratory chain disorders in children. *Brain* 126**,** 1905-1912.

Smith, R.L., Soeters, M.R., Wust, R.C.I., and Houtkooper, R.H. (2018). Metabolic Flexibility as an Adaptation to Energy Resources and Requirements in Health and Disease. *Endocr Rev* 39**,** 489-517.

Stendel, C., Neuhofer, C., Floride, E., Yuqing, S., Ganetzky, R.D., Park, J., Freisinger, P., Kornblum, C., Kleinle, S., Schols, L., Distelmaier, F., Stettner, G.M., Buchner, B., Falk, M.J., Mayr, J.A., Synofzik, M., Abicht, A., Haack, T.B., Prokisch, H., Wortmann, S.B., Murayama, K., Fang, F., Klopstock, T., and Group, A.T.P.S. (2020). Delineating MT-ATP6-associated disease: From isolated neuropathy to early onset neurodegeneration. *Neurol Genet* 6**,** e393.

Stephan Krahenbuhls, M.C.E.P.B., and Charles, L.H. (1991). Decreased Activities of Ubiquino1:Ferricytochrome c Oxidoreductase (Complex 111) and Ferrocytochrome c:Oxygen Oxidoreductase (Complex IV) in Liver Mitochondria from Rats with Hydroxycobalamin[c-lactam]-induced Methylmalonic Aciduria. *The Journal of biological chemistry.* 266**,** 20998-21003.

Tatuch, Y., Christodoulou, J., Feigenbaum, A., Clarke, J.T., Wherret, J., Smith, C., Rudd, N., Petrova-Benedict, R., and Robinson, B.H. (1992). Heteroplasmic mtDNA mutation (T----G) at 8993 can cause Leigh disease when the percentage of abnormal mtDNA is high. *Am J Hum Genet* 50**,** 852-858.

Taylor, R.W., Morris, A.A., Hutchinson, M., and Turnbull, D.M. (2002). Leigh disease associated with a novel mitochondrial DNA ND5 mutation. *Eur J Hum Genet* 10**,** 141-144.

Uziel, G., Moroni, I., Lamantea, E., Fratta, G.M., Ciceri, E., Carrara, F., and Zeviani, M. (1997). Mitochondrial disease associated with the T8993G mutation of the mitochondrial ATPase 6 gene: a clinical, biochemical, and molecular study in six families. *J Neurol Neurosurg Psychiatry* 63**,** 16-22.

Wallace, D.C., and Chalkia, D. (2013). Mitochondrial DNA genetics and the heteroplasmy conundrum in evolution and disease. *Cold Spring Harb Perspect Biol* 5**,** a021220.

Yamamoto, H., Morino, K., Mengistu, L., Ishibashi, T., Kiriyama, K., Ikami, T., and Maegawa, H. (2016). Amla Enhances Mitochondrial Spare Respiratory Capacity by Increasing Mitochondrial Biogenesis and Antioxidant Systems in a Murine Skeletal Muscle Cell Line. *Oxid Med Cell Longev* 2016**,** 1735841.

Zhadanov, S.I., Grechanina, E.Y., Grechanina, Y.B., Gusar, V.A., Fedoseeva, N.P., Lebon, S., Munnich, A., and Schurr, T.G. (2007). Fatal manifestation of a de novo ND5 mutation: Insights into the pathogenetic mechanisms of mtDNA ND5 gene defects. *Mitochondrion* 7**,** 260-266.

Zhang, G., Frederick, D.T., Wu, L., Wei, Z., Krepler, C., Srinivasan, S., Chae, Y.C., Xu, X., Choi, H., Dimwamwa, E., Ope, O., Shannan, B., Basu, D., Zhang, D., Guha, M., Xiao, M., Randell, S., Sproesser, K., Xu, W., Liu, J., Karakousis, G.C., Schuchter, L.M., Gangadhar, T.C., Amaravadi, R.K., Gu, M., Xu, C., Ghosh, A., Xu, W., Tian, T., Zhang, J., Zha, S., Liu, Q., Brafford, P., Weeraratna, A., Davies, M.A., Wargo, J.A., Avadhani, N.G., Lu, Y., Mills, G.B., Altieri, D.C., Flaherty, K.T., and Herlyn, M. (2016). Targeting mitochondrial biogenesis to overcome drug resistance to MAPK inhibitors. *J Clin Invest* 126**,** 1834-1856.

Zorov, D.B., Juhaszova, M., and Sollott, S.J. (2014). Mitochondrial reactive oxygen species (ROS) and ROS-induced ROS release. *Physiol Rev* 94**,** 909-950.

Chapter 4

5. Cell-permeable succinate, increases mitochondrial membrane potential and glycolysis in Leigh syndrome patient fibroblasts

5.1. Abstract

Mitochondrial (mt) disorders represent a large group of severe genetic disorders mainly impacting organ systems with high energy requirements. Leigh syndrome (LS) is a classic example of a mitochondrial disorder resulting from pathogenic mutations that disrupt OXPHOS capacities. Currently, evidence-based therapy directed towards treating LS is sparse. Recently, the cell-permeant substrates responsible for regulating the electron transport chain (ETC) have gained attention as therapeutic agents for mitochondrial diseases. We explored the therapeutic effects of introducing citric acid cycle (TCA) intermediate substrate, succinate, as a cell-permeable prodrug-NV118, to alleviate some of the mitochondrial dysfunction in LS. Results suggest that a 24-hour treatment with prodrug NV118 elicited an upregulation of glycolysis and mitochondrial membrane potential (MMP) while inhibiting intracellular reactive oxygen species in LS cells. The results from this study suggest an important role for TCA intermediates in the treatment of mitochondrial dysfunction in LS. We show here that NV118 could serve as a therapeutic agent for LS resulting from mutations in mtDNA resulting in complex I and complex V dysfunctions.

5.2. Introduction

Mitochondrial (mt) disorders represent a large group of severe genetic disorders mainly impacting organ systems with high energy requirements (McFarland et al., 2010;Maglioni et al., 2020). These disorders are clinically complex, often fatal, and occur at an estimated ratio of 1 in 10,000-15,000 live births (Khan et al., 2015;Lightowlers et al., 2015). Leigh syndrome (LS) is a

classic example of a mitochondrial disorder resulting from pathogenic mutations that disrupt oxidative phosphorylation (OXPHOS) capacities (Lightowlers et al., 2015). Currently, evidence-based therapy directed towards treating LS is sparse (Pfeffer et al., 2012;Lightowlers et al., 2015). Recently, cell-permeant substrates responsible for regulating the electron transport chain (ETC) have gained attention as therapeutic agents for mitochondrial diseases (Ehinger et al., 2016;Piel et al., 2018;Lee et al., 2019;Piel et al., 2020;Avram et al., 2021a;Avram et al., 2021b). These substrates work by increasing TCA cycle intermediates and providing alternative substrate sources for energy production in the mitochondria. One of the mitochondrial substrates that are currently being explored as a therapeutic option for LS is succinate (Ehinger et al., 2016;Piel et al., 2018;Owiredu et al., 2020a;Owiredu et al., 2020b;Piel et al., 2020;Avram et al., 2021a;Avram et al., 2021b). Conversion of succinyl-CoA by the enzyme succinyl-CoA synthetase yields free succinate as an intermediate substrate of the citric acid cycle, to form GTP which further donates its terminal phosphate group to ADP to form ATP (Johnson et al., 1998). Succinate is further dehydrogenated to fumarate by the flavoprotein succinate dehydrogenase (SDH), which is tightly embedded in the inner mitochondrial membrane. SDH also known as complex II contains a covalently bound Flavin adenine nucleotide (FAD) which gets simultaneously reduced to $FADH_2$. In turn, $FADH_2$ contributes to the ETC by transferring electrons to complex III when ubiquinone (CoQ) is further reduced to ubiquinol ($CoQH_2$) (Protti, 2018). Succinate is presumed to represent one of the major sources of electrons for mitochondrial reactive oxygen species (ROS) when it is oxidized by the ETC to reduce oxygen to superoxide (Vyssokikh et al., 2020). Succinate also contributes to the elimination of superoxide and H_2O_2 production (Quinlan et al., 2012), suggesting complex II to be an important contributor for regulating ROS homeostasis. Thus SDH, couples two major pathways in the mitochondria, the citric acid cycle and the ETC, both being essential for oxidative phosphorylation (Tretter et. al 2016).

In healthy mitochondria, CI-linked respiration is largely responsible for the ETC activity and subsequent ATP production by complexes, I II, III IV, and V (Protti, 2018). Consequently, inhibition of complex I (CI) activity can interfere with the majority of ATP production in the mitochondria. Chronic CI dysfunction can result in upregulation of the glycolytic pathway, elevated lactic acid production, and cell death. Succinate oxidation offers an alternate source of electron for OXPHOS, bypassing CI-linked respiration.

Succinate is a dicarboxylic acid that takes the form of an anion in living organisms. As such, it is not cell membrane permeable and has limited uptake into cells when given exogenously (Ehinger et al., 2016). To overcome this limitation, prodrugs of succinate were developed and screened for cell permeability (Ehinger et al., 2016). NV101-118 (NV118, diacetoxymethyl succinate), hereafter referred to as NV118, is one of the successful cell membrane-permeable prodrugs of succinate that was recently developed (Ehinger et al., 2016). Since its development, NV118 has been used as therapeutics for various diseases such as diabetes, carbon monoxide poisoning, and cardiovascular injury (Ehinger et al., 2016;Piel et al., 2018;Janowska et al., 2020;Owiredu et al., 2020a;Owiredu et al., 2020b;Piel et al., 2020;Avram et al., 2021a;Avram et al., 2021b). NV118 is currently in clinical trials and in use for various cellular models of diseases associated with CI-dysfunction (Ehinger et al., 2016;Piel et al., 2018;Janowska et al., 2020;Piel et al., 2020;Avram et al., 2021a;Avram et al., 2021b). In all of these models, NV118 improved mitochondrial functions, as evidenced by increased CII-linked respiration, membrane potential, ATP production, and a decrease in lactic acidosis (Ehinger et al., 2016;Piel et al., 2018;Janowska et al., 2020). Furthermore, recent studies have shown improvement in mitochondrial respiration with NV118 in cellular models with inhibition of downstream ETC enzymes like CIV (Owiredu et al., 2020a;Owiredu et al., 2020b). These studies suggest that NV118 can improve mitochondrial respiration by other means aside from elevating CII activity.

As described in chapters 2 (Bakare et al., 2021) and 3, we reported fragmented/hyper fused mitochondrial morphology, abnormal ETC enzyme activity, depressed mitochondrial function, decreased ROS, and membrane potential in fibroblast cells modeling for LS. The LS cells harbored pathogenic point mutation in the mtDNA at *T8993G* in the *MTATP6* gene causing complex V deficiency and *T10158C* in the *MTND3* gene and *T12706C* in *MTND5* gene causing complex I deficiency. A commercially available fibroblast cell line (BJ-FB) was used as a healthy control line.

In the present study, we used the same fibroblast cells modeling for LS and the control BJ cell line and treated them for 24 hours (Iyer et al., 2009;Keeney et al., 2009;Iyer et al., 2012) with varying concentrations of NV118 to measure changes in mitochondrial function and oxidative stress. Our results suggest that 24-hour treatment with 100µM NV118 can rescue some of the mitochondrial dysfunction in treated LS cells compared to the untreated cells. We report for the first time that after a 24-hour treatment with 100µM NV118 cellular bioenergetics improved as a result of upregulation of glycolysis, TCA cycle, and mitochondrial membrane potential (MMP). We show that the most sustained change was in glycolysis, as mitochondrial respiration remained the same after 24-hour treatment with NV118. Together, our results suggest that NV118 could serve as a therapeutic agent for the treatment of LS.

5.3. Results

5.3.1. Effect of NV118 on cell viability and mitochondrial respiration in non-permeabilized (intact) control BJ-FB cell line

We first assessed the effect of different concentrations of NV118 on the viability of intact control BJ-FB cells. Cell viability was measured following a 30-minutes exposure to 50µM, 100µM, or 150µM NV118. As a control, phenol red-free MEM (vehicle) was added to the wells without NV118 drug treatment. To ensure scientific rigor and reproducibility, analysis was

conducted on the control cell lines (n = 5) at passage eight. Results indicate no significant difference between the NV118 treated and untreated control BJ-FB cell lines (**Figure 5.3.1.a**).

Next, we assessed mitochondrial respiration in intact control BJ-FB cell line using the same NV118 concentrations and vehicle. Oxygen consumption rate (OCR) using a Seahorse XFe96 flux analyzer was measured after acute treatment with 50µM, 100µM, 150µM NV118, or vehicle. Basal respiration was recorded before injection of the different concentrations of NV118. Subsequently, other oxidative phosphorylation properties were measured including proton leak, maximal respiration, and non-mitochondrial respiration, after sequential injections of ATP synthase inhibitor oligomycin, the uncoupler carbonyl cyanide-4-(trifluoromethoxy) phenylhydrazone FCCP, complex I inhibitor Rotenone, and complex III inhibitor Antimycin A into the wells.

As expected, before NV118 was administered into the cell culture plates, the basal respiration for the control BJ-FB cell lines was similar between all treatment groups (**Figure 5.3.1.b**). The addition of NV118 resulted in a dose-dependent response of the oxidative phosphorylation properties recorded. Results show a significant increase ($p<0.0001$) in ATP production (**Figure 5.3.1.c**) in the NV118 treatment groups. The highest increase in ATP production was observed in the BJ-FB with 100µM NV118 treatment (23%), while both 50µM and 150µM NV118 treatment resulted in a 19% increase in ATP production relative to the untreated group. Although NV118 resulted in a significant increase in ATP rate, we also observed a significant increase ($p<0.01$) in proton leak (**Figure 5.3.1.d**) with 100µM (by 39%) and 150µM (by 49%) NV118 treatment relative to the untreated group. While the leak was not significantly different in the 50µM treatment group, proton leak increased by 26% relative to the untreated group. The increase in leak suggests that NV118 treatment results in mild uncoupling of the mitochondrial membrane. Indeed, there was a 3% and 4% decrease in coupling efficiency (**Figure 5.3.1.e**) for the 50µM and 100µM NV118 treatment respectively. While the decrease in

coupling efficiency was not significant in this treatment group, 150µM NV118 treatment significantly decreased (*p<0.05*) coupling efficiency by 5% compared to the untreated group. The maximum respiration rate (**Figure 5.3.1.f**) caused by the addition of FCCP showed a significant increase of 16% (*p<0.05*) in 50µM, 23% (*p<0.001*) increase in 100µM, and 22% (*p<0.001*) increase in 150µM NV118 treatment groups relative to the untreated BJ-FB cell lines. The observed significant increase in maximal respiration upon treatment suggests that NV118 increases the cells' ability to rapidly oxidize substrates when the metabolic need arises.

In our earlier work (*manuscript under review, chapter 3*) we have shown that spare respiratory capacity (SRC) is an important bioenergetics variable required by cells to adapt and respond to ATP demand (**see section 4.3.5).** The result in this study showed a significant increase (*p<0.05*) in SRC values (**Figure 5.3.1.g**) by 13% in the 50µM, and by 14% in the 100µM and 150µM treatment compared to the untreated group. The observed significant increase in SRC indicates that NV118 treatment could help BJ-FB cells adapt when there is a sudden increase in ATP demand. Finally, the mitochondrial respiration was inhibited by simultaneously treating cells with rotenone and antimycin A. Non-mitochondrial respiration, which is typically attributed to the non-ETC oxidases present in the cell (Hill et al., 2012) was significantly higher in the 50µM (20%) and 150µM (22%) treatment groups relative to the untreated cell lines (**Figure 5.3.1.h**). However, non-mitochondrial respiration was not significantly different when BJ-FB cell lines were treated with 100µM NV118.

Based on the dose-response and effects on non-mitochondrial respiration (**Figure 5.3.1.h**), ATP production (**Figure 5.3.1.c**), and the SRC (**Figure 5.3.1.g**), 100µM NV118 was selected as the optimal concentration for further evaluation on the diseased cell lines.

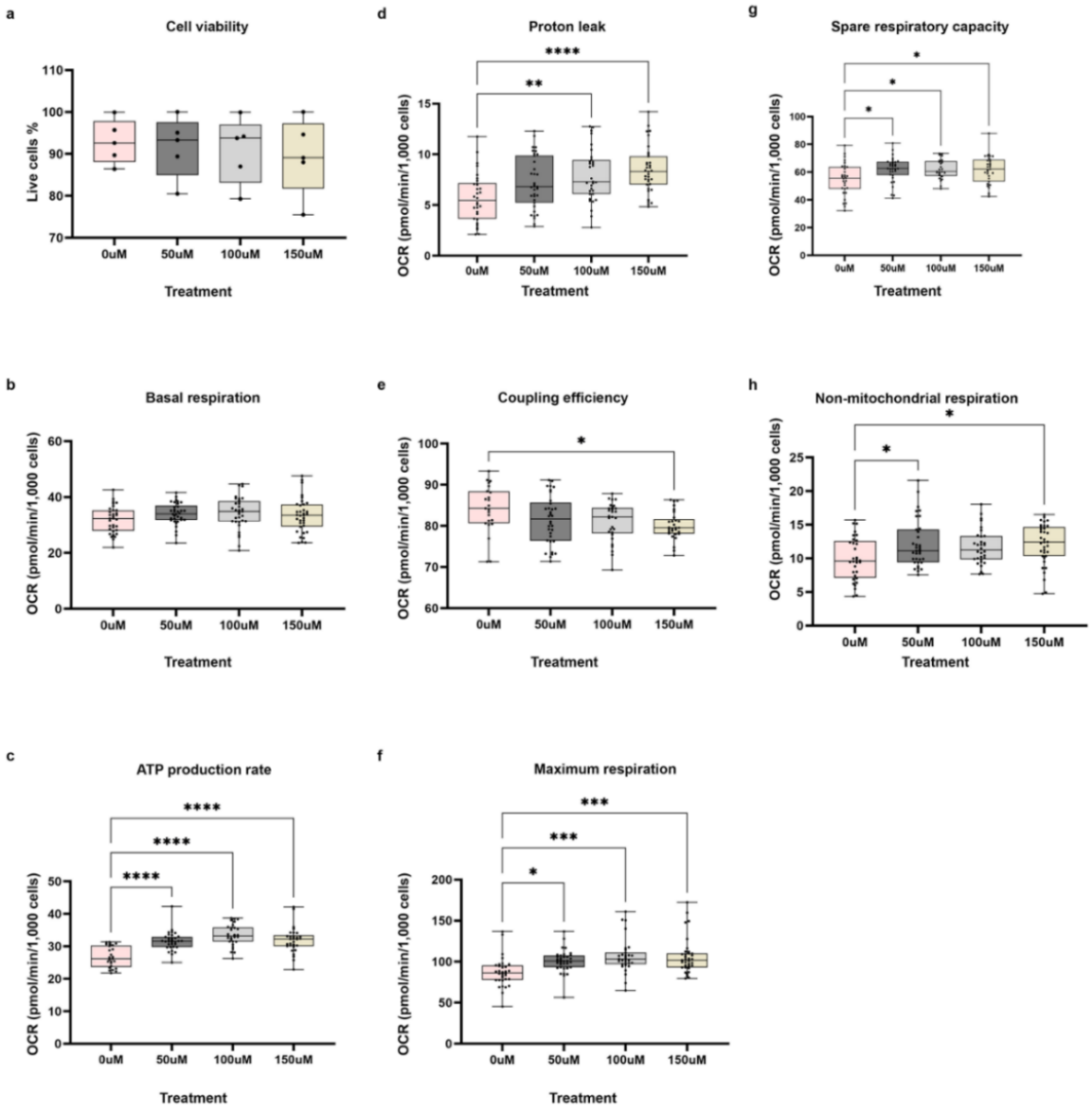

Figure 5.3.1. Cell viability and mitochondria respiration profile of CTL BJ-FB cell line after NV118 treatment. Control BJ-FB were treated with 0 µM, 50 µM, 100 µM, or 150 µM NV118 for 30-minutes, and (a) Cell viability was assessed. Oxygen consumption rate (OCR) under basal conditions and after the addition of NV118 was measured. The following respiration parameters were recorded (b) basal respiration, (c) ATP production rate, (d) proton leak, (e) coupling efficiency, (f) maximal respiration, (g) spare respiratory capacity, and (h) non-mitochondrial respiration after Rot/AA injection. All parameters are in pmol/min/1000 cells. Data are mean +/- SD. Experiments were repeated at least three times on different days under the same conditions. *p<0.05 **p<0.01 ***p<0.001 ****p<0.00001. Pink, dark gray, light gray, and tan bar represents treatment with 0 µM (vehicle), 50 µM, 100 µM, and 150 µM NV118 respectively.

5.3.2. The glycolytic pathway is upregulated in the control BJ-FB cell lines after 24-hour treatment with NV118

One of the hallmarks of LS is lactic acidosis resulting from the conversion of pyruvate to lactate to maintain the NAD+ pool (Ehinger et al., 2016). The result from the optimization studies led to the hypothesis that NV118 improves mitochondrial function and decreases the dependence of the cells on lactate production. Since succinate is a substrate that connects the TCA cycle with the ETC, we also wanted to understand how NV118 affects the TCA cycle and cellular respiration. Therefore, cellular glycolysis was examined to understand the impact of NV118 on this metabolic pathway. Using a Seahorse XFe96 flux analyzer, proton efflux rate (PER) rate was measured in the control BJ-FB cell line after a 24-hour treatment with 100µM NV118 or equivalent amount of vehicle (phenol-red free MEM). At the end of this assay, basal glycolysis, glycolysis-derived ATP, glycolytic capacity, and non-glycolytic respiration values were obtained. To ensure scientific rigor and reproducibility, analysis was conducted on the control cell line (n=3) at passage eight.

The results show a significant increase ($p<0.01$) by 15% in basal glycolysis (**Figure 5.3.2.a**) in the control BJ-FB upon +NV118 treatment when compared with the untreated group. This increase corresponded to a significant (by 13%; $p<0.01$) increase in the ATP derived (**Figure 5.3.2.b**) from glycolysis in the BJ-FB cell upon NV118 treatment. When the mitochondria were inhibited with rotenone and antimycin A to drive the cells' dependence on glycolysis, glycolytic capacity (**Figure 5.3.2.c**) significantly increased ($p<0.01$) by 13% in the NV118 treatment group relative to the untreated group. The addition of the glycolysis inhibitor, 2-deoxyglucose resulted in a significantly higher PER, as measured by an increase in post-2DG acidification (**Figure 5.3.2.d)** in BJ-FB ($p<0.01$, 20%) NV118 treatment group compared to the untreated group. These results together indicate that NV118 treatment increased utilization of TCA substrate; hence, the glycolytic pathway had to be upregulated to make pyruvate and acetyl-CoA shuttle

into the TCA cycle. The slight increase in mitoPER (by 2%) recorded in the BJ-FB (**Figure 5.3.2.e)** with NV118 treatment further supports this hypothesis. Furthermore, we observed a 2% decrease in glycoBHI (**Figure 5.3.2.f)**, further strengthening the possibility that NV118 upregulates the glycolytic pathway to contribute towards TCA substrates and not lactate production.

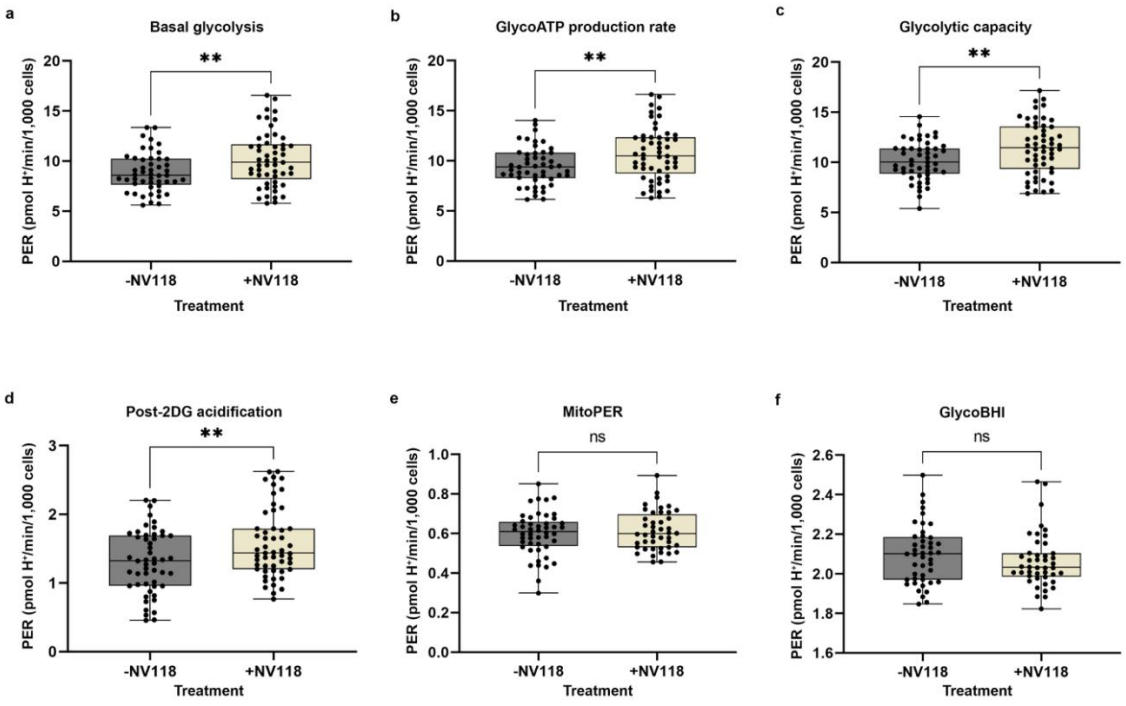

Figure 5.3.2. Glycolytic respiration profile of CTL BJ-FB cell line after NV118 treatment. Control BJ-FB was treated with 100 µM NV118 or vehicle (phenol-red free MEM) for 24-hours, and Proton Efflux Rate (PER) was measured at the end of the 24-hour treatment period. Cell line showing (a) basal glycolysis, (b) GlycoATP production rate, (c) glycolytic capacity after blocking ETC using Rot/AA, (d) post-2DG acidification (non-glycolytic acidification), (e) mitoPER, and (f) glycoBHI. All parameters are in pmol H^+/min/1000 cells. Data are mean +/- SD. Experiments were repeated at least three times on different days under the same conditions. **p<0.01, ns = not significant. Gray bar represents treatment with vehicle (-NV118), while tan bar represents treatment with 100 µM NV118 (+NV118).

5.3.3. Treatment with NV118 for 24-hours significantly increased glycolysis in LS cells harboring mtDNA mutation *T10158C* in *MTND3* gene but not in LS cells with mtDNA mutation *T12706C* in *MTND5* gene affecting CI function

Having examined the effect of NV118 on control BJ-FB lines, we proceeded to analyze the effect on diseased cell lines. We next examined the two cell lines modeling LS harboring pathogenic mutant DNA in *MTND3* (SBG4-FB (*T10158C*)), and *MTND5* (SBG5-FB (*T12706C*)) gene causing a complex I defect. Glycolytic rate assay was performed after 24-hour treatment with 100µM NV118 or equivalent amount of vehicle (phenol-red free MEM). The same glycolytic parameters were recorded as those of the BJ-FB cell lines.

Basal glycolysis (**Figure 5.3.3.1.a, 5.3.3.2.a**) was higher by 13% ($p<0.05$) and 9% in SBG4-FB (*T10158C*) and SBG5-FB (*T12706C*) respectively when NV118 was added. Glycolytic ATP production rate (glycoATP) was also higher in SBG4-FB (*T10158C*) (by 15%; $p<0.01$) (**Figure 5.3.3.1.b**) and SBG5-FB (*T12706C*) (9%) (**Figure 5.3.3.2.b**) cell lines in the NV118 treatment relative to the untreated group. When the mitochondria were inhibited with rotenone and antimycin A to induce glycolysis, glycolytic capacity also increased in both SBG4-FB (*T10158C*) (11%; $p<0.05$) (**Figure 5.3.3.1.c**) and SBG5-FB (*T12706C*) (12%) (**Figure 5.3.3.2.c**) in the presence of NV118. The addition of the glycolysis inhibitor, 2-deoxyglucose resulted in a significant increase ($p<0.01$) in post-2DG acidification in SBG4-FB (*T10158C*) (27%) (**Figure 5.3.3.1.d**), and SBG5-FB (*T12706C*) (27%) (**Figure 5.3.3.2.d**) in the NV118 treatment compared to untreated samples. Similar to the observation in the control BJ-FB, NV118 treatment increased utilization of TCA substrates; hence, leading to the upregulation of the glycolytic pathway in these cell lines. Although not statistically significant, the 5% increase in mitoPER recorded in the SBG5-FB (*T12706C*) (**Figure 5.3.3.2.e**) with NV118 treatment supports the increased activity of TCA cycle enzymes. In SBG4-FB (*T10158C*) cells with NV118 treatment, the results showed a decreased trend in mito PER values (**Fig. 5.3.3.1.e**). We

observed a trend towards a higher glycoBHI (**Figure 5.3.3.1.f**) in the SBG4-FB (*T10158C*) cells (3% increase) when NV118 was present, while the glycoBHI (**Figure 5.3.3.2.f**) stayed relatively the same in both the SBG5-FB (*T12706C*) treated and untreated samples Although NV118 treatment upregulated glycolysis in both cell lines, NV118 treatment in SBG4-FB (*T10158C*) does not result in a corresponding increase in TCA cycle substrate production, evidenced by the lower mitoPER (**Figure 5.3.3.1.e & 5.3.3.2.e**). Conversely, the upregulated glycolysis in SBG4-FB (*T10158C*) with NV118 treatment could be contributing to lactic acid production or other unknown pathways. Taken together, the results from the glycolytic respiration suggest that the location of the subunit affected by each mtDNA mutation influences the metabolic response with NV118 treatment.

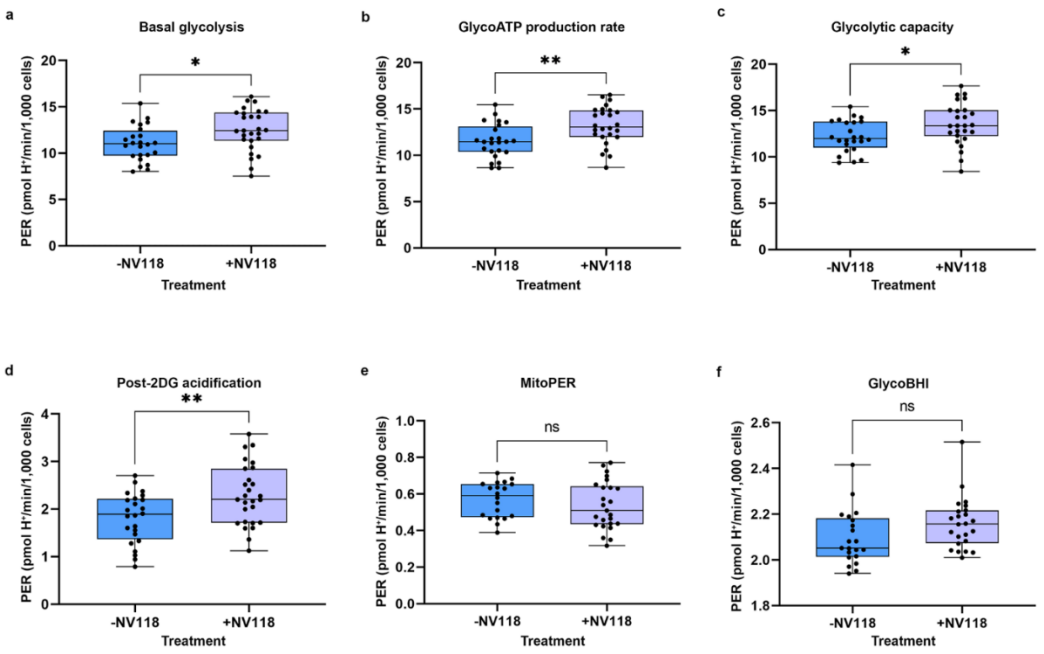

Figure 5.3.3.1. Glycolytic respiration profile of SBG4-FB (T10158C) cell line after NV118 treatment. SBG4-FB (*T10158C*) were treated with 100 µM NV118 or vehicle (phenol-red free MEM) for 24-hours, and Proton Efflux Rate (PER) was measured at the end of the 24-hour treatment period. Cell line showing (a) basal glycolysis, (b) GlycoATP production rate, (c) glycolytic capacity after blocking ETC using Rot/AA, (d) post-2DG acidification (non-glycolytic acidification), (e) mitoPER, and (f) glycoBHI. All parameters are in pmol H^+/min/1000 cells. Data are mean +/- SD. Experiments were repeated at least three times on different days under the same conditions. *p<0.05, **p<0.01, ns = not significant. The blue bar represents treatment with vehicle (-NV118), while the purple bar represents treatment with 100 µM NV118 (+NV118).

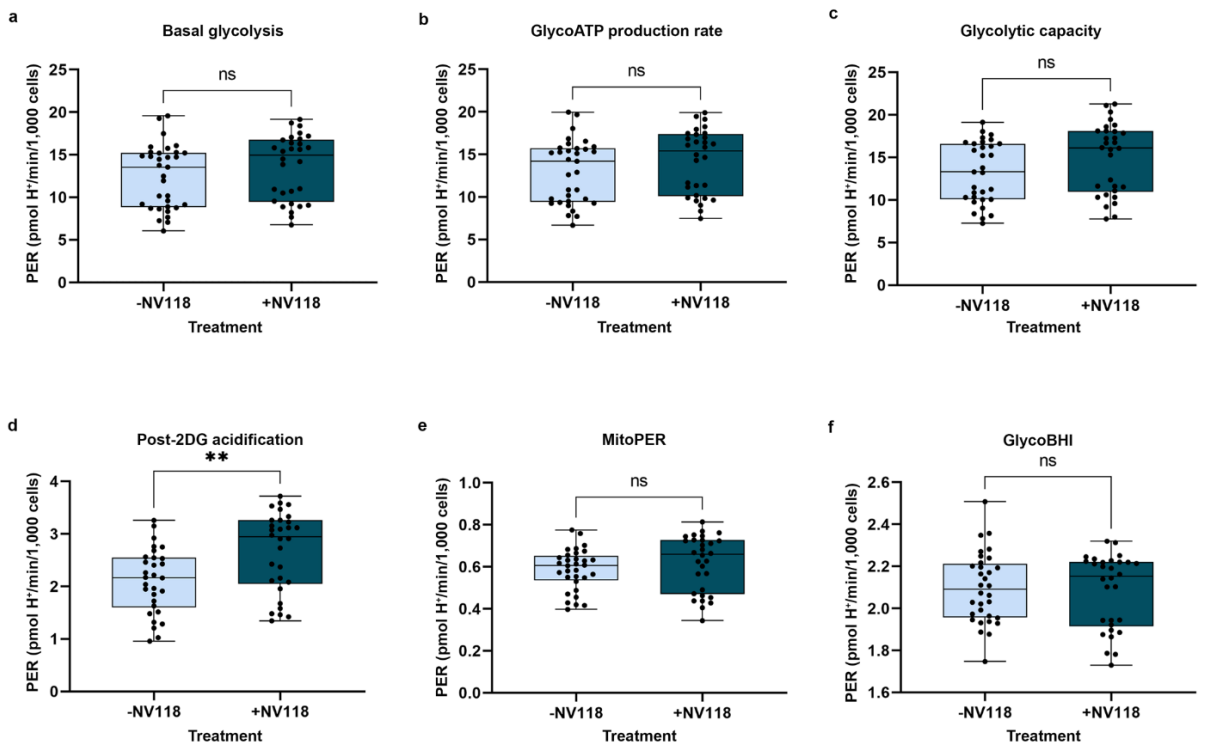

Figure 5.3.3.2. Glycolytic respiration profile of SBG5-FB (T12706C) cell line after NV118 treatment. SBG5-FB (*T12706C*) were treated with 100 µM NV118 or vehicle (phenol-red free MEM) for 24-hours, and Proton Efflux Rate (PER) was measured at the end of the 24-hour treatment period. Cell line showing (a) basal glycolysis, (b) GlycoATP production rate, (c) glycolytic capacity after blocking ETC using Rot/AA, (d) post-2DG acidification (non-glycolytic acidification), (e) mitoPER, and (f) glycoBHI. All parameters are in pmol H^+/min/1000 cells. Data are mean +/- SD. Experiments were repeated at least three times on different days under the same conditions. *p<0.05, **p<0.01, ns = not significant. The light blue bar represents treatment with vehicle (-NV118), while the green bar represents treatment with 100 µM NV118 (+NV118).

5.3.4. NV118 did not significantly increase glycolysis in LS cells harboring pathogenic mtDNA mutation (T8993G) in *MTATP6* gene affecting complex V

Most studies on administering succinate prodrug NV118 have focused on using it as therapy for disorders resulting from CI-deficiencies containing nuclear DNA mutations (Ehinger et al., 2016;Piel et al., 2018;Piel et al., 2020;Avram et al., 2021b). However, some recent studies have suggested improvement in mitochondrial function when NV118 was used to treat disorders resulting from CIV dysfunction (Owiredu et al., 2020a;Owiredu et al., 2020b). Since glycolysis was upregulated in the control BJ-FB without ETC defects, we wanted to investigate the effect

of NV118 on glycolysis in LS cell lines with mutations affecting CV (ATP synthase) of the ETC. For this purpose, two LS patient fibroblast cell lines carrying point mutation *T8993G* in *MTATP6 gene* (SBG1-FB (*T8993G*) with >96% heteroplasmy and SBG2-FB (*T8993G*) with >91% heteroplasmy) were selected for these experiments. Following the same approach as before, Glycolysis rate assays were estimated after a 24-hour treatment with 100µM NV118 or equivalent amount of vehicle (phenol-red free MEM) in all the cell lines.

There was statistically no significant difference in any of the parameters (**Figure 5.3.4.1. & 5.3.4.2.**) recorded for both SBG1-FB (*T8993G*) and SBG2-FB (*T8993G*) in the presence of NV118 when compared with the vehicle MEM treated cells (denoting –NV118). Although SBG1-FB (*T8993G*) and SBG2-FB (*T8993G*) cells showed trends towards an upregulation in the glycolytic pathway. In SBG1-FB (*T8993G*) cells, basal glycolysis, glycoATP, glycolytic capacity, and post-2DG acidification (**Figure 5.3.4.1.**) showed increasing trends by 24%, 23%, 23%, and 25% respectively in the NV118 treatment group relative to the untreated group. However, the increase was modest in the SBG2-FB (*T8993G*) cell lines. We recorded a 5%, 4%, 2%, and 4% increase in basal glycolysis, glycoATP, glycolytic capacity, and post-2DG acidification (**Figure 5.3.4.2.**) respectively in the SBG2-FB (*T8993G*) cell line after NV118 treatment. The mitoPER (**Figure 5.3.4.1.e**) in SBG1-FB (*T8993G*) exhibited a (2% increase) similar to what was estimated for SBG5-FB (*T12706C*) cells, while SBG2-FB (*T8993G*) (**Figure 5.3.4.2.e**) exhibited a (2% decrease) similar to what was observed for SBG4-FB (*T10158C*) cells. Overall, the glycoBHI for SBG1-FB (*T8993G*) decreased by (3%) (**Figure 5.3.4.1.f**) and decreased by (2%) in SBG2-FB (*T8993G*) cells (**Figure 5.3.4.2.f**) treated with NV118 compared to the untreated group.

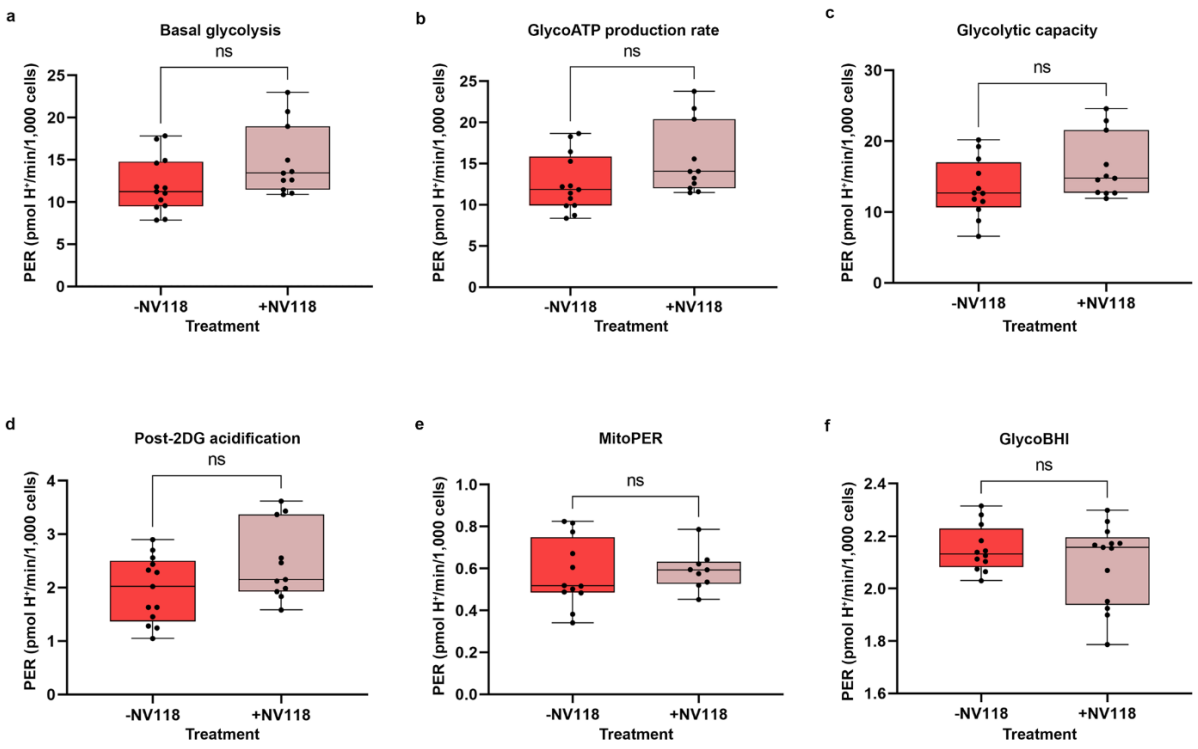

Figure 5.3.4.1. Glycolytic respiration profile of SBG1-FB (T8993G) cell line after NV118 treatment. SBG1-FB (*T8993G*) were treated with 100 µM NV118 or vehicle (phenol-red free MEM) for 24-hours, and Proton Efflux Rate (PER) was measured at the end of the 24-hour treatment period. Cell line showing (a) basal glycolysis, (b) GlycoATP production rate, (c) glycolytic capacity after blocking ETC using Rot/AA, (d) post-2DG acidification (non-glycolytic acidification), (e) mitoPER, and (f) glycoBHI. All parameters are in pmol H^+/min/1000 cells. Data are mean +/- SD. Experiments were repeated at least three times on different days under the same conditions. ns = not significant. The red bar represents treatment with vehicle (-NV118), while the pink bar represents treatment with 100 µM NV118 (+NV118).

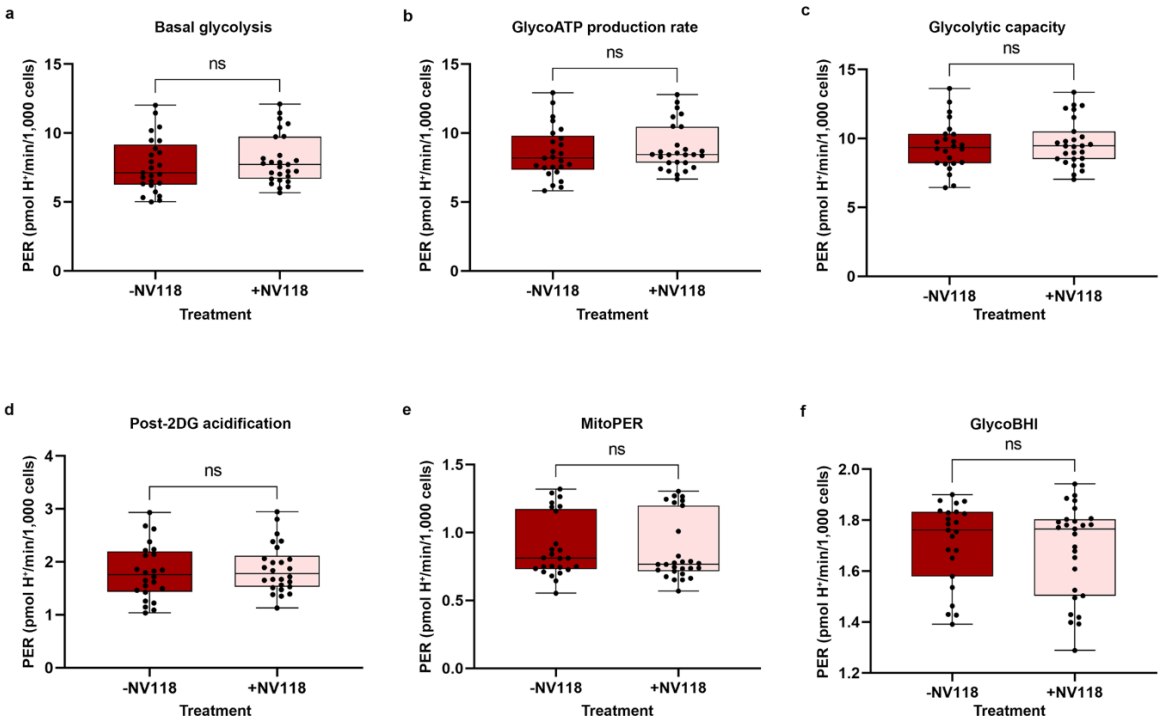

Figure 5.3.4.2. Glycolytic respiration profile of SBG2-FB (T8993G) cell line after NV118 treatment. SBG2-FB (*T8993G*) were treated with 100 µM NV118 or vehicle (phenol-red free MEM) for 24-hours, and Proton Efflux Rate (PER) was measured at the end of the 24-hour treatment period. Cell line showing (a) basal glycolysis, (b) GlycoATP production rate, (c) glycolytic capacity after blocking ETC using Rot/AA, (d) post-2DG acidification (non-glycolytic acidification), (e) mitoPER, and (f) glycoBHI. All parameters are in pmol H^+/min/1000 cells. Data are mean +/- SD. Experiments were repeated at least three times on different days under the same conditions. ns = not significant. The dark red bar represents treatment with vehicle (-NV118), while the pink bar represents treatment with 100 µM NV118 (+NV118).

5.3.5. 24-hour treatment with NV118 does not induce cellular ROS production in LS or control fibroblast cells

Next, we investigated the effects of NV118 on cellular ROS production in control and fibroblast cells modeling LS, and harboring pathogenic mtDNA variants (*T8993G*, *T10158C*, *T12706C*), in *MTATP6*, *MTND3,* and *MTND5* genes leading to complex V and I defect and depressed ATP production. Previous reports have shown that supplying mitochondria with a substantial increase in succinate concentration results in reverse electron transport (RET), consequently, increasing reactive oxygen species (ROS) production (Chance and Hollunger,

1961;Scialò et al., 2016;Scialo et al., 2017). Therefore, we wanted to test whether the four vulnerable LS cells treated with 100µM NV118 (succinate) for 24-hours would generate reactive oxygen species in the presence of NV118. LS and BJ control FB cells were grown to 80% confluency and treated with 20µM DCFDA/H_2DCFDA (2',7'-dichlorofluorescein diacetate) and vehicle for 24 hours (**see material methods for details**). The following day a BioTek plate reader was used to record the fluorescent intensity for each cell line. Data were background corrected to reduce background noise from excitation and emission crosstalk. DCFDA is a fluorogenic probe that diffuses freely into cells. When inside a cell, cellular esterases in the cells deacetylate this probe, converting it into a non-fluorescent compound. In the presence of hydroxyl, peroxyl, and other reactive oxygen species (ROS), DCFDCA gets oxidized to a highly fluorescent compound, DCF (2',7'-dichlorofluorescein) which can be detected by a plate reader with excitation/emission at 485nm/535nm.

Results indicate that there was no significant difference in ROS production between the NV118 treatment and untreated group in all cell lines (**Figure 5.3.5.**). It has been reported previously that high concentrations of succinate could exert inhibitory effects on mitochondrial respiration (Gonzalez-Meler et al., 1996;Tretter et al., 2016). Furthermore, high concentrations of succinate could result in upregulation of RET, contributing to an increase in ROS production and subsequent cellular apoptosis (Scialò et al., 2016;Tretter et al., 2016;Scialo et al., 2017). Treatment with NV118 did not result in any significant changes to cellular ROS production in either the control BJ-FB or any of the diseased cell lines. As indicated above, we expected that if NV118 results in RET, we would observe a significant increase in ROS production in all cell lines after NV118 treatment. Since we did not observe an increase in ROS in the presence of NV118, this indicates that the NV118 concentration (100µM) used in this study did not oversaturate the Quinone pool (Q-pool) nor increase RET in either the LS or control cell lines. Mutations resulting in disturbances to CII activity have been reported to result in ROS

production as well (Quinlan et al., 2012), our result further suggests that the addition of NV118 did not negatively affect the functions of CII.

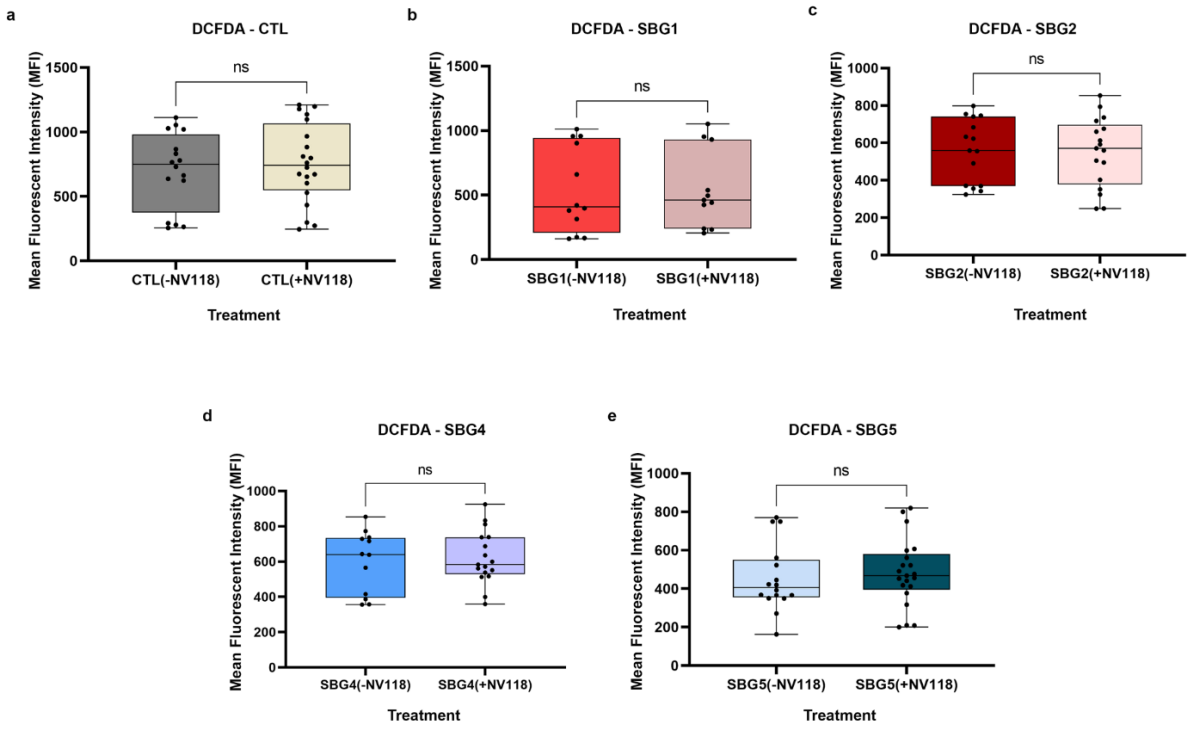

Figure 5.3.5. Cellular ROS production in CTL BJ-FB and LS diseased fibroblast. All cell lines were treated with 100 µM NV118 or vehicle (phenol-red free MEM) for 24-hours, and cellular ROS was measured at the end of the 24-hour treatment period using DCFDA/H_2DCFDA. Cellular ROS in a) control CTL BJ-FB cell lines and cell lines with (b-c) CV-defect (SBG1-FB (*T8993G*) and SBG2-FB (*T8993G*)), and (d-e) CI-defect with and without NV118 treatment. Data are mean +/- SD. Experiments were repeated at least three times on different days under the same conditions. *p<0.05, **p<0.01.

5.3.6. Mitochondrial membrane potential significantly improved in SBG4-FB (*T10158C*) and SBG5-FB (*T12706C*) exhibiting CI-defect and SBG2-FB (*T8993G*) with CV-defect after 24-hour treatment with NV118

Respiratory complex II oxidizes succinate to fumarate as part of the citric acid cycle and reduces ubiquinone to ubiquinol in the ETC. Previous experimental evidence suggested that prodrug NVII8 (complex II substrate, succinate) did not play a significant role in the production of physiological or pathological intracellular reactive oxygen species in LS or control BJ cells.

Therefore, we sought to understand the effects of prodrug NV118 treatment on mitochondrial membrane potential (MMP) in LS fibroblast cells and BJ control cells harboring pathogenic mtDNA (four LS: SBG1-FB (*MTATP6-T8993G*), SBG2-FB (*MTATP6-T8993G*), SBG4-FB (*MTND3-T10158C*), SBG5-FB (*MTND5-T12706C*) one CTL: BJ-FB). All cells were treated with 100μM NV118 or vehicle (phenol-red free MEM) for 24-hours and flow cytometry methods were used to measure MMP with TMRE (tetramethylrhodamine, ethyl ester) (see material and methods for details). TMRE is a positively charged dye that is attracted to the negative potential across the inner mitochondrial membrane and thus accumulates in functionally active mitochondria in live cells (Cottet-Rousselle et al., 2011). In active mitochondria, TMRE is sequestered in the matrix because of the negative charge in the matrix of these mitochondria. Depolarized or inactive mitochondria are not able to sequester TMRE as the MMP is compromised in these mitochondria. In this study, MMP was measured as mean fluorescent intensity (MFI) in all cell lines.

Results from this study showed that cells upon treatment with prodrug NV118, SBG2-FB (*T8993G*), SBG4-FB (*T10158C*), and SBG5-FB (*T12706C*) cells exhibited a significant increase in MMP by: 306% in SBG2-FB (*T8993G*) ($p<0.05$) (**Figure 5.3.6.3.a**), 329% in SBG4-FB (*T10158C*) ($p<0.01$) (**Figure 5.3.6.4.a**), and 66% in SBG5-FB (*T12706C*) ($p<0.05$) (**Figure 5.3.6.5.a**) compared to the untreated group. MMP stayed the same in the control BJ-FB (**Figure 5.3.6.1.a**) and SBG1-FB (*T8993G*) (**Figure 5.3.6.2.a**) cell line between the treated and untreated groups. This result suggests that prodrug NV118 increased electron flux and proton translocation into the mitochondrial intermembrane space (IMS) in the SBG2-FB (*T8993G*), SBG4-FB (*T10158C*), and SBG5-FB (*T12706C*), cell lines. The data is consistent with other reports elsewhere that have shown the addition of prodrug NV118 increased MMP indicative of mitochondrial oxidation of succinate via succinate dehydrogenase (complex II) (Ehinger et al., 2016).

When the uncoupler, cyanide p-trifluoromethoxyphenylhydrazone (FCCP), was added to depolarize the mitochondria, all cell lines responded to this treatment by exhibiting a decrease in MMP relative to the TMRE only treatment (**Figure 5.3.6.1.-6. d&e**). While TMRE+FCCP resulted in depolarization in all of the cell lines, a comparison between the untreated and NV118 treated groups showed that the SBG2-FB (*T8993G*) cells (**Figure 5.3.6.3.b**) revealed an additional defect apart from complex V deficiency. In our previous studies, we reported that SBG2-FB (*T8993G*) has an uncoupling defect (Bakare et al., 2021) because the cells were unresponsive to FCCP treatment. In this study, we observed that in the NV118 untreated group, MMP was indistinguishable between the TMRE only and TMRE+FCCP treatment group (**Figure 5.3.6.3.d**). Upon addition of NV118, there was an overall increase in MMP between TMRE and TMRE+FCCP treatment group, indicating succinate induced depolarization of the inner mitochondrial membrane upon addition of uncoupler-FCCP in SBG2-FB (*T8993G*) cells (**Figure 5.3.6.3.e**). This result suggests that the mutation in the SBG2-FB (*T8993G*) cells also affects the ability of this cell line to properly oxidize substrates.

Finally, we evaluated MMP in the presence of Oligomycin. As expected, the addition of Oligomycin resulted in hyperpolarization in all the cell lines in the NV118 untreated group (**Figure 5.3.6.1.-6.d**). In the presence of prodrug NV118 and oligomycin, the mitochondria became depolarized in most of the cell lines (**Figure 5.3.6.1.-6.e**). This is evident by the significant decrease in MMP in the SBG2-FB (*T8993G*) (by 67%; $p<0.01$) (**Figure 5.3.6.3.c**), SBG4-FB (*T10158C*) (by 60%; $p<0.0001$) (**Figure 5.3.6.4.c**), and SBG5-FB (*T12706C*) (by 65%; $p<0.01$) (**Figure 5.3.6.5.c**), and the trend towards a decrease in control BJ-FB (by 31%) (**Figure 5.3.6.1.c**) between the NV118 treated and untreated groups. This observation could be attributed to proton leak caused by inhibition of the ATP synthase. To maintain substrate oxidation by complex II when the ATP synthase activity is inhibited, some of the protons could

be leaking into the matrix to maintain the electron flux. Interestingly, there was no change in MMP in SBG1-FB (*T8993G*) cells (**Figure 5.3.6.2.c**) after the addition of Oligomycin.

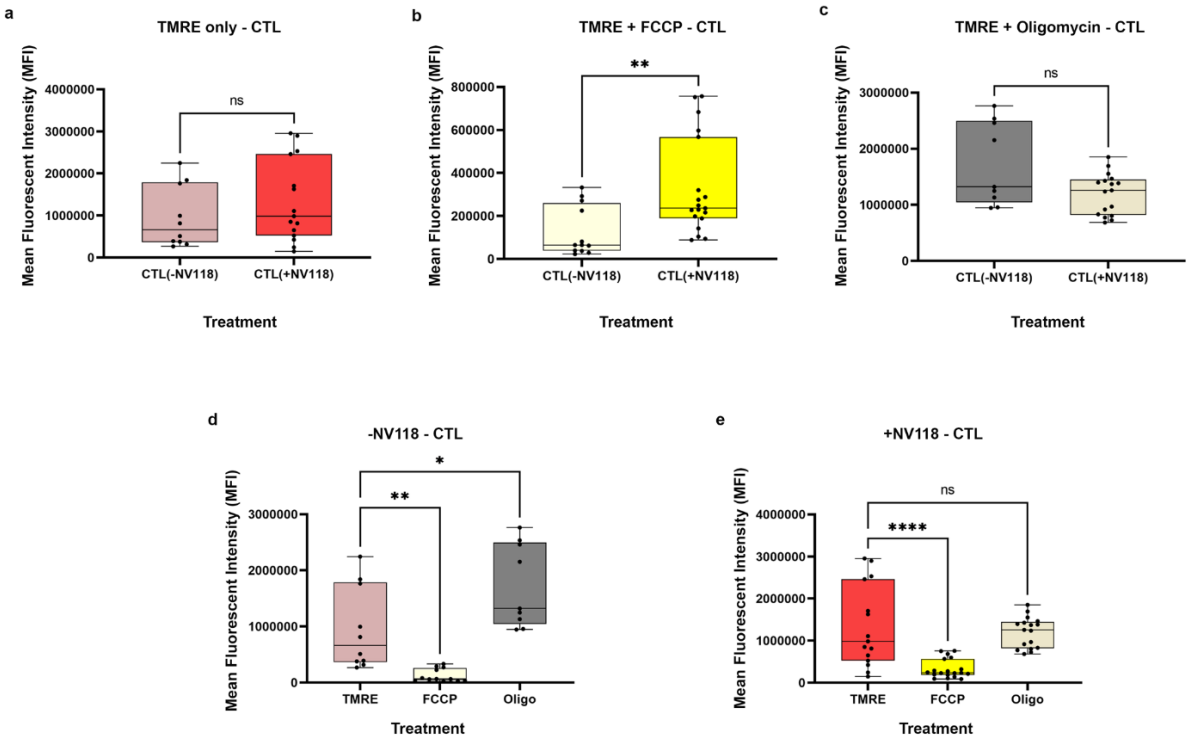

Figure 5.3.6.1. Mitochondrial membrane potential (MMP) analysis of BJ-FB with and without NV118. Using flow cytometry, along with membrane-potential sensitive dye (TMRE), MMP was evaluated. Mean fluorescence intensity (MFI) was calculated based on three independent runs and are shown for CTL BJ-FB. The top panel shows comparisons between NV118 treated and untreated groups when (a) stained with TMRE only (b) stained with TMRE+FCCP and (c) stained with TMRE+oligomycin. The bottom panel shows comparison between TMRE only, TMRE+FCCP, and TMRE+oligomycin in the d) NV118 untreated groups and e) NV118 treated group. *p<0.05** p<0.01*** p<0.001 ****p<0.00001. Light red, yellow, and dark gray bars represent treatment with vehicle (-NV118). While dark red, yellow, and tan bars represent NV118 treatment groups (+NV118).

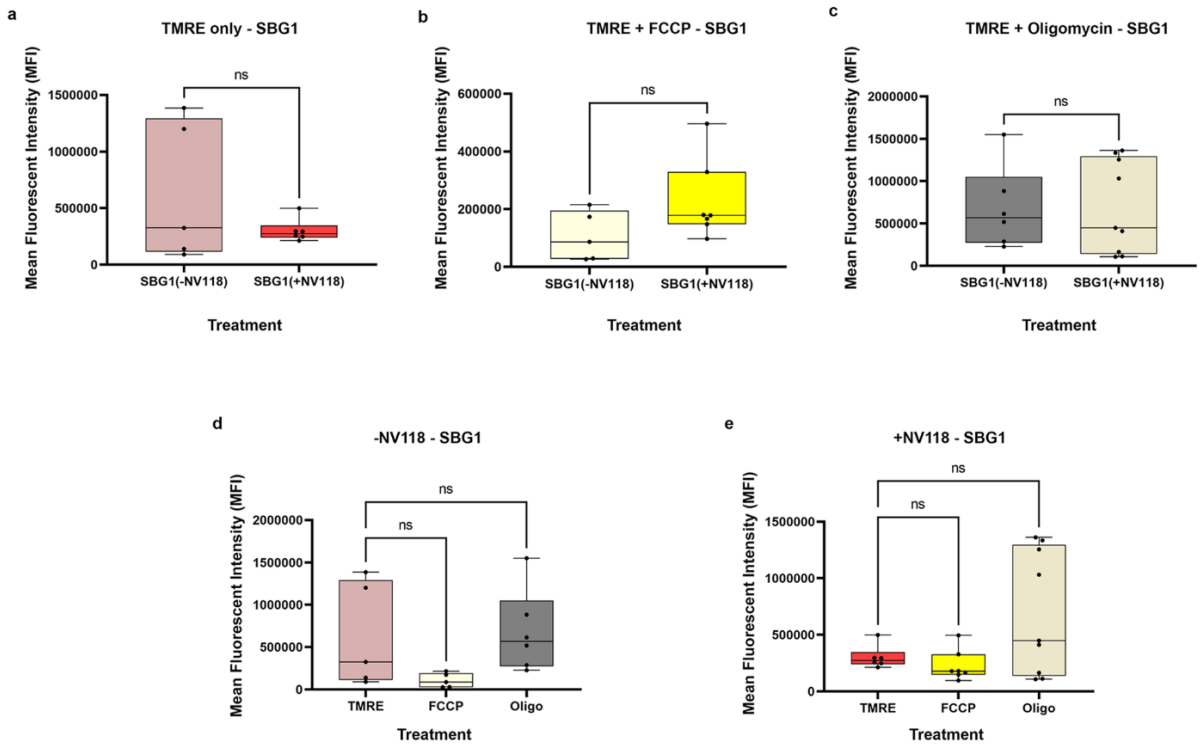

Figure 5.3.6.2. Mitochondrial membrane potential (MMP) analysis of SBG1-FB (T8993G) with and without NV118. Using flow cytometry, along with membrane-potential sensitive dye (TMRE), MMP was evaluated. Mean fluorescence intensity (MFI) was calculated based on three independent runs and are shown for SBG1-FB (*T8993G*). The top panel shows comparisons between NV118 treated and untreated groups when (a) stained with TMRE only (b) stained with TMRE+FCCP and (c) stained with TMRE+oligomycin. The bottom panel shows comparison between TMRE only, TMRE+FCCP, and TMRE+oligomycin in the d) NV118 untreated groups and e) NV118 treated group. *p<0.05** p<0.01*** p<0.001 ****p<0.00001. Light red, yellow, and dark gray bars represent treatment with vehicle (-NV118). While dark red, yellow, and tan bars represent NV118 treatment groups (+NV118).

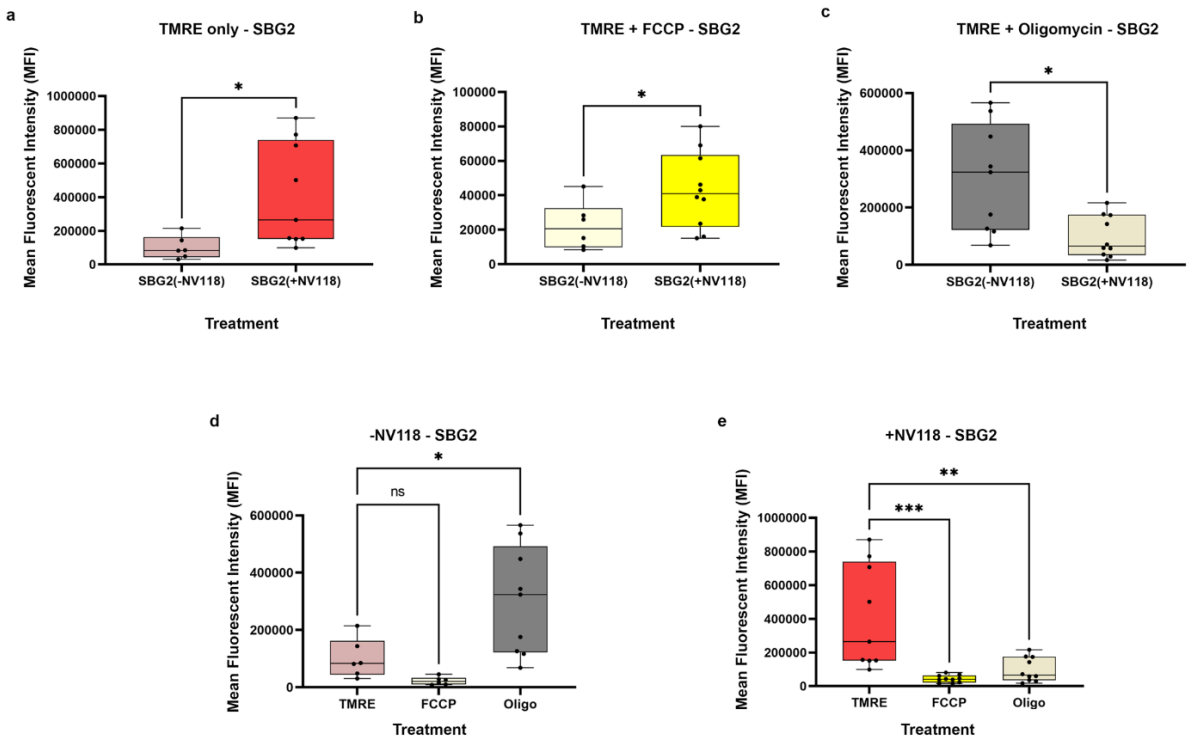

Figure 5.3.6.3. Mitochondrial membrane potential (MMP) analysis of SBG2-FB (T8993G) with and without NV118. Using flow cytometry, along with membrane-potential sensitive dye (TMRE), MMP was evaluated. Mean fluorescence intensity (MFI) was calculated based on three independent runs and are shown for SBG2-FB (*T8993G*). The top panel shows comparisons between NV118 treated and untreated groups when (a) stained with TMRE only (b) stained with TMRE+FCCP and (c) stained with TMRE+oligomycin. The bottom panel shows comparison between TMRE only, TMRE+FCCP, and TMRE+oligomycin in the d) NV118 untreated groups and e) NV118 treated group *p<0.05** p<0.01*** p<0.001 ****p<0.00001. Light red, yellow, and dark gray bars represent treatment with vehicle (-NV118). While dark red, yellow, and tan bars represent NV118 treatment groups (+NV118).

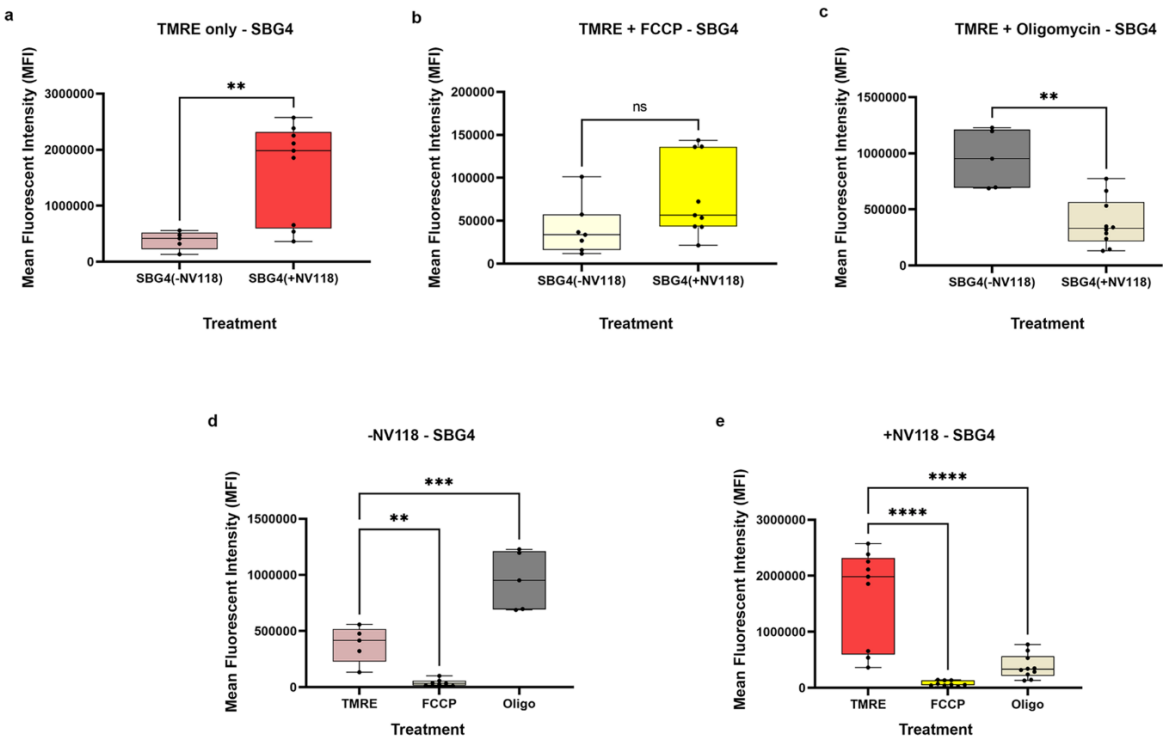

Figure 5.3.6.4. Mitochondrial membrane potential (MMP) analysis of SBG4-FB (T10158C) with and without NV118. Using flow cytometry, along with membrane-potential sensitive dye (TMRE), MMP was evaluated. Mean fluorescence intensity (MFI) was calculated based on three independent runs and are shown for SBG4-FB (*T10158C*). The top panel shows comparisons between NV118 treated and untreated groups when (a) stained with TMRE only (b) stained with TMRE+FCCP and (c) stained with TMRE+oligomycin. The bottom panel shows comparison between TMRE only, TMRE+FCCP, and TMRE+oligomycin in the d) NV118 untreated groups and e) NV118 treated group. *p<0.05** p<0.01*** p<0.001 ****p<0.00001. Light red, yellow, and dark gray bars represent treatment with vehicle (-NV118). While dark red, yellow, and tan bars represent NV118 treatment groups (+NV118).

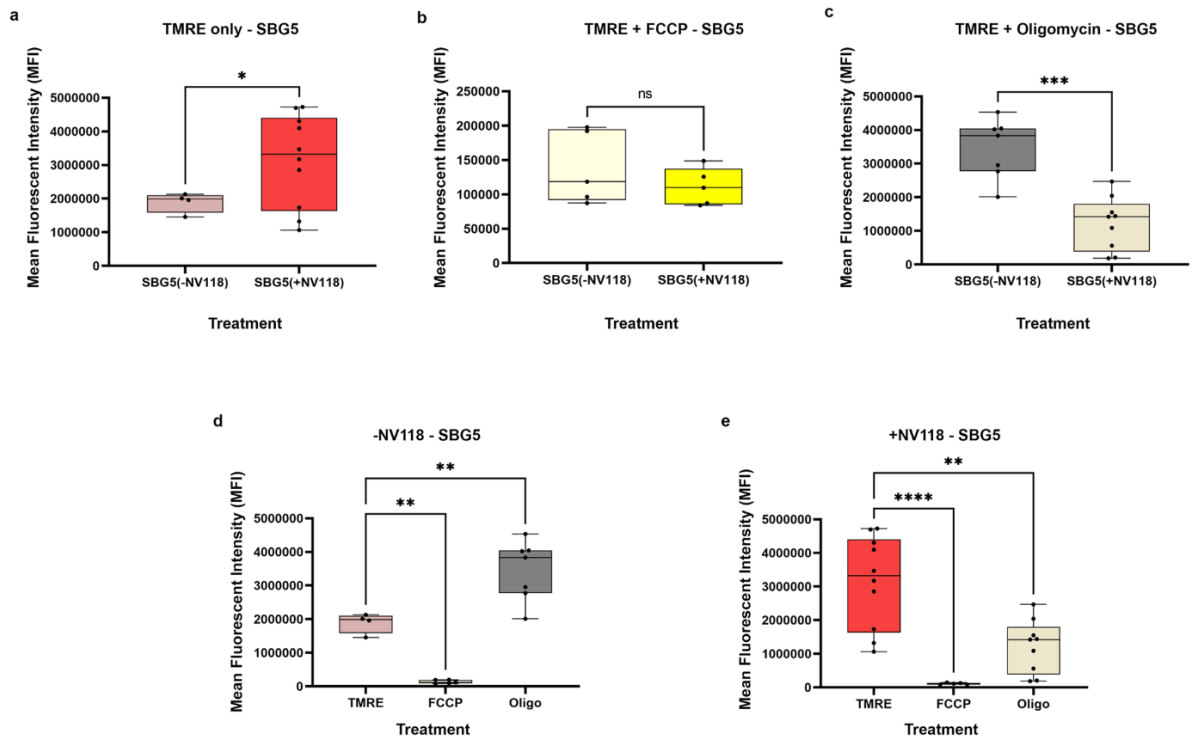

Figure 5.3.6.5. Mitochondrial membrane potential (MMP) analysis of SBG5-FB (T12706C) with and without NV118. Using flow cytometry, along with membrane-potential sensitive dye (TMRE), MMP was evaluated. Mean fluorescence intensity (MFI) was calculated based on three independent runs and are shown for SBG5-FB (*T12706C*). The top panel shows comparisons between NV118 treated and untreated groups when (a) stained with TMRE only (b) stained with TMRE+FCCP and (c) stained with TMRE+oligomycin. The bottom panel shows comparison between TMRE only, TMRE+FCCP, and TMRE+oligomycin in the d) NV118 untreated groups and e) NV118 treated group. *p<0.05** p<0.01*** p<0.001 ****p<0.00001. Light red, yellow, and dark gray bars represent treatment with vehicle (-NV118). While dark red, yellow, and tan bars represent NV118 treatment groups (+NV118).

5.3.7. Mitochondrial bioenergetics were not altered in LS cell lines after 24-hour treatment with prodrug NV118

We next hypothesized that an increase in MMP would perhaps contribute to mitochondrial respiration in the diseased LS cell lines. To test this hypothesis, a mitochondrial stress test was performed on the four LS cell lines and the control BJ-FB cell line. Using a Seahorse XFe96 flux analyzer, oxygen consumption rate was measured in all cell lines after a 24-hour treatment with 100µM NV118 or without NV118 (added equivalent amount of (phenol-red free MEM)) as vehicle controls. The following oxidative phosphorylation parameters were recorded: basal

respiration, leak, maximal respiration, and non-mitochondrial respiration, after sequential injections of ATP synthase inhibitor oligomycin, the uncoupler carbonyl cyanide-4-(trifluoromethoxy) phenylhydrazone FCCP, complex I inhibitor Rotenone, and complex III inhibitor Antimycin A into the wells. Analysis was conducted in all cell lines (n=3-4) at passage eight. We have reported previously that spare respiratory capacity (SRC) is an important variable in determining how flexible a cell is in responding to changes in energetic demand (**see Chapter 3**). Therefore, in addition to reporting the mitochondrial-derived ATP rate, we also examined the rate of SRC in all cell lines with or without NV118 treatment. Results suggest that NV118 did not significantly improve mitochondria respiration in any of the cell lines (**Figure 5.2.7.1.-5.**). This result is not consistent with other reports that have shown that NV118 treatment improves mitochondrial respiration (Ehinger et al., 2016;Piel et al., 2020) Although we observed improvement in mitochondrial respiration (**Figure 5.2.1.b-h**) in the optimization experiments during acute 20-minute exposure of prodrug NV118 in control BJ-FB cells, the result was different during the 24-hour treatment (**also see supplementary Figure 7.2.**). It is conceivable that once the prodrug NV118 (succinate) is oxidized to fumarate, malate, and oxaloacetate the cells are not able to sustain the CII-linked mitochondrial respiration because several reports have shown oxaloacetate competitively inhibits succinate dehydrogenase (Zeylemaker et al., 1969;Stepanova et al., 2016;Fink et al., 2018).

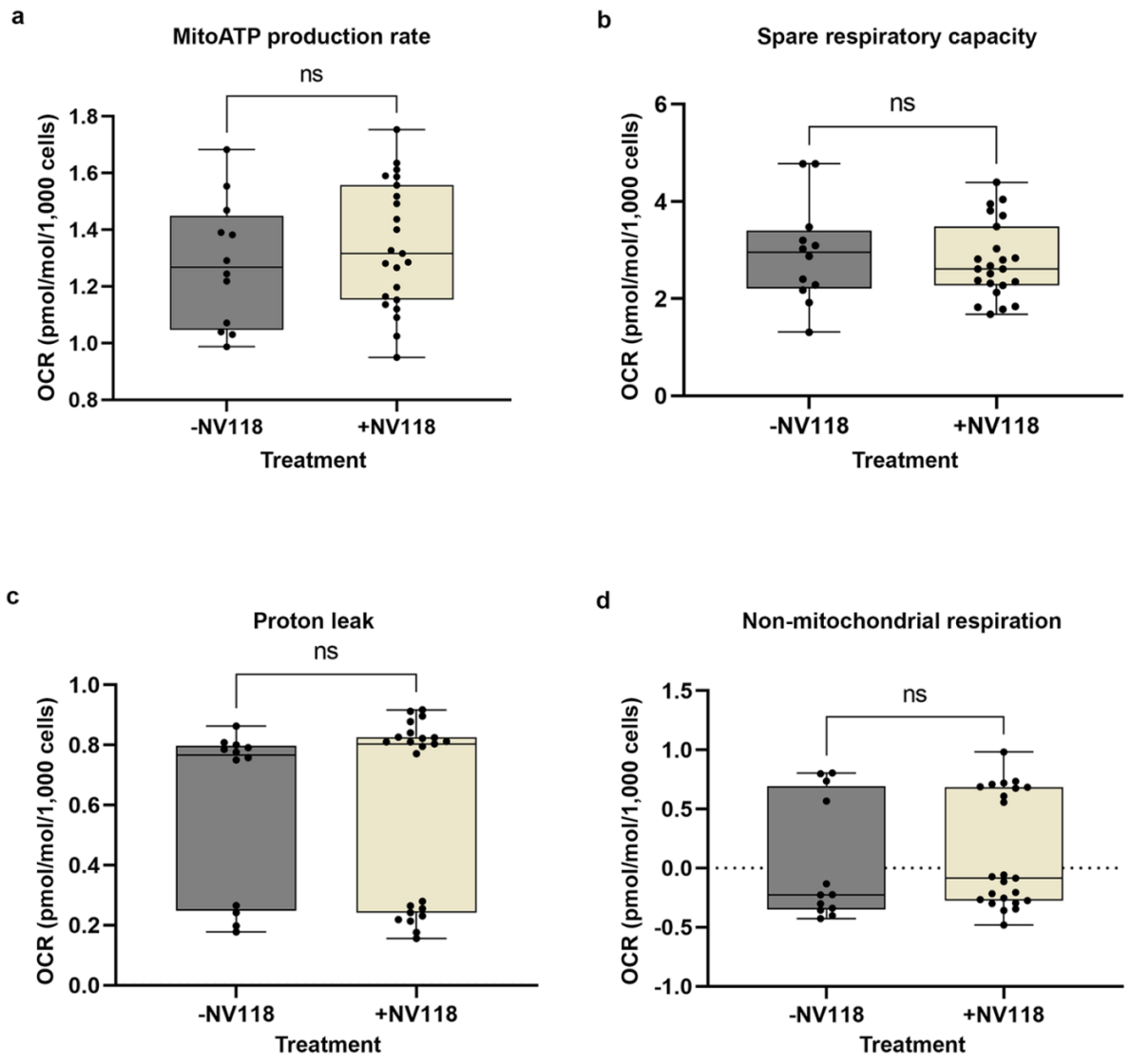

Figure 5.3.7.1. Mitochondrial respiration profile of CTL BJ-FB with and without NV118. CTL BJ-FB were treated with 100 µM NV118 or vehicle (phenol-red free MEM) for 24-hours, and Oxygen Consumption Rate (OCR) was measured at the end of the 24-hour treatment period. Cell line showing (a) mitoATP production rate, (b) spare respiratory capacity, (c) proton leak, (d) non-mitochondrial respiration. All parameters are in pmol/min/1000 cells. Data are mean +/- SD. Experiments were repeated at least three times on different days under the same conditions. ns = not significant. The dark gray bar represents treatment with vehicle (-NV118), while the tan bar represents treatment with 100 µM NV118 (+NV118).

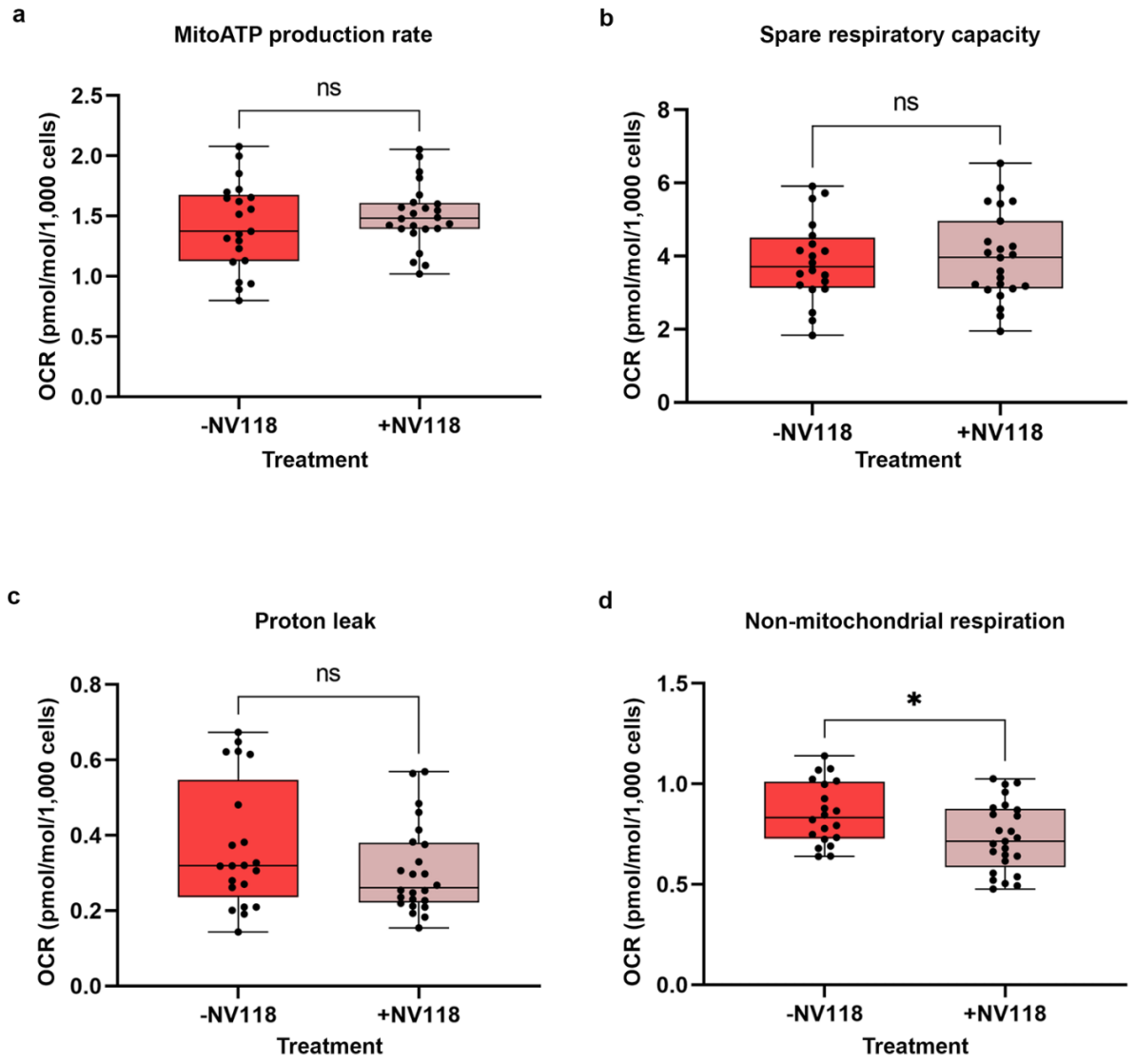

Figure 5.3.7.2. Mitochondrial respiration profile of SBG1-FB (*T8993G*) with and without NV118. SBG1-FB (*T8993G*) were treated with 100 µM NV118 or vehicle (phenol-red free MEM) for 24-hours, and Oxygen Consumption Rate (OCR) was measured at the end of the 24-hour treatment period. Cell line showing (a) mitoATP production rate, (b) spare respiratory capacity, (c) proton leak, (d) non-mitochondrial respiration. All parameters are in pmol/min/1000 cells. Data are mean +/- SD. Experiments were repeated at least three times on different days under the same conditions. *p< 0.05, ns = not significant. The red bar represents treatment with vehicle (-NV118), while the pink bar represents treatment with 100 µM NV118 (+NV118).

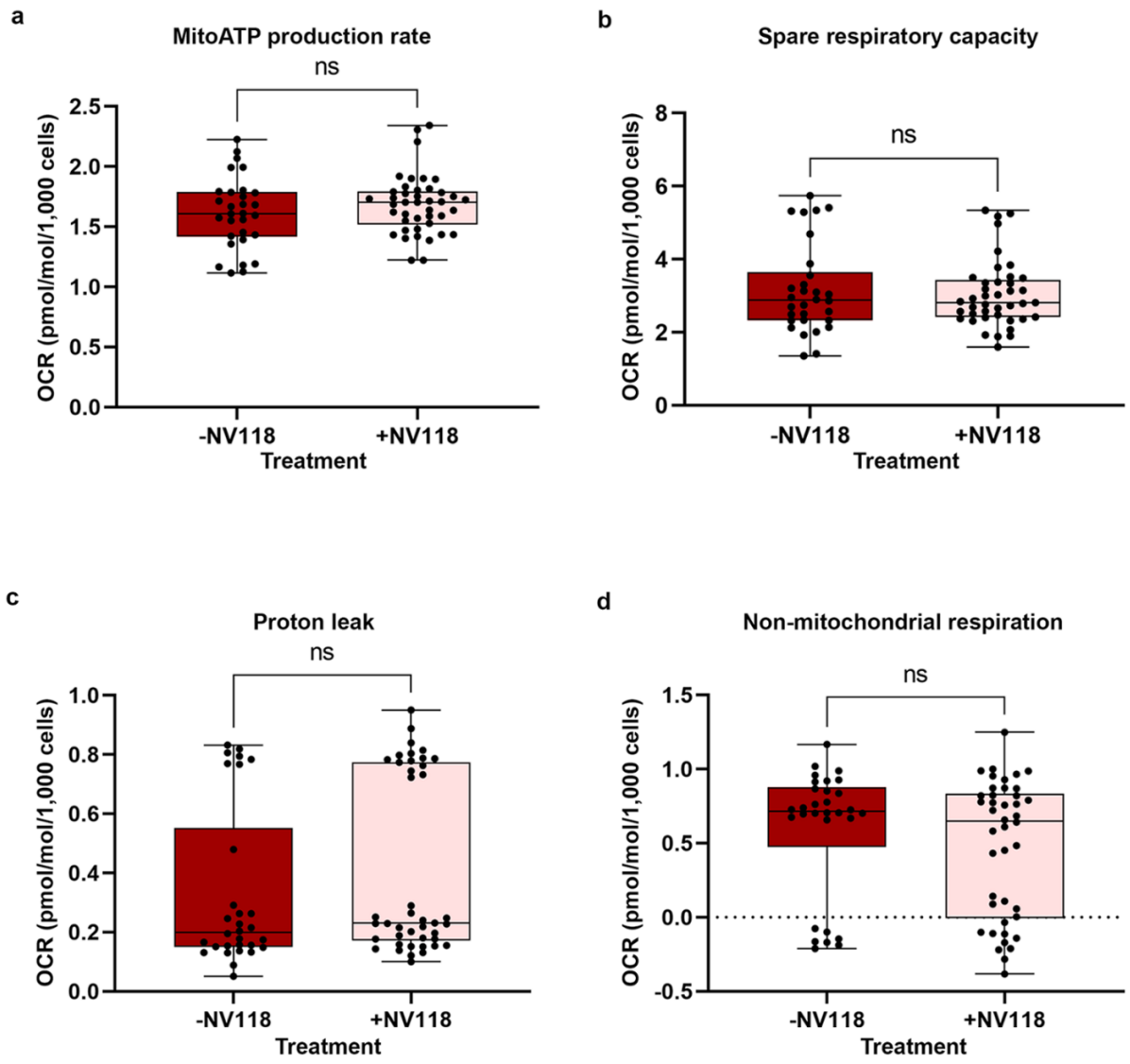

Figure 5.3.7.3. Mitochondrial respiration profile of SBG2-FB (*T8993G*) with and without NV118. SBG2-FB (*T8993G*) were treated with 100 µM NV118 or vehicle (phenol-red free MEM) for 24-hours, and Oxygen Consumption Rate (OCR) was measured at the end of the 24-hour treatment period. Cell line showing (a) mitoATP production rate, (b) spare respiratory capacity, (c) proton leak, (d) non-mitochondrial respiration. All parameters are in pmol/min/1000 cells. Data are mean +/- SD. Experiments were repeated at least three times on different days under the same conditions. *p< 0.05, ns = not significant. Dark red bars represent treatment with vehicle (-NV118), while pink bars represent treatment with 100 µM NV118 (+NV118).

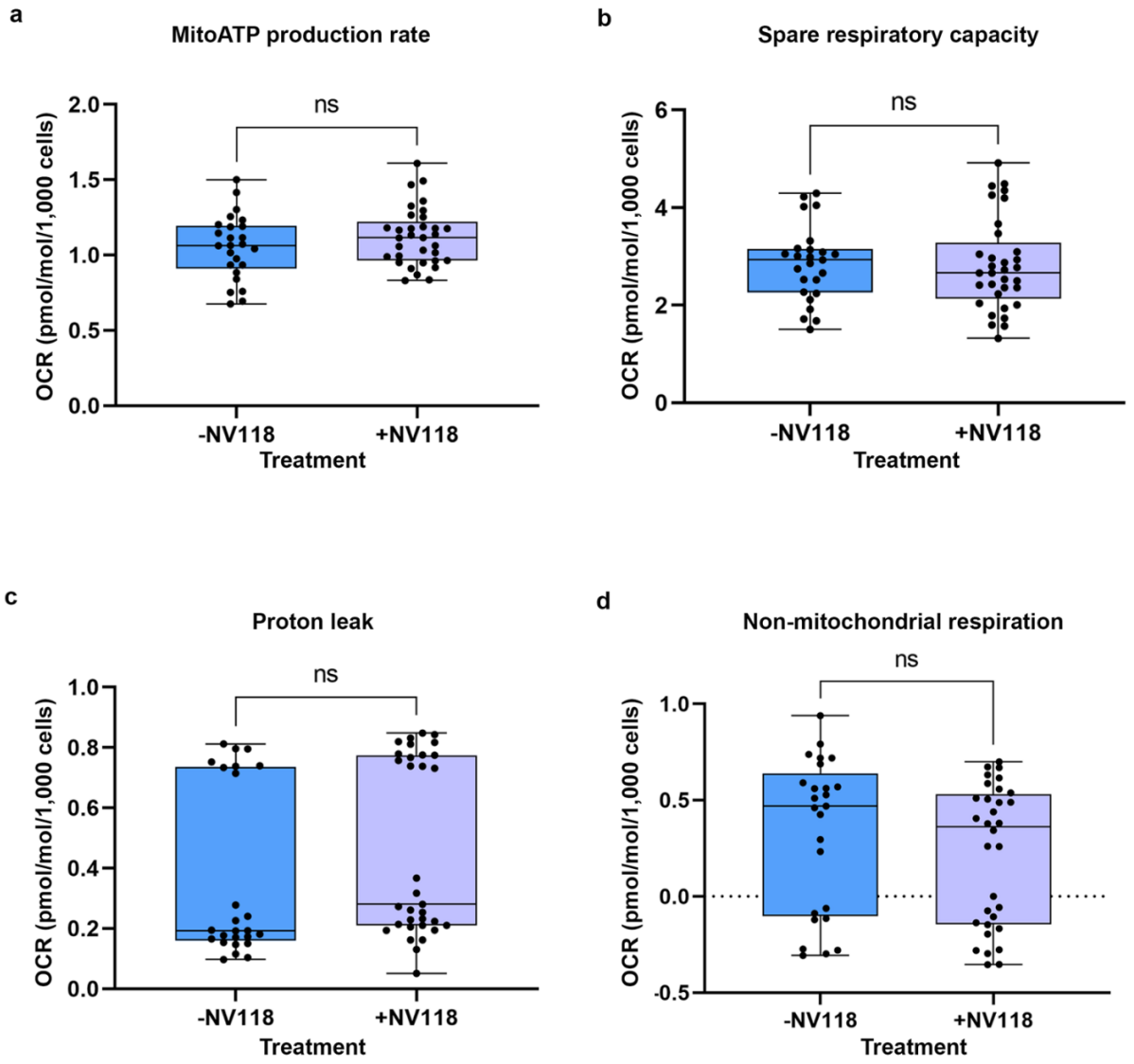

Figure 5.3.7.4. Mitochondrial respiration profile of SBG4-FB (*T10158C*) with and without NV118. SBG4-FB (*T10158C*) were treated with 100 µM NV118 or vehicle (phenol-red free MEM) for 24-hours, and Oxygen Consumption Rate (OCR) was measured at the end of the 24-hour treatment period. Cell line showing (a) mitoATP production rate, (b) spare respiratory capacity, (c) proton leak, (d) non-mitochondrial respiration. All parameters are in pmol/min/1000 cells. Data are mean +/- SD. Experiments were repeated at least three times on different days under the same conditions. *p< 0.05, ns = not significant. Blue bars represent treatment with vehicle (-NV118), while purple bars represent treatment with 100 µM NV118 (+NV118).

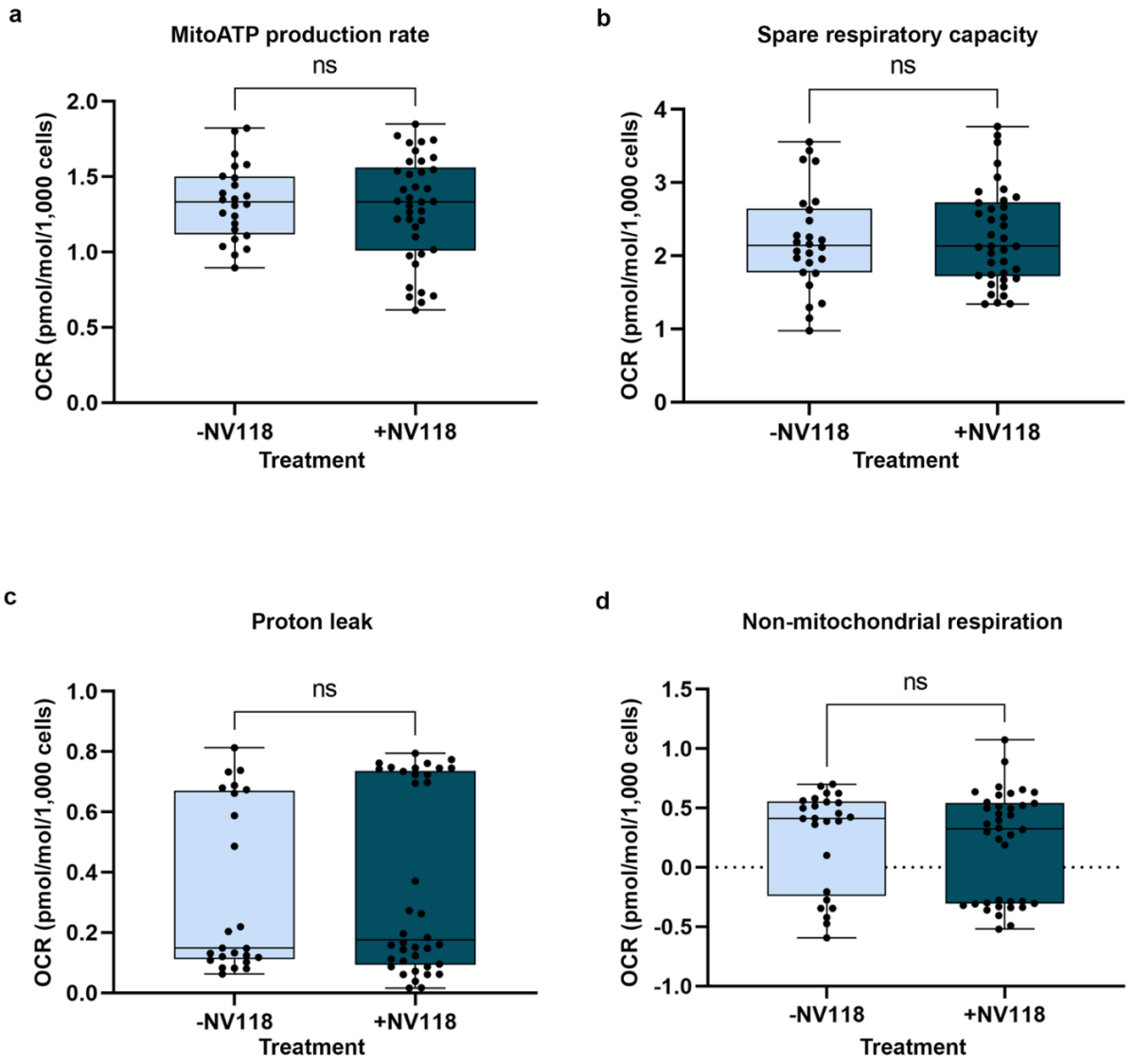

Figure 5.3.7.5. Mitochondrial respiration profile of SBG5-FB (*T12706C*) with and without NV118. SBG5-FB (*T12706C*) were treated with 100 µM NV118 or vehicle (phenol-red free MEM) for 24-hours, and Oxygen Consumption Rate (OCR) was measured at the end of the 24-hour treatment period. Cell line showing (a) mitoATP production rate, (b) spare respiratory capacity, (c) proton leak, (d) non-mitochondrial respiration. All parameters are in pmol/min/1000 cells. Data are mean +/- SD. Experiments were repeated at least three times on different days under the same conditions. *p< 0.05, ns = not significant. Light blue bars represent treatment with vehicle (-NV118), while green bars represent treatment with 100 µM NV118 (+NV118).

5.4. Discussion

To date there is no cure for patients affected with LS and patients usually pass away within a decade after their initial diagnosis (Baertling et al., 2014;Reynaud-Dulaurier et al., 2020). Recently, cell-permeant ETC substrates have been proposed as therapeutics for various ETC defects (Ehinger et al., 2016;Piel et al., 2020). In these studies, succinate prodrugs have been used as a bypass for disorders involving deficiencies in complex I. The succinate prodrugs have also been used to rescue mitochondrial disorders associated with a defect in complex IV, an ETC complex whose activity is downstream that of complex I (Owiredu et al., 2020a;Owiredu et al., 2020b). So far none of the studies have used succinate prodrugs for alleviating symptoms of LS harboring pathogenic mtDNA mutations in genes *MTATP6* affecting complex V and *MTND3* and *MTND5* affecting complex I. Therefore, we wanted to understand the mechanisms (**Figure 5.4.**) as well as alleviate the bioenergetic defects by providing TCA cycle intermediate substrate succinate, as a therapeutic drug (NV118) in the vulnerable LS cell lines containing pathogenic mtDNA mutations affecting complex I and complex V.

Optimization experiments for estimating the concentration of the drug were carried out on the control BJ-FB cell line to determine the appropriate NV118 concentration for use in this study (**Figure 5.3.1.**). It has been reported previously that high concentrations of succinate could exert inhibitory effects on mitochondrial respiration (Gonzalez-Meler et al., 1996;Tretter et al., 2016). Furthermore, high concentrations of succinate could result in upregulation of RET, contributing to an increase in ROS production and subsequent cellular apoptosis (Scialò et al., 2016;Tretter et al., 2016;Scialo et al., 2017). Therefore, the control BJ-FB cell line was treated with three different concentrations (50μM, 100μM, and 150μM) of NV118 and a vehicle (phenol red-free MEM) for 30-minutes (to evaluate acute response) before measuring cellular viability and mitochondrial respiration. While there was no significant difference in cell viability (**Figure 5.3.1.a**) between the NV118 treated and untreated groups, we observed a trend towards a slight

decrease in cell viability in the NV118 treatment group. The decrease in cell viability was dose-dependent, with 150μM NV118 treatment resulting in the highest decrease of 4%. However, the 50μM and 100μM NV118 treatment groups only resulted in a 1% and 2% decrease in cell viability respectively. The results from cell viability studies convinced us that the chosen concentrations were not toxic to the cells.

Next, we examined mitochondrial respiration in the control BJ-FB after treatment with the same three concentrations of NV118. Basal respiration (**Figure 5.3.1.b**) readings before injection of NV118 showed no significant difference between any of the treatment groups. After NV118 was added, however, the ATP production rate (**Figure 5.3.1.c**) increased significantly ($p<0.0001$) in the NV118 treatment group relative to the untreated group. The highest increase was observed in the group with 100μM NV118. The increase in ATP production correlated with a significant increase in maximal respiration (**Figure 5.3.1.f)**, and SRC (**Figure 5.3.1.g)** as well. Although it is worth noting that some of the increases in oxygen consumption contributed to a dose-dependent elevation of proton leak (**Figure 5.3.1.d)** with NV118 treatment. As a result, coupling efficiency (**Figure 5.3.1.e**) was also lower in a dose-dependent manner, with 150μM NV118 treatment resulting in a significant decrease ($p<0.05$) by 5% relative to the untreated group. Finally, when mitochondrial respiration was inhibited with rotenone and antimycin A, non-mitochondrial respiration (**Figure 5.3.1.h**) significantly increased ($p<0.05$) by 20% and 22% in the 50μM and 150μM NV118 treatment respectively relative to the untreated group. However, there was only an 18% increase in non-mitochondrial respiration in the 100μM NV118 treatment group. Non-mitochondrial respiration is typically attributed to the non-ETC oxidases present in the cell (Hill et al., 2012). This suggests that at 100μM NV118 concentration, there is less involvement of non-ETC oxidases. Owing to the significant decrease ($p<0.05$) in coupling efficiency (**Figure 5.3.1.e**) and the significant increase ($p<0.05$) in proton leak (**Figure 5.3.1.d)** and non-mitochondrial respiration (**Figure 5.3.1.h**), the 150μM NV118 concentration was

excluded. The 50μM NV118 concentration was also excluded because of the relatively high non-mitochondrial respiration. Together, the cell viability and the mitochondrial respiration studies were used to determine that 100μM NV118 concentration is optimal for our studies.

Once the optimal concentration was determined, we sought to understand how NV118 affects metabolism. First, glycolysis was evaluated after a 24-hour treatment with 100μM NV118. In the TCA cycle, oxidation of succinate results in the production of fumarate. Fumarate is further oxidized to malate, and malate becomes oxidized to produce oxaloacetate. In the absence of succinate, succinate dehydrogenase (SDH; CII) is inhibited and deactivated by oxaloacetate (Kearney et al., 1972;Kotlyar and Vinogradov, 1984;Stepanova et al., 2016). As a prodrug of succinate, the addition of NV118 for 20-mins resulted in a short-term increase in CII-respiration (**Figure 5.3.1.**). As a result, accumulation of TCA cycle intermediates upstream of succinate will occur. One of those intermediates is oxaloacetate (OAA), if not used up and continues to accumulate, could result in inhibition of CII activity. Therefore, we hypothesized that the addition of NV118 would result in the upregulation of glycolysis (**Figure 5.4.**). Glycolysis would produce pyruvate, which could be converted into acetyl-CoA, an important intermediate for the TCA cycle. Acetyl-CoA, together with oxaloacetate forms citrate to produce other TCA cycle substrates. Indeed, our results support this hypothesis as we observed a significant increase ($p<0.05$) in basal glycolysis and glycoATP production rate in the control BJ-FB (**Figure 5.3.2.a&b**) and the LS SBG4-FB (*T10158C*) cell line with complex I defect (**Figure 5.3.2.a&b**) when NV118 was added. In the other LS cell lines, SBG1-FB (*T8993G*), SBG2-FB (*T8993G*), and SBG5-FB (*T12706C*), glycolytic respiration (**Figure 5.3.4.1.b, 5.3.4.2.b, and 5.3.3.2.b**) trended up. Furthermore, when glycolysis was inhibited with 2-Deoxyglucose (2DG), there was a significant increase ($p<0.01$) and a trend towards an increase in post-2DG acidification in both the control BJ-FB and all the diseased FB cell lines (**Figure 5.3.2.-4.**). Since the addition of 2DG inhibits glycolysis and prevents lactate from being formed, acidification through the glycolytic

pathway is blocked. Furthermore, mitochondrial respiration through the ETC has also been inhibited with rotenone/antimycin A, preventing the oxidation of substrates through CI and CIII. Leaving the protons generated from the TCA cycle metabolism as the major contributor to acidification post-2DG. During cellular respiration, the CO_2 produced during oxidation reactions by TCA cycle dehydrogenases contribute to acidification (Divakaruni et al., 2014;Giorgi-Coll et al., 2017). This further supports the hypothesis that NV118 upregulates glycolysis to enhance the production of other TCA cycle substrates.

It is well known that reverse electron transport (RET) via complex I and NAD^+ dependent pathway occurs when there is an over-reduction of the CoQ pool by electrons from CII (Chance and Hollunger, 1961;Chouchani et al., 2016;Scialò et al., 2016;Scialo et al., 2017). To exclude the possibility that the treatment with NV118 was causing RET and contributing to reactive oxygen species production, we examined intracellular ROS levels using DCFDA/H_2DCFDA a fluorescent precursor, after 24-hour treatment with 100µM NV118. This dye measures hydroxyl, peroxyl, and other reactive oxygen species (ROS) within cells. Within the cells, DCFDA is hydrolyzed by esterases to release DCF, which is readily oxidized by intracellular ROS thus emitting a green fluorescence (Ex 485/Em 535). The results from ROS studies supported the observation made during the optimization studies with control BJFB cells. Treatment with 100µM NV118 did not result in a significant difference in intracellular ROS levels (**Figure 5.3.5.**) in any of the cell lines between the NV118 treated and untreated groups. Furthermore, the intracellular ROS levels are consistent with our previous results (**section 4.3.4.**), where LS diseased cell lines exhibited lower mitoROS levels compared to the control BJ-FB cells (*manuscript under review, chapter 3*). We conclude that the specific concentration of (succinate) produg NV118 used in this study did not contribute to complex I and NAD^+ mediated reverse electron transport (RET) or increase intracellular ROS levels in either the control or LS cell lines.

Knowing that the increase in CII-respiration did not result in elevated RET or ROS levels, we next examined MMP in the control and diseased FB in the presence and absence of prodrug NV118. As expected, we observed a significant increase ($p<0.05$) in MMP in both complex I defective LS (SBG4-FB (*T10158C*) and SBG5-FB (*T12706C*)) cells (**Figure 5.3.6.4.a & 5.3.6.5.a**) upon NV118 treatment compared to the untreated group. We also observed a significant increase ($p<0.05$) in MMP in SBG2-FB (*T8993G*) (**Figure 5.3.6.3.a**) with CV-defect after NV118 addition. In presence of NV118 prodrug in the control BJ-FB cells (**Figure 5.3.6.1.a**), there was a 39% increase (although not significant) in MMP relative to the untreated group. In the SBG1-FB (*T8993G*) (**Figure 5.3.6.2.a**), MMP stayed the same both in the NV118 treated and untreated groups. FCCP and Oligomycin were added as control, to depolarize and hyperpolarize MMP respectively. In both the untreated and NV118 treatment groups, FCCP resulted in depolarization (**Figure 5.3.6.1.-6. d&e**) as predicted. Interestingly, in the SBG2-FB (*T8993G*), the addition of NV118 rescued mitochondrial function (**Figure 5.3.6.3.d&e**). We have reported previously that SBG2-FB (*T8993G*) has an uncoupling defect (Bakare et al., 2021). The addition of exogenous substrate (NV118), helps rescue this problem, allowing for complete depolarization (significant decrease in MMP; $p<0.001$) when FCCP is added (**Figure 5.3.6.3.b**). When Oligomycin was added, we predicted hyperpolarization in the NV118 untreated group (**Figure 5.3.6.1.-6.d**). However, in the presence of NV118, all of the cell lines (**Figure 5.3.6.1.-6.e**) except SBG1-FB (*T8993G*) (**Figure 5.3.6.2.e**) experienced depolarization. Oligomycin is a complex V inhibitor, which prevents protons from getting back into the matrix, resulting in a relative decrease in proton gradient in the matrix, consequently making the matrix more negative relative to the IMS. We have shown above that MMP is generally higher with NV118 treatment (**Figure 5.4.**), therefore, inhibition of CV with oligomycin invariably affects the electron and proton flux. Proton leakage into the matrix through other channels independent of CV re-entry occurs to sustain the electron and proton flux. This increase in proton leak upon NV118

addition could explain why we observe depolarization when the CV is inhibited by oligomycin in the NV118 treatment group.

Finally, we examined mitochondrial respiration to check if the increased MMP corresponded with increased mitochondrial respiration. Our results show that mitochondrial respiration (**Figure 5.3.7.1.-5.**) remained the same after 24-hour treatment with NV118. In our optimization studies with the control BJ-FB, treatment with NV118 for 20-minutes before OCR measurements resulted in a significant increase ($p<0.05$) in mitoATP production, maximal respiration, and SRC (**Figure 5.3.1.c,f, & g.**). Therefore, this result shows that short-term treatment with NV118 results in changes to mitochondrial respiration, however, 24-hour treatment with NV118 results in inhibiting the SDH activity by OAA leading to no change in mitochondria respiration.

After 24-hour treatment with 100μM NV118, we observed changes in glycolysis (**Figure 5.3.2.-4.**) and MMP (**Figure 5.3.6.1.-6.**) that corresponded with the effect of the prodrug NV118. Our result suggests other mechanisms of action for the succinate prodrug, NV118. When NV118 has been used as therapy for CI-deficient cells, it has been suggested that the drug works by bypassing CI and upregulating CII-respiration (Ehinger et al., 2016;Piel et al., 2018;Janowska et al., 2020). While this explanation is valid in cell lines with CI-deficiencies, other labs have also shown improvement in mitochondrial function in cells with deficiencies in other ETC enzymes downstream of CI (Owiredu et al., 2020a;Owiredu et al., 2020b). In this situation, bypassing CI with NV118 does not fully explain how the disease phenotype is rescued in these cells. Our results suggest a pathway that involves upregulation of glycolysis (**Figure 5.3.2.-4.**) and the TCA cycle substrates. It has been demonstrated elsewhere that activated macrophages undergo metabolic alterations to support their pro-inflammatory functions (Mills et al., 2016). In these studies stimulation of macrophages with LPS (Lipopolysaccharides); endotoxins found in the outer membrane of Gram-negative bacteria, resulted in a switch to succinate-dependent respiration, and a subsequent increase in glycolysis and MMP. In

macrophages, the increased succinate oxidation resulted in ROS production and production of pro-inflammatory cytokines. While the addition of produg NV118 did not increase intracellular ROS levels (**Figure 5.3.5.**) in LS cell lines, we observed an increase in glycolysis (**Figure 5.3.2.-4.**) and MMP (**Figure 5.3.6.1.-6.**) consistent with other studies (Mills et al., 2016). We postulate that the addition of succinate (NV118) increases glycolysis to prevent the accumulation of oxaloacetate (a potent inhibitor of CII) (Priegnitz et al., 1973;Stepanova et al., 2016). The trend towards increased MitoPER and elevated post-2DG acidification (**Figure 5.3.2.-4.d&e**) in most of the cell lines in the presence of NV118 further supports this hypothesis. Since CO_2 from the TCA cycle can contribute to acidification (Divakaruni et al., 2014), when glycolysis is inhibited by the addition of 2DG, the other source of acidification could be from the TCA cycle. Upregulation of glycolysis by NV118 not only increases TCA cycle intermediates (**Figure 5.4.**) but also contributes to ATP production (Gullans et al., 1988). It is useful to note that succinate itself is a product of a substrate-level phosphorylation step in the TCA cycle (Tretter et al., 2016). Therefore, increasing TCA cycle intermediates could help provide additional ATP in cell lines with mutations affecting OXPHOS capacities.

LS is a disorder with no known cure, based on the results from this study, we have demonstrated the potential for NV118 as an LS therapeutic. To the best of our knowledge, we have also shown for the first time that in addition to rescuing mitochondrial dysfunction in cell lines with mutations impacting CI, NV118 has the potential to rescue mitochondrial dysfunction in cell lines with mutations impacting CV (ATP synthase). Although previous studies have focused on improving mitochondrial respiration, we show here that perhaps instead of trying to improve OXPHOS capacities in patients with LS, alternate therapies that focus on providing important TCA cycle intermediates could prove to be more beneficial. This is the first study that shows a therapeutic effect in four LS lines harboring mtDNA mutations (*T8993G*, *T10158C*, *T12706C*) while reducing intracellular ROS levels by 24 hours.

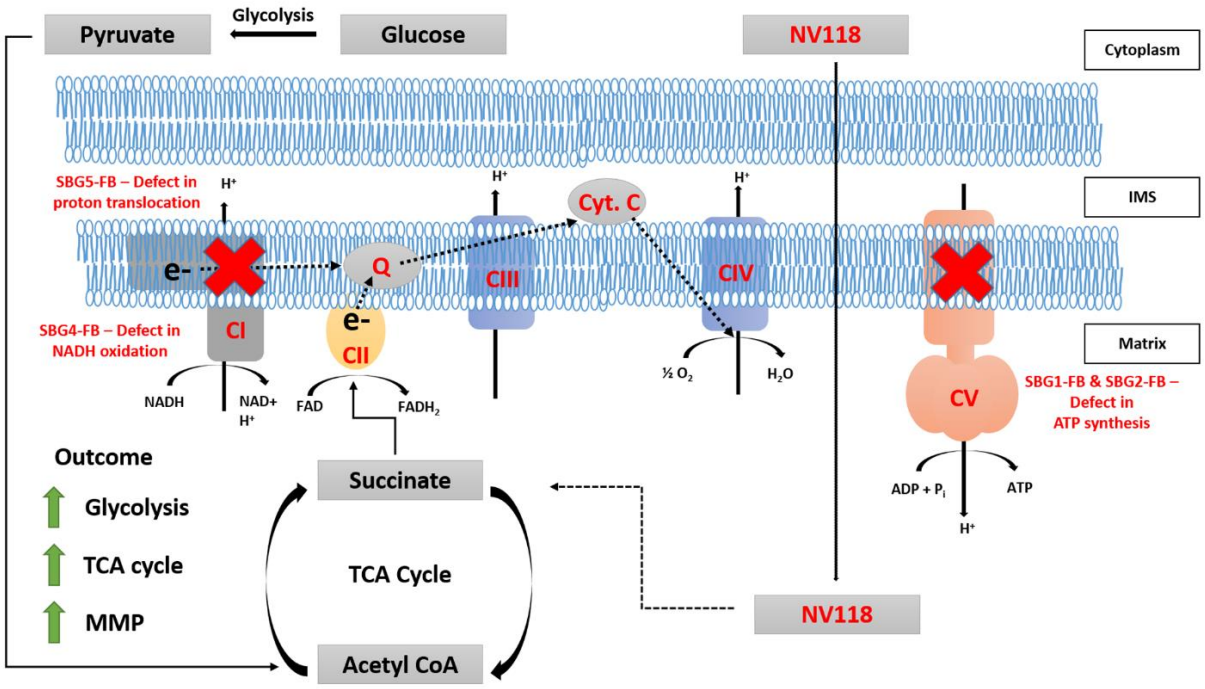

Figure 5.4. Summary figure describing the mechanism of action of NV118. NV118 is a succinate prodrug that is membrane permeable. In the mitochondria, NV118 (succinate) is oxidized by succinate dehydrogenase (CII). Under physiological conditions, both CI and CII contribute electrons (e-) to the quinone (Q) pool. Electrons from the Q pool are shuttled to CIII and then these electrons are donated to cytochrome c (Cyt. C) before they finally get donated to CIV when the final electron acceptor, oxygen (O_2) accepts these electrons and becomes reduced to water (H_2O). In addition to electron transport, CI, CIII, and CIV also translocate protons (H^+) from the matrix into the intermembrane space (IMS). This proton gradient is used by CV to generate ATP. Under physiological conditions, CI-linked respiration is favored, however, when CII substrates are in abundance CII-linked respiration becomes predominant. Since CII cannot shuttle protons, substrate oxidation increases to maintain MMP. Furthermore, to prevent the accumulation of oxaloacetate, a potent inhibitor of CII, glycolysis is upregulated. Together these processes drive an increase in TCA cycle enzyme activity. The red signs show that the mtDNA mutations in SBG1-FB (*T8993G*) and SBG2-FB (*T8993G*) result in CV dysfunction, while mutations in SBG4-FB (*T10158C*) and SBG5-FB (*T12706C*) result in CI dysfunction. After 24-hour treatment with 100uM NV118, a succinate prodrug, we observed an increase in glycolysis, MMP, and TCA cycle activity.

The results from this study has opened an avenue for further questions to be addressed in the future. For instance, did elevated succinate lead to the opening of the mitochondrial transition pore? What intervals of treatment is ideal to observe the full beneficial effect of NV118? In this study, all the LS cell lines used were derived from patients with early-onset LS. Clinical reports and metadata analysis are starting to suggest a difference in disease presentation and prognosis for patients with early-onset and late-onset LS (Gerards et al.,

2016;Wei et al., 2018). Perhaps, including cell lines (like SBG3-FB (*T9185C*)) derived from patients with late-onset LS presentation could provide insights into how late-onset LS disease responded to prodrug NV118 treatment. Nevertheless, this is the first study showcasing a single therapeutic dose of NV118 in LS patient cells harboring pathogenic mtDNA mutations in *MTATP6, MTND3*, *MTND5* genes affecting complex I and V of the electron transport chain.

5.5. Methods

5.5.1. Ethics statement

This study protocol conformed to the guidelines of the Declaration of Helsinki. The current study was conducted with patient fibroblasts provided by the Medical University of Salzburg (SBG), Austria. Fibroblasts were obtained for diagnostic purposes from patients with defined disorders. Informed consent was obtained to use these samples for research in an anonymized way. In accordance with federal regulations regarding the protection of human research subjects (32 CFR 219.101(b)(4)), the University of Arkansas Office of Research Compliance determined that the project was exempt from Institutional Review Board (IRB) oversight and human research subjects protection regulations.

5.5.2. NV118 drug preparation

The NV118, succinate prodrug (Oroboros Instruments Corporation, Innsbruck, Austria) was prepared following the manufacturer's instructions. Aliquots of the stock were stored in a -20^{o}C freezer until needed for experiments. Before each experiment, a fresh working solution was prepared by adding the appropriate volume of stock solution to phenol-red free MEM. The working solution (1mM) was prepared at 10X the final treatment concentration (100µM). The working solution was used up on the same day as they were prepared.

5.5.3. Cell culture

Cultures of healthy control and four patient-derived diseased fibroblast cell lines were maintained in a fibroblast expansion medium that consisted of minimal essential medium (MEM) (Thermo Fisher Scientific, Waltham, MA, USA) supplemented with 10% fetal bovine serum (FBS) (GE healthcare- HyClone^{TM}; Chicago, IL) and 2mM L-glutamine (Thermo Fisher Scientific, Waltham, MA, USA). All cell lines were cultured and maintained at 37^{o}C in a humidified atmosphere of 5% CO_2. The culture medium was replenished every two days and passaged when cells reached 80% confluence. Fibroblasts were enzymatically passaged in 0.05% Trypsin-EDTA (Thermo Fisher Scientific, Waltham, MA, USA). All experiments were performed with cells at passage 8 for consistency and to minimize experimental variability.

5.5.4. Mitochondrial oxygen consumption detection, glycolysis function test, and bioenergetics health index

Cells were maintained in culture following established protocols until the desired passage (Passage 8) is reached. A day before assay, 20,000 cells per well were plated and cultured in complete media (MEM supplemented with 10% FBS and 2mM L-glutamine). The drug treatment group also had 100µM NV118 added to each well, while the control groups had an equivalent volume of basal MEM added to each well. The cells were incubated with NV118 (or MEM) in a 37^{o}C incubator with a humidified atmosphere of 5% CO_2 for 24-hours. At the end of the 24-hour incubation period, mitochondrial and glycolytic metabolic profiles were assessed following steps below.

Changes in oxygen consumption were measured in real-time using an XFe96 extracellular flux analyzer. Seahorse XFe96 Cell Mito Stress Test Kit and glycolytic rate assay kit (Seahorse Biosciences, USA) were used as per the manufacturer's instructions. Prior to use in XFe96, fibroblasts were detached using mild trypsin and seed into the plates with a previously

optimized number of 20,000 cells per well. All fibroblasts were seeded in 8-12 replicate wells per plate, with the experiment repeated at least 3-5 times.

The cells were supplemented with 180 µl Mito-stress complete Seahorse medium, after which the cells were incubated in a non-CO_2 incubator at 37ºC for one hour. Respiration was measured using the classic mitochondrial inhibitors, specific for complex I and III subunits, such as Rotenone and Antimycin A (0.5 µM final concentrations each). Maximum respiration was measured by the addition of an uncoupler carbonyl cyanide-4-(trifluoromethoxy) phenylhydrazone- FCCP (0.7 µM final concentration); and Oligomycin (1 µM final concentration) was added to measure proton leak. The readouts were normalized to cell number and analyzed using Seahorse XF96 Wave software.

We also analyzed glycolytic function in the fibroblast cell lines. A classical glycolytic rate assay was performed using the XFe96 based on the following procedure: 1) cells were cultured in buffered (5 mM HEPES buffer) Seahorse medium supplemented with glucose and pyruvate; 2) the proton efflux rate (PER) was measured after the addition of saturating amounts of glucose; 3) rotenone and antimycin A were added to inhibit mitochondrial-derived ADP phosphorylation, and 4) 2-DG was added to inhibit glycolysis. The different assay parameters: basal glycolysis, compensatory glycolysis, total proton efflux, and post 2-DG acidification were normalized to cell number and analyzed using Seahorse XFe96 Wave software.

The mitochondrial-derived bioenergetic health index (mitoBHI), a composite index of mitochondrial quality was determined using the pre-defined formula - $\boldsymbol{Log}\,((\boldsymbol{mitoATP} * \boldsymbol{SRC})/(\boldsymbol{proton\ leak} * \boldsymbol{non-mito.resp.}))$. The glycolytic BHI (glycoBHI), an index of glycolytic respiration was determined using the formula - $\boldsymbol{Log}\,((\boldsymbol{glycoPER} * \boldsymbol{Comp.glycolysis})/(\boldsymbol{MitoPER} * \boldsymbol{post.2DG\ acid.}))$.

5.5.5. Mitochondrial membrane potential measurements

Cells were maintained in culture following established protocols until the desired passage (Passage 8) is reached. When cells reached 80-85% confluence they were treated with either 100µM NV118 or an equivalent volume of basal MEM and incubated for 24-hours. After the 24-hour incubation, mitochondrial membrane potential was evaluated following the procedure below.

On the day of the experiment, cells were enzymatically detached using 0.05% Trypsin-EDTA (Thermo Fisher Scientific) and centrifuged at 400xg for 5 mins. Cells were then resuspended in basal medium, after which the desired amount of tetramethylrhodamine, ethyl ester (TMRE-Abcam, Cambridge, MA, USA) was added (for a final concentration of 50nM). For FCCP and Oligomycin treatment groups, 20 µM and 5 µM of FCCP and Oligomycin were added respectively for 10 mins prior to treatment with TMRE. Cells were incubated with TMRE in a 37^{o}C 5% CO2 incubator for 25 mins. At the end of the incubation period, cells were centrifuged at 400xg for 5 mins. To wash off the excess dye, cells were resuspended in 1x dPBS solution and centrifuged for another 5 mins. At the end of the wash, the cells were resuspended in phenol-red free basal medium and transferred to Accuri C6 plus flow cytometer (BD Biosciences; Franklin Lakes, NJ, USA) for data acquisition. 20,000 events were recorded for each cell line. After data acquisition, the data were exported as FCS files and analyzed using FlowJo_v10.6.2 software. To gate for the TMRE-positive population, cells that were not stained with TMRE were used to gate for the TMRE negative cell populations. Mean fluorescent intensity (MFI) values, a measure of the geometric mean of TMRE positive cells was obtained for statistical analysis.

5.5.6. Intracellular ROS measurement

Cells were maintained in culture following established protocols until the desired passage (Passage 8) is reached. A day before assay, 20,000 cells per well were plated and cultured in complete media (MEM supplemented with 10% FBS and 2mM L-glutamine). In addition, the treatment groups had either 100μM NV118 or an equivalent volume of basal MEM in each well. After 24-hours, intracellular ROS levels were measured using the 2',7' –dichlorofluorescein diacetate (DCFDA/H_2DCFDA) a cell-permeable cellular ROS assay kit (Abcam). This dye measures hydroxyl (−OH), peroxyl (O_2^{2-}), and other reactive oxygen species (ROS). Within the cells, DCFDA is hydrolyzed by nonspecific esterases to release DCF, which is readily oxidized by intracellular ROS. The oxidized product emits green fluorescence at (Ex/Em: 485/535). Following the manufacturer's instructions, the cells were incubated with 10μM DCFDA. The cells were incubated in the dark for 45-minutes with this dye. As a positive control, 200μM TBHP was added for 60 mins before DCFDA treatment. At the end of the incubation period with DCFDA, the cells were washed once with phenol-red free MEM to get rid of excess dye. Finally, phenol-red-free MEM was added to each well, and cells were transferred to a plate reader (BioTek) for data acquisition. The fluorescent intensity was background corrected and adjusted by subtracting fluorescent intensity from blank wells.

5.5.7. Statistical analysis

All data were analyzed with GraphPad Prism 9 software (GraphPad Software, Inc.). Data presentation, number of separate measurements, and representative statistical analysis of each graph are described in the respective figure legends.

5.6. References

Avram, V.F., Bina, A.M., Sima, A., Aburel, O.M., Sturza, A., Burlacu, O., Timar, R.Z., Muntean, D.M., Elmer, E., and Cretu, O.M. (2021a). Improvement of Platelet Respiration by Cell-Permeable Succinate in Diabetic Patients Treated with Statins. *Life (Basel)* 11.

Avram, V.F., Chamkha, I., Asander-Frostner, E., Ehinger, J.K., Timar, R.Z., Hansson, M.J., Muntean, D.M., and Elmer, E. (2021b). Cell-Permeable Succinate Rescues Mitochondrial Respiration in Cellular Models of Statin Toxicity. *Int J Mol Sci* 22.

Baertling, F., Rodenburg, R.J., Schaper, J., Smeitink, J.A., Koopman, W.J., Mayatepek, E., Morava, E., and Distelmaier, F. (2014). A guide to diagnosis and treatment of Leigh syndrome. *J Neurol Neurosurg Psychiatry* 85**,** 257-265.

Bakare, A.B., Daniel, J., Stabach, J., Rojas, A., Bell, A., Henry, B., and Iyer, S. (2021). Quantifying Mitochondrial Dynamics in Patient Fibroblasts with Multiple Developmental Defects and Mitochondrial Disorders. *International Journal of Molecular Sciences* 22.

Chance, B., and Hollunger, G. (1961). The interaction of energy and electron transfer reactions in mitochondria. I. General properties and nature of the products of succinate-linked reduction of pyridine nucleotide. *J Biol Chem* 236**,** 1534-1543.

Chouchani, E.T., Kazak, L., Jedrychowski, M.P., Lu, G.Z., Erickson, B.K., Szpyt, J., Pierce, K.A., Laznik-Bogoslavski, D., Vetrivelan, R., Clish, C.B., Robinson, A.J., Gygi, S.P., and Spiegelman, B.M. (2016). Mitochondrial ROS regulate thermogenic energy expenditure and sulfenylation of UCP1. *Nature*.

Cottet-Rousselle, C., Ronot, X., Leverve, X., and Mayol, J.F. (2011). Cytometric assessment of mitochondria using fluorescent probes. *Cytometry A* 79**,** 405-425.

Divakaruni, A.S., Paradyse, A., Ferrick, D.A., Murphy, A.N., and Jastroch, M. (2014). Analysis and interpretation of microplate-based oxygen consumption and pH data. *Methods Enzymol* 547**,** 309-354.

Ehinger, J.K., Piel, S., Ford, R., Karlsson, M., Sjovall, F., Frostner, E.A., Morota, S., Taylor, R.W., Turnbull, D.M., Cornell, C., Moss, S.J., Metzsch, C., Hansson, M.J., Fliri, H., and Elmer, E. (2016). Cell-permeable succinate prodrugs bypass mitochondrial complex I deficiency. *Nat Commun* 7**,** 12317.

Fink, B.D., Bai, F., Yu, L., Sheldon, R.D., Sharma, A., Taylor, E.B., and Sivitz, W.I. (2018). Oxaloacetic acid mediates ADP-dependent inhibition of mitochondrial complex II-driven respiration. *J Biol Chem* 293**,** 19932-19941.

Gerards, M., Sallevelt, S.C., and Smeets, H.J. (2016). Leigh syndrome: Resolving the clinical and genetic heterogeneity paves the way for treatment options. *Mol Genet Metab* 117**,** 300-312.

Giorgi-Coll, S., Amaral, A.I., Hutchinson, P.J.A., Kotter, M.R., and Carpenter, K.L.H. (2017). Succinate supplementation improves metabolic performance of mixed glial cell cultures with mitochondrial dysfunction. *Sci Rep* 7**,** 1003.

Gonzalez-Meler, M.A., Ribas-Carbo, M., Siedow, J.N., and Drake, B.G. (1996). Direct Inhibition of Plant Mitochondrial Respiration by Elevated CO2. *Plant Physiol* 112**,** 1349-1355.

Gullans, S.R., Kone, B.C., Avison, M.J., and Giebisch, G. (1988). Succinate alters respiration, membrane potential, and intracellular K+ in proximal tubule. *Am J Physiol* 255**,** F1170-1177.

Hill, B.G., Benavides, G.A., Lancaster, J.R., Jr., Ballinger, S., Dell'italia, L., Jianhua, Z., and Darley-Usmar, V.M. (2012). Integration of cellular bioenergetics with mitochondrial quality control and autophagy. *Biol Chem* 393**,** 1485-1512.

Iyer, S., Bergquist, K., Young, K., Gnaiger, E., Rao, R.R., and Bennett, J.P. (2012). Mitochondrial gene therapy improves respiration, biogenesis, and transcription in G11778A Leber's hereditary optic neuropathy and T8993G Leigh's syndrome cells. *Human Gene Therapy* 23**,** 647-657.

Iyer, S., Thomas, R.R., Portell, F.R., Dunham, L.D., Quigley, C.K., and Bennett, J.P., Jr. (2009). Recombinant mitochondrial transcription factor A with N-terminal mitochondrial transduction domain increases respiration and mitochondrial gene expression. *Mitochondrion* 9**,** 196-203.

Janowska, J.I., Piel, S., Saliba, N., Kim, C.D., Jang, D.H., Karlsson, M., Kilbaugh, T.J., and Ehinger, J.K. (2020). Mitochondrial respiratory chain complex I dysfunction induced by N-methyl carbamate ex vivo can be alleviated with a cell-permeable succinate prodrug. *Toxicol In Vitro* 65**,** 104794.

Johnson, J.D., Mehus, J.G., Tews, K., Milavetz, B.I., and Lambeth, D.O. (1998). Genetic evidence for the expression of ATP- and GTP-specific succinyl-CoA synthetases in multicellular eucaryotes. *J Biol Chem* 273**,** 27580-27586.

Kearney, E.B., Ackrell, B.A., and Mayr, M. (1972). Tightly bound oxalacetate and the activation of succinate dehydrogenase. *Biochem Biophys Res Commun* 49**,** 1115-1121.

Keeney, P.M., Quigley, C.K., Dunham, L.D., Papageorge, C.M., Iyer, S., Thomas, R.R., Schwarz, K.M., Trimmer, P.A., Khan, S.M., Portell, F.R., Bergquist, K.E., and Bennett, J.P., Jr. (2009). Mitochondrial gene therapy augments mitochondrial physiology in a Parkinson's disease cell model. *Hum Gene Ther* 20**,** 897-907.

Khan, N.A., Govindaraj, P., Meena, A.K., and Thangaraj, K. (2015). Mitochondrial disorders: challenges in diagnosis & treatment. *Indian J Med Res* 141**,** 13-26.

Kotlyar, A.B., and Vinogradov, A.D. (1984). Interaction of the membrane-bound succinate dehydrogenase with substrate and competitive inhibitors. *Biochim Biophys Acta* 784**,** 24-34.

Lee, C.F., Caudal, A., Abell, L., Nagana Gowda, G.A., and Tian, R. (2019). Targeting NAD(+) Metabolism as Interventions for Mitochondrial Disease. *Sci Rep* 9**,** 3073.

Lightowlers, R.N., Taylor, R.W., and Turnbull, D.M. (2015). Mutations causing mitochondrial disease: What is new and what challenges remain? *Science* 349**,** 1494-1499.

Maglioni, S., Schiavi, A., Melcher, M., Brinkmann, V., Luo, Z., Raimundo, N., Laromaine, A., Meyer, J.N., Distelmaier, F., and Ventura, N. (2020). Lutein restores synaptic functionality in a C. elegans model for mitochondrial complex I deficiency. *bioRxiv***,** 2020.2002.2020.957225.

Mcfarland, R., Taylor, R.W., and Turnbull, D.M. (2010). A neurological perspective on mitochondrial disease. *The Lancet. Neurology* 9**,** 829-840.

Mills, E.L., Kelly, B., Logan, A., Costa, A.S.H., Varma, M., Bryant, C.E., Tourlomousis, P., Dabritz, J.H.M., Gottlieb, E., Latorre, I., Corr, S.C., Mcmanus, G., Ryan, D., Jacobs, H.T., Szibor, M., Xavier, R.J., Braun, T., Frezza, C., Murphy, M.P., and O'neill, L.A. (2016). Succinate Dehydrogenase Supports Metabolic Repurposing of Mitochondria to Drive Inflammatory Macrophages. *Cell* 167**,** 457-470 e413.

Owiredu, S., Ranganathan, A., Eckmann, D.M., Shofer, F.S., Hardy, K., Lambert, D.S., Kelly, M., and Jang, D.H. (2020a). Ex vivo use of cell-permeable succinate prodrug attenuates mitochondrial dysfunction in blood cells obtained from carbon monoxide-poisoned individuals. *Am J Physiol Cell Physiol* 319**,** C129-C135.

Owiredu, S., Ranganathan, A., Greenwood, J.C., Piel, S., Janowska, J.I., Eckmann, D.M., Kelly, M., Ehinger, J.K., Kilbaugh, T.J., and Jang, D.H. (2020b). In vitro comparison of hydroxocobalamin (B12a) and the mitochondrial directed therapy by a succinate prodrug in a cellular model of cyanide poisoning. *Toxicol Rep* 7**,** 1263-1271.

Pfeffer, G., Majamaa, K., Turnbull, D.M., Thorburn, D., and Chinnery, P.F. (2012). Treatment for mitochondrial disorders. *Cochrane Database Syst Rev***,** CD004426.

Piel, S., Chamkha, I., Dehlin, A.K., Ehinger, J.K., Sjovall, F., Elmer, E., and Hansson, M.J. (2020). Cell-permeable succinate prodrugs rescue mitochondrial respiration in cellular models of acute acetaminophen overdose. *PLoS One* 15**,** e0231173.

Piel, S., Ehinger, J.K., Chamkha, I., Frostner, E.A., Sjovall, F., Elmer, E., and Hansson, M.J. (2018). Bioenergetic bypass using cell-permeable succinate, but not methylene blue, attenuates metformin-induced lactate production. *Intensive Care Med Exp* 6**,** 22.

Priegnitz, A., Brzhevskaya, O.N., and Wojtczak, L. (1973). Tight binding of oxaloacetate to succinate dehydrogenase. *Biochem Biophys Res Commun* 51**,** 1034-1041.

Protti, A. (2018). Succinate and the shortcut to the cure of metformin-induced lactic acidosis. *Intensive Care Med Exp* 6**,** 35.

Quinlan, C.L., Orr, A.L., Perevoshchikova, I.V., Treberg, J.R., Ackrell, B.A., and Brand, M.D. (2012). Mitochondrial complex II can generate reactive oxygen species at high rates in both the forward and reverse reactions. *J Biol Chem* 287**,** 27255-27264.

Reynaud-Dulaurier, R., Benegiamo, G., Marrocco, E., Al-Tannir, R., Surace, E.M., Auwerx, J., and Decressac, M. (2020). Gene replacement therapy provides benefit in an adult mouse model of Leigh syndrome. *Brain* 143**,** 1686-1696.

Scialo, F., Fernandez-Ayala, D.J., and Sanz, A. (2017). Role of Mitochondrial Reverse Electron Transport in ROS Signaling: Potential Roles in Health and Disease. *Front Physiol* 8**,** 428.

Scialò, F., Sriram, A., Fernández-Ayala, D., Gubina, N., Lõhmus, M., Nelson, G., Logan, A., Cooper, H.M., Navas, P., Enríquez, J.A., Murphy, M.P., and Sanz, A. (2016). Mitochondrial ROS Produced via Reverse Electron Transport Extend Animal Lifespan. *Cell metabolism* 23**,** 725-734.

Stepanova, A., Shurubor, Y., Valsecchi, F., Manfredi, G., and Galkin, A. (2016). Differential susceptibility of mitochondrial complex II to inhibition by oxaloacetate in brain and heart. *Biochim Biophys Acta* 1857**,** 1561-1568.

Tretter, L., Patocs, A., and Chinopoulos, C. (2016). Succinate, an intermediate in metabolism, signal transduction, ROS, hypoxia, and tumorigenesis. *Biochim Biophys Acta* 1857**,** 1086-1101.

Vyssokikh, M.Y., Holtze, S., Averina, O.A., Lyamzaev, K.G., Panteleeva, A.A., Marey, M.V., Zinovkin, R.A., Severin, F.F., Skulachev, M.V., Fasel, N., Hildebrandt, T.B., and Skulachev, V.P. (2020). Mild depolarization of the inner mitochondrial membrane is a crucial component of an anti-aging program. *Proc Natl Acad Sci U S A* 117**,** 6491-6501.

Wei, Y., Cui, L., and Peng, B. (2018). Mitochondrial DNA mutations in late-onset Leigh syndrome. *J Neurol* 265**,** 2388-2395.

Zeylemaker, W.P., Klaasse, A.D., and Slater, E.C. (1969). Studies on succinate dehydrogenase. V. Inhibition by oxaloacetate. *Biochim Biophys Acta* 191**,** 229-238.

Chapter 5

6. Conclusion and general discussion

6.1. Overview of the key findings

The principal aim of this dissertation was to perform a thorough characterization of patient fibroblast cells modeling for LS, harboring some of the most prevalent pathogenic mtDNA variants (*T8993G*, *T9185C*, *T10158C*, *T12706C*) in *MTAP6*, *MTND3* and *MTND5* genes affecting the function of complex V and complex I.

Given the heterogeneity associated with genotypes and phenotypes, including the cross-talk pathways between nuclear and mitochondrial genomes associated with LS; in chapter 1 we conducted a much-needed comprehensive literature review to understand Leigh syndrome. This allowed us to address the unmet need in this dissertation and we **hypothesized** that patient cells modeling for LS, harboring a high percentage of pathogenic mtDNA mutations would generate abnormal mitochondrial morphologies, disrupt electron transfer, reduce proton translocation, and have defects in membrane potential and bioenergetics.

The influence of pathogenic mtDNA on mitochondrial structure and function in LS is unknown. Therefore, in chapter 2, we conducted a comprehensive MiNA analysis and identified five mitochondrial morphologies (i) individuals, (ii) networks, (iii) branches, (iv) length of branches, and (v) size of networks in single cells containing some of the most prevalent pathogenic mtDNA known to cause LS. Results indicated LS cells harboring pathogenic mtDNA (*T8993G*) predominantly contained individual mitochondrial with short branch lengths representative of fragmentation as the most predominant phenotype. This phenotype was also observed in other patient cells modeling for other mitochondrial disorders such as Mitochondrial Encephalopathy Lactic acidosis and Stroke-like episodes (MELAS), Kearns-Sayre Syndrome

(KSS), and Pearson Syndrome (PS) (Liu and Hajnoczky, 2011;Wu et al., 2011;Srinivasan et al., 2017;Tokuyama et al., 2020;Bakare et al., 2021). Another important result indicated that LS cells harboring pathogenic mutation (*T12706C*), exhibited fewer mitochondria and the mitochondrial networks had very long branches which appeared fused. We termed such an abnormal mitochondrial morphology as “hyperfused” mitochondria. The third important finding was that the inner mitochondrial membrane potential (MMP) was significantly decreased in all the patient lines harboring pathogenic mtDNA, modeling for LS when compared to the control cell line (Mortiboys et al., 2008;Iannetti et al., 2015;Esteras et al., 2020). It was concluded that low membrane potential was indicative of a low ATP/ADP ratio associated with complex V (ATP synthase) defect or complex I defect. In the course of our study we found out that the individual mitochondria were not resolved very well by the software used to generate the mitochondrial morphological readouts, therefore in this study, we were unable to distinguish between round, punctate, and rod mitochondrial morphologies. Nevertheless, this is the first study linking pathogenic mtDNA with associated abnormal mitochondrial morphologies and function in five patient lines modeling for several mitochondrial disorders (Bakare et al 2021).

In the summer of 2020, we initiated a collaborative study with Dr. Zhan’s laboratory to rewrite some of the codes in the MiNA software for parsing the individual mitochondrial morphologies and were able to design and develop a more high-throughput mitochondrial analysis tool termed Mitochondrial Cellular Phenotype (MitoCellPhe), which could now be used to distinguish subtle mitochondrial morphologies more accurately in physiological and pathological/pharmacological conditions in various cell types (Bakare et. al *manuscript under review*). One of the unexpected limitations of our experimental design was the use of a single control cell line for this study. During the time course of the study, the control BJ-FB cell line exhibited a lot of variability in several experiments trials leading to a compromise in scientific

rigor and reproducibility from our expectations. To overcome this problem, we have selected a few age-matched controls which will be used in future experiments.

In chapter 2 we have shown that cells modeling for LS harboring pathogenic mtDNA exhibited a low ATP/ADP ratio indicative of bioenergetics defects. Metabolic biomarkers that can sensitively assess the genotype-phenotype relationship in LS are lacking. Identification of a bioenergetics biomarker could aid in the early diagnosis of the disease. Therefore chapter 3 focused our efforts on genetics and biochemical analysis in these cell lines. Several clinical reports have shown that LS patients exhibit elevated lactate in blood and cerebrospinal fluid (CSF) (Sofou et al., 2014;Yu et al., 2018;Chang et al., 2020;Edwards et al., 2020). Yet other studies have shown conflicting results with normal lactate levels in both plasma and CSF, to elevated lactate in either/both plasma and CSF (Sofou et al., 2014;Sofou et al., 2018;Uittenbogaard et al., 2018;Edwards et al., 2020). It is now well established that early intervention is important to longevity in patients with LS (Hong et al., 2020;Ogawa et al., 2020). Therefore, the key findings in chapter 3 were estimating a novel glycolytic bioenergetics health index (gBHI) based on individual glycolytic parameters impacting glycolytic ATP production. gBHI turned out to be a more significant and sensitive indicator of cells that have mitochondrial dysfunction. Although earlier reports have proposed mitoBHI (mBHI) as an indicator of mitochondrial dysfunction (Chacko et al., 2014), results from the current study indicated that mBHI was highly variable given the persist mitochondrial dysfunction in these cell lines and gBHI was a more reliable indicator of bioenergetics defect. The second important finding in chapter 3 was that gBHI aided in computing a comprehensive mitochondrial/glycolytic bioenergetics health index ratio (mBHI/gBHI) termed (CBHI) in LS cells because the bioenergetics assays showed that LS cell lines relied on both mitochondrial bioenergetics (especially SRC) and glycolysis (basal glycolysis) for meeting energy requirements.

Furthermore, our results strongly suggest that bridging the CBHI bioenergetics parameter in the context of the specific pathogenic mtDNA variant is more informative than solely relying on the percentage heteroplasmy levels. This is consistent with clinical data that have shown high heteroplasmy levels in some patients without clinical presentations that are hallmarks of LS (Ganetzky et al., 2019). A few limitations in this study were the inherent difficulty growing very vulnerable LS cell lines without antibiotics harboring high levels of pathogenic mtDNA and the high variability associated with fibroblast cell culture. This led to an inability of obtaining heteroplasmy data in single cells which could be correlated with the abnormal mitochondrial morphologies observed in single cells in chapter 2. Reports have shown that during mitotic segregation, there is a shift in the mtDNA genotype of daughter cells (Wallace, 1999). We tried to minimize the variability to the best of our ability by performing all experiments at the same passage number (passage 8) so that robust statistics could be obtained for estimating the bioenergetics assays and for computing the gBHI and CBHI values in chapter 3.

In chapter 4 we further tested our hypothesis by exogenously introducing an important TCA cycle substrate, succinate, also important in regulating SRC, by activating complex II-mediated respiration when the main complex I pathway was defective. The cell-permeable succinate marketed under the new name, NV118, served as an alternate substrate and therapeutic agent in four early-onset LS cell lines harboring pathogenic mtDNA (SBG1-FB (*T8993G*), SBG2-FB (*T8993G*), SBG4-FB (*T10158C*), and SBG5-FB (*T12706C*)). To our knowledge, this is the first study where NV118 has been provided in cells modeling LS and harboring pathogenic mtDNA. The key findings from this study showed that NV118, a prodrug of succinate could serve as a therapeutic agent for LS resulting from defects in CI and CV. After 24-hour treatment, the most lasting effect of the drug was seen in the glycolytic pathway, TCA cycle, MMP and intercellular ROS levels. Studies reported in the literature have shown that succinate regulates a host of functions in the mitochondria. In addition to performing as an alternate substrate for cellular

energetics, it can also function as a signaling molecule to regulate ROS, and hypoxia (Mills et al., 2016;Tretter et al., 2016). In immune cells, increased succinate corresponds to upregulation in glycolysis and MMP (Kuschel et al., 2012;Mills et al., 2016). Succinate in turn signals for the upregulation of the Hypoxia-inducible factor 1-alpha (HIF-1α), resulting in a pro-inflammatory response (Kuschel et al., 2012;Mills et al., 2016). In our study, the addition of NV118 increased glycolysis and MMP in LS disease lines. We postulate this response was a result of high demand for TCA cycle intermediate Acetyl CoA, to ensure a continuous supply of substrate required for CII-linked respiration. It is worth noting that this experiment was performed without inhibiting the activity of CI. Another key finding from this study was that elevated glycolysis did not lead to an increase in intracellular ROS levels supporting earlier studies in the literature where succinate has been alluded to regulating ROS homeostasis in cells. The results from this study suggest an important role for TCA intermediates in the treatment of mitochondrial dysfunction in LS.

6.2. Future Directions

The work presented here has opened up several lines of investigation. Future experiments could be focused on understanding the metabolic pathways regulating levels of SRC in these lines as well as identifying novel methods of quantifying mtDNA mutant load at the mitochondrion level. This would open up several avenues for modeling and treating mitochondrial dysfunction.

Given the important role of the TCA cycle intermediates in alleviating some of the bioenergetics defects, metabolomics and optical redox ratio studies to access metabolic changes in LS (*Kolenc & Bakare, manuscript in preparation*) would be a worthwhile experiment for identifying the cross-talk pathways impacted between nuclear and mitochondrial genome due to pathogenic mtDNA. One could also conduct experiments to understand whether the

mitochondrial and redox defects could be reversed by NV118 treatment. It will be worthwhile to conduct further metabolomics studies comparing the results from LS cells with a CI dysfunction and those with a CV dysfunction after NV118 treatment to ascertain the mechanisms of action in these cell lines.

To understand the mechanisms behind the mitochondrial morphologies observed in LS cell lines, it would be interesting to block one or more genes regulating the fission and fusion pathways and estimate the changes in mitochondrial dynamics and function. This knowledge would be critical for understanding the relationship between inter-organelle communication that exists between the mitochondria and other cellular components.

6.3. Conclusion

In this dissertation, we were able to address the aims we set out at the beginning of this study. The comprehensive approach used in this study has provided valuable information that could enhance the diagnostic and therapeutic approach for LS. Through this study, it is evident that the best approach to therapy for LS might involve the regulation of TCA cycle intermediates to provide substrates for other alternative pathways that can be utilized for maintaining cellular functions in patients with LS. While fibroblast cell lines provide valuable information on LS, they are not the most appropriate model for LS. As described previously, LS is an early-onset neurological disorder. Therefore, it would be more appropriate to characterize mitochondrial structure and function in cell lines with neuronal lineage. Currently, experiments are underway in Dr. Iyer's lab to generate cardiac and neuronal cells from human induced pluripotent stem cell lines (hiPSC) derived from the fibroblast cell lines with LS. Given the neuromuscular involvement of LS, differentiation into neurons and cardiac muscle cells will provide valuable information on how the mtDNA mutations contribute to the pathologies and clinical symptoms observed in patients with LS. Furthermore, the hiPSCs and differentiated cell lines can be used

for high-throughput drug screening, to identify the effects of these drugs on various tissues affected in LS patients. In the long term, these types of studies can help physicians better diagnose and provide targeted therapies for patients with LS.

6.4. References

Bakare, A.B., Daniel, J., Stabach, J., Rojas, A., Bell, A., Henry, B., and Iyer, S. (2021). Quantifying Mitochondrial Dynamics in Patient Fibroblasts with Multiple Developmental Defects and Mitochondrial Disorders. *International Journal of Molecular Sciences* 22.

Chacko, B.K., Kramer, P.A., Ravi, S., Benavides, G.A., Mitchell, T., Dranka, B.P., Ferrick, D., Singal, A.K., Ballinger, S.W., Bailey, S.M., Hardy, R.W., Zhang, J., Zhi, D., and Darley-Usmar, V.M. (2014). The Bioenergetic Health Index: a new concept in mitochondrial translational research. *Clinical Science (London)* 127**,** 367-373.

Chang, X., Wu, Y., Zhou, J., Meng, H., Zhang, W., and Guo, J. (2020). A meta-analysis and systematic review of Leigh syndrome: clinical manifestations, respiratory chain enzyme complex deficiency, and gene mutations. *Medicine (Baltimore)* 99**,** e18634.

Edwards, L.S., Halmagyi, G.M., Mallawaarachchi, A., Thompson, E.O., and Kiernan, M.C. (2020). Fatal cerebellar oedema in adult Leigh syndrome. *Pract Neurol* 20**,** 336-337.

Esteras, N., Adjobo-Hermans, M.J.W., Abramov, A.Y., and Koopman, W.J.H. (2020). Visualization of mitochondrial membrane potential in mammalian cells. *Methods Cell Biol* 155**,** 221-245.

Ganetzky, R.D., Stendel, C., Mccormick, E.M., Zolkipli-Cunningham, Z., Goldstein, A.C., Klopstock, T., and Falk, M.J. (2019). MT-ATP6 mitochondrial disease variants: Phenotypic and biochemical features analysis in 218 published cases and cohort of 14 new cases. *Human Mutation* 40**,** 499-515.

Hong, C.M., Na, J.H., Park, S., and Lee, Y.M. (2020). Clinical Characteristics of Early-Onset and Late-Onset Leigh Syndrome. *Front Neurol* 11**,** 267.

Iannetti, E.F., Willems, P.H., Pellegrini, M., Beyrath, J., Smeitink, J.A., Blanchet, L., and Koopman, W.J. (2015). Toward high-content screening of mitochondrial morphology and membrane potential in living cells. *Int J Biochem Cell Biol* 63**,** 66-70.

Kuschel, A., Simon, P., and Tug, S. (2012). Functional regulation of HIF-1alpha under normoxia--is there more than post-translational regulation? *J Cell Physiol* 227**,** 514-524.

Liu, X., and Hajnoczky, G. (2011). Altered fusion dynamics underlie unique morphological changes in mitochondria during hypoxia-reoxygenation stress. *Cell Death Differ* 18**,** 1561-1572.

Mills, E.L., Kelly, B., Logan, A., Costa, A.S.H., Varma, M., Bryant, C.E., Tourlomousis, P., Dabritz, J.H.M., Gottlieb, E., Latorre, I., Corr, S.C., Mcmanus, G., Ryan, D., Jacobs, H.T., Szibor, M., Xavier, R.J., Braun, T., Frezza, C., Murphy, M.P., and O'neill, L.A. (2016). Succinate Dehydrogenase Supports Metabolic Repurposing of Mitochondria to Drive Inflammatory Macrophages. *Cell* 167**,** 457-470 e413.

Mortiboys, H., Thomas, K.J., Koopman, W.J., Klaffke, S., Abou-Sleiman, P., Olpin, S., Wood, N.W., Willems, P.H., Smeitink, J.A., Cookson, M.R., and Bandmann, O. (2008). Mitochondrial function and morphology are impaired in parkin-mutant fibroblasts. *Ann Neurol* 64**,** 555-565.

Ogawa, E., Fushimi, T., Ogawa-Tominaga, M., Shimura, M., Tajika, M., Ichimoto, K., Matsunaga, A., Tsuruoka, T., Ishige, M., Fuchigami, T., Yamazaki, T., Kishita, Y., Kohda, M., Imai-Okazaki, A., Okazaki, Y., Morioka, I., Ohtake, A., and Murayama, K. (2020). Mortality of Japanese patients with Leigh syndrome: Effects of age at onset and genetic diagnosis. *J Inherit Metab Dis* 43**,** 819-826.

Sofou, K., De Coo, I.F., Isohanni, P., Ostergaard, E., Naess, K., De Meirleir, L., Tzoulis, C., Uusimaa, J., De Angst, I.B., Lonnqvist, T., Pihko, H., Mankinen, K., Bindoff, L.A., Tulinius, M., and Darin, N. (2014). A multicenter study on Leigh syndrome: disease course and predictors of survival. *Orphanet J Rare Dis* 9**,** 52.

Sofou, K., De Coo, I.F.M., Ostergaard, E., Isohanni, P., Naess, K., De Meirleir, L., Tzoulis, C., Uusimaa, J., Lonnqvist, T., Bindoff, L.A., Tulinius, M., and Darin, N. (2018). Phenotype-genotype correlations in Leigh syndrome: new insights from a multicentre study of 96 patients. *J Med Genet* 55**,** 21-27.

Srinivasan, S., Guha, M., Kashina, A., and Avadhani, N.G. (2017). Mitochondrial dysfunction and mitochondrial dynamics-The cancer connection. *Biochim Biophys Acta Bioenerg* 1858**,** 602-614.

Tokuyama, T., Hirai, A., Shiiba, I., Ito, N., Matsuno, K., Takeda, K., Saito, K., Mii, K., Matsushita, N., Fukuda, T., Inatome, R., and Yanagi, S. (2020). Mitochondrial Dynamics Regulation in Skin Fibroblasts from Mitochondrial Disease Patients. *Biomolecules* 10.

Tretter, L., Patocs, A., and Chinopoulos, C. (2016). Succinate, an intermediate in metabolism, signal transduction, ROS, hypoxia, and tumorigenesis. *Biochim Biophys Acta* 1857**,** 1086-1101.

Uittenbogaard, M., Brantner, C.A., Fang, Z., Wong, L.C., Gropman, A., and Chiaramello, A. (2018). Novel insights into the functional metabolic impact of an apparent de novo m.8993T>G variant in the MT-ATP6 gene associated with maternally inherited form of Leigh Syndrome. *Mol Genet Metab* 124**,** 71-81.

Wallace, D.C. (1999). Mitochondrial Diseases in Man and Mouse. *Science* 283**,** 1482-1488.

Wu, S., Zhou, F., Zhang, Z., and Xing, D. (2011). Mitochondrial oxidative stress causes mitochondrial fragmentation via differential modulation of mitochondrial fission-fusion proteins. *FEBS J* 278**,** 941-954.

Yu, X.L., Yan, C.Z., Ji, K.Q., Lin, P.F., Xu, X.B., Dai, T.J., Li, W., and Zhao, Y.Y. (2018). Clinical, Neuroimaging, and Pathological Analyses of 13 Chinese Leigh Syndrome Patients with Mitochondrial DNA Mutations. *Chin Med J (Engl)* 131**,** 2705-2712.

7. Appendix A – Supplementary figures and tables

7.1. Population doubling (Chapter 2)

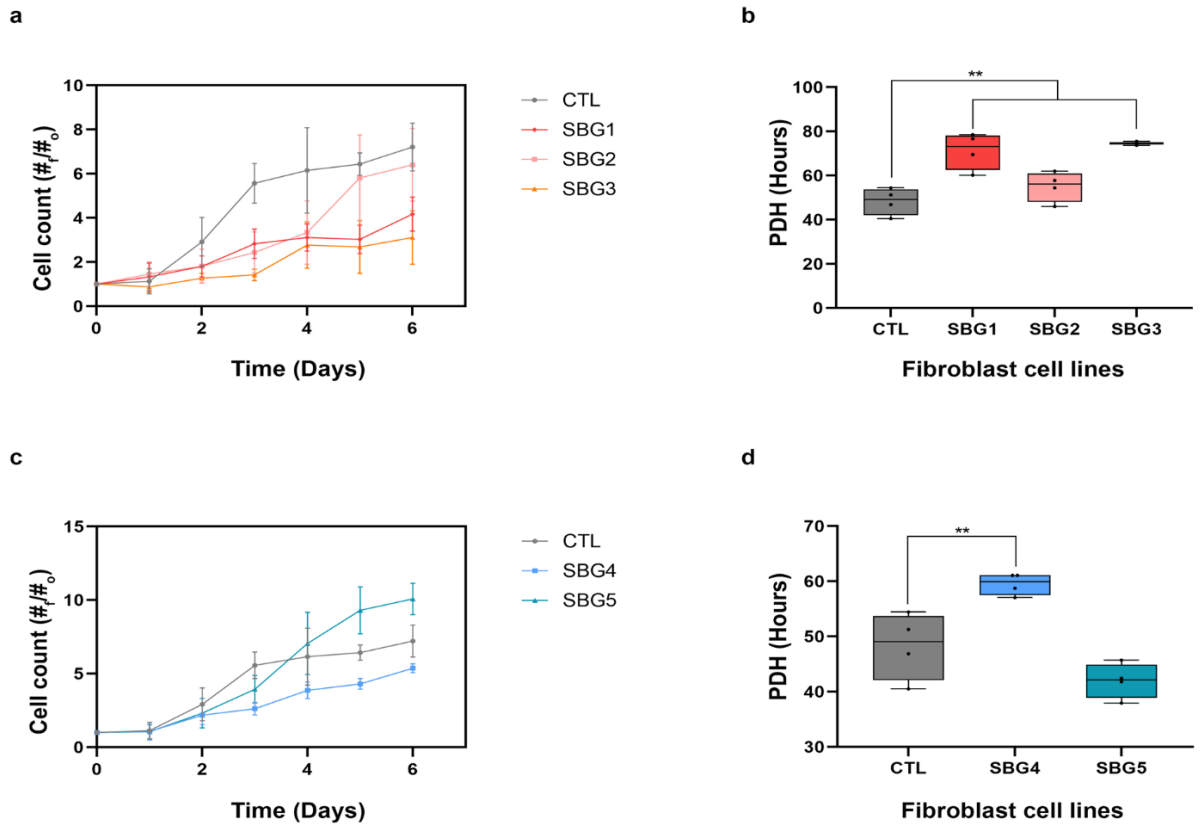

Supplementary Figure 7.1. Population doubling for fibroblast cell lines. Control BJ-FB, and diseased (SBG1-5) FB cells were counted everyday for 6-days. Cell counts and population doubling times are shown for cell lines with a-b) CV-defect c-d) CI-defect and the CTL BJ-FB. Data represents ±SD of at least three independent trials for all cell lines. Gray bar represents CTL BJ-FB, red bar represents SBG1-FB, pink bar represent SBG2-FB (*T8993G*), yellow bar represent SBG3-FB (*T9185C*), blue bar represent SBG4-FB (*T10158C*), and green bar represent SBG5-FB (*T12706C*). **p<0.01

7.2. Mitochondrial respiration with NV118 (Chapter 4)

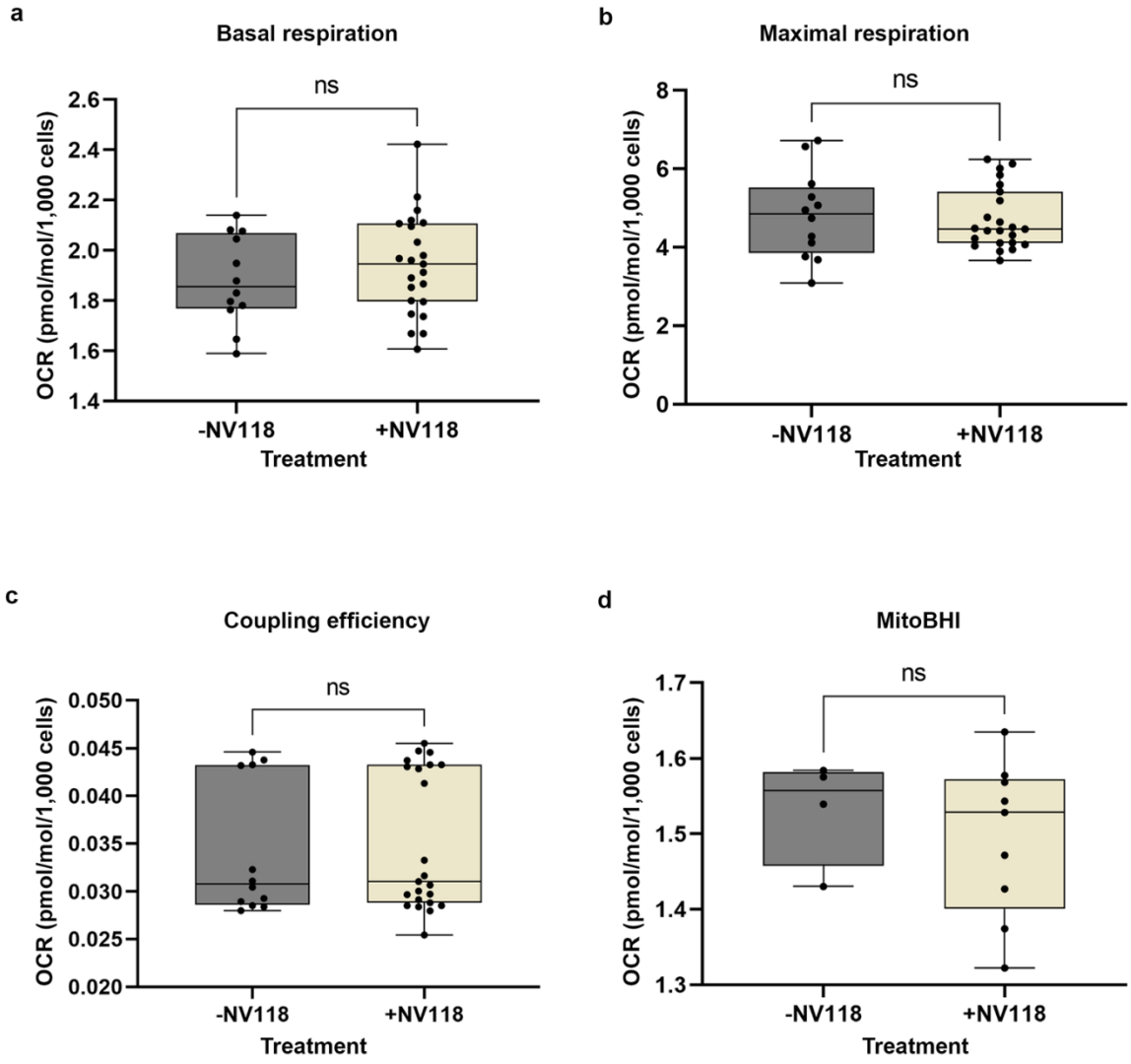

Supplementary Figure 7.2.1. Mitochondrial respiration profile of CTL BJ-FB with and without NV118. BJ-FB were treated with 100 µM NV118 or vehicle (phenol-red free MEM) for 24-hours, and Oxygen Consumption Rate (OCR) was measured at the end of the 24-hour treatment period. Cell line showing (a) Basal respiration, (b) maximal respiration, (c) coupling efficiency, (d) MitoBHI. All parameters are in pmol/min/1000 cells. Data are mean +/- SD. Experiments were repeated at least three times on different days under the same conditions. *p< 0.05, ns = not significant. Gray bar represents treatment with vehicle (-NV118), while tan bar represents treatment with 100 µM NV118 (+NV118).

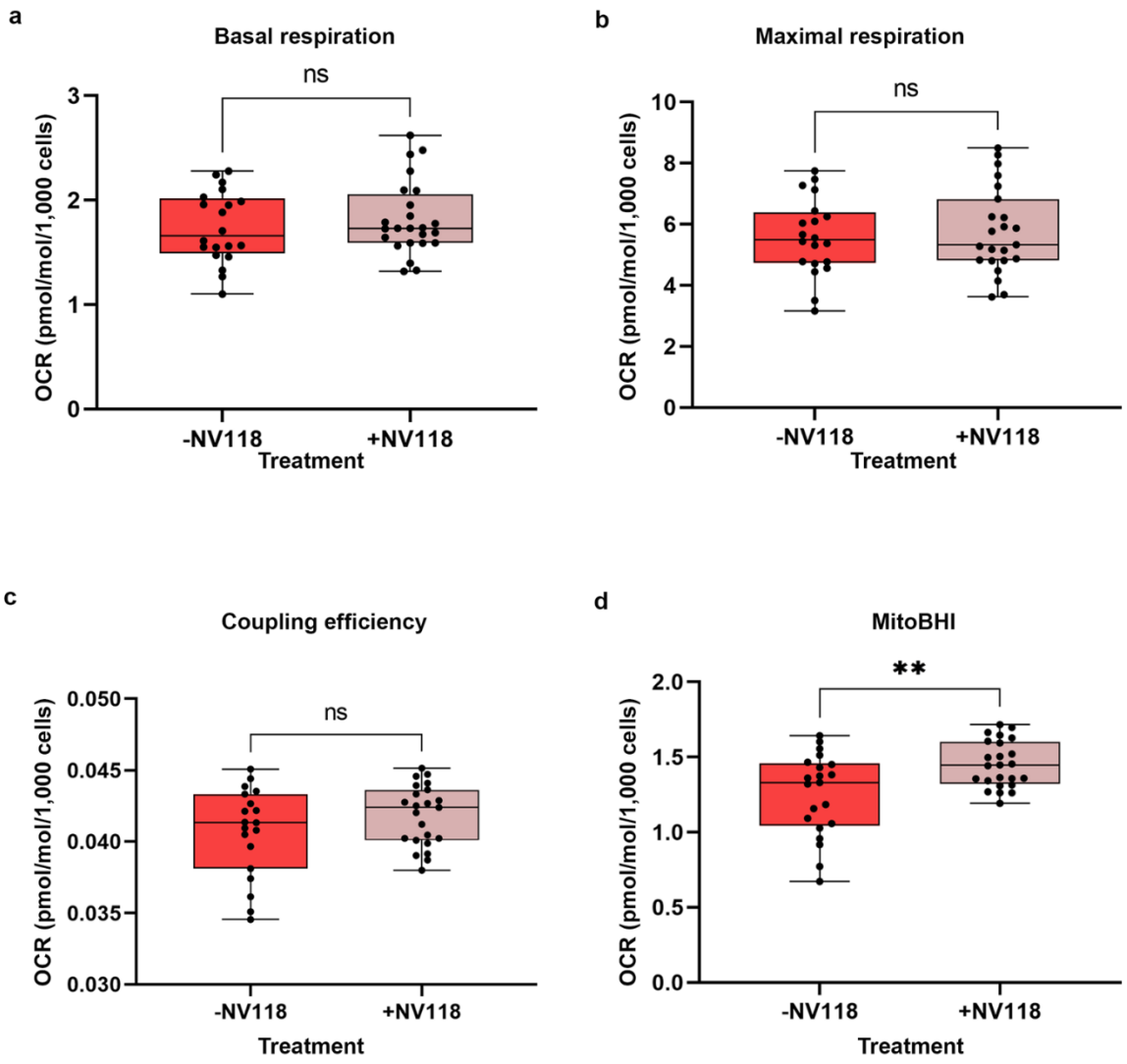

Supplementary Figure 7.2.2. Mitochondrial respiration profile of SBG1-FB (*T8993G*) with and without NV118. SBG1-FB (*T8993G*) were treated with 100 µM NV118 or vehicle (phenol-red free MEM) for 24-hours, and Oxygen Consumption Rate (OCR) was measured at the end of the 24-hour treatment period. Cell line showing (a) Basal respiration, (b) maximal respiration, (c) coupling efficiency, (d) MitoBHI. All parameters are in pmol/min/1000 cells. Data are mean +/- SD. Experiments were repeated at least three times on different days under the same conditions. *p< 0.05, ns = not significant. Red bar represents treatment with vehicle (-NV118), while pink bar represents treatment with 100 µM NV118 (+NV118).

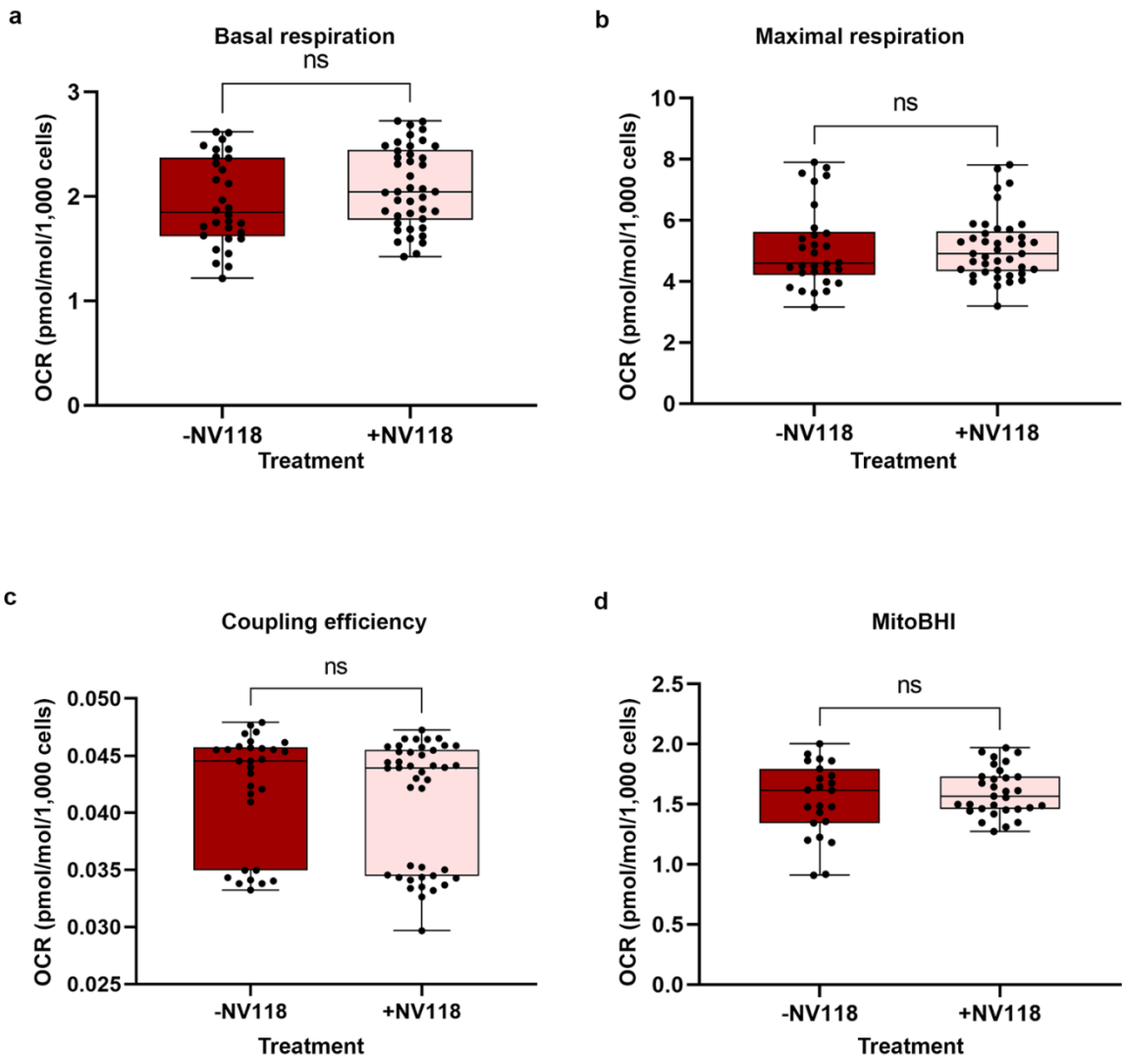

Supplementary Figure 7.2.3. Mitochondrial respiration profile of SBG2-FB (*T8993G*) with and without NV118. SBG2-FB (*T8993G*) were treated with 100 µM NV118 or vehicle (phenol-red free MEM) for 24-hours, and Oxygen Consumption Rate (OCR) was measured at the end of the 24-hour treatment period. Cell line showing (a) Basal respiration, (b) maximal respiration, (c) coupling efficiency, (d) MitoBHI. All parameters are in pmol/min/1000 cells. Data are mean +/- SD. Experiments were repeated at least three times on different days under the same conditions. *p< 0.05, ns = not significant. Red bar represents treatment with vehicle (-NV118), while pink bar represents treatment with 100 µM NV118 (+NV118).

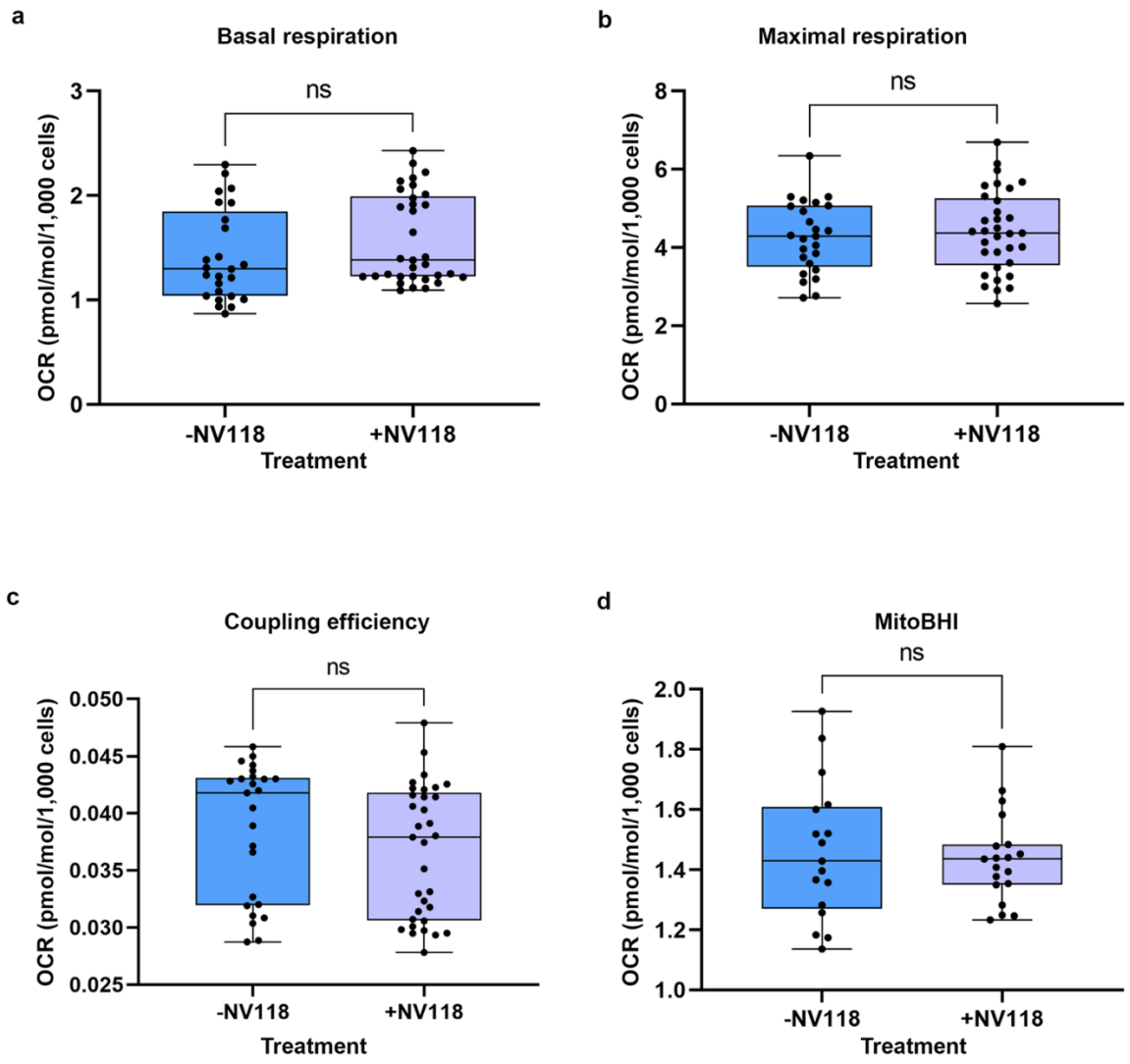

Supplementary Figure 7.2.4. Mitochondrial respiration profile of SBG4-FB (T10158C) with and without NV118. SBG4-FB (*T10158C*) were treated with 100 µM NV118 or vehicle (phenol-red free MEM) for 24-hours, and Oxygen Consumption Rate (OCR) was measured at the end of the 24-hour treatment period. Cell line showing (a) Basal respiration, (b) maximal respiration, (c) coupling efficiency, (d) MitoBHI. All parameters are in pmol/min/1000 cells. Data are mean +/- SD. Experiments were repeated at least three times on different days under the same conditions. *p< 0.05, ns = not significant. Blue bar represents treatment with vehicle (-NV118), while purple bar represents treatment with 100 µM NV118 (+NV118).

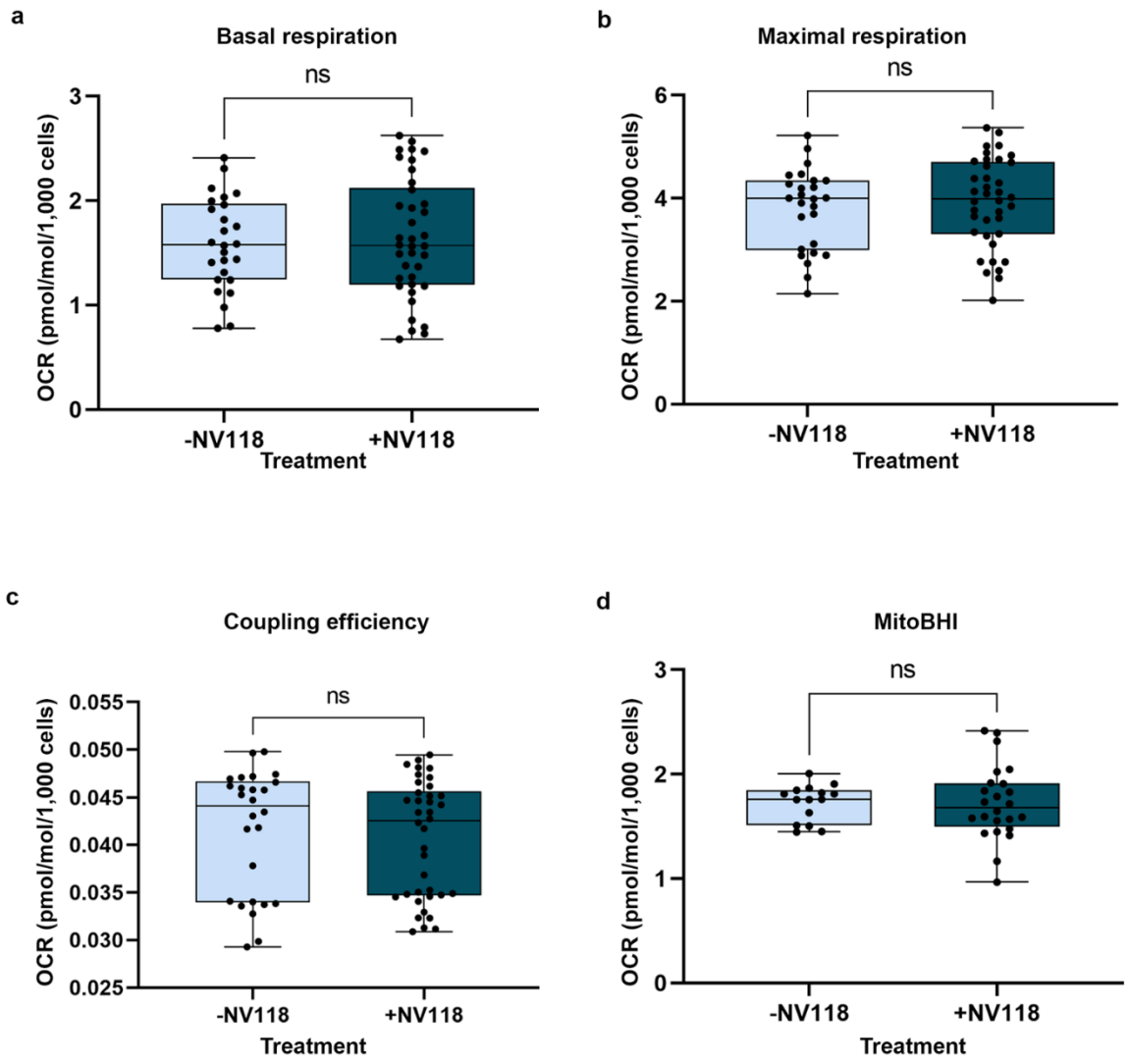

Supplementary Figure 7.2.5. Mitochondrial respiration profile of SBG5-FB (*T12706C*) with and without NV118. SBG5-FB (*T12706C*) were treated with 100 µM NV118 or vehicle (phenol-red free MEM) for 24-hours, and Oxygen Consumption Rate (OCR) was measured at the end of the 24-hour treatment period. Cell line showing (a) Basal respiration, (b) maximal respiration, (c) coupling efficiency, (d) MitoBHI. All parameters are in pmol/min/1000 cells. Data are mean +/- SD. Experiments were repeated at least three times on different days under the same conditions. *p< 0.05, ns = not significant. Blue bar represents treatment with vehicle (-NV118), while green bar represents treatment with 100 µM NV118 (+NV118).

7.3. Nuclear and mitochondrial DNA involvement in LS (Chapter 1)

Supplementary Table 7.3.1. Table showing nuclear genes involved in LS and LS-like disorders. The most prevalent mutations affecting the different ETC complexes are summarized with the genetic defect and corresponding biochemical and clinical manifestations.

Nuclear genes involved in LS and LS-like disorders

Complexes	Structural/ Assembly	Genes affected in LS	Genetic defect	Biochemical defect	Clinical manifestations	References
CI	Structural	NDUFA1	c.55C>T	Elevated blood/CSF lactate and pyruvate levels, isolated CI deficiency and decreased amount of fully assembled enzyme, depolarization of MMP, decreased carnitine, elevated alanine levels, hypoglycemia close to death, decreased CIII activity, elevated cytochrome c oxidase and citrate synthase activity, decreased pyruvate oxidation (normal succinate oxidation), increase CII-CIV activity, elevated CSF protein levels, Isolated PDHs activity in skeletal/cardiac muscle, brain, liver and skin fibroblast, elevated levels of fumarate and malate	Pyramidal tract dysfunction, ataxia, signs of brain stem dysfunction, oculomotor abnormalities, seizures, and lethargy, leukoencephalopathy, muscular hypotonia, myoclonic epilepsy, progressive macrocystic leukoencephalopathy with brain atrophy, and subsequent apnea, early-onset ophthalmoplegia, lethal encephalopathy	(Uehara et al., 2014)
			c.208+5G>A, c.875T>C, c.866+4A>G			(Hoefs et al., 2008;Tuppen et al., 2010;Schlehe et al., 2013)
	Structural	NDUFA2				(van den Bosch et al., 2012)
	Structural	NDUFA9	c.962G>C			(Hoefs et al., 2011)
	Structural	NDUFA10	c.1A>G, c.425A>G			(Ostergaard et al., 2011)
	Structural	NDUFA12	c.178C>T			(Bugiani et al., 2004;Tuppen et al., 2010)
	Structural	NDUFS1	c.1564C>A, c.1222C>T			(Bugiani et al., 2004)
	Structural	NDUFS2	c.671C>T, c.875T>C, c.866+4A>G			(Jaokar et al., 2013;Lou et al., 2018)
	Structural	NDUFS3	c.418C>T, c.595C>T			(Piekutowska-Abramczuk et al., 2018a)
	Structural	NDUFB8	c.227C>A, c.432C>G			(Budde et al., 2000)
	Structural	NDUFS4	c.289or290G, c.316C>T			(Bugiani et al., 2004;Lebon et al., 2007)
	Structural	NDUFS7	c.434G>A			(Loeffen et al., 1998)
	Structural	NDUFS8	c.C236T, c.G305A			

			c.1022C>T, c.1268C>T, c.640G>A, c.1294G>C, c.611A>G, c.616T>G			(Schuelke et al., 1999;Zafeiriou et al., 2008;Vilain et al., 2012;Incecik et al., 2018)
	Structural	NDUFV1				
	Structural	NDUFV2	c.IVS2 + 1delGTAA, c.669_670ins			(Cameron et al., 2015)
	Assembly	NDUFAF2	c.114C>G			(Hoefs et al., 2009)
	Assembly	NDUFAF4	c.194T>C			(Saada et al., 2008;Baertling et al., 2017)
	Assembly	NDUFAF5 (C20orf7)	c.477A>C			(Gerards et al., 2010)
	Assembly	NDUFAF6	c.532G>C, c.420+784C>T, c.554_558del, c.371 T>C			(Catania et al., 2018;Baide-Mairena et al., 2019)
	Assembly	NDUFAF8 (C17ORF89)	c.45_52dup, c.1A>G, c.165C>G			(Alston et al., 2020)
	Assembly	FOXRED1	c.1054C>T			(Fassone et al., 2010;Zurita Rendon et al., 2016)
	Assembly	NUBPL	c.166G>A, c.815-27T>C			(Calvo et al., 2010)
CII	Structural	SDHA	c.1684C>T, c1660C>T, c.1A>C, c.1571C>T, c.248C>T, c.356G>A, c.1664G>A	CII deficiency, elevated lactate, succinate, pyruvate, SDH deficiency	Developmental delay with axial hypotonia, generalised muscular hypotonia with axial predominance, bilateral horizontal nystagmus, seizures, tetraparetic, rapidly progressive psychomotor regression, lack of speech development, spastic quadriparesis and partial loss of postural control with dystonia	(Bourgeron et al., 1995;Horvath et al., 2006;Pagnamenta et al., 2006)
	Assembly	SDHAF1	c.169G>C, c.164G>C			(Ghezzi et al., 2009)

CIII	Structural	UQCRQ	c.208C>T	Mild to significantly elevated lactate levels, isolated CIII deficiency, increased citrate synthase, impaired respiration shown through decreased oxygen consumption	Severe psychomotor regression and extrapyramidal signs, dystonic postures, athetoid movements, ataxia, neurological regression, global dementia, progressive encephalopathy, early-onset developmental delay, spasticity, seizures, lactic acidosis, muscle hypotonia, failure to thrive, language regression, subacute rapid neurological failure	(Barel et al., 2008) (de Lonlay et al., 2001;Fernandez-Vizarra et al., 2007;Baker et al., 2019) (Ghezzi et al., 2011;Atwal, 2014)
			c.830G>A, c.296C>T, c.464, c.1,057G>A, c.217C>T, c.1102T>A, c.547C>T, c.550C>T			
	Assembly	BCS1L				
	Assembly	TTC19	c.577G>A, c.964_967del			
C IV	Structural	NDUFA4	c.42+1G>C	Deficient COX activity in galactose but not glucose media, lactic acidosis, Isolated COX deficiency, citric acid cycle metabolites, glycine, and alanine, CIV deficiencies, elevated plasma alanine and proline, OXPHOS dysfunction associated with ATPsynthase defect and assembly		(Pitceathly et al., 2013) (Hallmann et al., 2016)
	Structural	COX8A	c.115-1G>C c.743C>A, c.367_368del, c.772C>T, c.751C>T, c.833+1G>T, c.465_466del, c.532A>T, c.792_793del, c.845_846del, c.465_466del, c.826_827ins,		Bulbar dysfunction, dystonia, ataxia, spasticity, encephalopathy, pulmonary hypertension, recurrent vomiting, generalized epileptic tonic-clonic seizures, psychomotor retardation, microcephalus, enophthalmos, hypotonia, pigmentary retinopathy, developmental retardation and retrogression, hirsutism, growth retardation, nystagmus, hypoglycemia, metabolic acidosis, retinopathy, failure-to-thrive, hypertrophic cardiomyopathy, characteristic facial appearance, bilateral facial weakness, dysarthria and dysphagia	(Li et al., 2018)
	Assembly	SURF1	c.532A>T			(Antonicka et al., 2003) (Oquendo et al., 2004;Bugiani et al., 2005) (Joost et al., 2010) (Lim et al., 2014) (Mootha et al., 2003;Debray et al., 2011;Mourier et al., 2014) (Weraarpachai et al., 2009)
	Assembly	COX10	c.791C>A, c.878C>T			
	Assembly	COX15	c.C700T, c.503C>G, c.1081T>C			
	Assembly	SCO2	c.418G>A			
	Assembly	PET100	c.3G>C			
	Assembly	LRPPRC	c.1,119C>T			
	Assembly	TACO1	c.472C			
CV	Assembly	ATP5MD	c.87+1G>C	Elevated plasma alanine and lactate, reduction of CV dimerization, reduced ATP synthesis,	Gross motor developmental delay, gross motor regression, persistent hyperreflexia, bilateral plantar extensor signs, hypotonia, ocular movement abnormalities, ptosis, oro-motor incoordination, neurological regression, ataxia, hemiplegia, lethargic, bradycardia,	(Barca et al., 2018)

Supplementary Table 7.3.2. Table showing mitochondrial genes involved in LS and LS-like disorders. The most prevalent mutations affecting the different ETC complexes are summarized with the genetic defect and corresponding biochemical and clinical manifestations.

Mitochondrial genes involved in LS and LS-like disorders

Complexes	Genes affected in LS	Genetic defect	Biochemical defect	Clinical manifestations	References
CI	MT-ND1	m.3697G>A, m.3980G>A, m.3928G>C, m.3308T>C, m.3688G>A, m.3890G>A, m. 3460G>A, m.3946G>A	CI deficiency elevated Kreb cycle intermediate (especially fumarate and malate), elevated plasma and CSF lactate and pyruvic acid level, elevated alanine, Increased CI and CII activity, Elevated valine, isoleucine, and lysine levels, elevated 3-ketoglutaric acid levels	Ataxia, developmental delay, lactic acidosis, psychomotor developmental retardation, cardiomyopathy, dystonia, respiratory failure, progressive encephalomyopathy, strabismus convergens, scoliosis, hypotonia, myoclonic jerks, pyramidal syndrome, bradypnoea, bradycardia, ptosis, ophthalmoplegia, proteinuria, haematuria, tubulointerstitial nephropathy, hypertrophic cardiomyopathy, peripheral neuropathy, optic atrophy, diabetes mellitus, nystagmus, epilepsy, stroke-like episodes, cerebral paresis, facial weakness, impaired hearing, metabolic acidosis, drowsiness, vomiting, myoclonic jerks, hypothermia, stroke, oral-motor dyspraxia, spasticity, hemiparesis, dysarthria, drowsiness, vomiting, facial dyskinesia, generalized seizures, episodic central apneas	(Campos et al., 1997;Hinttala et al., 2006;Moslemi et al., 2008;Caporali et al., 2013;Wray et al., 2013;Negishi et al., 2014;Lee et al., 2016;Spangenberg et al., 2016;Ogawa et al., 2017)
	MT-ND2	m.4681T>C, m.4833A>G			(Hinttala et al., 2006;Ugalde et al., 2007;Ma et al., 2013;Lee et al., 2016)
	MT-ND3	m.10158T>C, m.10191T>C, m.10197G>A, m.10254G>A, 10134C>A			(Taylor et al., 2001;Lebon et al., 2003;Bugiani et al., 2004;Crimi et al., 2004;McFarland et al., 2004;Sarzi et al., 2007;Lim et al., 2009;Naess et al., 2009;Leshinsky-Silver et al., 2010;Miller et al., 2014;Han et al., 2015;Lee et al., 2016;Li et al., 2019)
	MT-ND4	m.11777C>A, m.11984T>C, m.11240C>T, m.11246G>A, m.11778G>A			(Komaki et al., 2003;Bugiani et al., 2004;Vanniarajan et al., 2006;Hadzsiev et al., 2010;Lee et al., 2016;Xu et al., 2017;Yu et al., 2018)
	MT-ND5	m.12706T>C, m.13513G>A, m.13084 A>T, m.13511A>T, m.13042G>A, m.13094T>C, m.12338T>C, m.13514A>G			(Corona et al., 2001;Taylor et al., 2002;Crimi et al., 2003;Kirby et al., 2003;Petruzzella et al., 2003;Blok et al.,

					2007;Ruiter et al., 2007;Shanske et al., 2008;Ching et al., 2013;Ma et al., 2013;Han et al., 2015;Lee et al., 2016)
	MT-ND6	m.14459G>A, m.14487T>C, m.14439G>A, m.14502T>C			(Kirby et al., 2000;Lebon et al., 2003;Bugiani et al., 2004;Gropman et al., 2004;Wang et al., 2009;Ronchi et al., 2011;Tarnopolsky et al., 2013;Uehara et al., 2014)
CIII	MT-CYB	m.14792C>G	Unlikely to have pathogenic significance	Unlikely to have pathogenic significance	(Andreu et al., 1999;Ronchi et al., 2011)
CIV	COXIII	m.9537Cinsertion, m.9952G>A	Normal CI & CII activity, elevated lactate, pyruvate, and alanine levels, decreased COX activity	Lactic acidosis, tetraparesis, ophthalmoparesis, convergent strabismus, reduced visual acuity, and moderate mental retardation	(Keightley et al., 1996;Hanna et al., 1998;Tiranti et al., 2000)
CV	MT-ATP6	m.8993T>C/G, m.9176T>C/G, m.9185T>C	Normal enzyme activity in some patients, Abnormal/normal ATP synthesis, Abnormal MMP, Increased ROS, Abnormal sensitivity to oligomycin, Impaired CV assembly	Ataxia, bulbar palsy, pyramidal tract involvement, stroke-like episodes, seizures	(Santorelli et al., 1993;Vilarinho et al., 2000;Carrozzo et al., 2001;Ogawa et al., 2017;Piekutowska-Abramczuk et al., 2018b;Wei et al., 2018;Ganetzky et al., 2019)

7.4. References

Alston, C.L., Veling, M.T., Heidler, J., Taylor, L.S., Alaimo, J.T., Sung, A.Y., He, L., Hopton, S., Broomfield, A., Pavaine, J., Diaz, J., Leon, E., Wolf, P., Mcfarland, R., Prokisch, H., Wortmann, S.B., Bonnen, P.E., Wittig, I., Pagliarini, D.J., and Taylor, R.W. (2020). Pathogenic Bi-allelic Mutations in NDUFAF8 Cause Leigh Syndrome with an Isolated Complex I Deficiency. *Am J Hum Genet* 106**,** 92-101.

Andreu, A.L., Tanji, K., Bruno, C., Hadjigeorgiou, G.M., Sue, C.M., Jay, C., Ohnishi, T., Shanske, S., Bonilla, E., and Dimauro, S. (1999). Exercise intolerance due to a nonsense mutation in the mtDNA ND4 gene. *Ann Neurol* 45**,** 820-823.

Antonicka, H., Leary, S.C., Guercin, G.H., Agar, J.N., Horvath, R., Kennaway, N.G., Harding, C.O., Jaksch, M., and Shoubridge, E.A. (2003). Mutations in COX10 result in a defect in mitochondrial heme A biosynthesis and account for multiple, early-onset clinical phenotypes associated with isolated COX deficiency. *Hum Mol Genet* 12**,** 2693-2702.

Atwal, P.S. (2014). Mutations in the Complex III Assembly Factor Tetratricopeptide 19 Gene TTC19 Are a Rare Cause of Leigh Syndrome. *JIMD Rep* 14**,** 43-45.

Baertling, F., Sanchez-Caballero, L., Van Den Brand, M.a.M., Wintjes, L.T., Brink, M., Van Den Brandt, F.A., Wilson, C., Rodenburg, R.J.T., and Nijtmans, L.G.J. (2017). NDUFAF4 variants are associated with Leigh syndrome and cause a specific mitochondrial complex I assembly defect. *Eur J Hum Genet* 2**5,** 1273-1277.

Baide-Mairena, H., Gaudo, P., Marti-Sanchez, L., Emperador, S., Sanchez-Montanez, A., Alonso-Luengo, O., Correa, M., Grau, A.M., Ortigoza-Escobar, J.D., Artuch, R., Vazquez, E., Del Toro, M., Garrido-Perez, N., Ruiz-Pesini, E., Montoya, J., Bayona-Bafaluy, M.P., and Perez-Duenas, B. (2019). Mutations in the mitochondrial complex I assembly factor NDUFAF6 cause isolated bilateral striatal necrosis and progressive dystonia in childhood. *Mol Genet Metab* 126**,** 250-258.

Baker, R.A., Priestley, J.R.C., Wilstermann, A.M., Reese, K.J., and Mark, P.R. (2019). Clinical spectrum of BCS1L Mitopathies and their underlying structural relationships. *Am J Med Genet A* 179**,** 373-380.

Barca, E., Ganetzky, R.D., Potluri, P., Juanola-Falgarona, M., Gai, X., Li, D., Jalas, C., Hirsch, Y., Emmanuele, V., Tadesse, S., Ziosi, M., Akman, H.O., Chung, W.K., Tanji, K., Mccormick, E.M., Place, E., Consugar, M., Pierce, E.A., Hakonarson, H., Wallace, D.C., Hirano, M., and Falk, M.J. (2018). USMG5 Ashkenazi Jewish founder mutation impairs mitochondrial complex V dimerization and ATP synthesis. *Hum Mol Genet* 27**,** 3305-3312.

Barel, O., Shorer, Z., Flusser, H., Ofir, R., Narkis, G., Finer, G., Shalev, H., Nasasra, A., Saada, A., and Birk, O.S. (2008). Mitochondrial complex III deficiency associated with a homozygous mutation in UQCRQ. *Am J Hum Genet* 82**,** 1211-1216.

Blok, M.J., Spruijt, L., De Coo, I.F., Schoonderwoerd, K., Hendrickx, A., and Smeets, H.J. (2007). Mutations in the ND5 subunit of complex I of the mitochondrial DNA are a frequent cause of oxidative phosphorylation disease. *J Med Genet* 44**,** e74.

Bourgeron, T., Rustin, P., Chretien, D., Birch-Machin, M., Bourgeois, M., Viegas-Pequignot, E., Munnich, A., and Rotig, A. (1995). Mutation of a nuclear succinate dehydrogenase gene results in mitochondrial respiratory chain deficiency. *Nat Genet* 11**,** 144-149.

Budde, S.M., Van Den Heuvel, L.P., Janssen, A.J., Smeets, R.J., Buskens, C.A., Demeirleir, L., Van Coster, R., Baethmann, M., Voit, T., Trijbels, J.M., and Smeitink, J.A. (2000). Combined enzymatic complex I and III deficiency associated with mutations in the nuclear encoded NDUFS4 gene. *Biochem Biophys Res Commun* 275**,** 63-68.

Bugiani, M., Invernizzi, F., Alberio, S., Briem, E., Lamantea, E., Carrara, F., Moroni, I., Farina, L., Spada, M., Donati, M.A., Uziel, G., and Zeviani, M. (2004). Clinical and molecular findings in children with complex I deficiency. *Biochim Biophys Acta* 1659**,** 136-147.

Bugiani, M., Tiranti, V., Farina, L., Uziel, G., and Zeviani, M. (2005). Novel mutations in COX15 in a long surviving Leigh syndrome patient with cytochrome c oxidase deficiency. *J Med Genet* 42**,** e28.

Calvo, S.E., Tucker, E.J., Compton, A.G., Kirby, D.M., Crawford, G., Burtt, N.P., Rivas, M., Guiducci, C., Bruno, D.L., Goldberger, O.A., Redman, M.C., Wiltshire, E., Wilson, C.J., Altshuler, D., Gabriel, S.B., Daly, M.J., Thorburn, D.R., and Mootha, V.K. (2010). High-throughput, pooled sequencing identifies mutations in NUBPL and FOXRED1 in human complex I deficiency. *Nat Genet* 42**,** 851-858.

Cameron, J.M., Mackay, N., Feigenbaum, A., Tarnopolsky, M., Blaser, S., Robinson, B.H., and Schulze, A. (2015). Exome sequencing identifies complex I NDUFV2 mutations as a novel cause of Leigh syndrome. *Eur J Paediatr Neurol* 19**,** 525-532.

Campos, Y., Martin, M.A., Rubio, J.C., Gutierrez Del Olmo, M.C., Cabello, A., and Arenas, J. (1997). Bilateral striatal necrosis and MELAS associated with a new T3308C mutation in the mitochondrial ND1 gene. *Biochem Biophys Res Commun* 238**,** 323-325.

Caporali, L., Ghelli, A.M., Iommarini, L., Maresca, A., Valentino, M.L., La Morgia, C., Liguori, R., Zanna, C., Barboni, P., De Nardo, V., Martinuzzi, A., Rizzo, G., Tonon, C., Lodi, R., Calvaruso, M.A., Cappelletti, M., Porcelli, A.M., Achilli, A., Pala, M., Torroni, A., and Carelli, V. (2013). Cybrid studies establish the causal link between the mtDNA m.3890G>A/MT-ND1 mutation and optic atrophy with bilateral brainstem lesions. *Biochim Biophys Acta* 1832**,** 445-452.

Carrozzo, R., Tessa, A., Vazquez-Memije, M.E., Piemonte, F., Patrono, C., Malandrini, A., Dionisi-Vici, C., Vilarinho, L., Villanova, M., Schagger, H., Federico, A., Bertini, E., and Santorelli, F.M. (2001). The T9176G mtDNA mutation severely affects ATP production and results in Leigh syndrome. *Neurology* 56**,** 687-690.

Catania, A., Ardissone, A., Verrigni, D., Legati, A., Reyes, A., Lamantea, E., Diodato, D., Tonduti, D., Imperatore, V., Pinto, A.M., Moroni, I., Bertini, E., Robinson, A., Carrozzo, R., Zeviani, M., and Ghezzi, D. (2018). Compound heterozygous missense and deep intronic variants in NDUFAF6 unraveled by exome sequencing and mRNA analysis. *J Hum Genet* 63**,** 563-568.

Ching, C.K., Mak, C.M., Au, K.M., Chan, K.Y., Yuen, Y.P., Yau, E.K., Ma, L.C., Chow, H.L., and Chan, A.Y. (2013). A patient with congenital hyperlactataemia and Leigh syndrome: an uncommon mitochondrial variant. *Hong Kong Med J* 19**,** 357-361.

Corona, P., Antozzi, C., Carrara, F., D'incerti, L., Lamantea, E., Tiranti, V., and Zeviani, M. (2001). A novel mtDNA mutation in the ND5 subunit of complex I in two MELAS patients. *Annals of Neurology* 49**,** 106-110.

Crimi, M., Galbiati, S., Moroni, I., Bordoni, A., Perini, M.P., Lamantea, E., Sciacco, M., Zeviani, M., Biunno, I., Moggio, M., Scarlato, G., and Comi, G.P. (2003). A missense

mutation in the mitochondrial ND5 gene associated with a Leigh-MELAS overlap syndrome. *Neurology* 60**,** 1857-1861.

Crimi, M., Papadimitriou, A., Galbiati, S., Palamidou, P., Fortunato, F., Bordoni, A., Papandreou, U., Papadimitriou, D., Hadjigeorgiou, G.M., Drogari, E., Bresolin, N., and Comi, G.P. (2004). A new mitochondrial DNA mutation in ND3 gene causing severe Leigh syndrome with early lethality. *Pediatr Res* 55**,** 842-846.

De Lonlay, P., Valnot, I., Barrientos, A., Gorbatyuk, M., Tzagoloff, A., Taanman, J.W., Benayoun, E., Chretien, D., Kadhom, N., Lombes, A., De Baulny, H.O., Niaudet, P., Munnich, A., Rustin, P., and Rotig, A. (2001). A mutant mitochondrial respiratory chain assembly protein causes complex III deficiency in patients with tubulopathy, encephalopathy and liver failure. *Nat Genet* 29**,** 57-60.

Debray, F.G., Morin, C., Janvier, A., Villeneuve, J., Maranda, B., Laframboise, R., Lacroix, J., Decarie, J.C., Robitaille, Y., Lambert, M., Robinson, B.H., and Mitchell, G.A. (2011). LRPPRC mutations cause a phenotypically distinct form of Leigh syndrome with cytochrome c oxidase deficiency. *J Med Genet* 48**,** 183-189.

Fassone, E., Duncan, A.J., Taanman, J.W., Pagnamenta, A.T., Sadowski, M.I., Holand, T., Qasim, W., Rutland, P., Calvo, S.E., Mootha, V.K., Bitner-Glindzicz, M., and Rahman, S. (2010). FOXRED1, encoding an FAD-dependent oxidoreductase complex-I-specific molecular chaperone, is mutated in infantile-onset mitochondrial encephalopathy. *Hum Mol Genet* 19**,** 4837-4847.

Fernandez-Vizarra, E., Bugiani, M., Goffrini, P., Carrara, F., Farina, L., Procopio, E., Donati, A., Uziel, G., Ferrero, I., and Zeviani, M. (2007). Impaired complex III assembly associated with BCS1L gene mutations in isolated mitochondrial encephalopathy. *Hum Mol Genet* 16**,** 1241-1252.

Ganetzky, R.D., Stendel, C., Mccormick, E.M., Zolkipli-Cunningham, Z., Goldstein, A.C., Klopstock, T., and Falk, M.J. (2019). MT-ATP6 mitochondrial disease variants: Phenotypic and biochemical features analysis in 218 published cases and cohort of 14 new cases. *Human Mutation* 40**,** 499-515.

Gerards, M., Sluiter, W., Van Den Bosch, B.J., De Wit, L.E., Calis, C.M., Frentzen, M., Akbari, H., Schoonderwoerd, K., Scholte, H.R., Jongbloed, R.J., Hendrickx, A.T., De Coo, I.F., and Smeets, H.J. (2010). Defective complex I assembly due to C20orf7 mutations as a new cause of Leigh syndrome. *J Med Genet* 47**,** 507-512.

Ghezzi, D., Arzuffi, P., Zordan, M., Da Re, C., Lamperti, C., Benna, C., D'adamo, P., Diodato, D., Costa, R., Mariotti, C., Uziel, G., Smiderle, C., and Zeviani, M. (2011). Mutations in TTC19 cause mitochondrial complex III deficiency and neurological impairment in humans and flies. *Nat Genet* 43**,** 259-263.

Ghezzi, D., Goffrini, P., Uziel, G., Horvath, R., Klopstock, T., Lochmuller, H., D'adamo, P., Gasparini, P., Strom, T.M., Prokisch, H., Invernizzi, F., Ferrero, I., and Zeviani, M. (2009). SDHAF1, encoding a LYR complex-II specific assembly factor, is mutated in SDH-defective infantile leukoencephalopathy. *Nat Genet* 41**,** 654-656.

Gropman, A., Chen, T.J., Perng, C.L., Krasnewich, D., Chernoff, E., Tifft, C., and Wong, L.J. (2004). Variable clinical manifestation of homoplasmic G14459A mitochondrial DNA mutation. *Am J Med Genet A* 124A**,** 377-382.

Hadzsiev, K., Maasz, A., Kisfali, P., Kalman, E., Gomori, E., Pal, E., Berenyi, E., Komlosi, K., and Melegh, B. (2010). Mitochondrial DNA 11777C>A mutation associated Leigh syndrome: case report with a review of the previously described pedigrees. *Neuromolecular Med* 12**,** 277-284.

Hallmann, K., Kudin, A.P., Zsurka, G., Kornblum, C., Reimann, J., Stuve, B., Waltz, S., Hattingen, E., Thiele, H., Nurnberg, P., Rub, C., Voos, W., Kopatz, J., Neumann, H., and Kunz, W.S. (2016). Loss of the smallest subunit of cytochrome c oxidase, COX8A, causes Leigh-like syndrome and epilepsy. *Brain* 139**,** 338-345.

Han, J., Lee, Y.M., Kim, S.M., Han, S.Y., Lee, J.B., and Han, S.H. (2015). Ophthalmological manifestations in patients with Leigh syndrome. *Br J Ophthalmol* 99**,** 528-535.

Hanna, M.G., Nelson, I.P., Rahman, S., Lane, R.J., Land, J., Heales, S., Cooper, M.J., Schapira, A.H., Morgan-Hughes, J.A., and Wood, N.W. (1998). Cytochrome c oxidase deficiency associated with the first stop-codon point mutation in human mtDNA. *Am J Hum Genet* 63**,** 29-36.

Hinttala, R., Smeets, R., Moilanen, J.S., Ugalde, C., Uusimaa, J., Smeitink, J.A., and Majamaa, K. (2006). Analysis of mitochondrial DNA sequences in patients with isolated or combined oxidative phosphorylation system deficiency. *J Med Genet* 43**,** 881-886.

Hoefs, S.J., Dieteren, C.E., Distelmaier, F., Janssen, R.J., Epplen, A., Swarts, H.G., Forkink, M., Rodenburg, R.J., Nijtmans, L.G., Willems, P.H., Smeitink, J.A., and Van Den Heuvel, L.P. (2008). NDUFA2 complex I mutation leads to Leigh disease. *Am J Hum Genet* 82**,** 1306-1315.

Hoefs, S.J., Dieteren, C.E., Rodenburg, R.J., Naess, K., Bruhn, H., Wibom, R., Wagena, E., Willems, P.H., Smeitink, J.A., Nijtmans, L.G., and Van Den Heuvel, L.P. (2009). Baculovirus complementation restores a novel NDUFAF2 mutation causing complex I deficiency. *Hum Mutat* 30**,** E728-736.

Hoefs, S.J., Van Spronsen, F.J., Lenssen, E.W., Nijtmans, L.G., Rodenburg, R.J., Smeitink, J.A., and Van Den Heuvel, L.P. (2011). NDUFA10 mutations cause complex I deficiency in a patient with Leigh disease. *Eur J Hum Genet* 19**,** 270-274.

Horvath, R., Abicht, A., Holinski-Feder, E., Laner, A., Gempel, K., Prokisch, H., Lochmuller, H., Klopstock, T., and Jaksch, M. (2006). Leigh syndrome caused by mutations in the flavoprotein (Fp) subunit of succinate dehydrogenase (SDHA). *J Neurol Neurosurg Psychiatry* 77**,** 74-76.

Incecik, F., Herguner, O.M., Besen, S., Bozdogan, S.T., and Mungan, N.O. (2018). Late-Onset Leigh Syndrome due to NDUFV1 Mutation in a 10-Year-Old Boy Initially Presenting with Ataxia. *J Pediatr Neurosci* 13**,** 205-207.

Jaokar, T.M., Patil, D.P., Shouche, Y.S., Gaikwad, S.M., and Suresh, C.G. (2013). Human mitochondrial NDUFS3 protein bearing Leigh syndrome mutation is more prone to aggregation than its wild-type. *Biochimie* 95**,** 2392-2403.

Joost, K., Rodenburg, R., Piirsoo, A., Van Den Heuvel, B., Zordania, R., and Õunap, K. (2010). A novel mutation in the SCO2 gene in a neonate with early-onset cardioencephalomyopathy. *Pediatric Neurology* 42**,** 227-230.

Keightley, J.A., Hoffbuhr, K.C., Burton, M.D., Salas, V.M., Johnston, W.S., Penn, A.M., Buist, N.R., and Kennaway, N.G. (1996). A microdeletion in cytochrome c oxidase (COX)

subunit III associated with COX deficiency and recurrent myoglobinuria. *Nat Genet* 12**,** 410-416.

Kirby, D.M., Boneh, A., Chow, C.W., Ohtake, A., Ryan, M.T., Thyagarajan, D., and Thorburn, D.R. (2003). Low mutant load of mitochondrial DNA G13513A mutation can cause Leigh's disease. *Annals of Neurology* 54**,** 473-478.

Kirby, D.M., Kahler, S.G., Freckmann, M.L., Reddihough, D., and Thorburn, D.R. (2000). Leigh disease caused by the mitochondrial DNA G14459A mutation in unrelated families. *Annals of Neurology* 48**,** 102-104.

Komaki, H., Akanuma, J., Iwata, H., Takahashi, T., Mashima, Y., Nonaka, I., and Goto, Y. (2003). A novel mtDNA C11777A mutation in Leigh syndrome. *Mitochondrion* 2**,** 293-304.

Lebon, S., Chol, M., Benit, P., Mugnier, C., Chretien, D., Giurgea, I., Kern, I., Girardin, E., Hertz-Pannier, L., De Lonlay, P., Rotig, A., Rustin, P., and Munnich, A. (2003). Recurrent de novo mitochondrial DNA mutations in respiratory chain deficiency. *J Med Genet* 40**,** 896-899.

Lebon, S., Rodriguez, D., Bridoux, D., Zerrad, A., Rotig, A., Munnich, A., Legrand, A., and Slama, A. (2007). A novel mutation in the human complex I NDUFS7 subunit associated with Leigh syndrome. *Mol Genet Metab* 90**,** 379-382.

Lee, J.S., Kim, H., Lim, B.C., Hwang, H., Choi, J., Kim, K.J., Hwang, Y.S., and Chae, J.H. (2016). Leigh Syndrome in Childhood: Neurologic Progression and Functional Outcome. *J Clin Neurol* 12**,** 181-187.

Leshinsky-Silver, E., Lev, D., Malinger, G., Shapira, D., Cohen, S., Lerman-Sagie, T., and Saada, A. (2010). Leigh disease presenting in utero due to a novel missense mutation in the mitochondrial DNA-ND3. *Mol Genet Metab* 100**,** 65-70.

Li, T.R., Wang, Q., Liu, M.M., and Lv, R.J. (2019). A Chinese Family With Adult-Onset Leigh-Like Syndrome Caused by the Heteroplasmic m.10191T>C Mutation in the Mitochondrial MTND3 Gene. *Front Neurol* 10**,** 347.

Li, Y., Wen, S., Li, D., Xie, J., Wei, X., Li, X., Liu, Y., Fang, H., Yang, Y., and Lyu, J. (2018). SURF1 mutations in Chinese patients with Leigh syndrome: Novel mutations, mutation spectrum, and the functional consequences. *Gene* 674**,** 15-24.

Lim, B.C., Park, J.D., Hwang, H., Kim, K.J., Hwang, Y.S., Chae, J.H., Cheon, J.E., Kim, I.O., Lee, R., and Moon, H.K. (2009). Mutations in ND subunits of complex I are an important genetic cause of childhood mitochondrial encephalopathies. *J Child Neurol* 24**,** 828-832.

Lim, S.C., Smith, K.R., Stroud, D.A., Compton, A.G., Tucker, E.J., Dasvarma, A., Gandolfo, L.C., Marum, J.E., Mckenzie, M., Peters, H.L., Mowat, D., Procopis, P.G., Wilcken, B., Christodoulou, J., Brown, G.K., Ryan, M.T., Bahlo, M., and Thorburn, D.R. (2014). A founder mutation in PET100 causes isolated complex IV deficiency in Lebanese individuals with Leigh syndrome. *American Journal of Human Genetics* 94**,** 209-222.

Loeffen, J., Smeitink, J., Triepels, R., Smeets, R., Schuelke, M., Sengers, R., Trijbels, F., Hamel, B., Mullaart, R., and Van Den Heuvel, L. (1998). The first nuclear-encoded complex I mutation in a patient with Leigh syndrome. *Am J Hum Genet* 63**,** 1598-1608.

Lou, X., Shi, H., Wen, S., Li, Y., Wei, X., Xie, J., Ma, L., Yang, Y., Fang, H., and Lyu, J. (2018). A Novel NDUFS3 mutation in a Chinese patient with severe Leigh syndrome. *J Hum Genet* 63**,** 1269-1272.

Ma, Y.Y., Wu, T.F., Liu, Y.P., Wang, Q., Song, J.Q., Li, X.Y., Shi, X.Y., Zhang, W.N., Zhao, M., Hu, L.Y., Yang, Y.L., and Zou, L.P. (2013). Genetic and biochemical findings in Chinese children with Leigh syndrome. *J Clin Neurosci* 20**,** 1591-1594.

Mcfarland, R., Kirby, D.M., Fowler, K.J., Ohtake, A., Ryan, M.T., Amor, D.J., Fletcher, J.M., Dixon, J.W., Collins, F.A., Turnbull, D.M., Taylor, R.W., and Thorburn, D.R. (2004). De novo mutations in the mitochondrial ND3 gene as a cause of infantile mitochondrial encephalopathy and complex I deficiency. *Annals of Neurology* 55**,** 58-64.

Miller, D.K., Menezes, M.J., Simons, C., Riley, L.G., Cooper, S.T., Grimmond, S.M., Thorburn, D.R., Christodoulou, J., and Taft, R.J. (2014). Rapid identification of a novel complex I MT-ND3 m.10134C>A mutation in a Leigh syndrome patient. *PLoS One* 9**,** e104879.

Mootha, V.K., Lepage, P., Miller, K., Bunkenborg, J., Reich, M., Hjerrild, M., Delmonte, T., Villeneuve, A., Sladek, R., Xu, F., Mitchell, G.A., Morin, C., Mann, M., Hudson, T.J., Robinson, B., Rioux, J.D., and Lander, E.S. (2003). Identification of a gene causing human cytochrome c oxidase deficiency by integrative genomics. *Proc Natl Acad Sci U S A* 100**,** 605-610.

Moslemi, A.R., Darin, N., Tulinius, M., Wiklund, L.M., Holme, E., and Oldfors, A. (2008). Progressive encephalopathy and complex I deficiency associated with mutations in MTND1. *Neuropediatrics* 39**,** 24-28.

Mourier, A., Ruzzenente, B., Brandt, T., Kühlbrandt, W., and Larsson, N.G. (2014). Loss of LRPPRC causes ATP synthase deficiency. *Human Molecular Genetics* 23**,** 2580-2592.

Naess, K., Freyer, C., Bruhn, H., Wibom, R., Malm, G., Nennesmo, I., Von Dobeln, U., and Larsson, N.G. (2009). MtDNA mutations are a common cause of severe disease phenotypes in children with Leigh syndrome. *Biochim Biophys Acta* 1787**,** 484-490.

Negishi, Y., Hattori, A., Takeshita, E., Sakai, C., Ando, N., Ito, T., Goto, Y., and Saitoh, S. (2014). Homoplasmy of a mitochondrial 3697G>A mutation causes Leigh syndrome. *J Hum Genet* 59**,** 405-407.

Ogawa, E., Shimura, M., Fushimi, T., Tajika, M., Ichimoto, K., Matsunaga, A., Tsuruoka, T., Ishige, M., Fuchigami, T., Yamazaki, T., Mori, M., Kohda, M., Kishita, Y., Okazaki, Y., Takahashi, S., Ohtake, A., and Murayama, K. (2017). Clinical validity of biochemical and molecular analysis in diagnosing Leigh syndrome: a study of 106 Japanese patients. *Journal of Inherited Metabolic Disease* 40**,** 685-693.

Oquendo, C.E., Antonicka, H., Shoubridge, E.A., Reardon, W., and Brown, G.K. (2004). Functional and genetic studies demonstrate that mutation in the COX15 gene can cause Leigh syndrome. *J Med Genet* 41**,** 540-544.

Ostergaard, E., Rodenburg, R.J., Van Den Brand, M., Thomsen, L.L., Duno, M., Batbayli, M., Wibrand, F., and Nijtmans, L. (2011). Respiratory chain complex I deficiency due to NDUFA12 mutations as a new cause of Leigh syndrome. *J Med Genet* 48**,** 737-740.

Pagnamenta, A.T., Hargreaves, I.P., Duncan, A.J., Taanman, J.W., Heales, S.J., Land, J.M., Bitner-Glindzicz, M., Leonard, J.V., and Rahman, S. (2006). Phenotypic variability of mitochondrial disease caused by a nuclear mutation in complex II. *Mol Genet Metab* 89**,** 214-221.

Petruzzella, V., Di Giacinto, G., Scacco, S., Piemonte, F., Torraco, A., Carrozzo, R., Vergari, R., Dionisi-Vici, C., Longo, D., Tessa, A., Papa, S., and Bertini, E. (2003). Atypical Leigh syndrome associated with the D393N mutation in the mitochondrial ND5 subunit. *Neurology* 61**,** 1017-1018.

Piekutowska-Abramczuk, D., Assouline, Z., Mataković, L., Feichtinger, R.G., Koňařiková, E., Jurkiewicz, E., Stawiński, P., Gusic, M., Koller, A., Pollak, A., Gasperowicz, P., Trubicka, J., Ciara, E., Iwanicka-Pronicka, K., Rokicki, D., Hanein, S., Wortmann, S.B., Sperl, W., Rötig, A., Prokisch, H., Pronicka, E., Płoski, R., Barcia, G., and Mayr, J.A. (2018a). NDUFB8 Mutations Cause Mitochondrial Complex I Deficiency in Individuals with Leigh-like Encephalomyopathy. *American Journal of Human Genetics* 102**,** 460-467.

Piekutowska-Abramczuk, D., Rutyna, R., Czyżyk, E., Jurkiewicz, E., Pronicka, K.I., Rokicki, D., Stachowicz, S., Strzemecka, J., Guz, W., Gawroński, M., Kosierb, A., Ligas, J., Puchala, M., Drelich-Zbroja, A., Bednarska-Makaruk, M., Dąbrowski, W., Ciara, E., Książyk, J.B., and Pronicka, E. (2018b). Leigh syndrome in individuals bearing m.9185T>C MTATP6 variant. Is hyperventilation a factor which starts its development? *Metabolic Brain Disease* 33**,** 191-199.

Pitceathly, R.D., Rahman, S., Wedatilake, Y., Polke, J.M., Cirak, S., Foley, A.R., Sailer, A., Hurles, M.E., Stalker, J., Hargreaves, I., Woodward, C.E., Sweeney, M.G., Muntoni, F., Houlden, H., Taanman, J.W., Hanna, M.G., and Consortium, U.K. (2013). NDUFA4 mutations underlie dysfunction of a cytochrome c oxidase subunit linked to human neurological disease. *Cell Rep* 3**,** 1795-1805.

Ronchi, D., Cosi, A., Tonduti, D., Orcesi, S., Bordoni, A., Fortunato, F., Rizzuti, M., Sciacco, M., Collotta, M., Cagdas, S., Capovilla, G., Moggio, M., Berardinelli, A., Veggiotti, P., and Comi, G.P. (2011). Clinical and molecular features of an infant patient affected by Leigh Disease associated to m.14459G>A mitochondrial DNA mutation: a case report. *BMC Neurology* 11**,** 85.

Ruiter, E.M., Siers, M.H., Van Den Elzen, C., Van Engelen, B.G., Smeitink, J.A., Rodenburg, R.J., and Hol, F.A. (2007). The mitochondrial 13513G > A mutation is most frequent in Leigh syndrome combined with reduced complex I activity, optic atrophy and/or Wolff-Parkinson-White. *Eur J Hum Genet* 15**,** 155-161.

Saada, A., Edvardson, S., Rapoport, M., Shaag, A., Amry, K., Miller, C., Lorberboum-Galski, H., and Elpeleg, O. (2008). C6ORF66 is an assembly factor of mitochondrial complex I. *Am J Hum Genet* 82**,** 32-38.

Santorelli, F.M., Shanske, S., Macaya, A., Devivo, D.C., and Dimauro, S. (1993). The mutation at nt 8993 of mitochondrial DNA is a common cause of Leigh's syndrome. *Annals of Neurology* 34**,** 827-834.

Sarzi, E., Brown, M.D., Lebon, S., Chretien, D., Munnich, A., Rotig, A., and Procaccio, V. (2007). A novel recurrent mitochondrial DNA mutation in ND3 gene is associated with isolated complex I deficiency causing Leigh syndrome and dystonia. *American Journal of Medical Genetics, Part A* 143A**,** 33-41.

Schlehe, J.S., Journel, M.S., Taylor, K.P., Amodeo, K.D., and Lavoie, M.J. (2013). The mitochondrial disease associated protein Ndufaf2 is dispensable for Complex-1 assembly but critical for the regulation of oxidative stress. *Neurobiol Dis* 58**,** 57-67.

Schuelke, M., Smeitink, J., Mariman, E., Loeffen, J., Plecko, B., Trijbels, F., Stockler-Ipsiroglu, S., and Van Den Heuvel, L. (1999). Mutant NDUFV1 subunit of mitochondrial complex I causes leukodystrophy and myoclonic epilepsy. *Nat Genet* 21**,** 260-261.

Shanske, S., Coku, J., Lu, J., Ganesh, J., Krishna, S., Tanji, K., Bonilla, E., Naini, A.B., Hirano, M., and Dimauro, S. (2008). The G13513A mutation in the ND5 gene of mitochondrial DNA as a common cause of MELAS or Leigh syndrome: evidence from 12 cases. *Arch Neurol* 65**,** 368-372.

Spangenberg, L., Grana, M., Greif, G., Suarez-Rivero, J.M., Krysztal, K., Tapie, A., Boidi, M., Fraga, V., Lemes, A., Guecaimburu, R., Cerisola, A., Sanchez-Alcazar, J.A., Robello, C., Raggio, V., and Naya, H. (2016). 3697G>A in MT-ND1 is a causative mutation in mitochondrial disease. *Mitochondrion* 28**,** 54-59.

Tarnopolsky, M., Meaney, B., Robinson, B., Sheldon, K., and Boles, R.G. (2013). Severe infantile leigh syndrome associated with a rare mitochondrial ND6 mutation, m.14487T>C. *Am J Med Genet A* 161A**,** 2020-2023.

Taylor, R.W., Morris, A.A., Hutchinson, M., and Turnbull, D.M. (2002). Leigh disease associated with a novel mitochondrial DNA ND5 mutation. *European Journal of Human Genetics* 10**,** 141-144.

Taylor, R.W., Singh-Kler, R., Hayes, C.M., Smith, P.E., and Turnbull, D.M. (2001). Progressive mitochondrial disease resulting from a novel missense mutation in the mitochondrial DNA ND3 gene. *Annals of neurology* 50**,** 104-107.

Tiranti, V., Corona, P., Greco, M., Taanman, J.W., Carrara, F., Lamantea, E., Nijtmans, L., Uziel, G., and Zeviani, M. (2000). A novel frameshift mutation of the mtDNA COIII gene leads to impaired assembly of cytochrome c oxidase in a patient affected by Leigh-like syndrome. *Hum Mol Genet* 9**,** 2733-2742.

Tuppen, H.A., Hogan, V.E., He, L., Blakely, E.L., Worgan, L., Al-Dosary, M., Saretzki, G., Alston, C.L., Morris, A.A., Clarke, M., Jones, S., Devlin, A.M., Mansour, S., Chrzanowska-Lightowlers, Z.M., Thorburn, D.R., Mcfarland, R., and Taylor, R.W. (2010). The p.M292T NDUFS2 mutation causes complex I-deficient Leigh syndrome in multiple families. *Brain* 133**,** 2952-2963.

Uehara, N., Mori, M., Tokuzawa, Y., Mizuno, Y., Tamaru, S., Kohda, M., Moriyama, Y., Nakachi, Y., Matoba, N., Sakai, T., Yamazaki, T., Harashima, H., Murayama, K., Hattori, K., Hayashi, J., Yamagata, T., Fujita, Y., Ito, M., Tanaka, M., Nibu, K., Ohtake, A., and Okazaki, Y. (2014). New MT-ND6 and NDUFA1 mutations in mitochondrial respiratory chain disorders. *Ann Clin Transl Neurol* 1**,** 361-369.

Ugalde, C., Hinttala, R., Timal, S., Smeets, R., Rodenburg, R.J., Uusimaa, J., Van Heuvel, L.P., Nijtmans, L.G., Majamaa, K., and Smeitink, J.A. (2007). Mutated ND2 impairs mitochondrial complex I assembly and leads to Leigh syndrome. *Mol Genet Metab* 90**,** 10-14.

Van Den Bosch, B.J., Gerards, M., Sluiter, W., Stegmann, A.P., Jongen, E.L., Hellebrekers, D.M., Oegema, R., Lambrichs, E.H., Prokisch, H., Danhauser, K., Schoonderwoerd, K., De Coo, I.F., and Smeets, H.J. (2012). Defective NDUFA9 as a novel cause of neonatally fatal complex I disease. *J Med Genet* 49**,** 10-15.

Vanniarajan, A., Rajshekher, G.P., Joshi, M.B., Reddy, A.G., Singh, L., and Thangaraj, K. (2006). Novel mitochondrial mutation in the ND4 gene associated with Leigh syndrome. *Acta Neurol Scand* 114**,** 350-353.

Vilain, C., Rens, C., Aeby, A., Baleriaux, D., Van Bogaert, P., Remiche, G., Smet, J., Van Coster, R., Abramowicz, M., and Pirson, I. (2012). A novel NDUFV1 gene mutation in complex I deficiency in consanguineous siblings with brainstem lesions and Leigh syndrome. *Clin Genet* 82**,** 264-270.

Vilarinho, L., Leao, E., Barbot, C., Santos, M., Rocha, H., and Santorelli, F.M. (2000). Clinical and molecular studies in three Portuguese mtDNA T8993G families. *Pediatric neurology* 22**,** 29-32.

Wang, J., Brautbar, A., Chan, A.K., Dzwiniel, T., Li, F.Y., Waters, P.J., Graham, B.H., and Wong, L.J. (2009). Two mtDNA mutations 14487T>C (M63V, ND6) and 12297T>C (tRNA Leu) in a Leigh syndrome family. *Mol Genet Metab* 96**,** 59-65.

Wei, Y., Cui, L., and Peng, B. (2018). Mitochondrial DNA mutations in late-onset Leigh syndrome. *J Neurol* 265**,** 2388-2395.

Weraarpachai, W., Antonicka, H., Sasarman, F., Seeger, J., Schrank, B., Kolesar, J.E., Lochmüller, H., Chevrette, M., Kaufman, B.A., Horvath, R., and Shoubridge, E.A. (2009). Mutation in TACO1, encoding a translational activator of COX I, results in cytochrome c oxidase deficiency and late-onset Leigh syndrome. *Nature Genetics* 41**,** 833-837.

Wray, C.D., Friederich, M.W., Du Sart, D., Pantaleo, S., Smet, J., Kucera, C., Fenton, L., Scharer, G., Van Coster, R., and Van Hove, J.L. (2013). A new mutation in MT-ND1 m.3928G>C p.V208L causes Leigh disease with infantile spasms. *Mitochondrion* 13**,** 656-661.

Xu, B., Li, X., Du, M., Zhou, C., Fang, H., Lyu, J., and Yang, Y. (2017). Novel mutation of ND4 gene identified by targeted next-generation sequencing in patient with Leigh syndrome. *J Hum Genet* 62**,** 291-297.

Yu, X.L., Yan, C.Z., Ji, K.Q., Lin, P.F., Xu, X.B., Dai, T.J., Li, W., and Zhao, Y.Y. (2018). Clinical, Neuroimaging, and Pathological Analyses of 13 Chinese Leigh Syndrome Patients with Mitochondrial DNA Mutations. *Chin Med J (Engl)* 131**,** 2705-2712.

Zafeiriou, D.I., Rodenburg, R.J., Scheffer, H., Van Den Heuvel, L.P., Pouwels, P.J., Ververi, A., Athanasiadou-Piperopoulou, F., and Van Der Knaap, M.S. (2008). MR spectroscopy and serial magnetic resonance imaging in a patient with mitochondrial cystic leukoencephalopathy due to complex I deficiency and NDUFV1 mutations and mild clinical course. *Neuropediatrics* 39**,** 172-175.

Zurita Rendon, O., Antonicka, H., Horvath, R., and Shoubridge, E.A. (2016). A Mutation in the Flavin Adenine Dinucleotide-Dependent Oxidoreductase FOXRED1 Results in Cell-Type-Specific Assembly Defects in Oxidative Phosphorylation Complexes I and II. *Mol Cell Biol* 36**,** 2132-2140.

8. Appendix B – List of publication (not included in dissertation)

Bakare, A.B., Meshrkey, F., Lowe, B., Molder, C., Rao, R.R., Zhan, J., Iyer, S. MitoCellPhe reveals mitochondrial morphologies in single fibroblasts and clustered stem cells. *American Journal of Physiology*. Submitted June 2021